Molecular and Bioinformatic Analysis of Neurotropic HIV Envelope Glycoproteins

HARVARD UNIVERSITY
Graduate School of Arts and Sciences

DISSERTATION ACCEPTANCE CERTIFICATE

The undersigned, appointed by the

Division of Medical Sciences

Committee on Virology

have examined a dissertation entitled

MOLECULAR AND BIOINFORMATIC ANALYSIS OF NEUROTROPIC HIV ENVELOPE GLYCOPROTEINS

presented by Megan Eileen Mefford

candidate for the degree of Doctor of Philosophy and hereby certify that it is worthy of acceptance.

Signature: _____

Typed Name: Dr. Michael Farzan

Signature: _____

Typed Name: Dr. Manish Sagar

Signature: _____

Typed Name: Dr. Paul Clapham

_____

Dr. David Knipe, Program Head

Date: April 20, 2012

_____

Dr. David Lopes Cardozo, Director of Graduate Studies

MOLECULAR AND BIOINFORMATIC ANALYSIS OF NEUROTROPIC HIV ENVELOPE GLYCOPROTEINS

A dissertation presented

by

Megan Eileen Mefford

to

The Division of Medical Sciences

in partial fulfillment of the requirements
for the degree of
Doctor of Philosophy
in the subject of

Virology

Harvard University
Cambridge, Massachusetts

April 2012

Dissertation Advisor: Dr. Dana Gabuzda **Author: Megan Eileen Mefford**

Molecular and Bioinformatic Analysis of Neurotropic HIV Envelope Glycoproteins

ABSTRACT

Human immunodeficiency virus (HIV) infection of macrophages in brain and other tissues plays an important role in development of HIV-associated neurological disorders and other aspects of disease pathogenesis. Macrophages express low levels of CD4, and macrophage-tropic HIV strains express envelope glycoproteins (Envs) adapted to overcome this restriction to virus entry by mechanisms that are not well characterized. One mechanism that influences this phenotype is increased exposure of the CD4 or CCR5 binding site, which may increase dissociation of soluble gp120 (sgp120) from Env trimers based on structural models. Little is known about spontaneous sgp120 shedding from primary HIV Envs or its biological significance. In this dissertation, we identify genetic determinants in brain-derived Envs that overcome the restriction imposed by low CD4, examine spontaneous sgp120 shedding by these Envs, and explore the biological significance of these findings. Sequence analysis of the gp120 β3 strand of the CCR5-binding site bridging sheet identified D197, which eliminates an N-linked glycosylation site, as a viral determinant associated with brain infection and HIV-associated dementia (HAD), and position 200 as a positively-selected codon in HAD patients. Mutagenesis studies showed that D197 and T/V200 enhance fusion and infection of macrophages and other cells expressing low CD4 by enhancing gp120 binding to CCR5. Sgp120 shedding from primary brain and lymphoid Envs was highly variable within and between patients, representing a spectrum rather than a categorical phenotype. Brain Envs with high sgp120 shedding mediated enhanced fusion and infection with cells expressing low CD4. Furthermore, viruses expressing

brain Envs with high sgp120 shedding had an increased capacity to induce lymphocyte activation during PBMC infection, despite similar levels of viral replication. Genetic analysis demonstrated greater entropy and positive selection in Envs with high versus low levels of sgp120 shedding, suggesting that diversifying evolution influences gp120-gp41 association. Finally, we examined V3 loop sequences from dual-tropic brain and lymphoid Envs and found that the frequency of R5X4 HIV-1 is underestimated by most predictive bioinformatic algorithms. Together, these studies provide a better understanding of how neurotropic HIV Envs adapt to target cells expressing low CD4, and possible roles of these viral adaptations in disease pathogenesis.

Dedicated to Todd,

my husband and best friend

ACKNOWLEDGEMENTS

A dissertation is never a solo effort, and I would like to thank a number of mentors, colleagues, and friends who contributed in their own ways to this work:

First, thank you to my advisor, Dana Gabuzda, for her seemingly unlimited supply of patience and advice.

I would also like to thank the members of my dissertation advisory committee, Jim Cunningham, Joe Sodroski, Bing Chen, and Ron Desrosiers, for helpful discussions, advice, and motivation.

Rebecca Dunfee and Elaine Thomas in the Gabuzda lab, who were there to help with the intricacies and frustrations of HIV Env when I was just beginning these projects.

Joya Mukerji and Will Yen, my fellow Gabuzda lab students, for helpful discussions, both scientific and otherwise.

Gabuzda lab members past and present, including Alex Holman, Kevin Olivieri, Anupa Kamat, Edana Cassol, Jianbin Wang, Erez Pery, Vikas Misra, and Andy Mehle, for helpful discussions and making the lab a fun and always interesting place to work.

Members of the Sodroski and Engelman labs, for sharing advice, frustrations, and friendship.

Virology students past and present, for friendship, advice, and making the transition from New Orleans to Boston not so terrible a shock.

My previous mentors, Preston Marx, Ron Veazey, and Kate Eaton, for encouraging my questions and curiosity.

I would especially like to thank my family, particularly my parents, Jim and Carol Hall, my brother Kyle, and future sister-in-law Cristie. I'd also like to thank my in-laws, Richard and Tommie Mefford, and Bill, Paula, Jake, Andy, and Will Lawson. Without your support I'd be lost. Look, I'm finally done!

Finally, Todd, for encouraging me and believing in me. Thank you for bringing so much love and happiness into my life.

TABLE OF CONTENTS

FIGURES

TABLES

CHAPTER 1: INTRODUCTION

The HIV/AIDS Pandemic

Since the first reports by the Centers for Disease Control of 5 cases of *Pneumocystis carinii* pneumonia in young men in Los Angeles on June 5, 1981, acquired immunodeficiency syndrome (AIDS) has become a worldwide pandemic (4). In 1984, human immunodeficiency virus (HIV) was isolated from an AIDS patient and identified as the causative agent of AIDS (5-7). Since that time, AIDS has resulted in more than 25 million deaths worldwide (UNAIDS 2011) and an estimated 34 million people are living with HIV infection (UNAIDS 2011). There were 2.7 million new HIV infections reported in 2010, down 21% from the peak of the global epidemic in 1997 (UNAIDS 2011). Encouragingly, nearly 6.6 million people in low and middle income countries were receiving HIV treatment at the end of 2010. As a consequence, HIV incidence in 33 countries, 22 of them in sub-Saharan Africa, continued to decline (UNAIDS Outlook Report 2010) and the number of people dying from AIDS-related causes fell to 1.8 million, down from a peak of 2.2 million in the mid-2000s (UNAIDS 2011). However, HIV incidence increased by more than 25% over this same period in 7 countries, 5 of which are located Eastern Europe and Central Asia (UNAIDS 2009).

HIV is a lentivirus of family *Retroviridae*. Two types of HIV (HIV-1 and HIV-2) circulate worldwide. HIV infection in humans is the result of several cross-species transmission events of simian immunodeficiency viruses (SIV): HIV-1 from a single chimpanzee to human transmission event (SIV_{cpz}) and HIV-2 most likely from a sooty mangaby transmission event (HIV_{smm}). HIV-1 is more common and virulent, with a prevalence of almost 90%. In contrast, HIV-2 is less easily transmitted, occurring in a few countries in Western Africa, Europe, and India (11-13) (hiv.lanl.gov).

HIV-1 infection is characterized by high levels of genetic diversity due to error-prone proofreading by the viral polymerase, high generation rate of viral particles, recombination, and hypermutagenesis induced by APOBEC3G (12-14). HIV-1 exists as 3 distinct genetic groups: M (major), O (outlier), and N (non-M or O) (Fig. 1.1). The M group consists of over 95% of global viral isolates and consists of at least 12 distinct phylogenetically associated subtypes or clades (A1, A2, B, C, D, E, F1, F2, G, H, J, and K) based on sequences of complete viral genomes (12-13). These clades represent different lineages of HIV, and have different geographical distributions. HIV isolates within a clade may exhibit nucleotide distances of up to 30%; interclade genetic variation can range between 30-40% depending on the gene analyzed (12-13). Furthermore, all retroviruses have a propensity to recombine, and in HIV-1 group M viruses this propensity has resulted in at least 46 circulating recombinant forms (CRFs) that arose due to infection of a single individual infected with 2 clades. Clade C viruses represent more than 50% of infections worldwide and are most prevalent in sub-Saharan Africa, China,

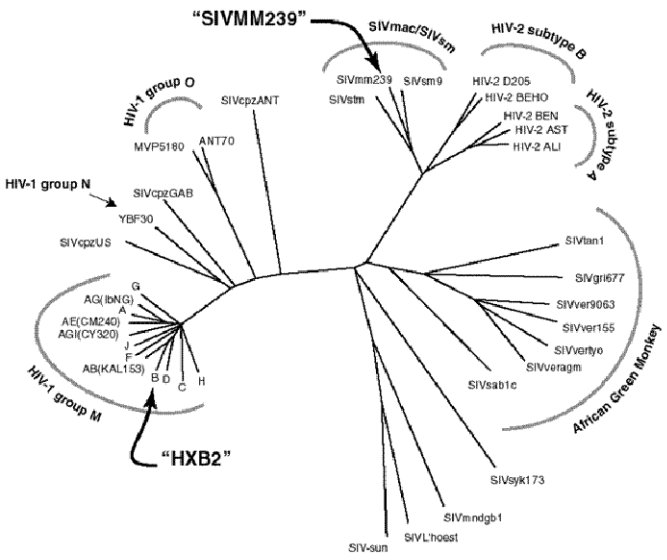

Figure 1.1 Phylogenetic analysis of HIV and SIV sequences from LANL.
A neighbor-joining phylogenetic tree was constructed to examine relationships between HIV and SIV sequences in the LANL database (hiv.lanl.gov). Groups are indicated with curved lines. Type sequences (HXB2 for HIV, SIVMM239 for SIV, are shown in bold type. Adapted from (Calef et al 2005) (8).

and India. Clade B viruses are most prevalent in western Europe, the Americas, and Oceania (12-13) (UNAIDS 2010) and are the most frequently studied clade.

Clinical Course of HIV infection

CD4+ T cells, macrophages, and other cells of the monocyte lineage are key targets of HIV infection. HIV is transmitted either by mucosal exposure during sex or breast feeding, or by direct blood-to-blood contact. The clinical course of HIV infection is characterized by an acute infection with high levels of viremia and irreversible damage to the immune system, in particular the gut-associated lymphoid tissue (GALT). This is followed by a chronic phase with persistent immune activation and slow depletion of CD4+ T cells, ultimately resulting in the progressive immune exhaustion and profound immunodeficiency that define AIDS (Fig. 1.2) (13, 16-18). The acute stage of HIV infection, which lasts from1-3 weeks post-exposure, is characterized by a peak in

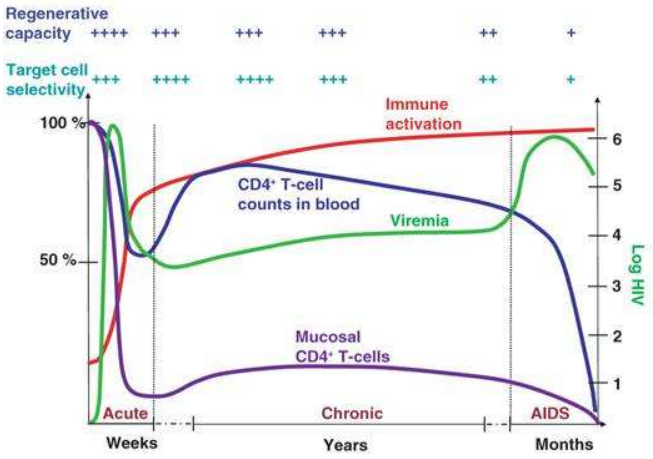

Figure 1.2. The clinical course of HIV infection. Changes in mucosal and blood CD4+T cell numbers and in viremia levels over the course of HIV infection are shown schematically in relation to changes in the relative level of immune activation. During acute infection, mucosal T cells (purple) drop, viremia (green) rapidly rises to a maximum peak, and CD4+ T cell counts (blue) decline sharply at first but then begin to rise to a moderately subnormal level. In the chronic phase, immune activation slowly increases (red). Mucosal CD4+ T cell numbers remain low, CD4+ T cell count slowly declines, and viremia rises. As overt AIDS is approached, changes seen in the chronic phase accelerate. Over the course of the chronic phase and into AIDS, the regenerative capacity of the immune system is destroyed (+++ to +), and target cell selectivity drops (++++ to +). Adapted from (van Marle et al 2005) (15).

viral replication and a dramatic decline in CD4+ T cells. CCR5+ CD4+ memory T cells are depleted from mucosal effector sites due to direct infection, bystander effects, and immune activation (17, 19). There is massive depletion of lamina propria CD4+ T cells in the first 3-6 weeks after transmission, and this cell loss is constant throughout the chronic stage of infection. After this peak in viremia, plasma RNA levels decrease over a 4-5 month period and CD4+ T cells subsets partially recover, though not to pre-infection levels (18, 20-21).

In the weeks to months after acute HIV infection, most individuals enter a clinically asymptomatic period characterized by low viremia (viral setpoint) and seroconversion. This chronic stage then lasts for approximately 10 years (17-18). During this time, steady-state viremia is fueled by rapid and continuous infection of target cells. Viral loads remains relatively constant in a given patient over a long period as equilibrium is reached between viral production and viral clearance. In reservoirs such as lymphoid tissue, there is a sharp decline in frequency of productively infected cells. Germinal center formation within lymphoid follicles becomes pronounced, and viral RNA corresponding to extracellular virions complexed with antibody and complement is detected in the network of follicular dendritic cell (FDC) processes. The massive numbers of virions trapped within the FDC network as well as latently infected cells (which harbor proviral DNA but do not express viral proteins) represent potentially continuous sources of virus for *de novo* infection of CD4+ T lymphocytes that are resident in or migrating through lymphoid tissues. Moreover, activation signals such as those delivered by proinflammatory cytokines, which are found in abundance within activated lymph nodes, are potent inducers of HIV replication in latently infected cells.

Lymphoid tissue remains the most important reservoir of systemic HIV infection throughout the course of disease. Thus, viral replication continues in the lymphoid compartment, and transient peaks in viremia may be detected throughout this period (17-18, 21).

During the course of the chronic stage of infection, there is a slow but steady decline in CD4+ lymphocytes and resulting impairment of the immune system. CD4+ T cells counts are an excellent marker of degree of immunodeficiency and can determine the immediate risk of opportunistic infections and other AIDS-related complications (17). Disease progression results in destruction of lymph node architecture as a consequence of viral replication and chronic immune activation. This leads to an increase in virus diffusion to surrounding CD4+ T-cells and favors HIV-1 spread within the local, regional and systemic lymphoid environment. Particularly at this stage, HIV infection is associated with an extensive replication in the gut lamina propria and submucosa and in draining lymph nodes, with local depletion of CD4+ T-cells (18, 21).

In the absence of virus containment, CD4+ T cell counts decrease below 200 cell/μl of blood, resulting in loss of cell-mediated immune responses and allowing ubiquitous environmental organisms with limited virulence to become life-threatening pathogens. The average time from infection to progression of AIDS is extremely variable, but is estimated to be on average 11 years (18). Incidence of AIDS-defining illnesses in industrialized nations has decreased sharply since 1996 due to highly active antiretroviral therapy (HAART) and improved access to health care (17).

Host Immune Responses to HIV infection

HIV infection is characterized by chronic immune activation and progressive depletion of CD4+ T cells, leading to immune system dysfunction and development of opportunistic infections and cancers that define AIDS (22). The level of chronic immune activation correlates with virus load and clinical outcome, with high immune activation associated with high viral loads and more rapid progression to AIDS and death (23).

HIV infection in humans is closely related to SIV infection in nonhuman primates. More than 40 species of nonhuman primates are endemically infected with species-specific SIVs, but unlike HIV, SIVs do not induce immunodeficiencies in their natural hosts. Differences that have been proposed to contribute to the lack of disease progression in SIV infection include preservation of healthy levels of peripheral CD4+ T cells and mucosal immunity, prevention of microbial translocation, maintenance of normal lymph node architecture and function, preferential sparing of central memory CD4+ T cells from infection, and lack of chronic immune activation (11).

One of the major challenges associated with HIV infection is that the correlates of protective immunity are not understood. During acute HIV-1 infection, there is a burst of inflammatory cytokines promoting cellular activation and potentially inducing proliferation of CD4+ T cell targets, which would fuel viral replication (24). During the transition from acute to chronic stages of HIV-1 infection, CD8+ cytotoxic T lymphocyte (CTL) responses correlate with an initial decline in virus replication. However, despite this decline in HIV-1 viremia, the majority of HIV-infected individuals are unable to control virus replication below the level of detection without antiretroviral therapy. Classic MHC class I-restricted, HIV-specific CTL responses have been demonstrated

against a variety of HIV proteins, including core proteins, reverse trancriptase (RT), Env, and regulatory proteins. In particular, a large body of evidence suggests that Gag-directed responses are immunodominant in chronic HIV infection and are associated with low viral loads (17, 25). CD4+ T cells, a major target of HIV infection, contribute to maintenance of host immunity by facilitating CTL and antibody response (26). Natural killer (NK) cells also contribute to the control of HIV-1 infection through clearance of infected cells via recognition of virally infected cells by activating and inhibitory killer immunoglobulin-like receptors (KIRs) and mediating antibody-dependent cellular cytotoxicity (ADCC) (27-28).

The initial antibody response appears at roughly two weeks post-exposure and is directed towards nonneutralizing epitopes on the envelope glycoprotein (Env) gp41 subunit. This response is followed within weeks by antibodies directed against the Env gp120 subunit and capsid (CA, p24) (17, 28-29). Neutralizing antibody (nAb) responses that block HIV infection of transmitted and early viruses are delayed, rising months after infection (28). NAbs may be type-specific (i.e. specific for one viral isolate) or broadly neutralizing (i.e. specific for a broad range of viral isolates), which are rare. NAbs are detected in circulation within the first year, but in most patients nAb responses lag behind viral escape and are generally not associated with control of viremia (17, 28, 30).

HIV infection is associated with increased expression of proinflammatory cytokines (including TNF-α IL-1β, and IL-6) secreted by PBMCs and macrophages. These cytokines are found at elevated levels in plasma, cerebral spinal fluid (CSF), and tissues. Chronically infected T cells and macrophages in lymphoid tissues also produce IFN-γ and IL-10. Disease progression is characterized by loss of the ability to produce

immunoregulatory cytokines such as IL-2 and IL-12, which are critical for effective cell mediated immune responses and required to stimulate proliferation and lytic activity of CTLs and NK cells (17).

During late stage infection, a decline in HIV-specific CTL activity correlates with disease progression. This loss of HIV-specific CTL activity is the result of downregulation of MHC class I molecules necessary for CTL recognition by viral proteins Tat, Nef, and Vpu (13, 17, 31) and loss of the IL-2 receptor (CD25) required for proliferation due to clonal exhaustion from high levels of viral antigens (17, 25). CD4+ T cells also develop an abnormal phenotype, characterized by loss of the CD25 marker and resulting in bystander apoptosis and clonal exhaustion or anergy (17, 32). Monocyte and macrophage dysfunction due to chronic immune activation can contribute to T cell dysfunction and results in impaired defenses against intracellular parasites (17).

The introduction of antiretroviral therapy (ART) has led to improved outcomes for individuals with HIV infection. A reduction in HIV viral replication is followed by recovery of CD4+ T cell lymphocyte numbers, at least partial restoration of overall immune function, and a reduction in the frequency of opportunistic infection. This process is known as immune reconstitution. However, some individuals on ART experience a clinical deterioration, termed immune reconstitution inflammatory syndrome, despite apparent virological and immunological response to therapy (33).

HIV Virus

Viral Genome Organization

HIV and SIV are members of the *Lentivirus* genus of the *Retroviridae* family, which are characterized by the ability to reverse transcribe RNA into DNA during viral replication. The retrovirus genome is composed of two identical copies of a positive-sense, single-stranded RNA molecule noncovalently linked near the 5' ends. The genomic RNA encodes the group-specific antigen (*gag)*, polymerase (*pol*), and envelope (*env*) structural genes, flanked by long terminal repeat (LTR) regions, and a complex combination of type-specific regulatory and accessory genes. The three primary structural gene products are initially synthesized as polyprotein precursors, which are subsequently processed by viral or cellular proteases into viral proteins (Fig. 1.3). Gag is cleaved into the matrix (MA), capsid (CA), nucleocapsid (NC), and p6 proteins. The Gag-Pol polyprotein is autocatalyzed into the protease (PR), reverse transcriptase (RT), and integrase (IN) proteins. Env is cleaved into the gp120 surface and gp41 transmembrane glycoproteins, which remain associated via noncovalent interactions. The remaining 6 HIV-1 encoded proteins (Vif, Vpr, Tat, Rev, Vpu, and Nef) are primary translation products of spliced mRNAs. In addition to gene products, the retroviral genome also contains structural regulatory motifs, such as the trans-active response element (TAR) and Rev response element (RRE), which are required for transcription and export of non-spliced and partially spliced viral mRNAs to the cytoplasm (13, 18, 34-35).

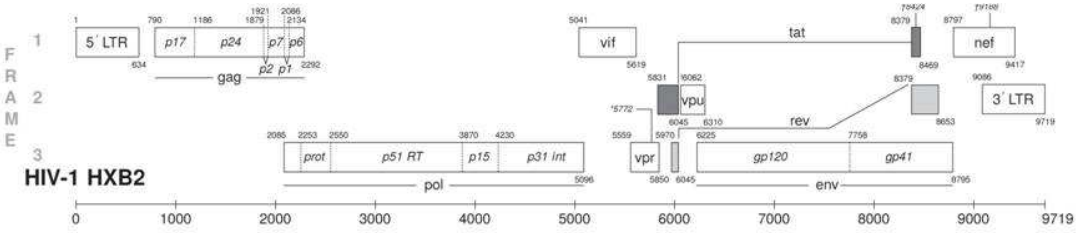

Figure 1.3. HIV-1 genome organization.
The ~9.7 kb HIV-1 genome encodes *gag*, *pol*, and *env* genes flanked by long terminal repeat (LTR) regions, and a number of accessory genes (*vif*, *vpu*, *vpr*, *rev*, *tat*, and *nef*) in 3 open reading frames. Numbering is relative to reference sequence HXB2. Adapted from (HIV Sequence Compendium, 2005).

HIV Life Cycle

HIV-1 is an enveloped retrovirus with a distinct cone-shaped core composed of CA (p24), which encases the viral genome (Fig. 1.4). Inside the core, the genome is bound to NC and complexed with IN and RT. The capsid is surrounded by a layer of MA (p17) proteins, which are anchored to the outer viral membrane, a lipid bilayer that includes trimeric Env spikes formed by the gp120 and gp41 subunits. The bilayer may also incorporate host cell membrane proteins during the budding process, including HLA class I and II proteins and adhesion proteins such as ICAM-1. Additional viral proteins, including p6, Vpr, and PR, and numerous cellular proteins, including cyclophilin A and APOBEC3G, are also incorporated into the viral particle (13, 18, 34, 36-37).

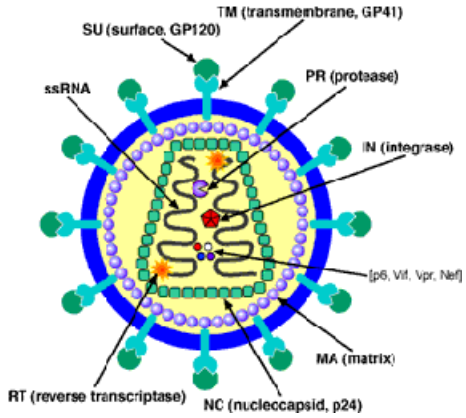

Figure 1.4. Organization of the HIV-1 virion.
HIV-1 virions consist of a conical core of capsid containing two copies of the RNA genome bound to nucleocapsid, and complexed with integrase and reverse transcriptase. The core is surrounded by matrix protein and is bound by a lipid envelope containing heterodimeric trimers of the Env transmembrane subunit (gp41) non-covalently attached to the surface subunit (gp120). Adapted from (http://www.brookscole.com/).

The HIV life cycle begins when gp120 binds to CD4 on the cell surface, triggering a cascade of conformational changes that result in fusion between the viral and host cell membranes (described in more detail later) (Fig.1.5). Following entry, the core is released into the cytoplasm, where partial uncoating occurs (18, 37-38). RT then converts the viral RNA into linear double-stranded viral DNA (13). The viral DNA is assembled along with cellular and viral proteins including MA, IN, and RT into a large nucleoprotein complex (preintegration complex, or PIC). Following dissolution of the partial CA core, the PIC is trafficked from the host cell periphery into the nucleus through the nuclear pore complex. The viral DNA is then integrated into the host cell genome by IN, which cleaves nucleotides of each of the 3' ends of the double helix DNA and transfers the modified provirus DNA into the host genome in a sequence-independent manner (13, 38-40). Following activation of the host cell, the RNA polymerase II holoenzyme is recruited to the LTR to transcribe proviral DNA into mRNA, initially resulting in early synthesis of regulatory proteins Tat, Nef, and Rev. Tat binds to the TAR site at the 5' end of the HIV RNA and stimulates transcription and formation of longer RNA transcripts. Nef activates viral transcription by inducing transcription factors that transactivate the LTR. Rev binds to the RRE and facilitates transcription of longer RNA transcripts, expression of structural and enzymatic genes, and inhibits production of regulatory proteins, thereby promoting formation of mature viral particles. Spliced and unspliced viral mRNA migrates into the cytoplasm, where structural proteins are produced (13, 31, 34, 38). The uncleaved Gag polyproteins are the major viral structural proteins and direct several activities necessary for viral particle formation. MA is responsible for targeting polyproteins and recruited essential viral components (including

the RNA genome and Env) to the viral assembly site located at the plasma membrane, while CA and NC drive multimerization and encapsidation of the viral genome. This immature particle migrates to the cell surface, where the Gag and Gag-Pol polyproteins are cleaved by PR, resulting in rearrangement of the virion and creating mature, infectious virus particles. P6 recruits the ESCRT complex (endosomal sorting complex required for transport) to mediate scission of the nascent budding virion from the host cell, where it acquires a lipid envelope containing the Env trimeric spikes (13, 36, 38, 41).

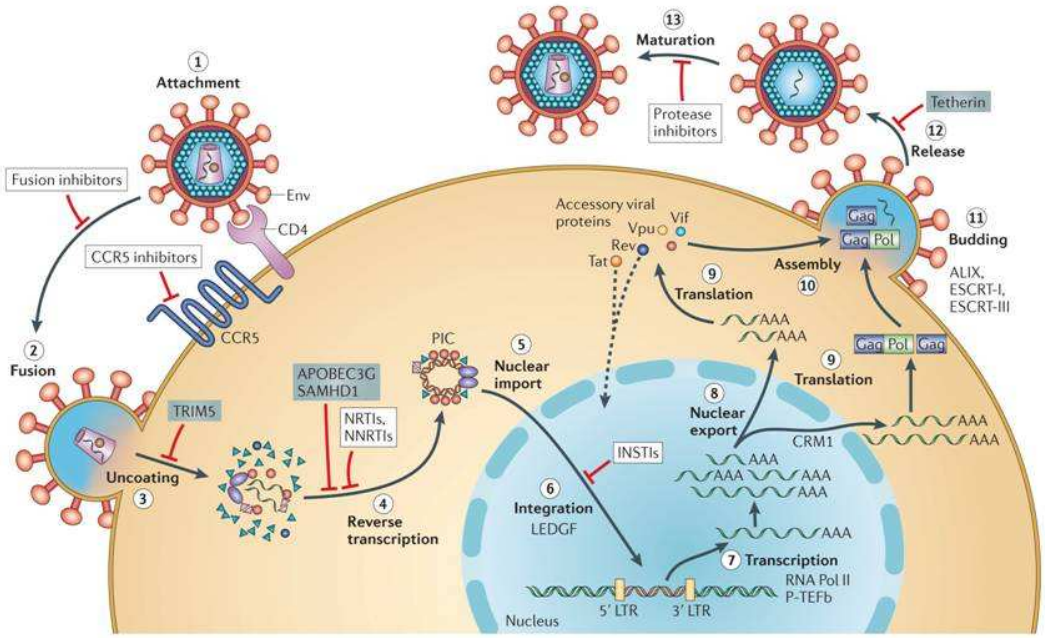

Figure 1.5. The HIV Life Cycle.
Steps in the HIV-1 replication cycle are shown in the context of the host cell and are described in the text. Adapted from (Engelman & Cherepanov 2012) (38).

During the HIV life cycle, the accessory proteins Vpu, Vif, Vpr, and Nef optimize viral replication. Vpu counteracts the type II transmembrane protein tethrin (CD317 or BST2), which inhibits release of budding particles by retaining them at the plasma membrane. Vif enhances viral infectivity by degrading the cellular antiviral factor

APOBEC3G. Vpr is part of the PIC and is involved in transport through the nuclear pore complex. Vpr also enhances replication by arresting infected cells in the G2 phase of the life cycle, and stimulates replication in MDM. Nef is a multifunctional protein with many roles during the HIV life cycle, including downregulation of CD4 and MHC class I, modulation of cellular signaling pathways, and enhancement of viral infectivity and replication (13, 31, 38, 42).

HIV Envelope Glycoprotein

HIV Env Synthesis and Processing

The HIV envelope glycoprotein (Env) is synthesized from a singly spliced 4.3-kb Vpu/Env bicistronic mRNA. The 160-kd polyprotein precursor is a type 1 integral membrane protein, which is anchored to cell membranes by a hydrophobic stop-transfer signal. The amino-terminal segment of the mRNA contains a short, hydrophobic signal peptide, which is recognized by the cellular signal recognition particle (SRP) and inserted into the bilayer of the rough endoplasmic reticulum (rER). Following translocation across the rER membrane, the signal peptide is cleaved by a cellular protease and gp160 is glycosylated. Env, particularly gp120, is heavily glycosylated, with half its molecular weight composed of oligosaccharide side chains. The sites of covalent attachment are Asn for N-linked sugars, at an Asn-x-Ser/Thr sequence, where x is any amino acid except Pro. These oligosaccharides are then processed, with the glucose removed to form high-mannose chains. In addition to the attachment of N-linked glycans, HIV Envs may also be modified with O-linked (or mucin-type) carbohydrates attached to the hydroxyl group of Ser and/or Thr (13, 43-44). Following modification, gp160 rapidly associates with host chaperone BiP/GRP78, forms disulfide bonds, and undergoes oligomerization. The

predominant oligomeric form is a trimer. As the ribosome approaches the end of the mRNA, the emergence of a long, hydrophobic amino acid sequence prevents the Env polyprotein from being released into the rER lumen. The amino acids following this membrane anchor extend into the cytosolic space and form the gp41 cytoplasmic tail (CT).

Gp160 is then transported to the Golgi, where it is proteolytically cleaved by furin or a furin-like protease following the sequence Arg-x-Lys/Arg-Arg to release the mature gp120 surface and gp41 transmembrane subunits. This cleavage is required for Env-induced fusion activity and infectivity. Subsequent to cleavage, gp120 and gp41 form a noncovalent association that is critical for transport of the Env complex from the Golgi to the cell surface, where it is incorporated into viral particles. Env on the cell surface is rapidly internalized unless stabilized by Pr^{55}Gag though a Tyr-x-x-Leu (YXXL) sequence in the gp41 CT. The YXXL motif interacts with clathrin adapter complexes, and is important for controlling Env expression levels on the cell surface (13, 44-45).

Sequence and Structure of HIV Env

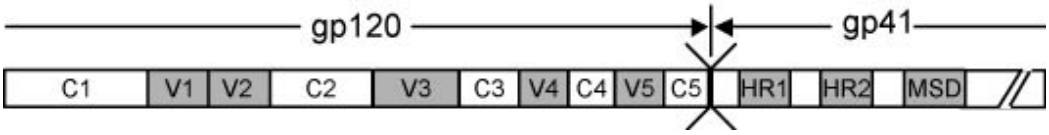

Figure 1.6. Organization of HIV-1 envelope glycoproteins.
HIV Env is translated as polyprotein precursor gp160 and cleaved by cellular proteases into surface subunit gp120 and transmembrane subunit gp41. C, conserved region. V, variable region. HR, heptad repeat region. MSD, membrane-spanning domain.

HIV Env consists of a surface-exposed gp120 and a transmembrane gp41 subunit (Fig. 1.6) (9). The gp120 subunit is approximately 550 amino acids in length and contains an average of 25 N-linked glycosylation motifs. Gp120 sequences are composed of five alternating conserved (C1 to C5) and variable (V1 to V5) regions. The conserved regions comprise the protein core, which contains an inner and an outer domain based on their orientation to the trimer axis (Fig. 1.7). The gp120 core outer domain is heavily glycosylated. This "glycan shield" is important for maintaining Env structure, providing protection against cellular proteases, and occluding receptor binding sites and neutralization epitopes (46). Intramolecular disulfide bonds result in arrangement of the first four variable regions into surface-exposed loops that extend from the core and partially occlude the coreceptor-binding site and neutralization epitopes (10, 47-49). The gp41 N-terminus (ectodomain) contains the fusion peptide, a domain of hydrophobic residues which inserts into the target cell membrane. There are 2 heptad repeat regions (HR1 and HR2), which are alpha-helical domains that form stable trimeric coiled-coils during membrane fusion (50-51). The gp41 subunit had a long cytoplasmic tail, which contains intracellular targeting signals and interacts with MA to allow efficient Env incorporation into virions (50). Residues

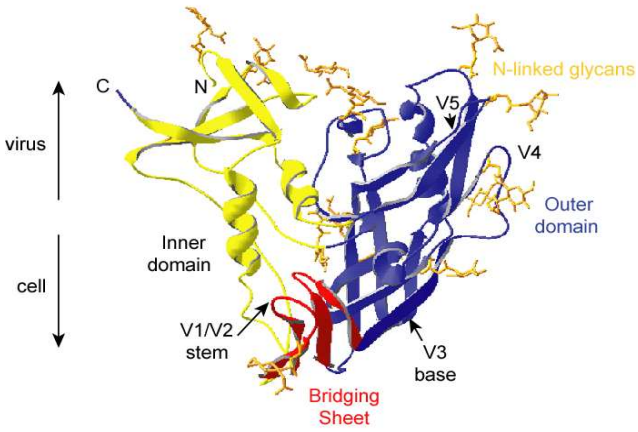

Figure 1.7. HIV gp120 core structure. Structure of HIV gp120 from the HXB2 gp120-CD4-mAb 17b complex crystal structure (1G9N) (Wyatt et al., 1998). Inner and outer domains are based on their relative orientation to the trimer axis. The orientation of gp120 relative to the viral membrane is indicated on the left N-linked glycans are shown on the outer domain. Adapted from (Wyatt et al 1998) (10).

identified as important contact points between gp120 and gp41 are located in the gp120 N-terminus, C2, and C4 regions and the gp41 N-terminus, HR2, membrane-spanning domain (MSD), and C-terminus (52-59).

HIV Env is organized into trimers on the surface of virions and infected cells, with the gp120 and gp41 subunits of each monomer remaining associated through noncovalent interactions (Fig. 1.8). In the CD4-bound state, two β-hairpins that extend from the inner domain (strands β2–β3) and outer domain (β20–β21) come together to form a four-stranded "bridging sheet" minidomain (3, 60). In contrast, a crystal structure of an unliganded SIV Env showed that in the unliganded core, neither the CD4 nor coreceptor binding sites were properly formed (Fig. 1.9). In this structure, the CD4-binding loop projected away from the center of the outer domain, with the β20-β21 ribbon tucked beneath it (3). The α-helices of the inner domain, the CD4-binding loop, and the β20-β21 ribbon created a long, narrow cavity lined principally with hydrophobic side chains (3). It was proposed that following CD4-binding to a face of the outer domain partly concealed within this cavity, the bridging sheet would close up to create the coreceptor binding site, flanked by the V1/V2 and V3 loops (3).

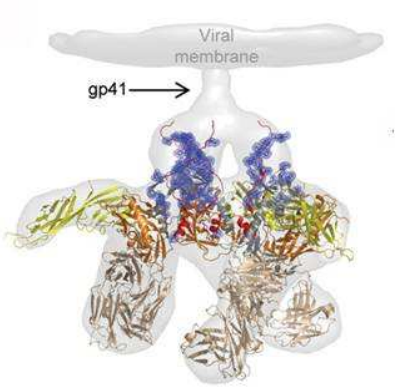

Figure 1.8. 3D structure of the HIV Env spike. Placement of the gp120-CD4-Fab 17b complex in the electron density map derived from cryoelectron tomography (light gray), with gp120 and residues involved in gp41 interactions colored in blue (balls and sticks), and Fab 17b in light brown. Adapted from (Pancera et al. 2010) (2).

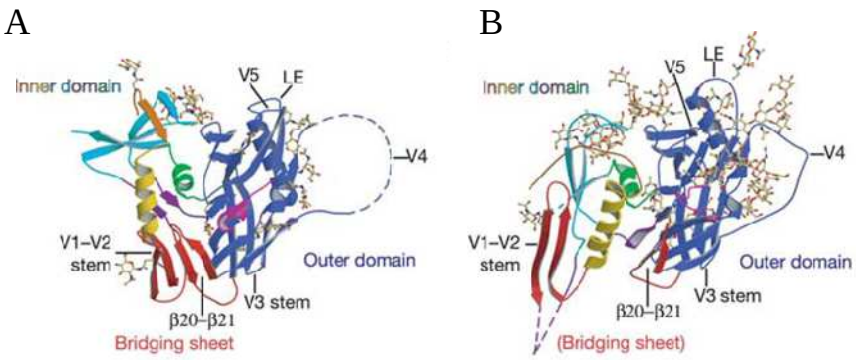

Figure 1.9. Crystal structure of liganded HIV and unliganded SIV gp120.
A) Conformation of the deglycosylated HIV gp120 core, complexed with CD4 and the Fab fragment of 17b, with the outer domain on the right and the inner domain on the left. CD4 and Fab have been omitted for clarity. Twelve disordered V4-loop residues are shown as a dashed line. Outer domain is in blue; inner domain, colored according to substructure (N terminus, orange; α1, yellow; three-strand sheet, cyan; outer/inner domain transition, purple; α5, green; bridging sheet, red). B) SIV gp120 core structure, in the same view and colors as (A). Adapted from (Chen et al. 2005) (3).

Recent mapping of ligand-induced changes in CD4-bound and unliganded HIV Env crystal structures revealed extensive conformational movement for these β-hairpin ribbons of the bridging sheet structure and much less movement for the outer domain. Quantification of these changes showed that the outer domain moved on average only ~2 Å, the inner domain ~ 4 Å, and the bridging sheet residues ~ 10 Å. These results suggested that the unliganded HIV gp120 core more closely resembled the CD4-bound state than the SIV unliganded Env (60).

Data from thermodynamic studies of gp120 binding to CD4 and to a number of CD4 binding-site antibodies, and from the SIV unliganded gp120 core structure, suggested that the structure of unliganded HIV-1 gp120 would be substantially different from the CD4-bound conformation. However, conformation-dependent ligands, including

CD4 and monoclonal antibodies (mAb) 17b, b12, b13, F105, and other antibodies that recognize non–CD4 bound conformations of gp120, recognized the unliganded Env constructs. These results suggest that ligand binding is not required for Env to obtain the CD4-bound conformation (60). However, these crystal studies rely on gp120 core structures that have the first three variable loops and parts of the gp120 core, including but not limited to the N- and C-termini, removed, possibly resulting in adoption of conformations that may not exist in the native trimer. Moreover, a number of biochemical studies have suggested that unliganded Env continuously samples different conformational states (53, 61-62), suggesting that gp120 core structures used for crystallization adopt the most energetically favorable of any number of possible conformations.

Although there are no high resolution structures of gp41, assumptions can be made based on structural and functional studies. Data support a trimeric model of gp41 in which the prehairpin intermediate state exists as a parallel trimer of fully-extended ectodomains between the HIV membrane and the fusion peptide inserted into the target cell membrane. There is also evidence for the final six-helix bundle (6HB) N-helix-turn-C-helix hairpin structure (63). Experimental evidence indicates that the membrane proximal external region (MPER), which is composed of the conserved cysteine-bound loop between HR1 and HR2 and a conserved region N-terminal to the MSD are surface exposed, as this region contains epitopes for antibodies directed against HIV (3, 64-66).

Recent cryoelectron tomographic studies of several HIV-1 and SIV strains have provided insights into the molecular architectures of trimeric Env displayed on native virions in unliganded, antibody-bound, and CD4-liganded states at resolutions of

approximately 20 *Å* (Fig. 1.10). These analyses have established that trimeric Env from HIV-1 undergoes a large structural transition from a "closed" unliganded state to an "open" liganded state when complexed to CD4 and 17b (Fig. 1.11). This appears to be coupled with a rearrangement of the gp41 region along the central axis of the trimer, leading to closer contact between the viral and target cell membranes. This quaternary structural change involves rotation of each gp120 protomer by about 45° around an axis parallel to the central threefold axis, coupled with an out-of-plane rotation of about 15°. In some strains, such as SIV CP-MAC, trimeric Env is already present in this open conformation even in the absence of soluble CD4 (sCD4), providing an explanation for CD4-independent viral entry by this strain (9, 67). Interestingly, these trimeric structures suggest that the gp120 V1/V2 and V3 loops come together to form the apex of the trimeric structure. This is supported by studies suggesting that V1/V2 and V3 participate in epitope masking in the trimeric structure. However, conflict exists over whether this epitope masking occurs on the same protomer (*cis* masking) or interprotomer (*trans* masking). The trimeric structures, however, seem to support a model of *trans* masking, with V1/V2 loops from one protomer making contacts with the V3 loop on a neighboring protomer within the trimer structure (55, 68-70). This issue remains to be elucidated by further structural modeling and functional studies.

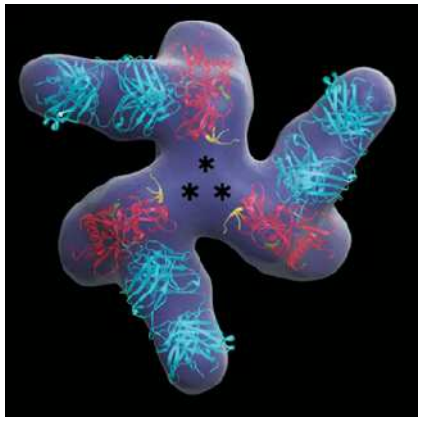

Figure 1.10. 3D representation of the HIV Env trimer.
Density map of structure of the HIV Env glycoprotein trimer spike. Monomeric CD4-liganded crystal structure is fit onto the model, with gp120 shown in red, and 17b Fab fragment in blue. Likely locations of V1/V2 loops and gp41 are indicated by asterisks. Adapted from (Liu et al. 2008) (9).

A

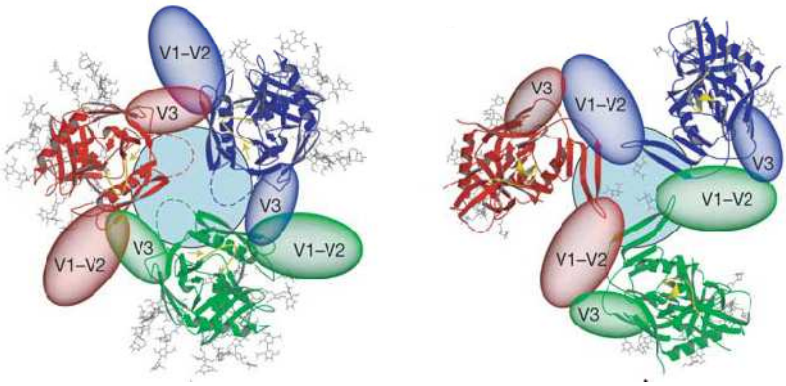

B

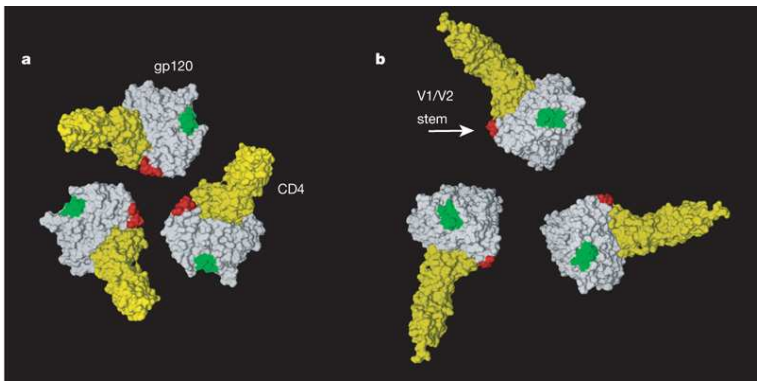

Figure 1.11. Changes in gp120 in Env trimer induced by CD4-binding.
A) SIV Env trimer modeled in the unliganded conformation (left panel) and CD4-bound conformation (right panel), viewed along the three-fold axis from outside the virion towards gp41. The polypeptide chain backbones are in ribbon representation; N-linked glycans are stick models; deleted V1–V2 and V3 segments are transparent balloons. The three monomers are in red, green and blue, respectively; the sugars, in grey. gp41 is shown as a circle in the rear. Adapted from (Chen et al 2005) (3). B) Model for the conformational change from the unliganded (left panel) to the CD4-bound state (right panel) shown as top view. The gp120 core, CD4, V1/V2 and V3 stems are shown in white, yellow, red and green, respectively. Adapted from (Liu et al 2008) (9).

HIV Fusion and Entry

HIV entry into cells is initiated by a high affinity interaction between gp120 and CD4 (Fig. 1.12). CD4 binding induces conformational changes in gp120 that involve rearrangements of the hypervariable loops and formation and exposure of the coreceptor binding site (71-72). In addition to gp120 rearrangements, the gp41 HR1 and HR2

domains are exposed and arrange into the prehairpin conformation. These conformational rearrangements are detected by exposure of the coreceptor-binding site following CD4-binding, and by reactivity of the CD4-bound Env with antibodies and synthetic peptides against the gp41 HR domains (72). CD4-induced conformational changes vary depending on experimental conditions and HIV isolates. Higher CD4 binding affinity from HIV strains adapted to grow on immortalized T-cell lines (lab-adapted isolates) results in greater HR1/HR2 exposure compared to primary isolates, which may require CCR5 binding to fully expose these regions. Pretreatment with high concentrations of sCD4 at physiological temperatures render virus noninfectious, proceeding through a transient activation of Env followed by irreversible loss of function. This may be associated with the observation that CD4 binding *in vitro* facilitates dissociation of gp120 from gp41, a phenomenon referred to as soluble gp120 (sgp120) shedding. It remains controversial whether gp120 needs to be shed from gp41 in order to trigger fusion (72). There are suggestions that sgp120 shedding may be required to overcome the large activation energy barrier at the post-coreceptor binding stage, thereby relieving restriction of gp41 refolding (61, 72).

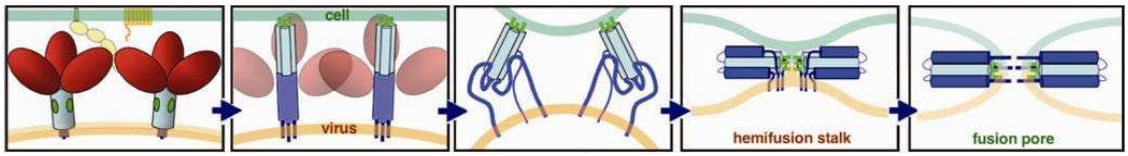

Figure 1.12. HIV Fusion with the Target Cell Membrane.
Steps in the membrane fusion process are shown with the viral membrane on the bottom and the target cell membrane on the top. Steps are described in detail in the text. Adapted from (Frey et al 2008) (1).

Current models suggest that formation of Env-CD4-coreceptor complexes leads to exposure of the gp41 fusion peptide, which interacts with the target cell membrane. The

pre-hairpin structure has a relatively long half-life and is a target for inhibitory peptides and neutralizing antibodies directed against HR1 and MPER. The pre-hairpin refolds into the final 6HB core structure consisting of the trimeric coiled coil. It is this transition that catalyzes membrane fusion by inserting the fusion peptide into the target cell membrane. Fusion progresses through a hemifusion intermediate, defined as a merger of contacting leaflets of 2 bilayers with their distal leaflets by forming a shared bilayer. Hemifusion is manifested by lipid mixing between virus and target cell membranes. There is conflicting evidence of whether the prehairpin intermediate or 6HB are implicated in pore formation, though there is experimental evidence that the energy released during gp41 refolding may be used to overcome the kinetic barrier, which is underlined by the high thermostability of the gp41 core structures (65, 72). The fusion pore is then enlarged, allowing the HIV core to enter the target cell (65, 72).

HIV Cellular Tropism

HIV infects CD4+ T cells and cells of the macrophage lineage through interaction of Env with CD4 and a chemokine coreceptor, typically CCR5 or CXCR4. CCR5 is expressed on memory T cells and cells of the macrophage lineage, and CXCR4 is expressed on naïve T cells [10-13]. Dual-tropic (R5X4) viruses can use either receptor for entry. The majority of transmitted viruses are CCR5-tropic (R5), and these R5 isolates remain throughout the course of infection. CXCR4-tropic (X4) isolates emerge during the late stages of disease in about 50% of individuals, and their emergence is typically associated with rapid disease progression (73-74). In addition, a variety of other coreceptors (CCR2, CCR3, CCR8, Apj, STRL33/BONZO/CXCR6, Gpr1, Gpr15/BOB,

CX_3CR1, ChemR23, RDC-1, and D6) may support entry of a subset of HIV isolates *in vitro*, but usage of coreceptors other than CCR5 or CXCR4 *in vivo* is rare (71, 75-77).

Cells of the macrophage lineage are primary infected by R5 HIV, but CCR5 usage alone is not necessary or sufficient for macrophage tropism (M-tropism) and X4 and R5X4 M-tropic isolates have been described (78-80) Receptor density also influences HIV infection of macrophages (81-82). Macrophages and microglia express lower cell surface levels of CD4 than CD4+ T cells in peripheral blood (83-84). The low levels of CD4 expressed on macrophages/microglia restrict infection by HIV strains with high dependence on CD4 for entry (85).

Neuropathogenesis of HIV/AIDS

Epidemiology of CNS Infection

HIV infection of the central nervous system (CNS) can cause neurological disorders, including HIV-associated dementia (HAD) and other neurological disorders, collectively termed HIV-associated neurocognitive disorders (HAND) (86). Before the widespread use of highly active antiretroviral therapy (HAART), the annual incidence of HAD , the most severe form of HAND, after AIDS diagnosis was 7% and the cumulative risk over the lifetime of an HIV-infected individual was 5-20%, with some estimates up to 50% prior to death (15, 87-88). Less severe forms of HAND, including minor cognitive motor disorder (MCMD) and neuropsychological impairment, were found in 30-60% of people living with HIV/AIDS (15, 89).

HAART reduces HIV RNA levels in plasma and cerebrospinal fluid (CSF) and improves neurocognitive function, although most antiviral drugs have poor CNS penetration. Currently, it is thought that patients who initiate HAART and achieve plasma

and CSF viral suppression and use CSF-penetrating regimens accrue the most benefit (89). Although the incidence of HAD dropped significantly after the introduction of HAART, incidence rates began to rise in 2003, suggesting possible viral escape (87). At the same time, milder forms of HAND continue to persist, and autopsy studies have shown that over 90% of patients dying with AIDS manifest some type of neurological disease (15, 88-89). As the number of individuals living with HIV/AIDS on HAART rises, the prevalence of HAD is actually increasing (87), which may be due in part to the increased risk of developing HAD as patients age (90-91). Thus, neurocognitive impairment continues to be a common complication of HIV/AIDS (12).

HAD is most common with infection of HIV clade B viruses, and is therefore a more common complication in the Western world. While patients infected with clade C HIV do develop cognitive disorders, the severity may be less, and previous studies have reported that clade C viruses may exhibit reduced potential for neuroinvasion compared to clade B viruses, though larger studies are needed to verify these findings (12, 92-93). Furthermore, reduced diagnosis of HAD with clade C infection in some areas may be associated with the difficulties of reaching a diagnosis in resource-poor settings, and the decreased time to the development of complicating opportunistic infections (94). Regardless of these confounding issues, target cells infected with HIV have been detected in brain tissue from patients infected with clade C viruses, but without the markers of neuroinflammation, including multinucleated giant cells, associated with clade B infection (12, 92-93, 95). The differences in neuropathogenesis of clade B and C HIV viruses has been partly attributed to the viral protein Tat, with studies reporting that clade C Tat exhibits reduced ability to recruit macrophages, stimulate production of

proinflammatory cytokines, and induce neuronal toxicity *in vitro* compared to clade B Tat (12, 93, 96-98). Recent work has also demonstrated that the Env gp120 subunit from clade B HIV may induce production of neurotoxic factors *in vitro* at a higher level than gp120 from clade C, suggesting that Env may also play a role in the decreased neurovirulence associated with clade C HIV infection (97). Thus, genetic variation in HIV genes between clades may contribute to neurodegeneration.

Neuroinvasion

HIV enters the brain during acute infection or shortly thereafter, most likely through trafficking of infected lymphocytes and monocytes across the blood brain barrier (BBB), though it is not clear whether early entry leads to viral persistence (15, 88, 99). Early colonization of the CNS by HIV is supported by the detection of HIV DNA in pure populations of perivascular macrophages, parenchymal microglia, and astrocytes from brain tissue of untreated individuals who died in the presymptomatic stage of infection from non-HIV causes, as well as high levels of colonization, inflammation, and markers of BBB disruption in CSF during the early stages of HIV infection (100-101). Several models of HIV neuroinvasion have been proposed. First, the CNS may suffer from repeated transitory exposures of HIV via trafficked lymphocytes and monocytes, followed by immune-mediated virus clearance. Alternatively, the CNS may serve as a relatively autonomous reservoir of infection, producing virus locally and evolving independently from other loci of infection within the body (88, 99, 102-103). A third possibility is that during end-stage infection, as a consequence of immune activation or other systemic events, there is increased trafficking of blood-born monocytes into the

brain (99, 102-103), which may increase virus entry into the CNS and/or increase target cell availability for infection and virus replication within the CNS.

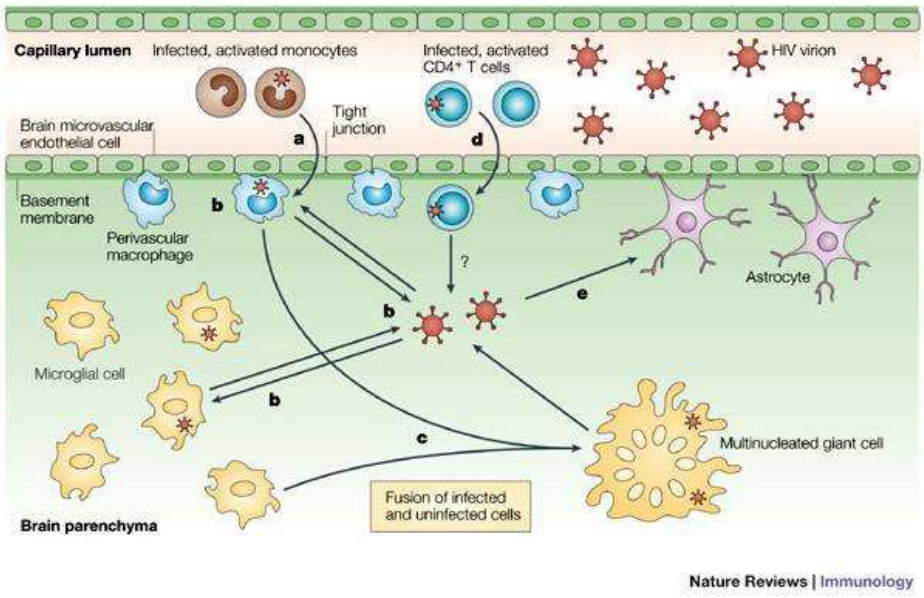

Figure 1.13. HIV Neuroinvasion.
HIV may enter the brain by the "Trojan horse" model pathway, in which HIV-infected monocytes and lymphocytes carry virus across the blood brain barrier. Once in the CNS, HIV-infected monocytes differentiate into perivascular macrophages. HIV released from these infected cells infects CNS resident cells, including macrophages, microglia, and astrocytes, leading to CNS viral persistence. Adapted from (Gonzalez-Scarano & Martin-Garcia 2005) (104).

To penetrate the CNS, HIV or HIV-infected cells must first cross the blood-brain barrier (BBB). The BBB is a selectively permeable, continuous cellular layer that consists of brain microvascular endothelial cells (BMVECs) linked to each other by tight junctions. These cells serve to regulate the traffic of cells and substances from the bloodstream to the CNS (104-106). Although a number of routes have been proposed for HIV entry across the BBB, the "Trojan horse" model is the most accepted. This model posits that infected monocytes transverse the BBB, where they differentiate into perivascular macrophages. Perivascular macrophages have a short half-life (30% in 90 days) and a high turnover rate, allowing for the potential of continuous delivery of new

HIV-infected cells to the CNS. This turnover can be greatly increased in inflammatory conditions, and HIV infected monocytes have been shown to cross the BBB more efficiently than noninfected monocytes. Studies have conclusively demonstrated that perivascular macrophages are the cell population most infected by HIV and SIV in the CNS, lending support to this model (15, 99, 104, 106).

HIV infection of the brain can contribute to further neuroinvasion by a number of mechanisms. BVMECs exposed to HIV up-regulate intracellular adhesion molecule 1 (ICAM-1) expression, which may facilitate leukocyte migration across the BBB. High levels of TNF-α, a proinflammatory cytokine secreted by HIV-infected macrophages, increases BBB permeability (107). Matrix metalloproteinases (MMPs), which are elevated in the CNS of HAD patients, can weaken basal membranes, facilitating leukocyte transport across the BBB (12). Finally, viral proteins, including HIV Env gp120 and Tat, have been shown to increase BBB permeability *in vitro* via a mechanism that is independent of viral replication (108-109). These mechanisms are especially important during the late stages of infection, when high peripheral viral loads and overall immunosuppression contribute to BBB breaches and macrophage trafficking of HIV into brain (12, 100, 102, 110).

HIV Target Cells in the CNS

Cells of the monocyte/macrophage lineage are the primary cells in the CNS that express CD4 and CCR5, and are the main target cells for productive HIV infection in brain. Although perivascular macrophages are the major reservoir of virus, resident microglia are also infected, particularly within areas of inflammation. Microglia have a

much lower turnover rate than macrophages (<1% over 90 days), and as terminally differentiated cells have a high level of CCR5 expression (83, 86, 104). However, M-tropic HIV Envs capable of using CXCR4 for entry have also been isolated from brain (78, 80, 111), suggesting that R5-tropism is not necessary for neurotropism.

HIV is occasionally found at low levels in other resident cell types within brain, including astrocytes and BVMECs, but HIV does not typically infect neurons. While astrocytes do express early, multiply spliced mRNAs, astrocyte infection is typically restricted and nonproductive due to defects at several stages of the virus life cycle that include viral entry, Rev-dependent transport of viral mRNAs into the cytoplasm, and translation (83). Therefore, while HIV infection of astrocytes is not likely to contribute to the viral load in the CNS, nonproductive infection impacts astrocyte function, which may affect neighboring cells or the BBB and contribute to the development of neurological complications (83, 112-114).

While most viruses isolated from the CNS are M-tropic, a recent study described a replicating population of R5-tropic T cell-tropic HIV viruses cloned from cerebral spinal fluid (CSF). While only low levels of HIV-infected CD4+ T cells have been identified in brain, it has been suggested that the presence of viral antigen during periods of increased HIV replication in CNS/CSF compartments could drive migration of both CD8+ and CD4 +T cells into the CNS/CSF. This may lead to persistence of compartmentalized virus through replication in CD4 T+ cells, resulting in the low numbers of cells detected in CSF and brain (90). Moreover, during late-stage disease, especially when complicated with other disease pathologies that could damage blood vessels or the BBB, viruses may leak at a higher rate from the blood vessels of the

meninges and accumulate in the tissues surrounding the brain, thereby increasing the likelihood for the migration of X4 viruses (6).

HIV Compartmentalization and Evolution in the CNS

A number of studies have analyzed paired HIV populations in blood and cerebral spinal fluid (CSF) during different stages of infection (115-120). CSF is an intermediate compartment between brain and the periphery, so viral populations in the CSF are genetically related to those in both compartments. Within 1 month of acute infection, similar populations were detected in blood and CSF. At later stages of disease, samples frequently demonstrate unique genetic variants in CSF compared to peripheral blood, implying the presence of genetic variants that evolved independently within CNS (83, 103). Moreover, CSF viral loads frequently correlate with the severity of HAD impairment in untreated patients (121). These results suggest that in the absence of treatment, high levels of viral replication contribute to BBB permeability, thereby permitting passage of virus between the CSF and brain.

The genetic evolution of HIV variants in brain is distinct from that in lymphoid tissues and other organs (83, 104, 111, 122-125). Phylogenetic reconstructions have shown clustering of sequences according to tissue of origin, indicating that CNS viruses from individuals are more closely related to each other than viruses originating from peripheral tissues (80, 111, 124, 126-129). Genetic compartmentalization of HIV within the brain suggests that selection and/or adaptive evolution may occur in the CNS in response to unique constraints of the brain microenvironment, including different target cell populations and immune selection pressures. Because many antiretroviral drugs have

poor CNS penetration, the CNS may serve as a sanctuary for HIV infection, and infected brain macrophages may comprise an important HIV reservoir during HAART (12). Furthermore, recent studies have suggested that HIV is capable of migrating out of brain via the meninges and reseeding the periphery, thereby potentially contributing to HAART resistance during late-stage AIDS (12, 102).

While macrophages and microglia are the primary target cells for HIV CNS infection, the ability to infect macrophages is not sufficient for neurovirulence and the presence of HIV in the CNS is not necessarily sufficient for cognitive impairment (130) (12, 15). HIV cloned from brain tissue of patients with HAD exhibit increased evidence of viral evolution and higher recombination rates compared to virus from patients without HAD (103). Consistent with this observation, certain HIV strains induce multinucleated giant cells or neuronal apoptosis *in vitro* in a manner that is independent of their replication capacities in macrophages and microglia (111, 123, 131-132). However, viral phenotypes that distinguish neurotropic and neurovirulent strains and increase risk of neurological disease are poorly understood.

Specific Env sequences, particularly in the gp120 V3 region, have been associated with brain compartmentalization (122-124, 132). Env sequences from AIDS patients with HAD are genetically and biologically distinct than those from patients without HAD (122-123, 125, 132-134), suggesting that particular Env variants may play an important role in CNS infections and the development of HAD. However, little is known about specific Env determinants that underlie that neurotropism and neurovirulence of HIV.

Mechanisms of HIV Neuropathogenesis

Although HIV infects the CNS during acute primary infection, the brain typically remains asymptomatic until after the development of immunosuppression and progression to AIDS (83, 104). HIV infection of the CNS is not sufficient for the development of neurological disorders. Factors that are thought to contribute to HIV neuropathogenesis include loss of immune control associated with disease progression, chronic immune activation, BBB abnormalities that allow increased trafficking of infected monocytes and T cells, and late emergence of viral variants that impact CNS disease progression (83, 122, 135-136).

Although the mechanisms by which HIV induces neurological damage are not well understood, several models have been proposed to explain how HIV infection contributes to neuronal injury. One model suggests that the release of soluble neurotoxic factors, including cytokines, chemokines, and small molecules such as nitric oxide, are produced by activated or infected macrophages and microglia as a consequence of HIV infection and may induce neurological damage (104, 137-140). Alternatively, HIV infection can cause direct injury to the CNS by the production of viral proteins, including the Env gp120 subunit, Vpr, and Tat, which have been shown to be neurotoxic *in vitro* (104, 132).

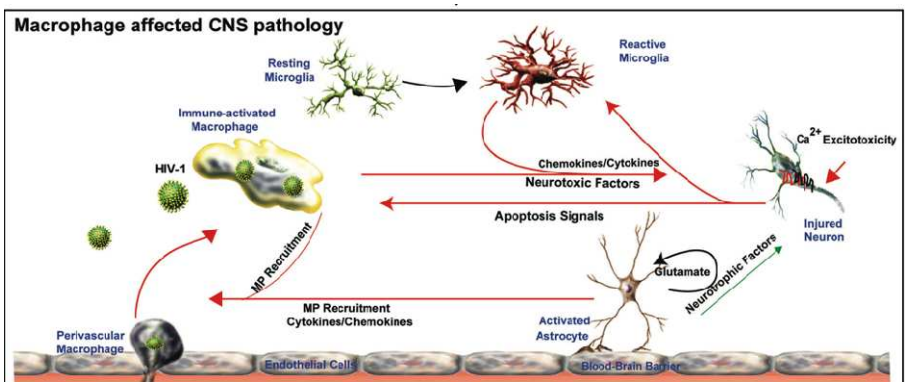

Figure 1.14. Model for macrophage-induced CNS pathology.
Once in brain, HIV-1 infection is perpetrated in both lymphocytes and macrophages where it can be latent or productive. Ultimately, persistently infected macrophages can cause tissue damage and disease in brain, where HIV-infected macrophages often become immune activated and develop a neurotoxic phenotype. Macrophage activation can lead to tissue damage and the development of neurological complications including HAD. Adapted from (Ciborowski et al 2006) (141).

The development of HAD, the most severe form of HAND, does not correlate with HIV viral infection in brain, leukoencephalopathy, axonal damage, or number of apoptotic neurons or neuronal cell loss. Indeed, the most important predictor of HAD seems to extensive macrophage and microglia infiltration (12, 86, 99). In HAD patients, levels of production of proinflammatory cytokines, including IL-1α/β, IFN-γ, TNF-α, TGF-β, and IL-6, correlate roughly with HAD. These cytokines may be secreted by macrophages, astrocytes, neurons, and endothelial cells when infected by HIV or stimulated by activated macrophages Neurotoxins produced by activated microglia include nitric oxide, superoxide anions, α-chemokines, MMPs, glutamate receptor agonists, proinflammatory cytokines, and growth factors, and have been linked to a number of chronic, progressive neurological disorders in addition to HAD (107, 142). Once initiated, chronic activation could be self-perpetuating, maintained in an autocrine or paracrine fashion by continued presence of macrophage-derived molecules, HIV

proteins, or downstream products from astrocytes or other cells expressed as consequence of microglial activation (99). Indeed, HIV infection may induce persistent inflammation in the CNS mediated by chronically activated microglia and other immune cells even after apparently successful antiretroviral therapy (ART) (86, 107, 143). Consistent with this, persistent neuroinflammation is observed at autopsy in brains of ART treated patients, with microglia and macrophages expressing high levels of CD14, CD16, CD68, and MHC class II molecules. HAD may therefore represent a condition in which microglial cell-driven inflammation is the primary cause of neurodegenerative disease (86, 107).

In addition to neurotoxins produced by activated cells, a number of viral products have been implicated in the development of HAD and milder forms of neurocognitive impairment, including the Env gp120 subunit, Tat, Nef, and Vpr. Gp120 neurotoxicity is indirect and relies on the production of toxic intermediate such as proinflammatory cytokines, arachidonic acid metabolites, and nitric oxide by activated cells, including macrophages, microglia, and astrocytes (12, 107, 144). Tat is secreted by infected cells and may induce neuronal apoptosis directly, via increases in intracellular calcium, thereby stimulating production of reactive oxygen intermediates and caspase activation, or indirectly, by stimulating macrophages to produce MMPs that induce neuronal apoptosis. Tat has also been associated with microglial migration, prolonged cytokine production, and induction of neuronal nitric oxide synthase (nNOS) via the NF-κB and C/EBP pathways. Furthermore, Tat has been implicated in formation of a macromolecular complex of low-density lipoprotein receptor-related protein (LRP), postsynaptic density protein-95 (PSD-95), N-methyl-D-aspartic acid (NMDA) receptors,

and nNOS at the neuronal plasma membrane, which is believed to trigger apoptosis (145-146). Both Tat and Nef increase production of neurotoxic quantities of quinolinic acid, a glutamate receptor agonist that induces apoptosis of neurons and astrocytes *in vitro* (107, 138, 147). Nef has also been shown to induce apoptosis of HBMECs *in vitro* (145), while Vpr may induce neuronal apoptosis *in vitro* and has been associated with neuronal cell loss in brain regions including the hippocampus and cortex (107, 145). Thus, HIV infection in the CNS likely contributes to neurocognitive disorders directly though viral infection of macrophages and microglia, and indirectly due to activation of infected and uninfected cells, resulting in the production of neurotoxic factors and neuronal cell loss.

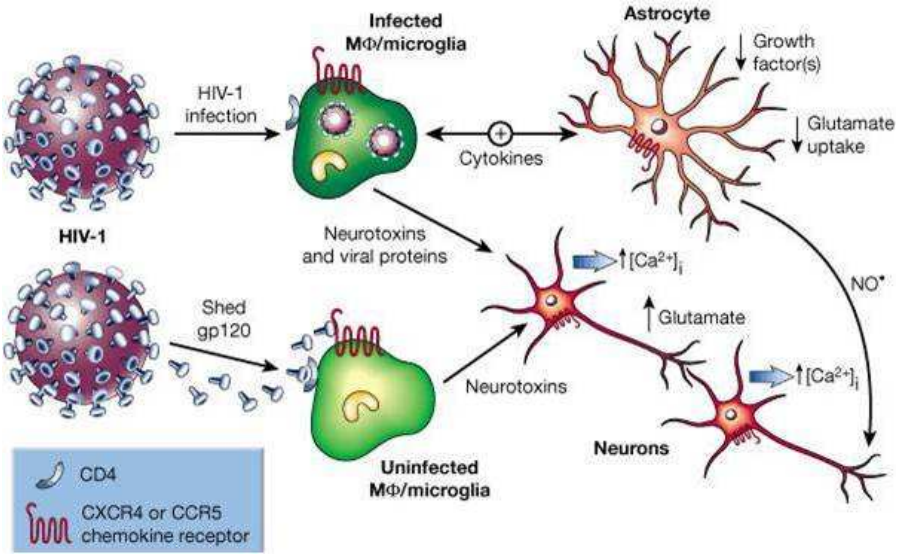

Fig. 1.15. Mechanisms by which gp120 may contribute to neuropathogenesis. Shedding of sgp120 from the surface of virions and infected cells in the CNS binds to and activates uninfected macrophages, microglia and astrocytes, leading to increased production of proinflammatory cytokines and neurotoxic factors, which may in turn promote neuronal injury and cell death, thereby contributing to processes involved in development of HAND. Adapted from (Kaul et al 2001) (137).

Scope of this Dissertation

HIV infection of macrophages in brain and other tissues plays an important role in the development of HIV-associated neurological disorders (HAND) and other aspects of disease pathogenesis. Infected macrophages show no obvious cytopathic effects of HIV infection and continue to shed virus for the duration of their normal lifespan, representing a long-lived reservoir for viral persistence (136). The major viral determinant of M-tropism is Env. Macrophages express lower levels of CD4 than CD4+ T cells in peripheral blood and are preferentially infected by viruses that can utilize low levels of CD4 for entry (84-85, 148-153).

Mechanisms that enhance Env interactions with CD4 include increased affinity for CD4 and increased exposure of the CD4-binding site (148, 152, 154-157). Another mechanism by which HIV Envs may overcome the restriction imposed by reduced CD4 on macrophages is through enhanced Env interactions with CCR5. Although several studies described M-tropic Envs with reduced CCR5 dependence, the genetic determinants in M-tropic Envs that contribute to this phenotype are poorly understood (124, 128, 158-159)

A second mechanism that influences this phenotype is increased exposure of the CD4 or CCR5 binding sites, which may also increase dissociation of soluble gp120 (sgp120) from the Env trimer based on structural models. While a large number of *in vitro* studies suggest a potential role for sgp120 in chronic activation and immune system dysfunction (108, 137-138, 160-176) (24-26), no studies have conclusively demonstrated that sgp120 contributes to HIV pathogenesis *in vivo*. Furthermore, little is known about spontaneous sgp120 shedding from primary HIV Envs or its biological significance.

In Chapter 2, we sought to identify determinants in M-tropic brain-derived Envs that contribute to reduced CD4-dependence by enhancing gp120 interactions with CCR5. To accomplish this goal, we examined brain and lymphoid gp120 sequences from the CCR5 binding site bridging sheet region from AIDS patients with or without HIV-associated dementia (HAD). Two determinants in the surface exposed β3 strand of the bridging sheet were identified. D197, which results in the elimination of an N-linked glycosylation site, was associated with brain infection and dementia. Position 200 was under positive selection in HAD patients. D197 and T/V200 enhanced fusion and entry with macrophages and other cells expressing low CD4 by enhancing gp120 binding to CCR5. The influence of T/V200 on fusion and entry was additive when combined with D197, suggesting that variants in β3 might enhance M-tropism cooperatively.

In Chapter 3 we analyzed spontaneous sgp120 shedding from a panel of 65 primary brain and lymphoid Envs from 12 AIDS patients. Sgp120 shedding from primary brain and lymphoid Envs was highly variable within and between patients, representing a spectrum rather than a categorical phenotype, and reached levels overlapping those shown to induce biological effects *in vivo*. Brain Envs with high sgp120 shedding mediated enhanced fusion and infection with cells expressing low CD4. Furthermore, viruses expressing brain Envs with high sgp120 shedding demonstrated an increased capacity to induce lymphocyte activation during infection of PBMC, despite similar levels of viral replication. Genetic analysis demonstrated greater entropy and positive selection in Envs with high versus low levels of sgp120 shedding, suggesting that diversifying evolution influences gp120-gp41 association.

In Chapter 4, we sequenced the gp120 coding region of nine full-length dual-tropic (R5X4) *env* genes cloned directly from autopsy brain and spleen tissue from an AIDS patient with severe HAD. We then compiled a dataset of 30 unique clade B R5X4 Env V3 sequences from this subject and 16 additional patients (*n*=4 brain and 26 lymphoid/blood Envs) and used it to compare the ability of six bioinformatic algorithms to correctly predict CXCR4 usage in R5X4 Envs. The results demonstrated that most predictive algorithms underestimated the frequency of R5X4 HIV-1 in brain and other tissues. $SVM_{geno2pheno}$ was the most accurate predictor of CXCR4 usage by R5X4 HIV-1.

In summary, we demonstrated that genetic determinants in the gp120 bridging sheet influence M-tropism by enhancing gp120 binding to CCR5. Furthermore, we demonstrated that a significant proportion of brain and lymphoid Envs readily shed sgp120 and present evidence that this phenotype is associated with enhanced interactions between gp120 from brain-derived Envs and CD4 and/or CCR5 and possibly with lymphocyte activation during PBMC infection. Our work provides a better understanding of the mechanisms by which gp120 determinants in brain Envs influence M-tropism. In addition, our findings demonstrate that spontaneous sgp120 shedding from primary brain and lymphoid Envs represents a phenotypic spectrum that may influence HIV pathogenesis by contributing to immune activation and bystander cell apoptosis.

REFERENCES

1. Frey G, Peng H, Rits-Volloch S, Morelli M, Cheng Y, Chen B. A fusion-intermediate state of HIV-1 gp41 targeted by broadly neutralizing antibodies. Proc Natl Acad Sci U S A. 2008;105(10):3739-44. PMCID: 2268799.

2. Pancera M, Majeed S, Ban YE, Chen L, Huang CC, Kong L, et al. Structure of HIV-1 gp120 with gp41-interactive region reveals layered envelope architecture and basis of conformational mobility. Proc Natl Acad Sci U S A. 2010;107(3):1166-71. PMCID: 2824281.

3. Chen B, Vogan EM, Gong H, Skehel JJ, Wiley DC, Harrison SC. Structure of an unliganded simian immunodeficiency virus gp120 core. Nature. 2005;433(7028):834-41.

4. MMWR Morb Mortal Wkly Rep. 1981;30:250-2.

5. Barre-Sinoussi F, Chermann JC, Rey F, Nugeyre MT, Chamaret S, Gruest J, et al. Isolation of a T-lymphotropic retrovirus from a patient at risk for acquired immune deficiency syndrome (AIDS). Science. 1983;220(4599):868-71.

6. Gallo RC, Sarin PS, Gelmann EP, Robert-Guroff M, Richardson E, Kalyanaraman VS, et al. Isolation of human T-cell leukemia virus in acquired immune deficiency syndrome (AIDS). Science. 1983;220(4599):865-7.

7. Levy JA, Hoffman AD, Kramer SM, Landis JA, Shimabukuro JM, Oshiro LS. Isolation of lymphocytopathic retroviruses from San Francisco patients with AIDS. Science. 1984;225(4664):840-2.

8. Calef C, Kuiken, C., Szinger, J., Gaschen, B., Abfalterer, W., Zhang, M., Tao, N., Funkhouser, R., Yusim, K., Flynn, M., Dalwani, A., Bruno, B., Foley, B., Leitner, T., Korber, B., editor. Gateway to tools of HIV and HCV Databases. Los Alamos, NM: Theoretical Biology and Biophysics Group, Los Alamos National Laboratory; 2005.

9. Liu J, Bartesaghi A, Borgnia MJ, Sapiro G, Subramaniam S. Molecular architecture of native HIV-1 gp120 trimers. Nature. 2008;455(7209):109-13.

10. Wyatt R, Kwong PD, Desjardins E, Sweet RW, Robinson J, Hendrickson WA, et al. The antigenic structure of the HIV gp120 envelope glycoprotein. Nature. 1998;393(6686):705-11.

11. Chahroudi A, Bosinger SE, Vanderford TH, Paiardini M, Silvestri G. Natural SIV hosts: showing AIDS the door. Science. 2012;335(6073):1188-93.

12. Rotta I, Almeida SM. Genotypical diversity of HIV clades and central nervous system impairment. Arq Neuropsiquiatr. 2011;69(6):964-72.

13. Freed EO, Martin, M.A. HIVs and their Replication. In: Knipe DM, Howley, P.M., editor. Fields Virology. Philadelphia, PA: Lippincott Williams & Wilkins; 2001. p. 1971-2041.

14. Dalmau J, Codoner FM, Erkizia I, Pino M, Pou C, Paredes R, et al. In-Depth Characterization of Viral Isolates from Plasma and Cells Compared with Plasma Circulating Quasispecies in Early HIV-1 Infection. PLoS One. 2012;7(2):e32714. PMCID: 3290612.

15. van Marle G, Power C. Human immunodeficiency virus type 1 genetic diversity in the nervous system: evolutionary epiphenomenon or disease determinant? J Neurovirol. 2005;11(2):107-28.

16. Becker C, Taube C, Bopp T, Michel K, Kubach J, Reuter S, et al. Protection from graft-versus-host disease by HIV-1 envelope protein gp120-mediated activation of human CD4+CD25+ regulatory T cells. Blood. 2009;114(6):1263-9.

17. Cohen OJ, Fauci, A.S. Pathogenesis and Medical Aspects of HIV Infection. In: Knipe DM, Howley, P.M., editor. Fields Virology. Philadelphia, PA: Lippincott Williams & Wilkins; 2001. p. 2043-94.

18. Fanales-Belasio E, Raimondo M, Suligoi B, Butto S. HIV virology and pathogenetic mechanisms of infection: a brief overview. Ann Ist Super Sanita. 2010;46(1):5-14.

19. Geldmacher C, Koup RA. Pathogen-specific T cell depletion and reactivation of opportunistic pathogens in HIV infection. Trends Immunol. 2012.

20. Fevrier M, Dorgham K, Rebollo A. CD4+ T cell depletion in human immunodeficiency virus (HIV) infection: role of apoptosis. Viruses. 2011;3(5):586-612. PMCID: 3185763.

21. Zeng M, Southern PJ, Reilly CS, Beilman GJ, Chipman JG, Schacker TW, et al. Lymphoid tissue damage in HIV-1 infection depletes naive T cells and limits T cell reconstitution after antiretroviral therapy. PLoS Pathog. 2012;8(1):e1002437. PMCID: 3252371.

22. Hazenberg MD, Hamann D, Schuitemaker H, Miedema F. T cell depletion in HIV-1 infection: how CD4+ T cells go out of stock. Nat Immunol. 2000;1(4):285-9.

23. Dalgleish AG, O'Byrne KJ. Chronic immune activation and inflammation in the pathogenesis of AIDS and cancer. Adv Cancer Res. 2002;84:231-76.

24. Riou C, Ganusov VV, Campion S, Mlotshwa M, Liu MK, Whale VE, et al. Distinct kinetics of gag-specific CD4(+) and CD8(+) T cell responses during acute HIV-1 infection. J Immunol. 2012;188(5):2198-206. PMCID: 3288487.

25. Freel SA, Saunders KO, Tomaras GD. CD8(+)T-cell-mediated control of HIV-1 and SIV infection. Immunol Res. 2011;49(1-3):135-46.

26. Letvin NL, Walker BD. Immunopathogenesis and immunotherapy in AIDS virus infections. Nat Med. 2003;9(7):861-6.

27. Alter G, Heckerman D, Schneidewind A, Fadda L, Kadie CM, Carlson JM, et al. HIV-1 adaptation to NK-cell-mediated immune pressure. Nature. 2011;476(7358):96-100. PMCID: 3194000.

28. Alter G, Moody MA. The humoral response to HIV-1: new insights, renewed focus. J Infect Dis. 2010;202 Suppl 2:S315-22. PMCID: 2945610.

29. Liu P, Overman RG, Yates NL, Alam SM, Vandergrift N, Chen Y, et al. Dynamic antibody specificities and virion concentrations in circulating immune complexes in acute to chronic HIV-1 infection. J Virol. 2011;85(21):11196-207. PMCID: 3194959.

30. Koff WC. HIV vaccine development: Challenges and opportunities towards solving the HIV vaccine-neutralizing antibody problem. Vaccine. 2011.

31. Arhel NJ, Kirchhoff F. Implications of Nef: host cell interactions in viral persistence and progression to AIDS. Curr Top Microbiol Immunol. 2009;339:147-75.

32. Stevceva L, Yoon V, Carville A, Pacheco B, Santosuosso M, Korioth-Schmitz B, et al. The efficacy of T cell-mediated immune responses is reduced by the envelope protein of the chimeric HIV-1/SIV-KB9 virus in vivo. J Immunol. 2008;181(8):5510-21.

33. Elston JW, Thaker H. Immune reconstitution inflammatory syndrome. Int J STD AIDS. 2009;20(4):221-4.

34. Simon-Loriere E, Rossolillo P, Negroni M. RNA structures, genomic organization and selection of recombinant HIV. RNA Biol. 2011;8(2):280-6.

35. Watts JM, Dang KK, Gorelick RJ, Leonard CW, Bess JW, Jr., Swanstrom R, et al. Architecture and secondary structure of an entire HIV-1 RNA genome. Nature. 2009;460(7256):711-6. PMCID: 2724670.

36. Briggs JA, Krausslich HG. The molecular architecture of HIV. J Mol Biol. 2011;410(4):491-500.

37. Arhel N. Revisiting HIV-1 uncoating. Retrovirology. 2010;7:96. PMCID: 2998454.

38. Engelman A, Cherepanov P. The structural biology of HIV-1: mechanistic and therapeutic insights. Nat Rev Microbiol. 2012;10(4):279-90.

39. Matreyek KA, Engelman A. The requirement for nucleoporin NUP153 during human immunodeficiency virus type 1 infection is determined by the viral capsid. J Virol. 2011;85(15):7818-27. PMCID: 3147902.

40. Woodward CL, Chow SA. The nuclear pore complex: a new dynamic in HIV-1 replication. Nucleus. 2010;1(1):18-22. PMCID: 3035120.

41. Jouvenet N, Neil SJ, Bess C, Johnson MC, Virgen CA, Simon SM, et al. Plasma membrane is the site of productive HIV-1 particle assembly. PLoS Biol. 2006;4(12):e435. PMCID: 1750931.

42. Wissing S, Galloway NL, Greene WC. HIV-1 Vif versus the APOBEC3 cytidine deaminases: an intracellular duel between pathogen and host restriction factors. Mol Aspects Med. 2010;31(5):383-97. PMCID: 2967609.

43. Stansell E, Desrosiers RC. Fundamental difference in the content of high-mannose carbohydrate in the HIV-1 and HIV-2 lineages. J Virol. 2010;84(18):8998-9009. PMCID: 2937622.

44. Coffin JM, Hughes, S.H., Varmus, H.E. Synthesis and Organization of Env Glycoproteins. In: Coffin JM, Hughes, S.H., Varmus, H.E., editor. Retroviruses. Cold Spring Harbor, NY: Cold Spring Harbor Laboratory Press; 1997.

45. Wyss S, Berlioz-Torrent C, Boge M, Blot G, Honing S, Benarous R, et al. The highly conserved C-terminal dileucine motif in the cytosolic domain of the human immunodeficiency virus type 1 envelope glycoprotein is critical for its association with the AP-1 clathrin adaptor [correction of adapter]. J Virol. 2001;75(6):2982-92. PMCID: 115924.

46. Dey B, Pancera M, Svehla K, Shu Y, Xiang SH, Vainshtein J, et al. Characterization of human immunodeficiency virus type 1 monomeric and trimeric gp120 glycoproteins stabilized in the CD4-bound state: antigenicity, biophysics, and immunogenicity. J Virol. 2007;81(11):5579-93.

47. Moore JP, Sodroski J. Antibody cross-competition analysis of the human immunodeficiency virus type I gp120 exterior envelope glycoprotein. Journal of Virology. 1996;79:11161-9.

48. Kwong PD, Wyatt R, Majeed S, Robinson J, Sweet RW, Sodroski J, et al. Structures of HIV-1 gp120 envelope glycoproteins from laboratory-adapted and primary isolates. Structure. 2000;8(12):1329-39.

49. Kwong PD, Wyatt R, Robinson J, Sweet RW, Sodroski J, Hendrickson WA. Structure of an HIV gp120 envelope glycoprotein in complex with the CD4 receptor and a neutralizing human antibody. Nature. 1998;393(6686):648-59.

50. Hunter E, editor. gp41, a multifunctional protein involved in HIV entry and pathogenesis. Los Alamos, NM: Theoretical Biology and Biophysics Groups, Los Alamos National Laboratory; 1997.

51. Bernstein HB, Tucker SP, Kar SR, McPherson SA, McPherson DT, Dubay JW, et al. Oligomerization of the hydrophobic heptad repeat of gp41. J Virol. 1995;69(5):2745-50. PMCID: 188967.

52. Finzi A, Xiang SH, Pacheco B, Wang L, Haight J, Kassa A, et al. Topological layers in the HIV-1 gp120 inner domain regulate gp41 interaction and CD4-triggered conformational transitions. Mol Cell. 2010;37(5):656-67. PMCID: 2854584.

53. Kassa A, Madani N, Schon A, Haim H, Finzi A, Xiang SH, et al. Transitions to and from the CD4-bound conformation are modulated by a single-residue change in the human immunodeficiency virus type 1 gp120 inner domain. J Virol. 2009;83(17):8364-78.

54. Koito A, Harrowe G, Levy JA, Cheng-Mayer C. Functional role of the V1/V2 region of human immunodeficiency virus type 1 envelope glycoprotein gp120 in infection of primary macrophages and soluble CD4 neutralization. J Virol. 1994;68(4):2253-9. PMCID: 236701.

55. Xiang SH, Finzi A, Pacheco B, Alexander K, Yuan W, Rizzuto C, et al. A V3 loop-dependent gp120 element disrupted by CD4 binding stabilizes the human immunodeficiency virus envelope glycoprotein trimer. J Virol. 2010;84(7):3147-61. PMCID: 2838131.

56. Poumbourios P, el Ahmar W, McPhee DA, Kemp BE. Determinants of human immunodeficiency virus type 1 envelope glycoprotein oligomeric structure. J Virol. 1995;69(2):1209-18.

57. Poumbourios P, Maerz AL, Drummer HE. Functional evolution of the HIV-1 envelope glycoprotein 120 association site of glycoprotein 41. J Biol Chem. 2003;278(43):42149-60.

58. Affranchino JL, Gonzalez SA. Mutations at the C-terminus of the simian immunodeficiency virus envelope glycoprotein affect gp120-gp41 stability on virions. Virology. 2006;347(1):217-25.

59. York J, Nunberg JH. Role of hydrophobic residues in the central ectodomain of gp41 in maintaining the association between human immunodeficiency virus type 1 envelope glycoprotein subunits gp120 and gp41. J Virol. 2004;78(9):4921-6. PMCID: 387687.

60. Kwon YD, Finzi A, Wu X, Dogo-Isonagie C, Lee LK, Moore LR, et al. Unliganded HIV-1 gp120 core structures assume the CD4-bound conformation with regulation by quaternary interactions and variable loops. Proc Natl Acad Sci U S A. 2012.

61. Haim H, Si Z, Madani N, Wang L, Courter JR, Princiotto A, et al. Soluble CD4 and CD4-mimetic compounds inhibit HIV-1 infection by induction of a short-lived activated state. PLoS Pathog. 2009;5(4):e1000360.

62. Haim H, Strack B, Kassa A, Madani N, Wang L, Courter JR, et al. Contribution of intrinsic reactivity of the HIV-1 envelope glycoproteins to CD4-independent infection and global inhibitor sensitivity. PLoS Pathog. 2011;7(6):e1002101. PMCID: 3121797.

63. Vogel EP, Curtis-Fisk J, Young KM, Weliky DP. Solid-state nuclear magnetic resonance (NMR) spectroscopy of human immunodeficiency virus gp41 protein that includes the fusion peptide: NMR detection of recombinant Fgp41 in inclusion bodies in whole bacterial cells and structural characterization of purified and membrane-associated Fgp41. Biochemistry. 2011;50(46):10013-26. PMCID: 3220598.

64. Zwick MB, Labrijn AF, Wang M, Spenlehauer C, Saphire EO, Binley JM, et al. Broadly neutralizing antibodies targeted to the membrane-proximal external region of human immunodeficiency virus type 1 glycoprotein gp41. J Virol. 2001;75(22):10892-905. PMCID: 114669.

65. Buzon MJ, Seiss K, Weiss R, Brass AL, Rosenberg ES, Pereyra F, et al. Inhibition of HIV-1 integration in ex vivo-infected CD4 T cells from elite controllers. J Virol. 2011;85(18):9646-50. PMCID: 3165766.

66. Zhu P, Liu J, Bess J, Jr., Chertova E, Lifson JD, Grise H, et al. Distribution and three-dimensional structure of AIDS virus envelope spikes. Nature. 2006;441(7095):847-52.

67. Harris A, Borgnia MJ, Shi D, Bartesaghi A, He H, Pejchal R, et al. Trimeric HIV-1 glycoprotein gp140 immunogens and native HIV-1 envelope glycoproteins display the same closed and open quaternary molecular architectures. Proc Natl Acad Sci U S A. 2011;108(28):11440-5. PMCID: 3136299.

68. Liu L, Cimbro R, Lusso P, Berger EA. Intraprotomer masking of third variable loop (V3) epitopes by the first and second variable loops (V1V2) within the native HIV-1 envelope glycoprotein trimer. Proc Natl Acad Sci U S A. 2011;108(50):20148-53. PMCID: 3250183.

69. Zhu CB, Zhu L, Holz-Smith S, Matthews TJ, Chen CH. The role of the third beta strand in gp120 conformation and neutralization sensitivity of the HIV-1 primary isolate DH012. Proc Natl Acad Sci U S A. 2001;98(26):15227-32.

70. Rusert P, Krarup A, Magnus C, Brandenberg OF, Weber J, Ehlert AK, et al. Interaction of the gp120 V1V2 loop with a neighboring gp120 unit shields the HIV envelope trimer against cross-neutralizing antibodies. J Exp Med. 2011;208(7):1419-33. PMCID: 3135368.

71. Doms RW. The plasma membrane as a combat zone in the HIV battlefield. Genes & Development. 2000;14:2677-88.

72. Melikyan GB. Membrane fusion mediated by human immunodeficiency virus envelope glycoprotein. Curr Top Membr. 2011;68:81-106.

73. Shankarappa R, Margolick JB, Gange SJ, Rodrigo AG, Upchurch D, Farzadegan H, et al. Consistent viral evolutionary changes associated with the progression of human immunodeficiency virus type 1 infection. J Virol. 1999;73(12):10489-502. PMCID: 113104.

74. van Rij RP, Visser JA, van Praag RM, Rientsma R, Prins JM, Lange JM, et al. Both R5 and X4 human immunodeficiency virus type 1 variants persist during prolonged therapy with five antiretroviral drugs. J Virol. 2002;76(6):3054-8. PMCID: 136002.

75. Gorry PR, Dunfee RL, Mefford ME, Kunstman K, Morgan T, Moore JP, et al. Changes in the V3 region of gp120 contribute to unusually broad coreceptor usage of an HIV-1 isolate from a CCR5 Delta32 heterozygote. Virology. 2007;362(1):163-78. PMCID: 1973138.

76. Zhang JL, Choe H, Dezube BJ, Farzan M, Sharma PL, Zhou XC, et al. The bis-azo compound FP-21399 inhibits HIV-1 replication by preventing viral entry. Virology. 1998;244(2):530-41.

77. Moore JP, Kitchen SG, Pugach P, Zack JA. The CCR5 and CXCR4 coreceptors--central to understanding the transmission and pathogenesis of human immunodeficiency virus type 1 infection. AIDS Res Hum Retroviruses. 2004;20(1):111-26.

78. Gorry PR, Bristol G, Zack JA, Ritola K, Swanstrom R, Birch CJ, et al. Macrophage tropism of human immunodeficiency virus type 1 isolates from brain and lymphoid tissues predicts neurotropism independent of coreceptor specificity. J Virol. 2001;75(21):10073-89.

79. Cheng-Mayer C, Liu R, Landau NR, Stamatatos L. Macrophage tropism of human immunodeficiency virus type 1 and utilization of the CC-CKR5 coreceptor. J Virol. 1997;71(2):1657-61.

80. Mefford ME, Gorry PR, Kunstman K, Wolinsky SM, Gabuzda D. Bioinformatic prediction programs underestimate the frequency of CXCR4 usage by R5X4 HIV type 1 in brain and other tissues. AIDS Res Hum Retroviruses. 2008;24(9):1215-20.

81. Kuhmann SE, Platt EJ, Kozak SL, Kabat D. Cooperation of multiple CCR5 coreceptors is required for infections by human immunodeficiency virus type 1. J Virol. 2000;74(15):7005-15.

82. Platt EJ, Wehrly K, Kuhmann SE, Chesebro B, Kabat D. Effects of CCR5 and CD4 cell surface concentrations on infections by macrophagetropic isolates of human immunodeficiency virus type 1. J Virol. 1998;72(4):2855-64.

83. Dunfee R, Thomas ER, Gorry PR, Wang J, Ancuta P, Gabuzda D. Mechanisms of HIV-1 neurotropism. Curr HIV Res. 2006;4(3):267-78.

84. Wang J, Crawford K, Yuan M, Wang H, Gorry PR, Gabuzda D. Regulation of CC chemokine receptor 5 and CD4 expression and human immunodeficiency virus type 1 replication in human macrophages and microglia by T helper type 2 cytokines. J Infect Dis. 2002;185(7):885-97.

85. Duenas-Decamp MJ, Peters P, Burton D, Clapham PR. Natural resistance of human immunodeficiency virus type 1 to the CD4bs antibody b12 conferred by a glycan and an arginine residue close to the CD4 binding loop. J Virol. 2008;82(12):5807-14.

86. Saijo K, Glass CK. Microglial cell origin and phenotypes in health and disease. Nat Rev Immunol. 2011;11(11):775-87.

87. McArthur JC. HIV dementia: an evolving disease. J Neuroimmunol. 2004;157(1-2):3-10.

88. Ances BM, Ellis RJ. Dementia and neurocognitive disorders due to HIV-1 infection. Semin Neurol. 2007;27(1):86-92.

89. Joska JA, Gouse H, Paul RH, Stein DJ, Flisher AJ. Does highly active antiretroviral therapy improve neurocognitive function? A systematic review. J Neurovirol. 2010;16(2):101-14.

90. Schnell G, Joseph S, Spudich S, Price RW, Swanstrom R. HIV-1 replication in the central nervous system occurs in two distinct cell types. PLoS Pathog. 2011;7(10):e1002286. PMCID: 3188520.

91. Jevtovic D, Salemovic D, Ranin J, Dulovic O, Ilic D, Brmbolic B. The prognosis of highly active antiretroviral therapy (HAART) treated HIV infected patients in Serbia, related to the time of treatment initiation. J Clin Virol. 2010;47(2):131-5.

92. Mahadevan A, Shankar SK, Satishchandra P, Ranga U, Chickabasaviah YT, Santosh V, et al. Characterization of human immunodeficiency virus (HIV)-infected cells in infiltrates associated with CNS opportunistic infections in patients with HIV clade C infection. J Neuropathol Exp Neurol. 2007;66(9):799-808.

93. Rao VR, Sas AR, Eugenin EA, Siddappa NB, Bimonte-Nelson H, Berman JW, et al. HIV-1 clade-specific differences in the induction of neuropathogenesis. J Neurosci. 2008;28(40):10010-6. PMCID: 2572723.

94. Patel VN, Mungwira RG, Tarumbiswa TF, Heikinheimo T, van Oosterhout JJ. High prevalence of suspected HIV-associated dementia in adult Malawian HIV patients. Int J STD AIDS. 2010;21(5):356-8.

95. Kaul M. HIV-1 associated dementia: update on pathological mechanisms and therapeutic approaches. Curr Opin Neurol. 2009;22(3):315-20. PMCID: 2779773.

96. Gandhi N, Saiyed ZM, Napuri J, Samikkannu T, Reddy PV, Agudelo M, et al. Interactive role of human immunodeficiency virus type 1 (HIV-1) clade-specific Tat

protein and cocaine in blood-brain barrier dysfunction: implications for HIV-1-associated neurocognitive disorder. J Neurovirol. 2010;16(4):294-305.

97. Samikkannu T, Agudelo M, Gandhi N, Reddy PV, Saiyed ZM, Nwankwo D, et al. Human immunodeficiency virus type 1 clade B and C gp120 differentially induce neurotoxin arachidonic acid in human astrocytes: implications for neuroAIDS. J Neurovirol. 2011;17(3):230-8.

98. Campbell GR, Watkins JD, Loret EP, Spector SA. Differential induction of rat neuronal excitotoxic cell death by human immunodeficiency virus type 1 clade B and C tat proteins. AIDS Res Hum Retroviruses. 2011;27(6):647-54. PMCID: 3101084.

99. Gartner S, Liu Y. Insights into the role of immune activation in HIV neuropathogenesis. J Neurovirol. 2002;8(2):69-75.

100. Thompson KA, Cherry CL, Bell JE, McLean CA. Brain cell reservoirs of latent virus in presymptomatic HIV-infected individuals. Am J Pathol. 2011;179(4):1623-9. PMCID: 3181362.

101. Spudich S, Gisslen M, Hagberg L, Lee E, Liegler T, Brew B, et al. Central nervous system immune activation characterizes primary human immunodeficiency virus 1 infection even in participants with minimal cerebrospinal fluid viral burden. J Infect Dis. 2011;204(5):753-60. PMCID: 3156103.

102. Lamers SL, Gray RR, Salemi M, Huysentruyt LC, McGrath MS. HIV-1 phylogenetic analysis shows HIV-1 transits through the meninges to brain and peripheral tissues. Infect Genet Evol. 2011;11(1):31-7. PMCID: 3005076.

103. Lamers SL, Salemi M, Galligan DC, Morris A, Gray R, Fogel G, et al. Human immunodeficiency virus-1 evolutionary patterns associated with pathogenic processes in the brain. J Neurovirol. 2010;16(3):230-41. PMCID: 2994721.

104. Gonzalez-Scarano F, Martin-Garcia J. The neuropathogenesis of AIDS. Nat Rev Immunol. 2005;5(1):69-81.

105. Roberts TK, Buckner CM, Berman JW. Leukocyte transmigration across the blood-brain barrier: perspectives on neuroAIDS. Front Biosci. 2010;15:478-536.

106. Ivey NS, MacLean AG, Lackner AA. Acquired immunodeficiency syndrome and the blood-brain barrier. J Neurovirol. 2009;15(2):111-22. PMCID: 2744422.

107. Albright AV, Martin J, O'Connor M, Gonzalez-Scarano F. Interactions between HIV-1 gp120, chemokines, and cultured adult microglial cells. J Neurovirol. 2001;7(3):196-207.

108. Yang B, Akhter S, Chaudhuri A, Kanmogne GD. HIV-1 gp120 induces cytokine expression, leukocyte adhesion, and transmigration across the blood-brain barrier: modulatory effects of STAT1 signaling. Microvasc Res. 2009;77(2):212-9.

109. Banks WA, Robinson SM, Nath A. Permeability of the blood-brain barrier to HIV-1 Tat. Exp Neurol. 2005;193(1):218-27.

110. Shiramizu B, Williams AE, Shikuma C, Valcour V. Amount of HIV DNA in peripheral blood mononuclear cells is proportional to the severity of HIV-1-associated neurocognitive disorders. J Neuropsychiatry Clin Neurosci. 2009;21(1):68-74. PMCID: 2668129.

111. Ohagen A, Devitt A, Kunstman KJ, Gorry PR, Rose PP, Korber B, et al. Genetic and functional analysis of full-length human immunodeficiency virus type 1 env genes derived from brain and blood of patients with AIDS. J Virol. 2003;77(22):12336-45.

112. Kramer-Hammerle S, Rothenaigner I, Wolff H, Bell JE, Brack-Werner R. Cells of the central nervous system as targets and reservoirs of the human immunodeficiency virus. Virus Res. 2005;111(2):194-213.

113. Churchill MJ, Wesselingh SL, Cowley D, Pardo CA, McArthur JC, Brew BJ, et al. Extensive astrocyte infection is prominent in human immunodeficiency virus-associated dementia. Ann Neurol. 2009;66(2):253-8.

114. Eugenin EA, Clements JE, Zink MC, Berman JW. Human immunodeficiency virus infection of human astrocytes disrupts blood-brain barrier integrity by a gap junction-dependent mechanism. J Neurosci. 2011;31(26):9456-65. PMCID: 3132881.

115. Ritola K, Robertson K, Fiscus SA, Hall C, Swanstrom R. Increased human immunodeficiency virus type 1 (HIV-1) env compartmentalization in the presence of HIV-1-associated dementia. J Virol. 2005;79(16):10830-4. PMCID: 1182623.

116. Ellis RJ, Gamst AC, Capparelli E, Spector SA, Hsia K, Wolfson T, et al. Cerebrospinal fluid HIV RNA originates from both local CNS and systemic sources. Neurology. 2000;54(4):927-36.

117. Ellis RJ, Hsia K, Spector SA, Nelson JA, Heaton RK, Wallace MR, et al. Cerebrospinal fluid human immunodeficiency virus type 1 RNA levels are elevated in neurocognitively impaired individuals with acquired immunodeficiency syndrome. HIV Neurobehavioral Research Center Group. Ann Neurol. 1997;42(5):679-88.

118. Harrington PR, Haas DW, Ritola K, Swanstrom R. Compartmentalized human immunodeficiency virus type 1 present in cerebrospinal fluid is produced by short-lived cells. J Virol. 2005;79(13):7959-66. PMCID: 1143772.

119. McArthur JC, McClernon DR, Cronin MF, Nance-Sproson TE, Saah AJ, St Clair M, et al. Relationship between human immunodeficiency virus-associated dementia and viral load in cerebrospinal fluid and brain. Ann Neurol. 1997;42(5):689-98.

120. Spudich SS, Nilsson AC, Lollo ND, Liegler TJ, Petropoulos CJ, Deeks SG, et al. Cerebrospinal fluid HIV infection and pleocytosis: relation to systemic infection and antiretroviral treatment. BMC Infect Dis. 2005;5:98. PMCID: 1299327.

121. Robertson K, Fiscus S, Kapoor C, Robertson W, Schneider G, Shepard R, et al. CSF, plasma viral load and HIV associated dementia. J Neurovirol. 1998;4(1):90-4.

122. Gartner S, McDonald RA, Hunter EA, Bouwman F, Liu Y, Popovic M. Gp120 sequence variation in brain and in T-lymphocyte human immunodeficiency virus type 1 primary isolates. J Hum Virol. 1997;1(1):3-18.

123. Power C, McArthur JC, Johnson RT, Griffin DE, Glass JD, Dewey R, et al. Distinct HIV-1 env sequences are associated with neurotropism and neurovirulence. Curr Top Microbiol Immunol. 1995;202:89-104.

124. Thomas ER, Dunfee RL, Stanton J, Bogdan D, Taylor J, Kunstman K, et al. Macrophage entry mediated by HIV Envs from brain and lymphoid tissues is determined by the capacity to use low CD4 levels and overall efficiency of fusion. Virology. 2007;360(1):105-19. PMCID: 1890014.

125. Wang TH, Donaldson YK, Brettle RP, Bell JE, Simmonds P. Identification of shared populations of human immunodeficiency virus type 1 infecting microglia and tissue macrophages outside the central nervous system. J Virol. 2001;75(23):11686-99.

126. Lamers SL, Salemi M, Galligan DC, de Oliveira T, Fogel GB, Granier SC, et al. Extensive HIV-1 intra-host recombination is common in tissues with abnormal histopathology. PLoS One. 2009;4(3):e5065.

127. Keele BF, Tazi L, Gartner S, Liu Y, Burgon TB, Estes JD, et al. Characterization of the follicular dendritic cell reservoir of human immunodeficiency virus type 1. J Virol. 2008;82(11):5548-61.

128. Gorry PR, Taylor J, Holm GH, Mehle A, Morgan T, Cayabyab M, et al. Increased CCR5 affinity and reduced CCR5/CD4 dependence of a neurovirulent primary human immunodeficiency virus type 1 isolate. J Virol. 2002;76(12):6277-92.

129. Korber BT, Kunstman KJ, Patterson BK, Furtado M, McEvilly MM, Levy R, et al. Genetic differences between blood- and brain-derived viral sequences from human immunodeficiency virus type 1-infected patients: evidence of conserved elements in the V3 region of the envelope protein of brain-derived sequences. J Virol. 1994;68(11):7467-81.

130. Gendelman HE, Lipton SA, Tardieu M, Bukrinsky MI, Nottet HS. The neuropathogenesis of HIV-1 infection. J Leukoc Biol. 1994;56(3):389-98.

131. Adamson DC, Dawson TM, Zink MC, Clements JE, Dawson VL. Neurovirulent simian immunodeficiency virus infection induces neuronal, endothelial, and glial apoptosis. Mol Med. 1996;2(4):417-28.

132. Power C, McArthur JC, Nath A, Wehrly K, Mayne M, Nishio J, et al. Neuronal death induced by brain-derived human immunodeficiency virus type 1 envelope genes

differs between demented and nondemented AIDS patients. J Virol. 1998;72(11):9045-53.

133. Shapshak P, Segal DM, Crandall KA, Fujimura RK, Zhang BT, Xin KQ, et al. Independent evolution of HIV type 1 in different brain regions. AIDS Res Hum Retroviruses. 1999;15(9):811-20.

134. Smit TK, Brew BJ, Tourtellotte W, Morgello S, Gelman BB, Saksena NK. Independent evolution of human immunodeficiency virus (HIV) drug resistance mutations in diverse areas of the brain in HIV-infected patients, with and without dementia, on antiretroviral treatment. J Virol. 2004;78(18):10133-48.

135. Martin-Garcia J, Cocklin S, Chaiken IM, Gonzalez-Scarano F. Interaction with CD4 and antibodies to CD4-induced epitopes of the envelope gp120 from a microglial cell-adapted human immunodeficiency virus type 1 isolate. J Virol. 2005;79(11):6703-13.

136. Gorry PR, Churchill M, Crowe SM, Cunningham AL, Gabuzda D. Pathogenesis of macrophage tropic HIV-1. Curr HIV Res. 2005;3(1):53-60.

137. Kaul M, Garden GA, Lipton SA. Pathways to neuronal injury and apoptosis in HIV-associated dementia. Nature. 2001;410(6831):988-94.

138. Kaul M, Zheng J, Okamoto S, Gendelman HE, Lipton SA. HIV-1 infection and AIDS: consequences for the central nervous system. Cell Death Differ. 2005;12 Suppl 1:878-92.

139. Nath A. Human immunodeficiency virus (HIV) proteins in neuropathogenesis of HIV dementia. J Infect Dis. 2002;186 Suppl 2:S193-8.

140. Wesselingh SL, Thompson KA. Immunopathogenesis of HIV-associated dementia. Curr Opin Neurol. 2001;14(3):375-9.

141. Ciborowski P. Biomarkers of HIV-1-associated neurocognitive disorders: challenges of proteomic approaches. Biomark Med. 2009;3(6):771-85.

142. Boven LA, Middel J, Verhoef J, De Groot CJ, Nottet HS. Monocyte infiltration is highly associated with loss of the tight junction protein zonula occludens in HIV-1-associated dementia. Neuropathol Appl Neurobiol. 2000;26(4):356-60.

143. Robertson KR, Smurzynski M, Parsons TD, Wu K, Bosch RJ, Wu J, et al. The prevalence and incidence of neurocognitive impairment in the HAART era. Aids. 2007;21(14):1915-21.

144. Corasaniti MT, Bagetta G, Rotiroti D, Nistico G. The HIV envelope protein gp120 in the nervous system: interactions with nitric oxide, interleukin-1beta and nerve growth factor signalling, with pathological implications in vivo and in vitro. Biochem Pharmacol. 1998;56(2):153-6.

145. Sharma D, Bhattacharya J. Cellular & molecular basis of HIV-associated neuropathogenesis. Indian J Med Res. 2009;129(6):637-51.

146. Hahn YK, Vo P, Fitting S, Block ML, Hauser KF, Knapp PE. beta-Chemokine production by neural and glial progenitor cells is enhanced by HIV-1 Tat: effects on microglial migration. J Neurochem. 2010;114(1):97-109. PMCID: 2992981.

147. Guillemin GJ, Kerr SJ, Brew BJ. Involvement of quinolinic acid in AIDS dementia complex. Neurotox Res. 2005;7(1-2):103-23.

148. Dunfee RL, Thomas ER, Gorry PR, Wang J, Taylor J, Kunstman K, et al. The HIV Env variant N283 enhances macrophage tropism and is associated with brain infection and dementia. Proc Natl Acad Sci U S A. 2006;103(41):15160-5. PMCID: 1586182.

149. Gray L, Sterjovski J, Churchill M, Ellery P, Nasr N, Lewin SR, et al. Uncoupling coreceptor usage of human immunodeficiency virus type 1 (HIV-1) from macrophage tropism reveals biological properties of CCR5-restricted HIV-1 isolates from patients with acquired immunodeficiency syndrome. Virology. 2005;337(2):384-98.

150. Walter BL, Wehrly K, Swanstrom R, Platt E, Kabat D, Chesebro B. Role of low CD4 levels in the influence of human immunodeficiency virus type 1 envelope V1 and V2 regions on entry and spread in macrophages. J Virol. 2005;79(8):4828-37.

151. Bannert N, Schenten D, Craig S, Sodroski J. The level of CD4 expression limits infection of primary rhesus monkey macrophages by a T-tropic simian immunodeficiency virus and macrophagetropic human immunodeficiency viruses. J Virol. 2000;74(23):10984-93.

152. Martin-Garcia J, Cao W, Varela-Rohena A, Plassmeyer ML, Gonzalez-Scarano F. HIV-1 tropism for the central nervous system: Brain-derived envelope glycoproteins with lower CD4 dependence and reduced sensitivity to a fusion inhibitor. Virology. 2006;346(1):169-79.

153. Peters PJ, Bhattacharya J, Hibbitts S, Dittmar MT, Simmons G, Bell J, et al. Biological analysis of human immunodeficiency virus type 1 R5 envelopes amplified from brain and lymph node tissues of AIDS patients with neuropathology reveals two distinct tropism phenotypes and identifies envelopes in the brain that confer an enhanced tropism and fusigenicity for macrophages. J Virol. 2004;78(13):6915-26.

154. Peters PJ, Duenas-Decamp MJ, Sullivan WM, Brown R, Ankghuambom C, Luzuriaga K, et al. Variation in HIV-1 R5 macrophage-tropism correlates with sensitivity to reagents that block envelope: CD4 interactions but not with sensitivity to other entry inhibitors. Retrovirology. 2008;5:5.

155. Dunfee RL, Thomas ER, Wang J, Kunstman K, Wolinsky SM, Gabuzda D. Loss of the N-linked glycosylation site at position 386 in the HIV envelope V4 region

enhances macrophage tropism and is associated with dementia. Virology. 2007;367(1):222-34. PMCID: 2201988.

156. Duenas-Decamp MJ, Peters PJ, Burton D, Clapham PR. Determinants flanking the CD4 binding loop modulate macrophage tropism of human immunodeficiency virus type 1 R5 envelopes. J Virol. 2009;83(6):2575-83.

157. Sterjovski J, Churchill MJ, Ellett A, Gray LR, Roche MJ, Dunfee RL, et al. Asn 362 in gp120 contributes to enhanced fusogenicity by CCR5-restricted HIV-1 envelope glycoprotein variants from patients with AIDS. Retrovirology. 2007;4:89. PMCID: 2225424.

158. Sterjovski J, Roche M, Churchill MJ, Ellett A, Farrugia W, Gray LR, et al. An altered and more efficient mechanism of CCR5 engagement contributes to macrophage tropism of CCR5-using HIV-1 envelopes. Virology. 2010;404(2):269-78.

159. Peters PJ, Duenas-Decamp MJ, Sullivan WM, Clapham PR. Variation of macrophage tropism among HIV-1 R5 envelopes in brain and other tissues. J Neuroimmune Pharmacol. 2007;2(1):32-41.

160. Trushin SA, Bren GD, Badley AD. CD4 T Cells Treated with gp120 Acquire a CD45R0+/CD45RA+ Phenotype. Open Virol J. 2009;3:21-5. PMCID: 2703203.

161. Mogensen TH, Melchjorsen J, Larsen CS, Paludan SR. Innate immune recognition and activation during HIV infection. Retrovirology. 2010;7:54. PMCID: 2904714.

162. Rychert J, Strick D, Bazner S, Robinson J, Rosenberg E. Detection of HIV gp120 in plasma during early HIV infection is associated with increased proinflammatory and immunoregulatory cytokines. AIDS Res Hum Retroviruses. 2010;26(10):1139-45. PMCID: 2982714.

163. Gemma C, Smith EM, Hughes TK, Jr., Opp MR. Human immunodeficiency virus glycoprotein 160 induces cytokine mRNA expression in the rat central nervous system. Cell Mol Neurobiol. 2000;20(4):419-31.

164. Cicala C, Arthos J, Censoplano N, Cruz C, Chung E, Martinelli E, et al. HIV-1 gp120 induces NFAT nuclear translocation in resting CD4+ T-cells. Virology. 2006;345(1):105-14.

165. Ameglio F, Capobianchi MR, Castilletti C, Cordiali Fei P, Fais S, Trento E, et al. Recombinant gp120 induces IL-10 in resting peripheral blood mononuclear cells; correlation with the induction of other cytokines. Clin Exp Immunol. 1994;95(3):455-8. PMCID: 1535081.

166. Kinter AL, Umscheid CA, Arthos J, Cicala C, Lin Y, Jackson R, et al. HIV envelope induces virus expression from resting CD4+ T cells isolated from HIV-infected

individuals in the absence of markers of cellular activation or apoptosis. J Immunol. 2003;170(5):2449-55.

167. Biancotto A, Iglehart SJ, Vanpouille C, Condack CE, Lisco A, Ruecker E, et al. HIV-1 induced activation of CD4+ T cells creates new targets for HIV-1 infection in human lymphoid tissue ex vivo. Blood. 2008;111(2):699-704. PMCID: 2200839.

168. Medders KE, Sejbuk NE, Maung R, Desai MK, Kaul M. Activation of p38 MAPK is required in monocytic and neuronal cells for HIV glycoprotein 120-induced neurotoxicity. J Immunol. 2010;185(8):4883-95.

169. Selliah N, Shackelford J, Wang JF, Traynor F, Yin J, Finkel TH. T cell signaling and apoptosis in HIV disease. Immunol Res. 2003;27(2-3):247-60.

170. Ullrich CK, Groopman JE, Ganju RK. HIV-1 gp120- and gp160-induced apoptosis in cultured endothelial cells is mediated by caspases. Blood. 2000;96(4):1438-42.

171. Garg H, Blumenthal R. HIV gp41-induced apoptosis is mediated by caspase-3-dependent mitochondrial depolarization, which is inhibited by HIV protease inhibitor nelfinavir. J Leukoc Biol. 2006;79(2):351-62.

172. Garg H, Joshi A, Blumenthal R. Altered bystander apoptosis induction and pathogenesis of enfuvirtide-resistant HIV type 1 Env mutants. AIDS Res Hum Retroviruses. 2009;25(8):811-7. PMCID: 2791676.

173. Anand AR, Ganju RK. HIV-1 gp120-mediated apoptosis of T cells is regulated by the membrane tyrosine phosphatase CD45. J Biol Chem. 2006;281(18):12289-99.

174. Garden GA, Guo W, Jayadev S, Tun C, Balcaitis S, Choi J, et al. HIV associated neurodegeneration requires p53 in neurons and microglia. FASEB J. 2004;18(10):1141-3.

175. Jana A, Pahan K. Human immunodeficiency virus type 1 gp120 induces apoptosis in human primary neurons through redox-regulated activation of neutral sphingomyelinase. J Neurosci. 2004;24(43):9531-40. PMCID: 1955476.

176. Singh IN, Goody RJ, Dean C, Ahmad NM, Lutz SE, Knapp PE, et al. Apoptotic death of striatal neurons induced by human immunodeficiency virus-1 Tat and gp120: Differential involvement of caspase-3 and endonuclease G. J Neurovirol. 2004;10(3):141-51.

.

CHAPTER 2: GENETIC DETERMINANTS IN THE HIV gp120 β3 STRAND OF THE BRIDGING SHEET INFLUENCE MACROPHAGE TROPISM BY ENHANCING ENV INTERACTIONS WITH CCR5

Megan E. Mefford[a], Kevin Kunstman[b], Steven M. Wolinsky[b], and Dana Gabuzda[a, c]

[a]Department of Cancer Immunology and AIDS, Dana-Farber Cancer Institute, Boston, MA, USA

[b]Northwestern University Medical School, Chicago, IL, USA

[c]Department of Neurology, Harvard Medical School, Boston, MA, USA

SUPPLEMENTARY DATA FOR CHAPTER 2 IS LOCATED IN APPENDIX A ON PAGE 175.

ABSTRACT

Macrophages and microglia are the main target cells for HIV infection of the central nervous system (CNS). Macrophages/microglia express lower levels of CD4 compared to CD4+ T cells, and macrophage-tropic (M-tropic) HIV strains express envelope glycoproteins (Envs) that have adapted to overcome this restriction to viral entry by mechanisms that are poorly characterized. One mechanism that influences this phenotype is enhanced binding of the HIV Env gp120 subunit to CCR5, but viral determinants of this phenotype in M-tropic strains have not been characterized. Here, we identified two genetic determinants in the HIV gp120 β3 strand of the bridging sheet in the CCR5 binding site that enhance M-tropism of primary brain-derived Envs. D197, which results in the loss of an N-linked glycosylation site, was associated with brain infection and HIV-associated dementia (HAD), while position 200 was identified as a codon under positive selection in HAD patients. Mutagenesis studies showed that D197 and T/V200 enhance fusion and infection of macrophages and other cells expressing low CD4 in a strain-dependent manner by enhancing gp120 binding to CCR5. This phenotype was not associated with increased neutralization sensitivity to monoclonal antibodies 17b and 412d, which recognize epitopes overlapping the CCR5-binding site. However, exposure to low levels of sCD4 increased neutralization sensitivity of some viruses expressing D197 and T/V200 to 17b. These findings suggest that genetic determinants in the β3 strand of the bridging sheet of HIV gp120 overcome the restriction to macrophage infection imposed by low CD4 by enhancing Env interactions with CCR5, thereby contributing to infection of the CNS and other macrophage-rich tissues.

INTRODUCTION

Human immunodeficiency virus type I (HIV) infects CD4+ T cells and cells of the macrophage lineage. Tissues harboring persistently infected macrophages include brain, lung, liver, spleen, small bowel, colon, and bone marrow (1-3). In these tissues, infected macrophages show no obvious cytopathic effects of HIV infection and continue to shed virus for the duration of their normal lifespan, representing a long-lived reservoir for viral persistence (1). Infected macrophages also contribute to disease pathogenesis in brain and other tissues by producing proinflammatory cytokines and other soluble factors, which in turn can induce bystander cell activation and apoptosis (1). Furthermore, macrophage reservoirs the brain represent a barrier to virus eradication due to limited penetration by antiretroviral therapy (1, 4-9).

The major determinant of M-tropism is the viral envelope glycoprotein (Env). The HIV Env, which consists of a surface-exposed gp120 and a transmembrane gp41 subunit, is organized into trimers on the surface of virions and infected cells (10). The gp120 subunit core is composed of an inner domain, a heavily glycosylated outer domain, and 4 surface exposed variable loops that extend from the core and partially occlude the coreceptor binding site and neutralization epitopes (11-12). HIV entry into cells is initiated by a high affinity interaction between gp120 and CD4, which induces conformational changes in gp120 resulting in formation of the coreceptor binding site (13). CCR5 is the primary coreceptor for virus entry into macrophages/microglia; however, CCR5 usage alone is neither necessary nor sufficient for M-tropism (14-15). Moreover, HIV M-tropism of CCR5-using (R5) isolates represents a spectrum rather than a categorical phenotype, with up to a 1000-fold variation in replication capacity in primary monocyte-derived macrophages (MDM) (8, 14, 16-18). One factor that

contributes to this spectrum of M-tropism is receptor density (19-20). Macrophages express lower levels of CD4 than CD4+ T cells in peripheral blood and are preferentially infected by viruses that can utilize low levels of CD4 for entry (18, 21-27). Determinants of reduced CD4-dependence or CD4-independence have been mapped to the HIV and SIV gp120 V1/V2, V3, and V4 variable loops, C2 and C3 regions, and regions of gp41 (21, 23, 28-34).

Mechanisms that enhance Env interactions with CD4 include increased affinity for CD4 and increased exposure of the CD4-binding site (21, 26, 28, 35-37). Another mechanism by which HIV Envs may overcome the restriction imposed by reduced CD4 on macrophages is through enhanced Env interactions with CCR5. Although several studies described M-tropic Envs with reduced CCR5 dependence, the genetic determinants in M-tropic Envs that contribute to this phenotype are poorly understood (16, 38-40). Genetic determinants that enhance gp120-CCR5 interactions in a strain-dependent manner have been mapped to the CCR5-binding site, which includes residues in the gp120 V3 loop, inner domain, and bridging sheet (11, 41-43). The bridging sheet is a 4-strand β-sheet formed by the β20/β21 strands, located between the inner and outer domains, and surface-exposed β2/β3 strands, which serve as the conserved stem of the V1/V2 loop (11, 37, 41-44). Genetic determinants in the β20/β21 strands that disrupt the hairpin structure have been shown to eliminate gp120 binding to CCR5 (45). Genetic determinants in the β3 strand have been shown to reduce Env binding to CCR5 and decrease membrane fusion efficiency in a strain-dependent manner (44). Moreover, amino acid variants in β3 may compromise interactions between the V1/V2 variable loops, which occlude the CCR5-binding site, and the V3 loop (46-47), possibly

disrupting the inter-protomer interactions that stabilize the unliganded Env trimer (47-48). Because the bridging sheet region undergoes structural rearrangements following CD4 binding, determinants in this region are likely to influence receptor-induced conformational changes that affect the viral entry process.

In this study, we identified viral determinants in the β3 strand of the HIV gp120 bridging sheet region that contribute to enhanced macrophage entry of brain-derived Envs. D197, which eliminates an N-linked glycosylation site, was associated with brain infection, and position 200 was a positively selected codon in patients with HIV-associated dementia (HAD). Mutagenesis studies showed that D197 and T/V200 enhanced macrophage entry in a strain-dependent manner, a phenotype that was associated with enhanced fusion and infection of cells expressing low CD4 due to enhanced gp120 binding to CCR5. These findings suggest that the β3 strand of the HIV gp120 bridging sheet in M-tropic Envs contains determinants that can overcome the restriction imposed by low CD4 for entry by enhancing Env interactions with CCR5.

MATERIALS AND METHODS

Sequence Analysis. Nucleotide sequences from published studies and Genbank were aligned using ClustalX2. Gp120 V1-V5 region sequences were examined using three different approaches to identify codons under positive selection: single likelihood ancestor counting (SLAC), fixed-effects likelihood (FEL), and internal fixed effects likelihood (IFEL) (HyPhy software, datamonkey web server). SLAC and FEL detect sites under selection at external branches of the phylogenetic tree, while IFEL identifies sites along internal branches (49-51). Sites were classified as positively selected when a significant p-value ($p<0.05$) was estimated by a minimum of 2 methods. To identify determinants associated with brain compartmentalization or dementia, gp120 β2 and β3 strand amino acid sequences were aligned using ClustalX2. Stratified 2x2 contingency tables were used to account for sequence correlations within each patient. P values were assigned using Fisher's exact test with $p<0.05$ considered significant.

Cells. 293T and TZM-bl cells, a HeLa cell clone engineered to express CD4 and CCR5 that contains integrated reporter genes for firefly luciferase and *E. coli* β-galactosidase under control of HIV-1 LTR, were cultured in DMEM media supplemented with 10% (vol/vol) fetal bovine serum (FBS) and 100 μg/ml penicillin and streptomycin. CF2-Luc cells, which are derived from canine thymocyte cell line CF2th and stably express firefly luciferase under control of HIV-1 LTR (52), and CF2th-synCCR5 cells, which express a codon-optimized version of human CCR5 containing a C-terminal nonapeptide (TETSQVAPA) tag derived from bovine rhodopsin (38), were cultured in medium supplemented with 0.7 mg/ml G418 (Mediatech, Herndon, VA). Affinofile cells were

cultured in DMEM supplemented with 10% dialyzed FBS (Gibco, Grand Island, NY), 100 μg/ml penicillin and streptomycin, and 50 μg/ml blasticidin S HCl (Invitrogen, Grand Island, NY) (53). Monocyte-derived macrophages (MDM) were derived from peripheral blood mononuclear cells (PBMC) isolated from healthy HIV-negative donors. As previously described, MDM were isolated from PBMC by plastic adherence and cultured in RPMI 1640 medium supplemented with 10% FBS, 100 μg/ml penicillin and streptomycin, and 10 ng/ml macrophage colony stimulating factor (M-CSF, R&D Systems, Minneapolis, MN) (38). TZM-bl cells were provided by Norm Letvin. Affinofile cells were provided by Benhur Lee.

Viruses and Mutagenesis. Primary clade B *env* genes from AIDS patients with HIV-associated dementia were cloned into pCR3.1 as previously described (16, 38). Env expression and processing was verified by Western blotting with goat anti-gp120 (AIDS Research and Reference Reagent Program, Division of AIDS, NIAID, NIH, Bethesda, MD) (21, 28). Mutant Env plasmids with changes at positions 197 and 200 (HXB2 numbering) were created by PCR-based mutagenesis and verified by DNA sequencing.

Entry Assays. HIV luciferase reporter viruses were generated by cotransfection of 293T cells with pNL4-3env-luc, an HIV provirus with *env* deleted and *nef* replaced with luciferase, and an Env-expressing plasmid as described (38). TZM-bl cells were seeded into 96-well plates in media supplemented with 15 μg/ml DEAE-dextran and infected with 10^4 ^{3}H cpm reverse transcriptase (RT) units of virus stock. Cells were lysed 48 hours post-infection and assayed for luciferase activity. MDM were prepared in 48-well plates

and infected overnight with 2 x 10^4 RT units of virus stock in media supplemented with 2 μg/ml polybrene. Cells were lysed 6 days post-infection and assayed for luciferase activity. Affinofile cells were seeded into 96-well plates and treated for 20 hours with serial dilutions of 0-3 ng/ml doxycycline (Clontech, Mountain View, CA) to induce CD4 expression and 0-2 μM Ponasterone A (Invitrogen) to induce CCR5 expression (53). Cells were then infected with 10^4 RT units of virus stock, lysed 2 days post-infection, and assayed for luciferase activity. Mock infected cells were used as negative controls. Background luciferase levels were subtracted from all results.

Fusion Assays. 293T cells were cotransfected with 2 μg pCR3.1 Env-expressing plasmid and 0.2 μg pLTR-Tat using calcium phosphate. Cf2-Luc cells were cotransfected with 0.1 (low), 1 (medium), or 10 μg (high) amounts of pcDNA3-CD4 and 10 μg (high) pcDNA3-CCR5 using Lipofectamine 2000 (Invitrogen). 2.5 x 10^4 293T cells and 2.5 x 10^5 CF2-Luc cells were mixed in 48-well plates and incubated for 5-8 hours. Cells were then lysed and analyzed for luciferase activity. 293T cells cotransfected with a nonfunctional Env (pSVIII-ΔKSenv) and pLTR-Tat were used to determine background levels of luciferase.

Flow Cytometry. Cell surface expression of CD4 and CCR5 on induced Affinofile and transfected CF2-Luc cells was analyzed by collecting cells with 5 mM EDTA in PBS and staining with anti-CD4-PE (BD Biosciences, San Jose, CA) and anti-CCR5-PE (BD Pharmingen, San Diego, CA). Cell surface staining was analyzed using a FACSCantoII flow cytometer (BD Biosciences). The approximate number of CD4 and CCR5 molecules

per cell was calculated using FACS analysis of Quantibrite beads according to manufacturer's instructions (BD Biosciences).

ELISA. ELISAs were based on previously described methods (54-56) with several modifications. Briefly, 96-well microplates were coated overnight with sheep antibody D7324 at 5 μg/ml in PBS (AALTO Bioproducts, Ltd., Ireland). Wells were washed 3 times with PBS supplemented with 2.5% Tween-20 (PBS-T) and blocked for 1 hour at room temperature with PBS-T supplemented with 3% BSA. Supernatants were incubated in the wells for 3 hours, followed by 10 washes with PBS-T and 1 hour incubation with polyclonal rabbit anti-gp120 (American Biotechnologies Inc.). After 10 additional washes with PBS-T, wells were incubated with anti-rabbit-HRP (GE Healthcare). The reaction was developed using BM chemiluminescence ELISA substrate (Roche) according to the manufacturer's instructions. The reaction was read on a luminometer (Viktor2, Perkin Elmer, Waltham, MA). Calculations of sgp120 concentrations were based on a standard curve of purified gp120 (21). Supernatant from cells transfected with empty pcDNA3 vector was used to determine background.

CCR5-Binding Assays. Plasmids expressing soluble gp120 (sgp120) glycoproteins were constructed by introducing a frameshift in gp120 that resulted in a truncation at position 518 (HXB2 numbering). Supernatants from 293T cells transfected with the Env-expressing plasmids were collected 48 hours post-transfection and cleared by centrifugation at 2000 rpm for 5 minutes. Supernatants were stored at -80ºC until used. Supernatants were concentrated by centrifugation using Amicon Ultra columns with a 30-

kD cutoff (Millipore, Billerica, MA). Sgp120 concentrations in concentrated supernatants were determined by ELISA. Equal concentrations of sgp120 were incubated with or without 1 μg/ml soluble CD4 (sCD4, Immunodiagnostics, Woburn, MA) for 30 minutes at 37ºC prior to incubation with CF2-synCCR5 cells. Binding of sgp120 to cells was detected by staining with mAb C11, followed by anti-human-PE (Bio-Rad, Hercules, CA), and was analyzed by flow cytometry. Specificity of gp120 interaction with CCR5 was verified by pre-incubating CF2-synCCR5 cells with 100 nM TAK-779 (obtained through the AIDS Research and Reference Reagents Program, Division of AIDS, NIAID, NIH, Bethesda, MD) (57) for 1 hour at 37ºC prior to incubation with sgp120.

Neutralization Assays. HIV luciferase reporter viruses were incubated with a range of concentrations of sCD4, monoclonal antibody (mAb) 17b (obtained from the NIH AIDS Research and Reference Reagent Program, Division of AIDS, NIAID, NIH, from Dr. James E. Robinson), or 0.1 μg/ml sCD4 and a range of concentrations of 17b in combination for 1 hour at 37ºC prior to infection of TZM-BL cells. Cells were harvested 48 hours post-infection and assayed for luciferase activity (58).

RESULTS

Identification of determinants in the gp120 bridging sheet associated with brain infection and HAD. The genetic evolution of HIV variants in brain is distinct from that in lymphoid tissues and other organs (3, 16, 59-63). Furthermore, diversifying evolution associated with CNS infection can result in nonsynonymous substitutions that affect protein structure and function (51, 64-67). The gp120 CCR5-binding site includes residues in the V3 loop, the inner domain, and the bridging sheet. The bridging sheet is formed following gp120 binding to CD4, and residues in this region have been shown to impact gp120 interactions with CCR5 in a strain-specific manner by influencing gp120 binding to CCR5 and positioning of the V1/V2 loops, thereby increasing exposure of the CCR5 binding site (29, 45-47). Therefore, to investigate whether M-tropic HIV brain-derived Envs contain genetic determinants in the gp120 bridging sheet that enhance gp120 interactions with CCR5, analyzed viral sequences in this region.

To identify potential sites of positive selection in the gp120 bridging sheet, brain-derived gp120 V1-V5 region sequences from patients diagnosed with or without clinical dementia were analyzed (n=336 unique sequences from 19 HAD subjects and 119 from 11 non-HAD subjects) (16, 18, 26, 61, 63, 68-72). The SLAC, FEL, and IFEL methods (datamonkey web server) were used to calculate the probability that codon variation was due to positive selection (Fig. 2.1) (49-50, 73). A total of 29 and 14 sites were estimated to be under positive selection in brain sequences from patients with or without HAD, respectively (p<0.05 in a minimum of 2 methods) (Table S2.1). In the bridging sheet region, only position 200, located in the surface-exposed β3 strand, was estimated to be under positive selection in brain sequences from HAD patients (p=0.02) (Table 2.1).

When the dataset was expanded to include blood and lymphoid-derived Env sequences matched to the brain sequences, the prediction of positive selection at position 200 in HAD patients was strengthened (p=0.005) (Fig. S2.1). However, position 200 was not estimated to be under positive selection in either brain or brain and blood/lymphoid sequences in non-HAD patients. Thus, position 200 in the β3 strand is a positively selected codon in brain and blood/lymphoid-derived sequences in HAD patients

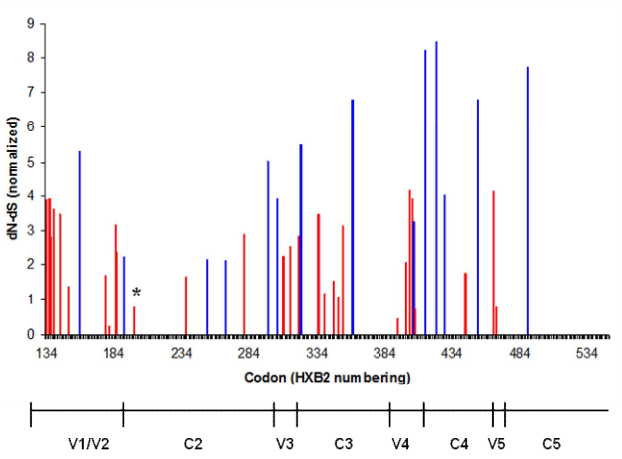

Figure 2.1. Predicted sites of positive selection in brain Envs from subjects with or without HAD. Brain-derived Env sequences from AIDS patients with or without HAD (n=336 and 119 sequences from patients with or without HAD, respectively) were aligned using ClustalX2. dN-dS values were estimated by SLAC, FEL, and IFEL and normalized by total codon tree length using the datamonkey web server. dN-dS values shown are averages calculated for any codon with p<0.05 by a minimum of 2 methods. Sites from HAD subjects are shown in red and from non-HAD subjects in blue. Codons were numbered according to codon *env* position of HIV-1 HXB2 reference strain. *indicates position 200 in the β3 strand of the gp120 bridging sheet.

Table 2.1. Position 200 in the gp120 β3 strand is estimated to be under positive selection in HAD patients.

Alignment	Codon	Region	Average dN-dS	Average p-value[a]
HAD brain[b]	200	β3	0.8	0.021 (FEL, IFEL)
HAD lymphoid[c]	200	β3	2.6	0.005 (all 3)
Non-HAD brain[d]	NS	NS	NS	NS
Non-HAD lymphoid[e]	NS	NS	NS	NS

[a] SLAC, FEL, and IFEL analyses (HyPhy software package) were used to reconstruct ancestral sequences at each node of a phylogenetic tree (data not shown). Substitutions are calculated at each branch and terminal node. P-values are averaged for methods in parentheses.
[b] n=336 unique brain-derived gp120 V1-V5 region sequences from 19 HAD subjects
[c] n=171 unique blood/lymphoid-derived gp120 V1-V5 region sequences from 15 HAD subjects
[d] n=119 unique brain-derived gp120 V1-V5 region sequences from 11 non-HAD subjects
[e]n=66 unique blood/lymphoid-derived gp120 V1-V5 region sequences from 7 non-HAD subjects

Position 200 is located in the surface-exposed β3 strand of the gp120 bridging sheet. The β2/β3 hairpin structure forms the conserved stem of the V1/V2 loops. Genetic determinants in the V1/V2 stem region can increase Env interactions with CCR5 by influencing the position of the V1/V2 loops, which occlude the coreceptor binding site in unliganded gp120 (20, 33, 47). Thus, determinants in the β2/β3 strands may enhance reduced CD4 dependence by increasing gp120 affinity for CCR5 or increasing exposure of the CCR5-binding site. To determine whether determinants at position 200 or other positions in the β2/β3 hairpin were associated with brain infection, we examined 796 matched brain- and blood/lymphoid-derived β2 and β3 strand sequences from 26 patients (*n*=498 brain sequences, range 3-89 sequences/patient; median=8 sequences/patient; and 298 blood/lymphoid sequences, range 2-57 sequences/patient; median 5 sequences/patient) (16, 18, 26, 36, 61, 63, 68, 71-72, 74-76). While more common in

brain-derived sequences, the most common variant at position 200 (Thr) was not associated with brain infection, appearing in 15% of brain and 10% of blood/lymphoid sequences (Table 2.2). However, elimination of the N-linked glycosylation site (PNGS) at position 197 was associated with brain infection, appearing in 8% of brain sequences and 1% of blood/lymphoid sequences (p=0.03, Fisher's exact test). No other determinants associated with brain infection were identified in the β2 or β3 strands (Table 2.2 and data not shown). Because position 200 was under positive selection in sequences from HAD patients, the dataset of brain-derived sequences from patients with or without HAD was expanded to include patients without matched lymphoid sequences (n=419 sequences from HAD patients, range 1-89 sequences/patient; median=5 sequences/patient; and 163 sequences from non-HAD patients, range 1-81 sequences/patient; median 4 sequences/patient) (16, 61, 63, 68-71, 75, 77). This dataset was then used to determine association with dementia. In this dataset, elimination of the PNGS at 197 appeared in 10% of brain sequences from HAD patients and 0% of brain sequences from non-HAD patients (p=0.001). T200 appeared in 10% of sequences from HAD patients and 17% of sequences from non-HAD patients. Thus, the elimination of the PNGS at position 197 in β3, while rare, is associated with brain compartmentalization and dementia.

Table 2.2. Loss of N-linked glycosylation site at position 197 in gp120 β3 strand is associated with brain infection and dementia.

	Variant Amino Acid Frequency [a]					
By Tissue (n=26 subjects)	**197Ψ [b]**	**A198[c]**	**T199 [c]**	**T200 [c]**	**V201 [c]**	**A202 [c]**
Brain (n=498)	**8%* (3)**	4% (1)	0.2% (1)	15% (4)	8% (2)	0.5% (1)
Blood/Lymphoid (n=298)	1% (2)	4% (1)	0% (0)	10% (3)	7% (2)	0.8% (1)
Brain, by disease[d]						
Dementia (n=419)	**10%** (5)**	4% (1)	0% (0)	10% (2)	4% (1)	0.5% (0)
No dementia (n=163)	0% (0)	0% (0)	0% (0)	17% (2)	5% (1)	0% (0)

[a] Variant amino acid frequency calculated as number of sequences containing most common variant/number of sequences containing any other amino acid (including clade B consensus) for each position. Sequences are correlated within each patient. The number in parentheses indicates the number of patients who have sequences containing the most common variant.

[b] Ψ indicates the presence of any amino acid that results in elimination of the N-linked glycosylation site

[c] Amino acid designation reflects the most common variant at each position.

[d] n=419 brain-derived sequences from 27 subjects with HAD and 163 brain-derived sequences from 18 non-HAD subjects

*p=0.03; ** p=0.001, Fisher's Exact Test

Determinants at 197 and 200 enhance macrophage entry by increasing fusion and infection of cells expressing low CD4. Many N-linked glycans that compose the "glycan shield" of the gp120 outer domain are highly conserved and essential for proper protein folding, stability, and interactions between gp120, CD4, and CCR5 (12, 64, 78). Moreover, studies in rhesus macaques infected with SIV and SHIV suggest that loss of specific PNGS sites in the V1/V2 loop region may affect viral replication, sensitivity to antibody neutralization, and M-tropism, possibly by increasing exposure of the CCR5-binding site (32, 79). Therefore, determinants at position 197 may influence macrophage

infection by enhancing Env interactions with CD4 and CCR5. To investigate this question, we used mutagenesis to introduce N197D (the most common variant) and V200T into a brain-derived Env cloned from a weakly M-tropic isolate (MACS2br13, hereafter referred to as M2br) and reciprocal changes to clade B consensus amino acids (D197N and T200V) into a highly M-tropic brain-derived Env cloned from autopsy brain tissue (UK1br2-14, hereafter referred to as UK1br) (Fig. 2.2A) (16, 21, 38). In addition, a double mutant (N197D/V200T) expressing both determinants was introduced into M2br. The parental and mutant Envs were processed to gp120 and gp41 and expressed on the cell surface at similar levels (Fig. 2.2B). Viruses expressing the parental and mutant Envs mediated similar levels of virus entry into control TZM-BL cells expressing high CD4 and CCR5, with viruses expressing UK1br Envs mediating high levels of entry, comparable to virus expressing the control ADA Env (Fig. 2.2C). M2br N197D and N197D/V200T exhibited significantly increased entry into monocyte-derived macrophages (MDM) compared to the parental Env ($p<0.01$, student's *t* test), while M2br V200T, which contains the PNGS at position 197, mediated entry at levels similar to the parental M2br Env (Fig. 2.2D). UK1br T200V exhibited increased macrophage entry compared to the parental Env ($p=0.05$), while similar levels of entry were observed for viruses expressing parental UK1br and UK1br D197N Envs (Fig. 2.2D). These results suggest either a Val or Thr at position 200 contributes to enhanced macrophage entry in a strain-dependent manner when combined with Asp at position 197.

Figure 2.2. Determinants at positions 197 and 200 enhance macrophage entry in a strain-dependent manner. A) HIV UK1br and M2br gp120 β3 sequences were previously published (16, 38) and were aligned against the clade B consensus sequence. Dots represent residues identical to the Clade B consensus sequence. Positions 197 and 200 are shown in red. B) 293T cells transfected with pCR3.1 Env expression plasmids were analyzed by Western blotting with polyclonal rabbit anti-gp120. ADA and YU2 Envs were used as assay controls. C) TZM-bl cells expressing high levels of CD4 and CCR5 were infected with HIV luciferase reporter viruses expressing UK1br and M2br parental and mutant Envs, lysed 48 hours after infection, and analyzed for luciferase activity. D) Monocyte-derived macrophages (MDM) were infected with reporter viruses expressing the parental and mutant Envs, lysed 6 days after infection, and analyzed for luciferase activity. For data in *C* and *D*, relative luciferase units (RLU) with background subtracted are shown for viruses expressing no Env (mock), ADA, UK1br, and M2br Envs on the left. Data on the right are presented as percentage of wild-type entry and represent duplicate wells of a single experiment. Error bars represent standard deviations. The experiment was repeated a minimum of 3 times for each Env set. *$p<0.05$, student's T test.

Fig. 2.2, Continued

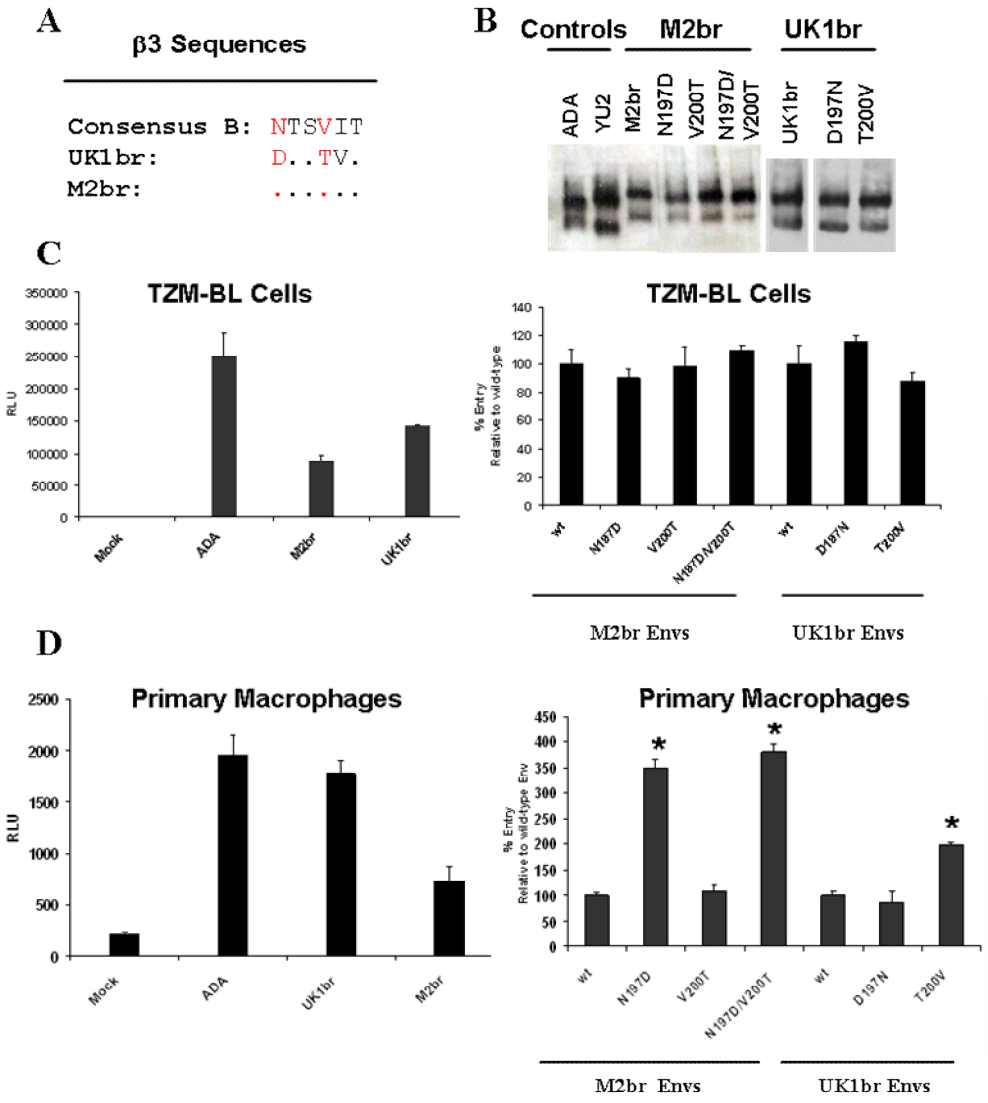

Macrophages express low CD4 compared to CD4+ T cells, so M-tropic Envs must overcome this restriction for virus entry. Therefore, we tested the capacity of the parental and mutant Envs to initiate fusion with cells expressing low levels of CD4 (Fig. 2.3A) (38). M2br N197D and N197D/V200T enhanced the overall efficiency of fusion compared to parental M2br (p=0.14, 0.03, and 0.06 for N197D and 0.03, 0.05, and 0.02 for N197D/V200T, for cells expressing low, medium, and high CD4, respectively, student's t test), but M2br V200T, which contained the PNGS at 197, did not enhance fusion compared to the wild-type M2br Env (Fig. 2.3C, left panel). M2br N197D/V200T mediated fusion with cells expressing very low CD4 levels, but was not CD4-independent (data not shown). UK1br T200V enhanced fusion with cells expressing low and medium levels of CD4 compared to the parental Env (p=0.2 and 0.05, respectively). UK1br D197N exhibited decreased fusion with cells expressing reduced CD4 compared to the parental Env (p=0.08, medium CD4) (Fig. 2.3C, right panel).

Figure 2.3. D197 and T/V200 enhance capacity of Envs to use low CD4 and CCR5 for fusion and entry. A) Env cell surface expression of CD4 on transfected CF2-Luc cells (left panel) or CD4 and CCR5 on induced Affinofile cells (middle and right panels) determined by flow cytometry. Estimated CD4 and CCR5 antibody binding sites (ABS) on Affinofile cells are calculated using QuantiBrite beads (Invitrogen). (B) 293T cells expressing control ADA Env, M2br parental and mutant Envs (left panel), and UK1br parental and mutant Envs (right panel) were mixed with CF2luc cells expressing low, medium, or high levels of CD4 as indicated. Fusion was measured by analyzing luciferase activity at 5 (UK1br) or 8 hours (M2br) depending on the kinetics of fusion. Background luciferase activity, measured as luciferase activity for 293T cells expressing the nonfunctional ΔKS Env, was subtracted from each time point. Results are expressed as mean percentages of fusion of the parental Env with cells expressing high CD4 and CCR5 and represent duplicate wells of a single experiment. Error bars represent standard deviations. The experiment was repeated a minimum of 3 times for each Env set. C) Affinofile cells were induced with doxycycline and Ponasterone A for 20 hours, then infected with HIV luciferase reporter viruses pseudotyped with UK1br and M2br wild-type and mutant Envs. Infection was quantified after 48 hours by analyzing luciferase activity. Background luciferase activity, measured as luc activity for Affinofile cells infected with *env*- virus, was subtracted. Results are presented as percentage of infection of cells expressing high CD4 and CCR5 for virus expressing the parental Env. $*p<0.05$, student's T test.

Figure 2.3, Continued

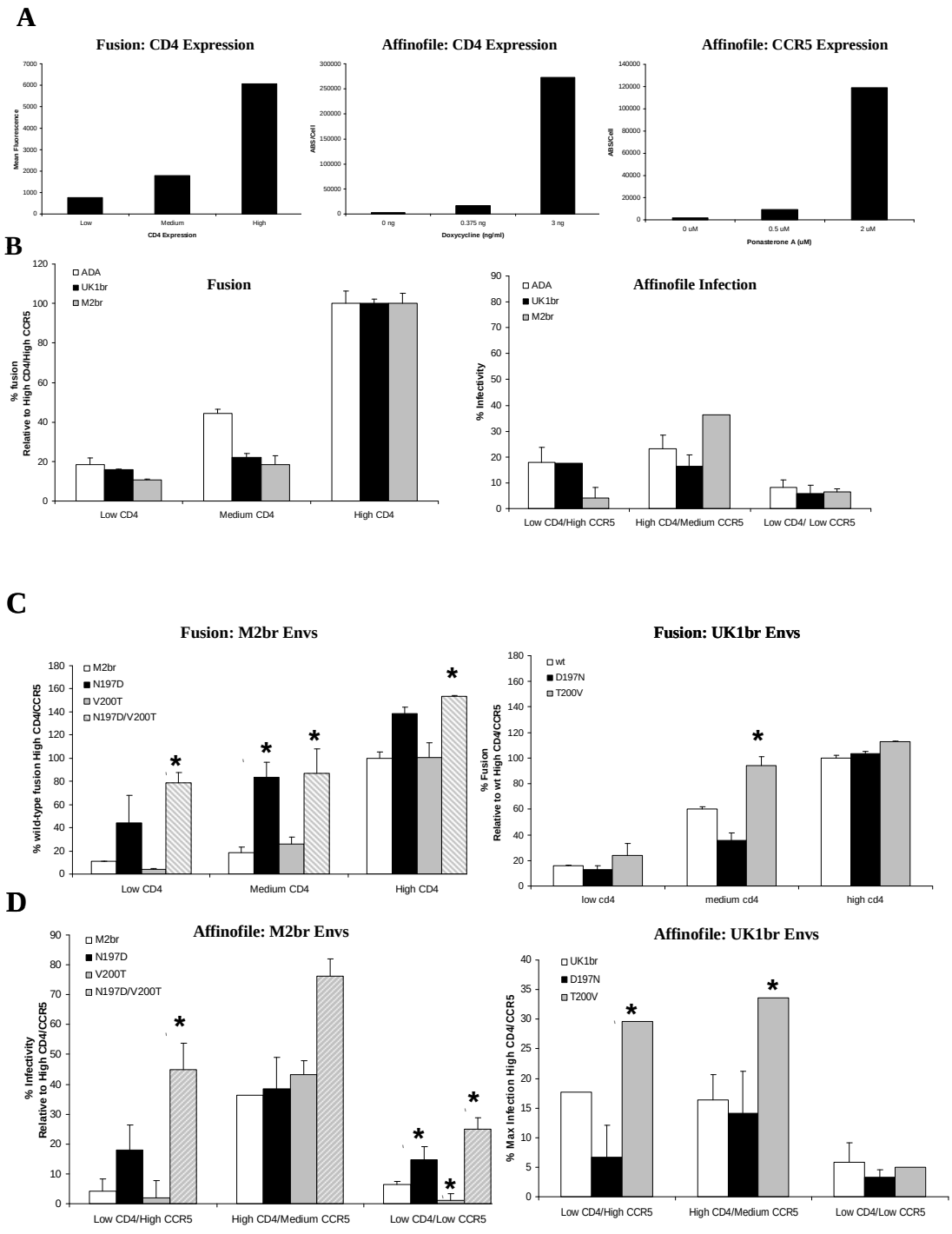

We next investigated whether Envs with enhanced capacity to fuse with cells expressing low CD4 also mediated enhanced entry into cells expressing low CD4 using the Affinofile cell line (53). Affinofile cells are a dually inducible cell line with independent regulation of CD4 and CCR5 expression. The use of 3 serial dilutions each of doxycyline and Ponasterone A to regulate CD4 and CCR5 expression, respectively, created a matrix of 9 conditions to analyze CD4 and CCR5 usage (Fig. 2.3A). Consistent with the fusion assay, viruses expressing M2br N197D, M2br N197D/V200T, and UK1br T200V mediated enhanced entry into Affinofile cells expressing low CD4 and high CCR5 compared to viruses expressing the parental Envs ($p<0.05$, student's *t* test) (Fig. 2.3D). Furthermore, UK1br T200V and M2br N197D/V200T mediated enhanced entry into Affinofile cells expressing lower CCR5 in combination with high CD4 compared to the parental Envs, and M2br N197D and N197D/V200T had the capacity to infect cells expressing low CD4 and CCR5 ($p<0.05$). Interestingly, M2br V200T, which contains the PNGS at 197, exhibited reduced entry into cells expressing low CD4 and CCR5 compared to the parental Envs. Furthermore, the ability to use low CD4 and CCR5 for fusion and entry was associated with enhanced macrophage entry (Fig. S2.2). Thus, D197 and T/V200 increased infection of cells expressing low CD4 and CCR5, suggesting that these determinants enable Envs to overcome restrictions imposed by low CD4 by enhancing interactions with CCR5.

Determinants at 197 and 200 increase Env interactions with CCR5. To investigate the mechanism by which D197 and T/V200 contribute to reduced CD4-dependence, we investigated binding of the parental and mutant Envs to cell-surface CCR5. UK1br

T200V bound to CF2 cells expressing high CCR5 with a 3-fold increase in the presence of sCD4 and a 10-fold increase in the absence of sCD4 compared to the parental Env (Fig. 2.4). These results suggest that enhanced fusion and infection of cells expressing low CD4 is due to enhanced gp120 affinity for CCR5.

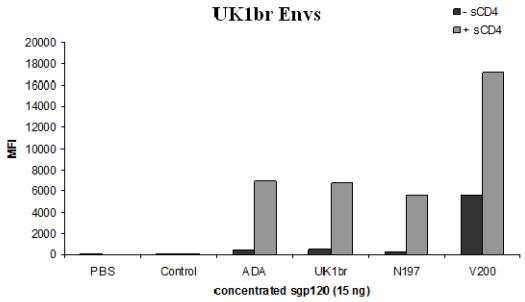

Figure 2.4 V200 enhances macrophage entry mediated by UK1br by increasing gp120 binding to CCR5. Soluble gp120 (sgp120) from the wild-type and mutant Envs was produced by transfected 293T cells with Env plasmids containing a stop codon at position 518. Concentrations of sgp120 in the supernatant were determined using ELISA and verified by Western blotting. Concentrated sgp120s were incubated with CF2th-synCCR5 cells with or without preincubation with sCD4. Binding of sgp120 to CCR5 on the cell surface was determined by flow cytometry. Results are representative of 3 independent experiments.

N-linked glycosylation is integral to maintaining Env structure and occluding conserved structural epitopes, including the CCR5-binding site, from neutralizing antibodies (80-83). Loss of the PNGS at 197 in Envs adapted to grow on immortalized T cell lines (lab-adapted Envs) influences sensitivity to neutralizing antibodies in a strain-specific manner (45, 80, 84-85). Therefore, we measured neutralization sensitivity of the parental and mutant Envs to soluble CD4 (sCD4) and monoclonal antibodies (mAb) 17b and 412. 17b has been used as a surrogate for CCR5-binding to probe conformational changes in gp120 (86), and 412d recognizes a CD4-induced (CD4i) epitope. Viruses expressing the M2br parental and mutant Envs were resistant to neutralization by sCD4 at concentrations up to 50 μg/ml, consistent with published results (Table 2.3 and Fig. S2.3) (45, 84). UK1br Envs containing the loss of the PNGS at position 197 (UK1br and UK1br T200V) were sensitive to sCD4 neutralization, with IC_{50} values of 1.3 and 0.4

μg/ml, respectively. As previously reported, the change to Asn at position 197 in the UK1br Env resulted in increased resistance to sCD4 neutralization, with a 12-fold increase in the IC_{50} compared to the parental UK1br (IC50=16.0 μg/ml) (78, 80, 84-85, 87). Despite previous reports that the loss of the PNGS at position 197 resulted in increased sensitivity to 17b neutralization (45, 84-85), only virus expressing the control ADA Env was neutralized by 17b. Viruses expressing the UK1br and M2br parental and mutant Envs were resistant to neutralization by 17b at concentrations up to 40 μg/ml or 412d at concentrations up to 10 μg/ml (Table 2.3, Fig. S2.3, and data not shown). Preincubation of the viruses with a combination of sCD4 and 17b increased neutralization sensitivity of M2br N197D and N197D/V200T, with IC50 values of 26 and 0.22 μg/ml, respectively. However, the M2br Envs containing N197 and all UK1br Envs remained resistant at concentrations of 17b up to 25 μg/ml. Together, these results suggest that changes in amino acid sequence in β3 that include D197 in combination with T/V200 may affect stability and exposure of the CCR5-binding site following interactions with CD4.

Table 2.3. Neutralization of parental and mutant Envs by sCD4 and 17b.[a]

Virus	sCD4	17b	sCD4 + 17b
ADA	1.7	4.4	ND
M2br	>50	>40	>25
N197D	>50	>40	26.0
V200T	>50	>40	>25
N197D/V200T	>50	>40	0.22
UK1br	1.3	>40	>25
D197N	16.0	>40	>25
T200V	0.4	>40	>25

[a]Values (μg/ml) represent IC50 values calculated from neutralization curves.

DISCUSSION

In this study, we identified viral determinants in the HIV gp120 β3 strand of the bridging sheet that were associated with brain infection and dementia. D197, which results in the loss of a PNGS, is associated with brain infection and dementia, and T/V200 is under positive selection in HAD patients. D197 and T/V200 enhanced fusion and infection of cells expressing low CD4, including macrophages. Viruses expressing Envs containing D197 and T/V200 also mediated enhanced entry into Affinofile cells expressing low CD4 and CCR5 (Fig. 2.3). UK1br T200V exhibited increased gp120 binding to CCR5, reaching levels 10-fold those of the parental Env, suggesting that D197 and T/V200 contribute to high-affinity interactions between M-tropic brain-derived Envs and CCR5.

The PNGS at 197 is highly conserved among clade B Envs. Determinants that eliminate this PNGS were found in only 8% of brain-derived and 1% of blood/lymphoid-derived Envs from our dataset (Table 2.2). Based on previous studies (80, 84-85, 88), we expected to find that the loss of the PNGS at 197 would increase exposure of the CCR5-binding site and corresponding neutralization epitopes. Unexpectedly, viruses expressing both the UK1br and M2br Envs containing D197 were not neutralization sensitive to mAb 17b at concentrations up to 40 μg/ml (Table 2.2 and Fig. S2.3). However, incubation with both sCD4 and 17b increased neutralization sensitivity of viruses expressing M2br N197D and N197D/V200T (IC50=26.0 and 0.2 μg/ml, respectively), but not the UK1br Envs. These results suggest that in M2br, D197 and T200 may enhance gp120 interactions with CCR5 by stabilizing the region of the 17b epitope following interactions with low concentrations of sCD4. Viruses expressing the UK1br

Envs were sensitive to neutralization by sCD4, with a 12-fold increase in neutralization resistance associated with the addition of the PNGS at position 197 (IC50=16.0 and 1.3 μg/ml for UK1br D197N and UK1br, respectively). Haim et al demonstrated that Envs have different susceptibilities to inactivation by sCD4, which may be linked to reactivity and a propensity to sample different conformations, resulting in increased sCD4-induced sgp120 shedding and virus inactivation (89-90). Thus, these results suggest that D197 and T/V200 enhance gp120-CCR5 affinity by context-specific mechanisms.

Previous mutagenesis studies investigated the effects of eliminating the PNGS at 197 in both primary and lab-adapted HIV Envs (38, 45, 78, 80, 84, 87-88, 91-92). These studies reported strain-dependent sensitivity to entry inhibitor BMS-806, sCD4, and a number of monoclonal antibodies, including 17b, b3, b12, F105, 2G12, and patient sera, and binding to sCD4 and CCR5. These results may reflect context-specific differences in the position of the V1/V2 loops, resulting in exposure of the CCR5-binding site or disrupting interactions between the V1/V2 and V3 loops, which may result from enhanced Env affinity for CCR5. Our data show that the effect of T/V200 on fusion and entry into cells expressing low CD4 is additive when combined with D197. Therefore, determinants in the β3 strand may act cooperatively to enhance gp120 interactions with CCR5.

Genetic evolution of HIV Env occurs in response to selection pressures, which include adaptation to target cell populations and immune evasion. However, the selection pressures *in vivo* that drive changes in M-tropism of R5 Envs are poorly understood (17). Analysis of diversifying selection in the bridging sheet region of the CCR5-binding site identified position 200 under positive selection in both brain and blood/lymphoid

sequences from patients with HAD. Position 200 is located in several overlapping immunodominant cytotoxic T lymphocyte (CTL) epitopes (LANL CTL/CD8+ T Cell Database); diversifying selection at this position may therefore be a consequence of immune evasion. The association between positive selection at position 200 and HAD patients may reflect the greater genetic diversity of the *env* gene that is associated with HAD (93-94).

In summary, this study identified determinants in the gp120 β3 strand from M-tropic brain-derived HIV Envs that increase gp120 binding to CCR5, thereby enhancing macrophage entry. T/V200 enhanced fusion and entry when combined with D197, suggesting that the sequence context of the β3 strand in M-tropic Envs is important for influencing gp120 interactions with CCR5. These findings suggest that genetic determinants in the β3 strand of the bridging sheet of HIV gp120 overcome the restriction to macrophage infection imposed by low CD4 by enhancing Env interactions with CCR5, thereby contributing to infection of the CNS and other macrophage-rich tissues.

ACKNOWLEDGEMENTS

We thank J. Cunningham, J. Sodroski, and B. Chen for helpful discussions, N. Letvin for providing TZM-bl cells, B. Lee for providing Affinofile cells, and D. Kabat for providing attenuated CCR5 plasmids. The following reagent was obtained through the NIH AIDS Research and Reference Reagent Program, Division of AIDS, NIAID: monoclonal antibody 17b from Dr. James E. Robinson and TAK-779. This work was supported by NIH Grants NS37277 and MH83588. M.M. was supported in part by NIH fellowship 1F31NS060611-01. Core facilities were supported by Harvard Medical School Center for AIDS Research (CFAR) and DFCI/Harvard Cancer Center grants.

REFERENCES

1. Gorry PR, Churchill M, Crowe SM, Cunningham AL, Gabuzda D. Pathogenesis of macrophage tropic HIV-1. Curr HIV Res. 2005;3(1):53-60.

2. Pierson T, McArthur J, Siliciano RF. Reservoirs for HIV-1: mechanisms for viral persistence in the presence of antiviral immune responses and antiretroviral therapy. Annu Rev Immunol. 2000;18:665-708.

3. Wang TH, Donaldson YK, Brettle RP, Bell JE, Simmonds P. Identification of shared populations of human immunodeficiency virus type 1 infecting microglia and tissue macrophages outside the central nervous system. J Virol. 2001;75(23):11686-99.

4. Dayton AI. Hitting HIV where it hides. Retrovirology. 2008;5:15. PMCID: 2253557.

5. Hogg RS, O'Shaughnessy MV, Gataric N, Yip B, Craib K, Schechter MT, et al. Decline in deaths from AIDS due to new antiretrovirals. Lancet. 1997;349(9061):1294.

6. Le Douce V, Herbein G, Rohr O, Schwartz C. Molecular mechanisms of HIV-1 persistence in the monocyte-macrophage lineage. Retrovirology. 2010;7:32. PMCID: 2873506.

7. Chun TW, Carruth L, Finzi D, Shen X, DiGiuseppe JA, Taylor H, et al. Quantification of latent tissue reservoirs and total body viral load in HIV-1 infection. Nature. 1997;387(6629):183-8.

8. Duncan CJ, Sattentau QJ. Viral determinants of HIV-1 macrophage tropism. Viruses. 2011;3(11):2255-79. PMCID: 3230851.

9. Smurzynski M, Wu K, Letendre S, Robertson K, Bosch RJ, Clifford DB, et al. Effects of central nervous system antiretroviral penetration on cognitive functioning in the ALLRT cohort. Aids. 2011;25(3):357-65. PMCID: 3022370.

10. Liu J, Bartesaghi A, Borgnia MJ, Sapiro G, Subramaniam S. Molecular architecture of native HIV-1 gp120 trimers. Nature. 2008;455(7209):109-13.

11. Moore JP, Sodroski J. Antibody cross-competition analysis of the human immunodeficiency virus type I gp120 exterior envelope glycoprotein. Journal of Virology. 1996;79:11161-9.

12. Dey B, Pancera M, Svehla K, Shu Y, Xiang SH, Vainshtein J, et al. Characterization of human immunodeficiency virus type 1 monomeric and trimeric gp120 glycoproteins stabilized in the CD4-bound state: antigenicity, biophysics, and immunogenicity. J Virol. 2007;81(11):5579-93.

13. Doms RW. The plasma membrane as a combat zone in the HIV battlefield. Genes & Development. 2000;14:2677-88.

14. Gorry PR, Bristol G, Zack JA, Ritola K, Swanstrom R, Birch CJ, et al. Macrophage tropism of human immunodeficiency virus type 1 isolates from brain and lymphoid tissues predicts neurotropism independent of coreceptor specificity. J Virol. 2001;75(21):10073-89.

15. Cheng-Mayer C, Liu R, Landau NR, Stamatatos L. Macrophage tropism of human immunodeficiency virus type 1 and utilization of the CC-CKR5 coreceptor. J Virol. 1997;71(2):1657-61.

16. Thomas ER, Dunfee RL, Stanton J, Bogdan D, Taylor J, Kunstman K, et al. Macrophage entry mediated by HIV Envs from brain and lymphoid tissues is determined by the capacity to use low CD4 levels and overall efficiency of fusion. Virology. 2007;360(1):105-19. PMCID: 1890014.

17. Richards KH, Aasa-Chapman MM, McKnight A, Clapham PR. Modulation of HIV-1 macrophage-tropism among R5 envelopes occurs before detection of neutralizing antibodies. Retrovirology. 2010;7:48. PMCID: 2890664.

18. Peters PJ, Bhattacharya J, Hibbitts S, Dittmar MT, Simmons G, Bell J, et al. Biological analysis of human immunodeficiency virus type 1 R5 envelopes amplified from brain and lymph node tissues of AIDS patients with neuropathology reveals two distinct tropism phenotypes and identifies envelopes in the brain that confer an enhanced tropism and fusigenicity for macrophages. J Virol. 2004;78(13):6915-26.

19. Kuhmann SE, Platt EJ, Kozak SL, Kabat D. Cooperation of multiple CCR5 coreceptors is required for infections by human immunodeficiency virus type 1. J Virol. 2000;74(15):7005-15.

20. Platt EJ, Wehrly K, Kuhmann SE, Chesebro B, Kabat D. Effects of CCR5 and CD4 cell surface concentrations on infections by macrophagetropic isolates of human immunodeficiency virus type 1. J Virol. 1998;72(4):2855-64.

21. Dunfee RL, Thomas ER, Gorry PR, Wang J, Taylor J, Kunstman K, et al. The HIV Env variant N283 enhances macrophage tropism and is associated with brain infection and dementia. Proc Natl Acad Sci U S A. 2006;103(41):15160-5. PMCID: 1586182.

22. Gray L, Sterjovski J, Churchill M, Ellery P, Nasr N, Lewin SR, et al. Uncoupling coreceptor usage of human immunodeficiency virus type 1 (HIV-1) from macrophage tropism reveals biological properties of CCR5-restricted HIV-1 isolates from patients with acquired immunodeficiency syndrome. Virology. 2005;337(2):384-98.

23. Walter BL, Wehrly K, Swanstrom R, Platt E, Kabat D, Chesebro B. Role of low CD4 levels in the influence of human immunodeficiency virus type 1 envelope V1 and V2 regions on entry and spread in macrophages. J Virol. 2005;79(8):4828-37.

24. Wang J, Crawford K, Yuan M, Wang H, Gorry PR, Gabuzda D. Regulation of CC chemokine receptor 5 and CD4 expression and human immunodeficiency virus type 1

replication in human macrophages and microglia by T helper type 2 cytokines. J Infect Dis. 2002;185(7):885-97.

25. Bannert N, Schenten D, Craig S, Sodroski J. The level of CD4 expression limits infection of primary rhesus monkey macrophages by a T-tropic simian immunodeficiency virus and macrophagetropic human immunodeficiency viruses. J Virol. 2000;74(23):10984-93.

26. Martin-Garcia J, Cao W, Varela-Rohena A, Plassmeyer ML, Gonzalez-Scarano F. HIV-1 tropism for the central nervous system: Brain-derived envelope glycoproteins with lower CD4 dependence and reduced sensitivity to a fusion inhibitor. Virology. 2006;346(1):169-79.

27. Duenas-Decamp MJ, Peters P, Burton D, Clapham PR. Natural resistance of human immunodeficiency virus type 1 to the CD4bs antibody b12 conferred by a glycan and an arginine residue close to the CD4 binding loop. J Virol. 2008;82(12):5807-14.

28. Dunfee RL, Thomas ER, Wang J, Kunstman K, Wolinsky SM, Gabuzda D. Loss of the N-linked glycosylation site at position 386 in the HIV envelope V4 region enhances macrophage tropism and is associated with dementia. Virology. 2007;367(1):222-34. PMCID: 2201988.

29. Kolchinsky P, Kiprilov E, Bartley P, Rubinstein R, Sodroski J. Loss of a single N-linked glycan allows CD4-independent human immunodeficiency virus type 1 infection by altering the position of the gp120 V1/V2 variable loops. J Virol. 2001;75(7):3435-43.

30. Chenine AL, Pion M, Matouskova E, Gondois-Rey F, Vigne R, Hirsch I. Adaptation of a CXCR4-using human immunodeficiency type 1 NDK virus in intestinal cells is associated with CD4-independent replication. Virology. 2002;304(2):403-14.

31. Puffer BA, Altamura LA, Pierson TC, Doms RW. Determinants within gp120 and gp41 contribute to CD4 independence of SIV Envs. Virology. 2004;327(1):16-25.

32. Puffer BA, Pohlmann S, Edinger AL, Carlin D, Sanchez MD, Reitter J, et al. CD4 independence of simian immunodeficiency virus Envs is associated with macrophage tropism, neutralization sensitivity, and attenuated pathogenicity. J Virol. 2002;76(6):2595-605.

33. Otto C, Puffer BA, Pohlmann S, Doms RW, Kirchhoff F. Mutations in the C3 region of human and simian immunodeficiency virus envelope have differential effects on viral infectivity, replication, and CD4-dependency. Virology. 2003;315(2):292-302.

34. LaBranche CC, Hoffman TL, Romano J, Haggarty BS, Edwards TG, Matthews TJ, et al. Determinants of CD4 independence for a human immunodeficiency virus type 1 variant map outside regions required for coreceptor specificity. J Virol. 1999;73(12):10310-9.

35. Peters PJ, Duenas-Decamp MJ, Sullivan WM, Brown R, Ankghuambom C, Luzuriaga K, et al. Variation in HIV-1 R5 macrophage-tropism correlates with sensitivity to reagents that block envelope: CD4 interactions but not with sensitivity to other entry inhibitors. Retrovirology. 2008;5:5.

36. Duenas-Decamp MJ, Peters PJ, Burton D, Clapham PR. Determinants flanking the CD4 binding loop modulate macrophage tropism of human immunodeficiency virus type 1 R5 envelopes. J Virol. 2009;83(6):2575-83.

37. Sterjovski J, Churchill MJ, Ellett A, Gray LR, Roche MJ, Dunfee RL, et al. Asn 362 in gp120 contributes to enhanced fusogenicity by CCR5-restricted HIV-1 envelope glycoprotein variants from patients with AIDS. Retrovirology. 2007;4:89. PMCID: 2225424.

38. Gorry PR, Taylor J, Holm GH, Mehle A, Morgan T, Cayabyab M, et al. Increased CCR5 affinity and reduced CCR5/CD4 dependence of a neurovirulent primary human immunodeficiency virus type 1 isolate. J Virol. 2002;76(12):6277-92.

39. Sterjovski J, Roche M, Churchill MJ, Ellett A, Farrugia W, Gray LR, et al. An altered and more efficient mechanism of CCR5 engagement contributes to macrophage tropism of CCR5-using HIV-1 envelopes. Virology. 2010;404(2):269-78.

40. Peters PJ, Duenas-Decamp MJ, Sullivan WM, Clapham PR. Variation of macrophage tropism among HIV-1 R5 envelopes in brain and other tissues. J Neuroimmune Pharmacol. 2007;2(1):32-41.

41. Kwong PD, Wyatt R, Majeed S, Robinson J, Sweet RW, Sodroski J, et al. Structures of HIV-1 gp120 envelope glycoproteins from laboratory-adapted and primary isolates. Structure. 2000;8(12):1329-39.

42. Chen B, Vogan EM, Gong H, Skehel JJ, Wiley DC, Harrison SC. Structure of an unliganded simian immunodeficiency virus gp120 core. Nature. 2005;433(7028):834-41.

43. Huang CC, Lam SN, Acharya P, Tang M, Xiang SH, Hussan SS, et al. Structures of the CCR5 N terminus and of a tyrosine-sulfated antibody with HIV-1 gp120 and CD4. Science. 2007;317(5846):1930-4.

44. Reeves JD, Gallo SA, Ahmad N, Miamidian JL, Harvey PE, Sharron M, et al. Sensitivity of HIV-1 to entry inhibitors correlates with envelope/coreceptor affinity, receptor density, and fusion kinetics. Proc Natl Acad Sci U S A. 2002;99(25):16249-54.

45. Rizzuto CD, Wyatt R, Hernandez-Ramos N, Sun Y, Kwong PD, Hendrickson WA, et al. A conserved HIV gp120 glycoprotein structure involved in chemokine receptor binding. Science. 1998;280(5371):1949-53.

46. Pan Y, Ma B, Nussinov R. CD4 binding partially locks the bridging sheet in gp120 but leaves the beta2/3 strands flexible. J Mol Biol. 2005;350(3):514-27.

47. Zhu CB, Zhu L, Holz-Smith S, Matthews TJ, Chen CH. The role of the third beta strand in gp120 conformation and neutralization sensitivity of the HIV-1 primary isolate DH012. Proc Natl Acad Sci U S A. 2001;98(26):15227-32.

48. Xiang SH, Finzi A, Pacheco B, Alexander K, Yuan W, Rizzuto C, et al. A V3 loop-dependent gp120 element disrupted by CD4 binding stabilizes the human immunodeficiency virus envelope glycoprotein trimer. J Virol. 2010;84(7):3147-61. PMCID: 2838131.

49. Pond SL, Frost SD. A genetic algorithm approach to detecting lineage-specific variation in selection pressure. Mol Biol Evol. 2005;22(3):478-85.

50. Pond SL, Frost SD, Grossman Z, Gravenor MB, Richman DD, Brown AJ. Adaptation to different human populations by HIV-1 revealed by codon-based analyses. PLoS Comput Biol. 2006;2(6):e62.

51. Pond SLK, A.F.Y. Poon, S. Zarate, D.M. Smith, S.J. Little, S.K. Pillai, R.J. Ellis, J.K. Wong, A.J. Leigh Brown, D.D. Richman, and S.D.W. Frost. Estimating selection pressures on HIV-1 using phylogenetic likelihood models. Stastistics in Medicine. 2008;27(23):4779-89.

52. Etemad-Moghadam B, Sun Y, Nicholson EK, Fernandes M, Liou K, Gomila R, et al. Envelope glycoprotein determinants of increased fusogenicity in a pathogenic simian-human immunodeficiency virus (SHIV-KB9) passaged in vivo. J Virol. 2000;74(9):4433-40. PMCID: 111962.

53. Johnston SH, Lobritz MA, Nguyen S, Lassen K, Delair S, Posta F, et al. A quantitative affinity-profiling system that reveals distinct CD4/CCR5 usage patterns among human immunodeficiency virus type 1 and simian immunodeficiency virus strains. J Virol. 2009;83(21):11016-26.

54. Si Z, Madani N, Cox JM, Chruma JJ, Klein JC, Schon A, et al. Small-molecule inhibitors of HIV-1 entry block receptor-induced conformational changes in the viral envelope glycoproteins. Proc Natl Acad Sci U S A. 2004;101(14):5036-41.

55. Moore PL, Gray ES, Choge IA, Ranchobe N, Mlisana K, Abdool Karim SS, et al. The c3-v4 region is a major target of autologous neutralizing antibodies in human immunodeficiency virus type 1 subtype C infection. J Virol. 2008;82(4):1860-9.

56. Bowley DR, Labrijn AF, Zwick MB, Burton DR. Antigen selection from an HIV-1 immune antibody library displayed on yeast yields many novel antibodies compared to selection from the same library displayed on phage. Protein Eng Des Sel. 2007;20(2):81-90.

57. Baba M, Nishimura O, Kanzaki N, Okamoto M, Sawada H, Iizawa Y, et al. A small-molecule, nonpeptide CCR5 antagonist with highly potent and selective anti-HIV-1 activity. Proc Natl Acad Sci U S A. 1999;96(10):5698-703. PMCID: 21923.

58. Binley JM, Wrin T, Korber B, Zwick MB, Wang M, Chappey C, et al. Comprehensive cross-clade neutralization analysis of a panel of anti-human immunodeficiency virus type 1 monoclonal antibodies. J Virol. 2004;78(23):13232-52.

59. Dunfee R, Thomas ER, Gorry PR, Wang J, Ancuta P, Gabuzda D. Mechanisms of HIV-1 neurotropism. Curr HIV Res. 2006;4(3):267-78.

60. Gartner S, McDonald RA, Hunter EA, Bouwman F, Liu Y, Popovic M. Gp120 sequence variation in brain and in T-lymphocyte human immunodeficiency virus type 1 primary isolates. J Hum Virol. 1997;1(1):3-18.

61. Ohagen A, Devitt A, Kunstman KJ, Gorry PR, Rose PP, Korber B, et al. Genetic and functional analysis of full-length human immunodeficiency virus type 1 env genes derived from brain and blood of patients with AIDS. J Virol. 2003;77(22):12336-45.

62. Power C, McArthur JC, Johnson RT, Griffin DE, Glass JD, Dewey R, et al. Distinct HIV-1 env sequences are associated with neurotropism and neurovirulence. Curr Top Microbiol Immunol. 1995;202:89-104.

63. Lamers SL, Salemi M, Galligan DC, de Oliveira T, Fogel GB, Granier SC, et al. Extensive HIV-1 intra-host recombination is common in tissues with abnormal histopathology. PLoS One. 2009;4(3):e5065.

64. Poon AF, Lewis FI, Pond SL, Frost SD. Evolutionary interactions between N-linked glycosylation sites in the HIV-1 envelope. PLoS Comput Biol. 2007;3(1):e11. PMCID: 1779302.

65. Olivieri KC, Agopian KA, Mukerji J, Gabuzda D. Evidence for adaptive evolution at the divergence between lymphoid and brain HIV-1 nef genes. AIDS Res Hum Retroviruses. 2010;26(4):495-500. PMCID: 2933169.

66. Huang KJ, Alter GM, Wooley DP. The reverse transcriptase sequence of human immunodeficiency virus type 1 is under positive evolutionary selection within the central nervous system. J Neurovirol. 2002;8(4):281-94.

67. Gray LR, Gabuzda D, Cowley D, Ellett A, Chiavaroli L, Wesselingh SL, et al. CD4 and MHC class 1 down-modulation activities of nef alleles from brain- and lymphoid tissue-derived primary HIV-1 isolates. J Neurovirol. 2011;17(1):82-91.

68. Mefford ME, Gorry PR, Kunstman K, Wolinsky SM, Gabuzda D. Bioinformatic prediction programs underestimate the frequency of CXCR4 usage by R5X4 HIV type 1 in brain and other tissues. AIDS Res Hum Retroviruses. 2008;24(9):1215-20.

69. Shapshak P, Segal DM, Crandall KA, Fujimura RK, Zhang BT, Xin KQ, et al. Independent evolution of HIV type 1 in different brain regions. AIDS Res Hum Retroviruses. 1999;15(9):811-20.

70. Anand R, Thayer R, Srinivasan A, Nayyar S, Gardner M, Luciw P, et al. Biological and molecular characterization of human immunodeficiency virus (HIV-1BR) from the brain of a patient with progressive dementia. Virology. 1989;168(1):79-89.

71. Liu Y, Tang XP, McArthur JC, Scott J, Gartner S. Analysis of human immunodeficiency virus type 1 gp160 sequences from a patient with HIV dementia: evidence for monocyte trafficking into brain. J Neurovirol. 2000;6 Suppl 1:S70-81.

72. Brown RJ, Peters PJ, Caron C, Gonzalez-Perez MP, Stones L, Ankghuambom C, et al. Intercompartmental recombination of HIV-1 contributes to env intrahost diversity and modulates viral tropism and sensitivity to entry inhibitors. J Virol. 2011;85(12):6024-37. PMCID: 3126287.

73. Poon AF, Frost SD, Pond SL. Detecting signatures of selection from DNA sequences using Datamonkey. Methods Mol Biol. 2009;537:163-83.

74. Keele BF, Tazi L, Gartner S, Liu Y, Burgon TB, Estes JD, et al. Characterization of the follicular dendritic cell reservoir of human immunodeficiency virus type 1. J Virol. 2008;82(11):5548-61.

75. Morris A, Marsden M, Halcrow K, Hughes ES, Brettle RP, Bell JE, et al. Mosaic structure of the human immunodeficiency virus type 1 genome infecting lymphoid cells and the brain: evidence for frequent in vivo recombination events in the evolution of regional populations. J Virol. 1999;73(10):8720-31.

76. Hughes ES, Bell JE, Simmonds P. Investigation of the dynamics of the spread of human immunodeficiency virus to brain and other tissues by evolutionary analysis of sequences from the p17gag and env genes. J Virol. 1997;71(2):1272-80.

77. Monken CE, Wu B, Srinivasan A. High resolution analysis of HIV-1 quasispecies in the brain. Aids. 1995;9(4):345-9.

78. Pikora C, Wittish C, Desrosiers RC. Identification of two N-linked glycosylation sites within the core of the simian immunodeficiency virus glycoprotein whose removal enhances sensitivity to soluble CD4. J Virol. 2005;79(19):12575-83.

79. Igarashi T, Imamichi H, Brown CR, Hirsch VM, Martin MA. The emergence and characterization of macrophage-tropic SIV/HIV chimeric viruses (SHIVs) present in CD4+ T cell-depleted rhesus monkeys. J Leukoc Biol. 2003;74(5):772-80.

80. Huang X, Jin W, Hu K, Luo S, Du T, Griffin GE, et al. Highly conserved HIV-1 gp120 glycans proximal to CD4-binding region affect viral infectivity and neutralizing antibody induction. Virology. 2012;423(1):97-106.

81. Musich T, Peters PJ, Duenas-Decamp MJ, Gonzalez-Perez MP, Robinson J, Zolla-Pazner S, et al. A conserved determinant in the V1 loop of HIV-1 modulates the V3 loop to prime low CD4 use and macrophage infection. J Virol. 2011;85(5):2397-405. PMCID: 3067776.

82. Watkins JD, Diaz-Rodriguez J, Siddappa NB, Corti D, Ruprecht RM. Efficiency of neutralizing antibodies targeting the CD4-binding site: influence of conformational masking by the V2 loop in R5-tropic clade C simian-human immunodeficiency virus. J Virol. 2011;85(23):12811-4. PMCID: 3209380.

83. Liu L, Cimbro R, Lusso P, Berger EA. Intraprotomer masking of third variable loop (V3) epitopes by the first and second variable loops (V1V2) within the native HIV-1 envelope glycoprotein trimer. Proc Natl Acad Sci U S A. 2011;108(50):20148-53. PMCID: 3250183.

84. Kolchinsky P, Kiprilov E, Sodroski J. Increased neutralization sensitivity of CD4-independent human immunodeficiency virus variants. J Virol. 2001;75(5):2041-50.

85. Li Y, Cleveland B, Klots I, Travis B, Richardson BA, Anderson D, et al. Removal of a single N-linked glycan in human immunodeficiency virus type 1 gp120 results in an enhanced ability to induce neutralizing antibody responses. J Virol. 2008;82(2):638-51. PMCID: 2224603.

86. Zhang W, Godillot AP, Wyatt R, Sodroski J, Chaiken I. Antibody 17b binding at the coreceptor site weakens the kinetics of the interaction of envelope glycoprotein gp120 with CD4. Biochemistry. 2001;40(6):1662-70.

87. Pantophlet R, Ollmann Saphire E, Poignard P, Parren PW, Wilson IA, Burton DR. Fine mapping of the interaction of neutralizing and nonneutralizing monoclonal antibodies with the CD4 binding site of human immunodeficiency virus type 1 gp120. J Virol. 2003;77(1):642-58.

88. Ly A, Stamatatos L. V2 loop glycosylation of the human immunodeficiency virus type 1 SF162 envelope facilitates interaction of this protein with CD4 and CCR5 receptors and protects the virus from neutralization by anti-V3 loop and anti-CD4 binding site antibodies. J Virol. 2000;74(15):6769-76.

89. Haim H, Si Z, Madani N, Wang L, Courter JR, Princiotto A, et al. Soluble CD4 and CD4-mimetic compounds inhibit HIV-1 infection by induction of a short-lived activated state. PLoS Pathog. 2009;5(4):e1000360.

90. Haim H, Strack B, Kassa A, Madani N, Wang L, Courter JR, et al. Contribution of intrinsic reactivity of the HIV-1 envelope glycoproteins to CD4-independent infection and global inhibitor sensitivity. PLoS Pathog. 2011;7(6):e1002101. PMCID: 3121797.

91. Madani N, Perdigoto AL, Srinivasan K, Cox JM, Chruma JJ, LaLonde J, et al. Localized changes in the gp120 envelope glycoprotein confer resistance to human immunodeficiency virus entry inhibitors BMS-806 and #155. J Virol. 2004;78(7):3742-52.

92. Saphire EO, Parren PW, Barbas CF, 3rd, Burton DR, Wilson IA. Crystallization and preliminary structure determination of an intact human immunoglobulin, b12: an

antibody that broadly neutralizes primary isolates of HIV-1. Acta Crystallogr D Biol Crystallogr. 2001;57(Pt 1):168-71.

93. van Marle G, Power C. Human immunodeficiency virus type 1 genetic diversity in the nervous system: evolutionary epiphenomenon or disease determinant? J Neurovirol. 2005;11(2):107-28.

94. Ritola K, Robertson K, Fiscus SA, Hall C, Swanstrom R. Increased human immunodeficiency virus type 1 (HIV-1) env compartmentalization in the presence of HIV-1-associated dementia. J Virol. 2005;79(16):10830-4. PMCID: 1182623.

Chapter 3: Spontaneous Shedding of Soluble gp120 from Primary HIV Envelopes Is Associated with Enhanced Infection of Cells Expressing Low CD4 and Activation of Bystander Cells

Megan E. Mefford[a], Elaine Thomas[a], Paul J. Peters[b], Kevin Kunstman[c], Steven M. Wolinsky[c], Paul R. Clapham[b], and Dana Gabuzda[a, d]

[a]Department of Cancer Immunology and AIDS, Dana-Farber Cancer Institute, Boston, MA, USA
[b]Center for AIDS Research, Program in Molecular Medicine and Department of Molecular Genetics and Microbiology, 373 Plantation Street, University of Massachusetts Medical School, Worcester, Massachusetts 01605
[c]Northwestern University Medical School, Chicago, IL, USA
[d]Department of Neurology, Harvard Medical School, Boston, MA, USA

SUPPLEMENTARY DATA FOR CHAPTER 3 IS LOCATED
IN APPENDIX A ON PAGE 182.

ABSTRACT

The HIV envelope glycoprotein (Env) soluble gp120 (sgp120) subunit induces biological effects *in vitro,* that include activation of signaling pathways and proinflammatory cytokine production in bystander T cells and macrophages and altered T cell migration. Sgp120 shedding from HIV virions and infected cells can occur spontaneously due to weak noncovalent interactions with gp41 or be induced following Env binding to CD4. Although sgp120 has been detected in plasma and tissues from HIV-infected individuals by ELISA, the range and variability of sgp120 shedding from primary Envs in patients is unknown. Here, we analyzed spontaneous sgp120 shedding from primary *env* clones and explored the biological significance of these findings. Full-length *env* genes (n = 65 Envs)were amplified from brain and lymphoid tissue from 12 AIDS patients and spontaneous sgp120 shedding was quantified by Western blotting and ELISA. Relationships between shedding and biological data were examined. Sgp120 shedding from primary brain and lymphoid Envs was highly variable within and between patients, representing a spectrum rather than a categorical phenotype, with concentrations overlapping those shown to induce biological effects *in vitro*. Brain Envs with high sgp120 shedding exhibited enhanced fusion and infection with cells expressing low CD4 and an increased capacity to induce T cell activation during infection of PBMC, despite similar levels of viral replication. Genetic analysis demonstrated greater entropy and positive selection in Envs with high versus low levels of sgp120 shedding, suggesting that diversifying evolution influences gp120-gp41 association. These findings suggest that increased spontaneous shedding of sgp120 may be a viral phenotype that contributes to HIV pathogenesis by enhancing bystander T cell activation.

INTRODUCTION

The HIV envelope glycoproteins (Env) bind to CD4 and CCR5 or CXCR4 on target cells, resulting in fusion and viral entry. The multimeric Env complex, which consists of surface-exposed gp120 subunits held together by noncovalent interactions with transmembrane gp41 subunits, is organized into trimeric spikes on the surface of virions and infected cells (4-5). HIV entry is mediated by high affinity interactions between gp120 and CD4, triggering a cascade of conformational changes that include formation and exposure of the coreceptor binding site and the gp41 prehairpin conformation. Subsequent binding of CD4-bound gp120 to CCR5 or CXCR4 triggers formation of the gp41 6-helix bundle and initiates membrane fusion (6). The relatively weak interactions mediating gp120 association with gp41 allow the soluble gp120 (sgp120) subunit to be readily shed from Env trimers, either spontaneously or following receptor binding. Spontaneous dissociation of sgp120 occurs in a subset of Envs and is influenced by viral determinants in regions important for gp120-gp41 association (7-10). Sgp120 shedding can also be induced in a strain-dependent manner following binding of gp120 to the soluble subunit form of CD4 (sCD4) *in vitro* (11-18).

Many studies have demonstrated that sgp120 can induce biological effects *in vitro* (19-29), but the relevance of these results to pathogenesis *in vivo* is unknown. Sgp120 has been detected by ELISA in plasma and tissues from a subset of AIDS patients and SHIV-infected macaques. Sgp120 concentrations detected in plasma range from less than 20 to 800 pM, depending on the ELISA protocol and stage of HIV infection, and in excess of 4 nM in lymph nodes and spleen (21, 30-34). Purified sgp120 at concentrations overlapping those detected *in vivo* has been shown to induce many biological effects *in vitro*. Sgp120 binds to CD4 on uninfected T cells and macrophages, resulting in cellular activation and production of

proinflammatory cytokines (21-23, 35-40). In one study, sgp120 concentrations measured by ELISA in plasma from patients in the early stages of HIV infection correlated with higher levels of plasma IL-6, IL-10, and TNF-α compared to subjects without detectable sgp120 in plasma (21). Sgp120-induced activation of T cells and macrophages can induce apoptosis of uninfected T cells and neurons, (19-20, 24-26, 35, 39, 41-45), a mechanism proposed to contribute to T-cell depletion and the development of HIV-associated neurological disorders (HAND) (19-20, 46). Furthermore, incubation of T cells and dendritic cells with purified sgp120 alters cell chemotaxis and migration (27-29). While these studies suggest a potential role for sgp120 in chronic activation and immune system dysfunction, no studies have conclusively demonstrated that sgp120 contributes to HIV pathogenesis *in vivo*.

The majority of *in vitro* studies investigating sgp120-induced biological effects used sgp120 purified from lab-adapted HIV isolates that were adapted to grow on immortalized T-cell lines (23-26, 35, 38, 42, 47-48). However, Envs from primary HIV isolates differ markedly from lab-adapted Envs. For example, lab-adapted isolates are more sensitive to neutralization by polyclonal sera from HIV-infected individuals, monoclonal antibodies, and recombinant sCD4 (11, 49), suggesting they adopt conformations in which gp120 neutralization epitopes that are normally concealed on primary Envs are exposed. Therefore, biological effects induced by sgp120 from lab-adapted strains may not be indicative of the ability of primary Envs to contribute to HIV pathogenesis. Furthermore, *in vitro* studies often use sgp120 derived from a single HIV isolate to analyze biological effects (23-26, 35-36, 38, 43-45, 47-48). While some studies utilized purified sgp120 from 2-5 isolates (27-28, 39, 47, 50-52), the range and variability of spontaneous sgp120 shedding from primary Envs is unknown.

Here, we investigated spontaneous shedding of sgp120 from 65 primary HIV Envs cloned from brain and lymphoid tissues from 12 AIDS patients. We demonstrate that spontaneous shedding of sgp120 from primary brain and lymphoid Envs is highly variable within and between patients, representing a spectrum rather than a categorical phenotype. Sgp120 concentrations shed by a subset of brain and lymphoid Envs overlapped concentrations previously shown to induce biological effects *in vitro*. Brain Envs with high sgp120 shedding mediated enhanced fusion and infection with cells expressing low CD4, and viruses expressing these Envs demonstrated an increased capacity to induce lymphocyte activation during infection of PBMC despite similar levels of viral replication. Genetic analysis demonstrated greater entropy and positive selection in Envs with high versus low levels of shedding, suggesting that diversifying evolution influences gp120-gp41 association. These findings suggest that increased spontaneous shedding of sgp120 may be a viral phenotype that contributes to pathogenesis by enhancing T cell activation.

MATERIALS AND METHODS

Cells and HIV Env clones. 293T and TZM-bl cells were cultured in DMEM media supplemented with 10% (vol/vol) fetal bovine serum (FBS) and 100 μg/ml penicillin and streptomycin. CF2-Luc cells, which are derived from canine thymocyte cell line CF2th and stably express firefly luciferase under control of HIV-1 LTR, were cultured in medium supplemented with 0.7 mg/ml G418 (Mediatech, Herndon, VA) (53-54). Affinofile cells were cultured in DMEM supplemented with 10% dialyzed FBS (Gibco), 100 μg/ml penicillin and streptomycin, and 50 μg/ml blasticidin S HCl (Invitrogen) (55). All primary clade B *env* genes were amplified directly from brain and lymphoid tissue as previously described. Briefly, primary *env* genes from AIDS patients UK1, UK7, MACS2 (M2), MACS3 (M3), and MACS1 (M1) were cloned into pCR3.1 (1-2, 56). Primary *env* genes from AIDS patients A, B, C, and D were subcloned into pSVIIIenv using the KpnI to BamHI fragment (57). Primary *env* genes from AIDS patients NA118, NA20, and NA420 were cloned into pSVIIIenv using the KpnI to KpnI fragment (3). Reference Envs, including primary Envs ADA, YU2, JRFL, and JRCSF, and lab-adapted Env HXB2, were cloned into pcDNA3.1 (Invitrogen, Grand Island, NY). TZM-bl cells were provided by Norm Letvin. Affinofile cells were provided by Benhur Lee. NA118, NA20, and NA420 Env expression plasmids were provided by Paul Clapham.

Detection of sgp120 shedding by Western blotting. 293T cells were transfected with pCR3.1Env or pSVIIIEnv plus pLTR-Tat at a 1:10 ratio using calcium phosphate transfection (1, 53, 58-59). Cells were washed after 18 hours and incubated in media containing 0.3 μg/ml sodium butyrate. Cell lysates and supernatant were collected after 48 hours, centrifuged for 5 minutes at 2000 rpm to remove cell debris, and stored at -80ºC prior to analysis. Gp120 in cell

lysates and supernatants was detected by Western blotting with polyclonal rabbit anti-gp120 (American Biotechnologies Inc.), a pool of 2 patient sera and monoclonal human anti-gp120 (Immunodiagnostics, Woburn, MA), or a pool of monoclonal antibodies 2G12 (NIH AIDS Research and Reference Reagent Program, Division of AIDS, NIAID, NIH, from Dr. Hermann Katinger), b12 (NIH AIDS Research and Reference Reagent Program, Division of AIDS, NIAID, NIH, from Dr. Dennis Burton and Carlos Barbas), and human anti-gp120 (60). Bands were visualized using Pierce ECL Western Blotting Substrate (Thermo Scientific, Billerica, MA). Blots were scanned into Photoshop to analyze mean band intensity. Results are presented as % sgp120 shedding, calculated as [sgp120 (supernatant)/gp120 (lysate)] x 100. All results are representative of at least 3 independent experiments.

ELISA. The ELISA assay was based on previously described methods (59, 61-62) with several modifications. Briefly, 96-well microplates were coated overnight with sheep antibody D7324 at 5 μg/ml in PBS (AALTO Bioproducts, Ltd., Ireland). Wells were washed 3 times with PBS supplemented with 2.5% Tween-20 (PBS-T) and blocked for 1 hour at room temperature with PBS-T supplemented with 3% BSA. Supernatants were incubated in the wells for 3 hours, followed by 10 washes with PBS-T and 1 hour incubation with polyclonal rabbit anti-gp120 (American Biotechnologies Inc.). After 10 more washes with PBS-T, wells were incubated with anti-rabbit-HRP (GE Healthcare). The reaction was developed using BM chemiluminescence ELISA substrate (Roche) according to the manufacturer's instructions. The reaction was read on a luminometer (Viktor2, Perkin Elmer, Waltham, MA). Calculations of sgp120 concentrations were based on a standard curve of purified HIV_{IIIB} (Immunodiagnostics). Background calculated from 293T cells transfected with empty pcDNA3.1 was subtracted from each well.

Entry Assays. HIV luciferase reporter viruses were generated by cotransfection of 293T cells with pNL4-3ΔenvLuc, an HIV provirus with *env* deleted and *nef* replaced with luciferase, and an Env-expression plasmid as described (53). To investigate sgp120 shedding following incubation at 37ºC, 10^4 ^{3}H cpm reverse transcriptase (RT) units of virus stock were incubated at 37ºC for 0, 2, or 6 hours prior to infection of TZM-BL cells seeded into 96-well plates. Cells were lysed with passive lysis buffer (Promega) after 48 hours of incubation and virus infection was quantified by luciferase activity (Promega). Affinofile cells were seeded into 96-well plates and treated for 20 hours with serial dilutions of 0-3 ng/ml doxycycline (Clontech, Mountain View, CA) to induce CD4 expression and 0-2 μM Ponasterone A (Invitrogen) to induce CCR5 expression (55). Cells were then infected with 10^4 RT units of virus stock, lysed 2 days post-infection, and assayed for luciferase activity. Cell surface CD4 and CCR5 levels were analyzed by collecting cells with 5 mM EDTA in PBS and staining with anti-CD4-PE (BD Biosciences, San Jose, CA) and anti-CCR5-PE (BD Pharmingen, San Diego, CA). Cell surface staining was analyzed using a FACSCantoII flow cytometer (BD Biosciences). The approximate number of CD4 and CCR5 molecules per cell was calculated using FACS analysis of Quantibrite beads according to manufacturer's instructions (BD Biosciences). Mock infected cells were used as negative controls. Single-round infection of CF2th CD4+/CCR5+ cells, HeLa hiCD4/hiCCR5 cells, and monocyte-derived macrophages (MDM) were previously described (1, 3).

Fusion Assays. 293T cells were cotransfected with 2 μg Env-expression plasmid and 0.2 μg pLTR-Tat using calcium phosphate. Cf2-Luc cells were cotransfected with 0.1 (low) or 10 μg (high) amounts of pcDNA3-CD4 and 10 μg (high) pcDNA3-CCR5 using Lipofectamine 2000 (Invitrogen). Cell surface expression levels of CD4 and CCR5 were verified by flow cytometry as described for Affinofile cells. 2.5×10^4 293T cells and 2.5×10^5 CF2-Luc cells were mixed in 48-well plates and incubated for 8 hours. Cells were then lysed and analyzed for luciferase activity. 293T cells cotransfected with a nonfunctional Env (pSVIII-ΔKSenv) and pLTR-Tat were used to determine background levels of luciferase.

PBMC Activation Assays. Healthy HIV-/HCV- donor blood provided by Research Blood Components (Boston, MA) was collected into EDTA vacutainer tubes. The protocol for obtaining blood was approved by the Dana-Farber Cancer Institute IRB. After collection, 10 ml of fresh blood were diluted 1:1 with PBS and layered over 15 ml Ficoll Histopaque 1077 (Sigma) and spun at 2000 × g for 20 min at room temperature. 5 ml of PBMC containing serum were collected at the interface and diluted with 20 ml of PBS. The diluted cells were pelleted at 1000 × g for 10 min at 4°C, resuspended in 10 ml of PBS, and pelleted again at 1000 × g for 10 min. The cell pellet was resuspended in 10 mls of RPMI-1640 (Invitrogen) and pelleted at 1000 × g for 10 min. Cells were counted and resuspended at 2×10^6/ml in RPMI-1640 with 10% FBS and 100 μg/ml penicillin/streptomycin. PBMC were incubated with a low concentration of PHA (1 ug/ml) for 2 days, followed by a 24 hour incubation with a low concentration of human IL-2 (10 U/ml). 250,000 cells were incubated in round-bottom 96-well plates with 10,000 ^{3}H cpm RT units of virus stock for 3 h at 37^{o}C. Fifty percent medium changes were performed every 3 to 4 days for 14 days and replication was monitored by p24 antigen ELISA (Perkin Elmer, Boston,

MA). Cells were collected for FACS analysis at days 3, 6, 10, and 14 post-infection and stained with combinations of anti-CD3-PE-Cy5, anti-CD4-FITC, anti-CD8-PE, anti-CD25-APC-Cy7, anti-HLA-DR-PE, anti-CD69-PE-Cy5, anti-TNF-α-APC, anti-IL-1β-PE, and anti-IL-6-V450 (BD Biosciences) to monitor cell activation. Alternatively, cells were stained with a combination of anti-CD4-FITC or anti-CD8-FITC, Annexin V V450, and 7-AAD (BD Biosciences) to monitor apoptosis. Fluorescent cells were detected using a FACSCantoII flow cytometer (BD Biosciences). Data were analyzed using FACSDiva software (BD Biosciences).

Sequence Analysis. Primary brain and blood/lymphoid-derived Envs were characterized as high shedding (% sgp120 shedding >20%) or low shedding (% sgp120 shedding <20%) based on Western blotting. Gp160 nucleotide and protein sequences for both groups were aligned using ClustalX2. The entropy at each position in the protein alignment was measured with Shannon's entropy using EntropyOne (LANL). Detection of N-linked glycosylation sites was performed with Glycosite (LANL). Selection pressures over gp160 for each group were examined with methods available on the datamonkey web server. Three different approaches were used to identify codons under positive selection: single likelihood ancestor counting (SLAC), fixed-effects likelihood (FEL), and internal fixed effects likelihood (IFEL). SLAC and FEL detect sites under selection at the external branches of the phylogenetic tree, while IFEL identifies sites along the internal branches (63-65). Sites were classified as positively selected with $p<0.1$ at least 2 methods. Bootstrapped phylogenetic trees for each group were created by the neighbor-joining method using ClustalX2 and visualized using Treeview.

Statistical Analysis. Data were analyzed using analysis of variance (ANOVA), Mann Whitney test, unpaired *t* test with Welch's correction, and Spearman correlation using GraphPad Prism software. Differences were considered significant at $p \leq 0.05$.

RESULTS

Characteristics of Study Subjects and Envelope Clones. Low concentrations (<100 ng/ml) of purified HIV sgp120 can induce apoptosis of uninfected neurons *in vitro* (19, 41-45), a mechanism proposed to contribute to the development of HIV-associated neurological disorders (HAND) (19, 46). However, sgp120 shedding from HIV in the brain has not been examined. Given that, HIV adaptation to macrophages, which express low levels of CD4 and are the main target cells for infection in the brain, can result in adoption of more "open" Env conformations (1, 3, 53, 58, 66-69) that enhance gp120-receptor interactions, but may also may increase spontaneous shedding of sgp120 (5, 7-8). We predicted that HIV Envs in the brain would shed sgp120 at higher levels than Envs in blood/lymphoid tissues. To address this question, we compiled a panel of 65 primary Envs cloned from brain and blood or lymphoid tissue (hereafter referred to as lymphoid) from 12 AIDS patients that were previously characterized for biological functions including cell tropism and neutralization sensitivity (1, 3, 56-57). Viral loads from these tissues ranged from 301 to 100,841 HIV copies per million cells (Table S3.1). As detailed in Table 3.1, 7 patients were diagnosed with HAD and 8 patients showed evidence of HIV encephalitis (1, 3, 56-57, 70). All samples were collected prior to the advent of the HAART era; the patients received limited or no antiretroviral therapy. There were an average of 4 brain and 4 lymphoid Envs per patient (range 1-5 Envs from brain and lymphoid tissue per patient). Mean pairwise genetic distance of *env* clones from each tissue within each patient ranged from 0.002 to 0.057 and was independent of tissue viral load (Table S3.1 and data not shown). There was evidence of genetic compartmentalization between Envs from brain and lymphoid tissues ($p<0.1$, Slatkin-Maddison) for 5 patients (Table S3.1). As reference controls we used a panel of 5 well-

characterized Envs (primary Envs ADA, YU2, JRFL and JRCSF, and lab-adapted Env HXB2) for which spontaneous levels of sgp120 shedding were previously reported (9, 18, 71-72).

Table 3.1. Clinical Characteristics of 12 AIDS Patients

Patient[a]	Risk Factor[b]	Clinical Dementia	HIV Encephalitis	Coreceptor Usage[c]	# SGA Clones		Source
					Brain	LN/SP/BL[d]	
M2[e]	MSM	Severe	Moderate	R5	4	3	Thomas 2007
M3[e]	MDM	Severe	Moderate	R5	3	3	Thomas 2007
UK1	IVDU	Severe	Moderate	R5	5	3	Thomas 2007
UK7	IVDU	Severe	Severe	R5	5	1	Thomas 2007
M1[e]	MSM	Yes	Severe	R5X4	3	1	Mefford 2008
NA118	IVDU	Yes	Severe	R5	1	2	Peters 2004
NA20	Hemophilia	Mild	Mild	R5	3	5	Peters 2004
NA420	IVDU	No	Mild	R5	3	2	Peters 2004
A	MSM	No	No	R5, X4	2	2	Ohagen 2003
B	MSM	No	No	R5	2	2	Ohagen 2003
C	MSM	No	No	R5	2	2	Ohagen 2003
D	MSM	No	No	R5X4	1	5	Ohagen 2003

[a]All samples were taken in the pre-HAART era and patients received either no ART or single drug regimens (1-2, 70)
[b] MSM, men who have sex with men; IVDU, intravenous drug user
[c] R5, CCR5; X4, CXCR4; R5X4, dual tropic (CCR5 and CXCR4)
[d] LN, lymph node; SP, spleen; BL, blood
[e] M2, MACS2; M3, MACS3; M1, MACS1

Spontaneous shedding of sgp120 from primary brain and lymphoid Envs is highly variable within and between patients. To investigate levels of spontaneous sgp120 shedding from primary Envs, sgp120 levels in supernatants and cell lysates from 293T cells transfected with Env-expression plasmids were analyzed by Western blotting (Fig. 3.1A). Median levels of spontaneous sgp120 shedding were highly variable between patients (Fig. 3.1B; $p<0.0001$, ANOVA). Percent sgp120 shedding relative to gp120 levels in cell lysates ranged from 24.4% to 97.8% for the reference control Envs and 0% to 84.6% for the panel of primary Envs. At least 1 Env from 10 of the subjects had high levels of spontaneous sgp120 shedding, while Envs from the remaining 2 subjects exhibited little to no sgp120 shedding. Further analysis demonstrated a range of sgp120 shedding levels for the primary and control Envs, independent of patient or tissue of origin (Fig. 3.1C, Table S3.2). Additionally, mean sgp120 shedding calculated for brain and lymphoid tissues within each patient did not correlate with tissue viral load or mean pairwise genetic distance of the *env* clones (Fig. S3.1, $p=0.4$, $r=0.3$ and $p=0.2$,$r=0.3$, respectively, Spearman correlation) (1). Sgp120 shedding into supernatants was not associated with levels of gp120 in cell lysates (Fig. S3.2B; $p=0.9$, $r=-0.01$). These results suggest sgp120 from primary Envs is highly variable both within and between patients, and represents a spectrum rather than a categorical phenotype.

Fig. 3.1. Detection of sgp120 spontaneously shed from primary brain and lymphoid Envs by Western blotting.
293T cells were transfected with Env-expression plasmids. Gp120 was detected in cell lysates and supernatants by Western blotting or ELISA following 48 hours of incubation. A) Representative Western blots depicting gp160 and gp120 bands in cell lysates (top gel) and supernatants (bottom gel) from 293T cells expressing brain and lymphoid Envs from 7 patients. Reference Envs depicted include ADA, YU2, and JRFL. B) Sgp120 shedding from 65 Envs from 12 AIDS patients and 5 reference Envs (ADA, YU2, JRFL, JRCSF, HXB2) detected by Western blotting were compared. Mean band intensity was determined using Photoshop. Percent sgp120 shedding was calculated as [sgp120 (supernatant)/gp120 (cell lysate)] x 100, with a range of 0% (no sgp120 detected in supernatant) to nearly 100% (equal amounts of sgp120 detected in supernatant and cell lysate). Scatter plots showing average % sgp120 shedding values from a minimum of 3 independent experiments were created using Graphpad Prism software. Brain Envs are depicted with red circles, lymphoid Envs with blue circles, and control Envs with black circles Median levels of sgp120 shedding (black lines) from combined brain and lymphoid Envs within each patient differed significantly (p>0.0001, ANOVA). C) Range of sgp120 shedding detected by Western blotting. Error bars represent standard deviations from at least 3 independent experiments. D) Median levels of sgp120 shedding were compared for brain and lymphoid Envs from patients diagnosed with or without clinical dementia. Median levels of shedding for each group are depicted with a line.

Fig. 3.1, Continued

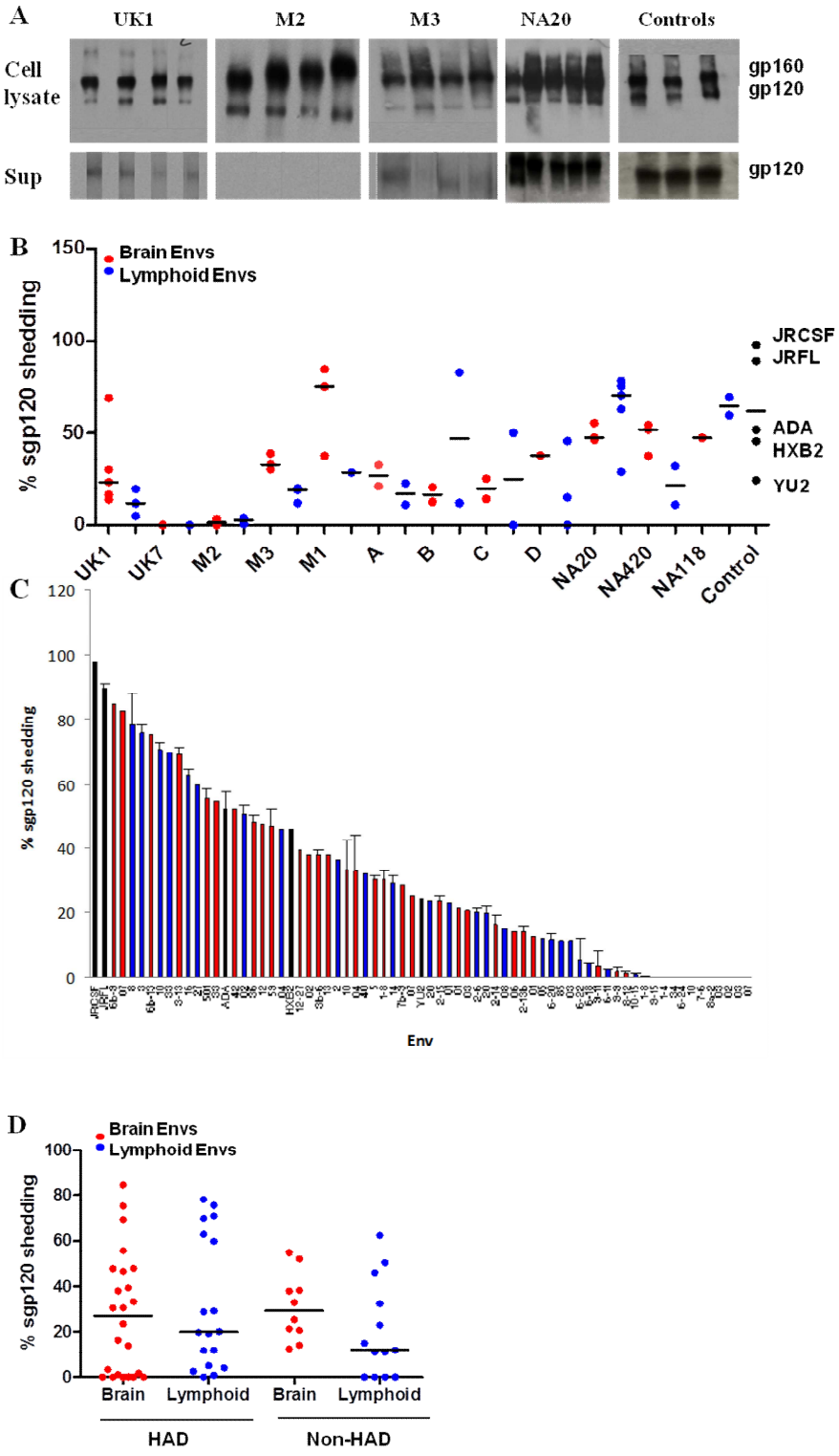

We also compared sgp120 shedding from brain-derived Envs from HAD compared to non-HAD patients. Overall, there was a trend towards higher levels of sgp120 shedding from brain compared to lymphoid Envs, although these differences did not reach statistical significance (Fig. 3.1D; p=0.5 and 0.09 for HAD and non-HAD patients, respectively, Mann Whitney). Furthermore, median levels of sgp120 shedding were similar for brain-derived Envs from patients with and without HAD (Fig. 3.1D). These results suggest that for patients with late-stage AIDS, Envs with high levels of sgp120 shedding are not significantly associated with brain infection or dementia.

Previous studies have used ELISAs to measure the concentration of sgp120 shed from viruses and cells (11, 60, 73-75). ELISA is a more sensitive method than Western blotting, but does not allow quantitation of gp120 levels in cell lysates to normalize results for differences in cell surface expression. To validate the results obtained by Western blotting, we compared detection of sgp120 in transfected 293T cell supernatants by Western blot and gp120 sandwich ELISA. Sgp120 concentrations in the cell supernatants detected by ELISA ranged from below the threshold of detection (1 ng/ml) to in excess of 1.5 ug/ml (Fig. 3.2A, Table S3.2) and median levels of sgp120 detected in supernatants were highly variable between patients (p<0.0001, ANOVA). The levels of sgp120 shedding detected in supernatants of transfected 293T cells by ELISA were consistent with those detected by Western blotting (Fig. 3.2B, p<0.0001, r=0.6, Spearman correlation). For 66.1% of the primary Envs, levels of sgp120 measured in supernatant exceeded concentrations shown to induce biological effects *in vitro* (27, 36, 41, 43-45, 50).

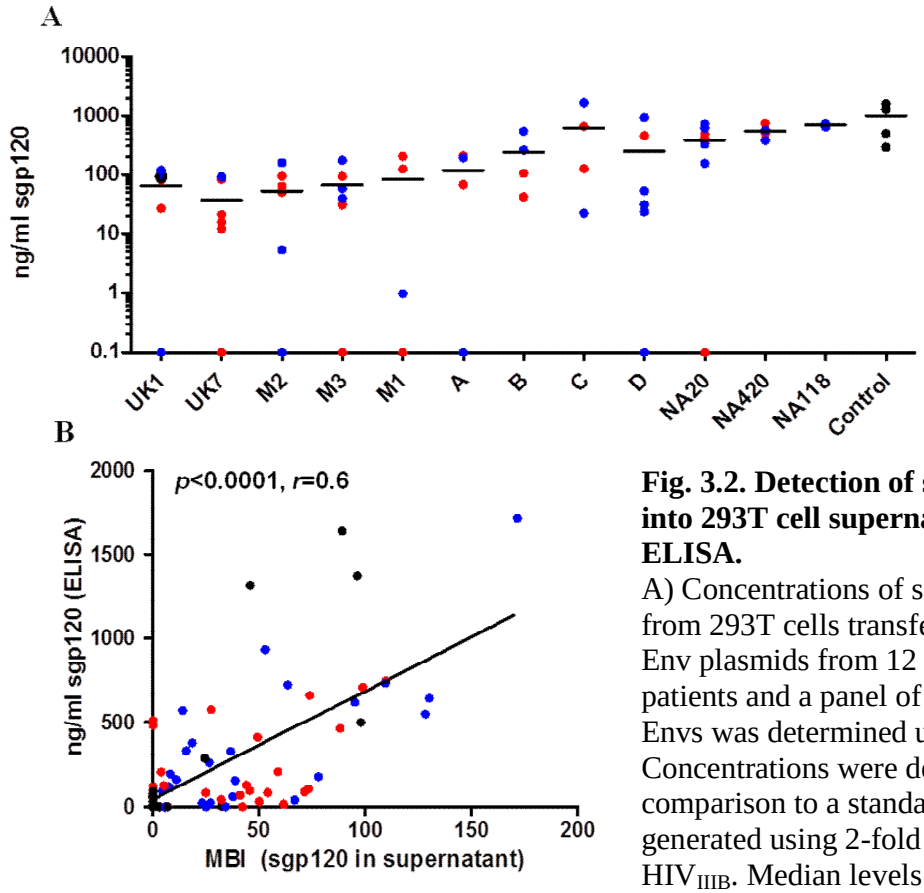

Fig. 3.2. Detection of sgp120 shed into 293T cell supernatants by ELISA.
A) Concentrations of sgp120 shed from 293T cells transfected with 65 Env plasmids from 12 AIDS patients and a panel of 5 reference Envs was determined using ELISA. Concentrations were determined by comparison to a standard curve generated using 2-fold dilutions of HIV_{IIIB}. Median levels of sgp120 shedding (black lines) from combined brain and lymphoid Envs within each patient differed significantly (p>0.0001, ANOVA). B) Comparison of methods of detection of sgp120 in supernatants of transfected 293T cells in a single representative experiment. P and R values were calculated using Spearman correlation on GraphPad Prism software.

High levels of sgp120 shedding are not associated with reduced infectivity. High levels of sgp120 shedding from primary Envs on virions can be detrimental to infectivity. Indeed, this was clearly seen for a series of mutants constructed in the YU2 Env in a study by Finzi et al, where Envs with the highest levels of sgp120 shedding had the lowest infectivity (Fig. S3.3) (7). However, when we compared sgp120 shedding from a subset of primary Envs to viral infectivity measured during single-round infection of CF2 CD4+/CCR5+ cells, we found no relationship. Incubation of virus at 37ºC has been shown to increase sgp120 dissociation of sgp120 from a subset of Envs (11, 60). Therefore, we examined the relationship between virus inactivation due

to increased sgp120 shedding at 37C and viral infectivity by analyzing infectivity of TZM-bl cells for HIV reporter viruses expressing a subset of the primary R5-tropic Envs (*n*=16 Envs from 7 patients; 8 Envs each from brain and lymphoid tissues) following incubation at 37ºC for 0, 2, or 6 hours. As previously reported, a wide range of infectivity was observed following 2 hours incubation at 37ºC (Fig. 3.3A). When Envs were divided into 2 groups based on tissue of origin, mean infectivity at both 2 and 6 hours was higher for viruses expressing brain compared to lymphoid Envs (Fig. 3.3B, *p*=0.01 and 0.02, respectively, unpaired *t* test with Welch's correction). These results suggest that high levels of sgp120 shedding from brain Envs are not necessarily detrimental to viral infectivity.

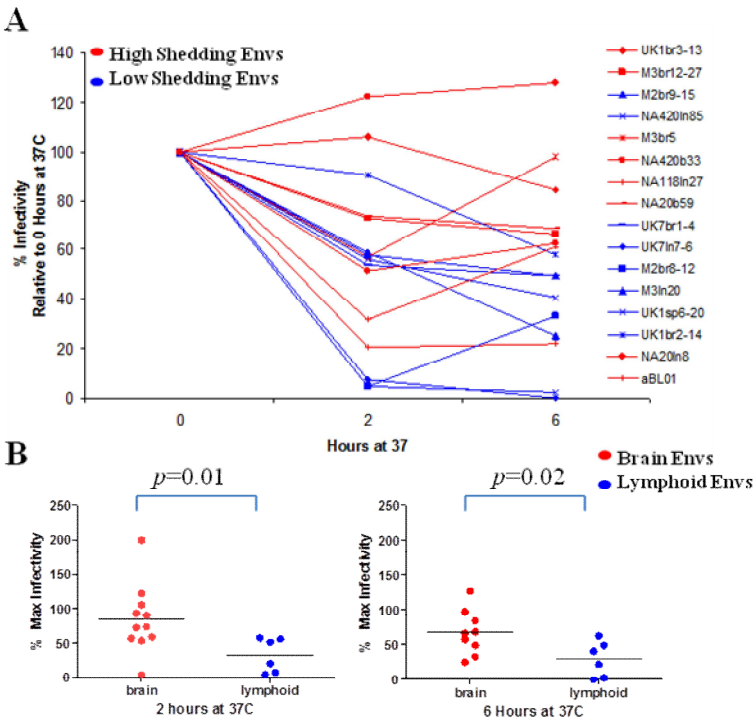

Fig. 3.3. Decreased infectivity following incubation at 37ºC is associated with tissue of origin but not levels of sgp120 shedding.
A) HIV luciferase reporter viruses pseudotyped with primary brain and lymphoid Envs from 7 patients were incubated at 0, 2, and 6 hours at 37ºC prior to infection of TZM-BL cells. Cells were lysed 48 hours after infection and assayed for luciferase activity. Envs with high levels of shedding (>20%) are shown in red and Envs with low levels of shedding (<20%) are shown in blue. B) Comparison of infectivity following 2 and 6 hours incubation at 37ºC for brain and lymphoid Envs. Lines depict mean % infectivity compared to viruses with no incubation at 37C for each group. P-values were calculated using unpaired t test with Welch's correction.

Brain Envs with high levels of spontaneous sgp120 shedding exhibit enhanced fusion and infection with cells expressing low CD4. Brain Envs have adapted to infect target cells expressing low levels of CD4 (50, 54, 58). One mechanism that influences this phenotype is increased exposure of the CD4 or CCR5 binding sites, a phenotype that may also increase sgp120 shedding (8, 66-69). To determine whether brain Envs with high levels of sgp120 shedding are associated with enhanced infection of cells expressing low CD4, we analyzed infection of Affinofile cells expressing low CD4 and CCR5 for viruses expressing a subset of matched brain and lymphoid primary Envs from 6 patients (n=14 Envs; 8 from brain and 6 from lymphoid tissues). Viruses expressing brain Envs mediated enhanced infection of cells expressing low CD4 and high CCR5 compared to lymphoid Envs (Fig. 3.4A, p=0.05). Viruses expressing lymphoid Envs mediated higher infection with cells expressing high CD4 and medium CCR5 compared to brain Envs, as previously reported (data not shown) (76). Further analysis revealed that Envs with high sgp120 shedding exhibited enhanced infection of cells expressing low CD4 compared to those with low sgp120 shedding (Fig. 3.4B, p=0.02). In this dataset, the majority of the brain Envs fell into the high shedding category. These results suggest that mechanisms used by brain Envs to utilize reduced CD4 for entry may decrease gp120-gp41 association.

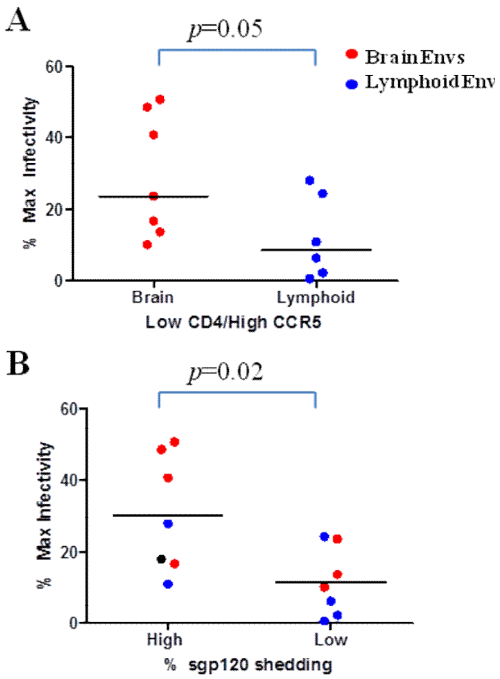

Fig. 3.4. Primary Envs from brain with high levels of sgp120 shedding are associated with enhanced infection of Affinofile cells expressing low CD4. Affinofile cells expressing low CD4 and high CCR5 were infected with HIV luciferase reporter viruses pseudotyped with primary brain and lymphoid Envs from 6 patients. Cells were lysed 48 hours after infection and assayed for luciferase activity. Brain Envs are shown in red and lymphoid Envs are shown in blue. A) Comparison of infectivity for brain and lymphoid Envs. Lines depict mean % infectivity of cells expressing high CD4 and CCR5. B) Comparison of infectivity for Envs grouped according to % sgp120 shedding (high shedding > 20%; low shedding < 20%). P-values were calculated using unpaired t test with Welch's correction.

Next, we examined the association between sgp120 shedding from brain and lymphoid Envs and interaction with cells expressing low CD4 using a larger dataset. Cell-cell fusion assays were performed with CF2Luc cells expressing low or high levels of CD4 (MFI low CD4 ≤15% MFI high CD4) and high CCR5 for Envs from 8 patients (n=44 Envs from 7 patients with HAD and 1 patient with no HAD). Results are presented as fusion with cells expressing low CD4/fusion with cells expressing high CD4 (Fig. 3.5A/B). There was an association between high levels of sgp120 shedding from CCR5-tropic brain but not lymphoid Envs and relative enhancement of fusion with cells expressing low CD4 compared to high CD4 (p= 0.02 and 0.47, respectively, Spearman correlation) (1). We then compared the relationship between sgp120 shedding from brain Envs and enhanced infection of cells expressing low CD4 using Envs from 7 patients (n=34 Envs from 6 patients with HAD and 1 patient with no HAD) (1, 3). Results are presented as infection of cells expressing low CD4/high CD4 (Fig. 3.5 C/D). There was a

correlation between brain Envs with high levels of shedding and enhanced infection of cells expressing low CD4 (p=0.01). Furthermore, an inverse correlation was observed between lymphoid Envs with high levels of shedding and infection of cells expressing low CD4 (p=0.01). Thus, the association between reduced CD4-dependence and high levels of sgp120 shedding may reflect CNS-specific adaptations.

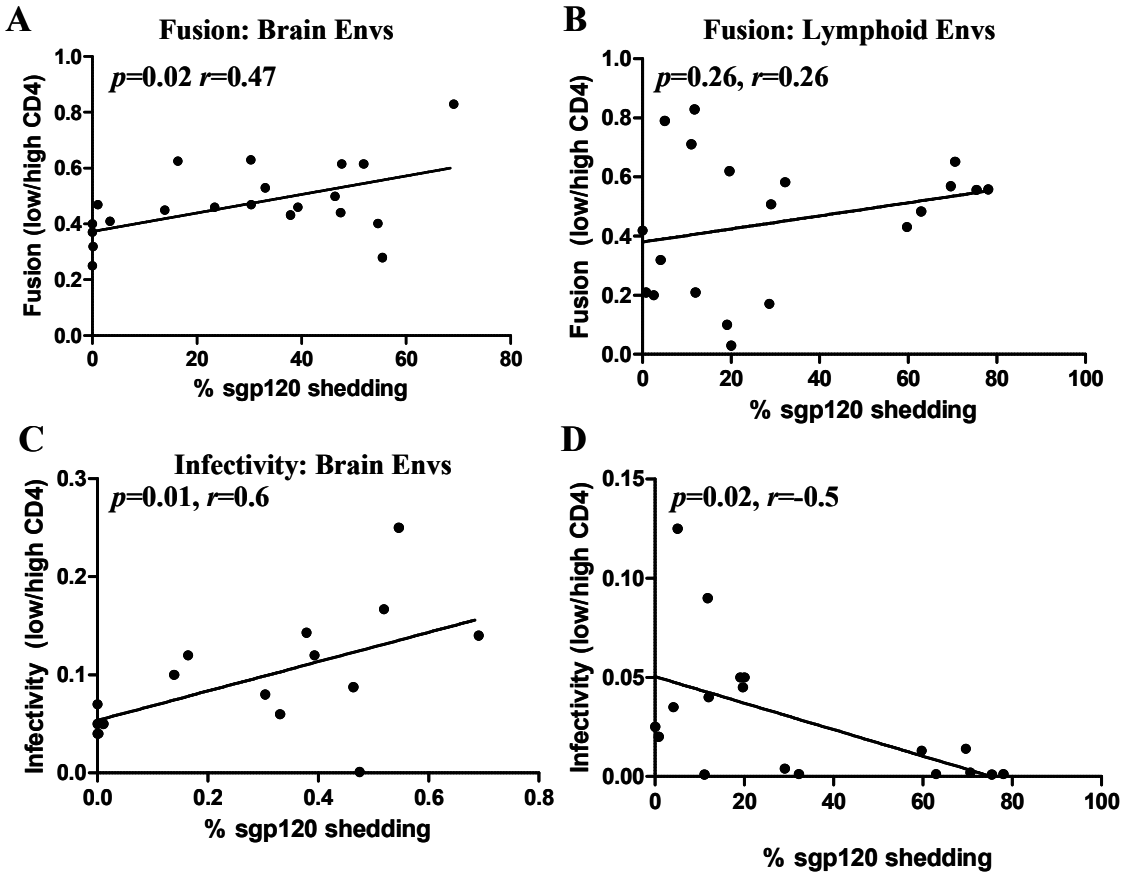

Fig. 3.5. Association between brain Envs with high levels of sgp120 shedding and enhanced fusion and infection of cells expressing low CD4.
Percent sgp120 shedding from 293T cells transfected with primary brain and lymphoid CCR5-tropic Envs from a subset of 7 AIDS patients was compared to relative fusion (A, B) and infectivity (C, D) of cells expressing low CD4/high CD4 (1, 3, 56). P and R values were calculated using Spearman correlation on GraphPad Prism software.

Macrophages and microglia, the target cells of HIV in brain, express low levels of CD4. Therefore, HIV viruses from brain express Envs adapted to overcome this restriction on infection (3, 58, 68, 77-81). Because brain Envs with high levels of sgp120 shedding mediated enhanced infection into cells expressing low CD4, we investigated whether these Envs also mediated enhanced entry into monocyte-derived macrophages (MDM). However, we found no relationship between brain Envs with high levels of sgp120 shedding and MDM entry (p=0.48, r=-0.18) (Fig. 3.6A). This may reflect the different mechanisms used by HIV Envs to mediate efficient entry

into MDMs. Interestingly, there was a stronger association between the Envs that mediated high infectivity in TZM-bl cells (infectivity >0.05) following 2 hours of incubation at 37ºC and enhanced MDM entry (n=8 Envs, 7 brain and 1 lymphoid from 5 patients; p=0.06, r=0.68) (Fig. 3.6B). TZM-bl cells express high levels of CD4 and CCR5, and the subset of Envs was mixed between high and low levels of sgp120 shedding (n=4 Envs with % sgp120 shedding >20% and 4 Envs with %sgp120 shedding <20%). These results suggest that understanding the relationship between Envs with high levels of sgp120 shedding and the mechanisms by which brain and lymphoid Envs contribute to M-tropism requires further investigation.

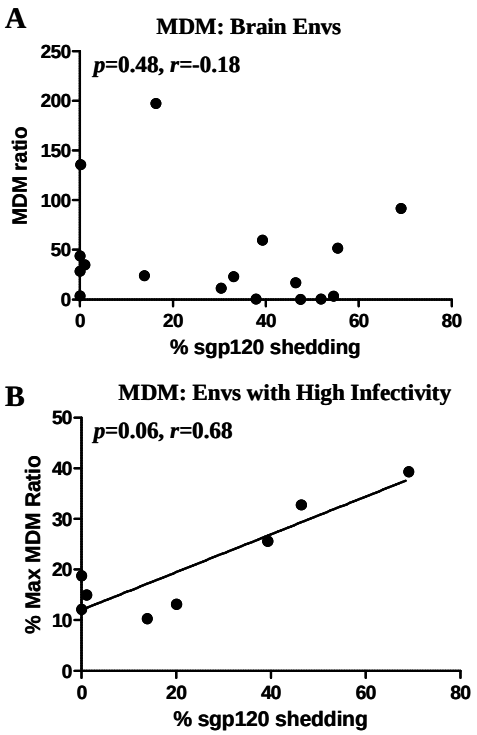

Figure 3.6. Brain Envs with high levels of sgp120 shedding are not associated with enhanced entry into primary macrophages.
A) Relative entry into macrophages of viruses expressing brain-derived Envs from 7 AIDS patients was compared to sgp120 shedding. % Max MDM ratio is calculated as [(MDM entry/entry into cells)/maximum MDM ratio for each study]*100 (thomas, peters) to control for inter-study variations.. P values were calculated using Spearman correlation on Graphpad Prism software. P values <0.05 were considered significant. B) Relative entry into macrophages was compared with % sgp120 shedding by brain and lymphoid Envs (n=8 Envs, 7 brain and 1 lymphoid, from 5 patients) that mediated high levels of infectivity in TZM-bl cells following 2 hours of incubation at 37ºC.

One mechanism proposed to reduce CD4-dependence of brain-derived Envs is increased exposure of the CD4 or CCR5 binding sites, which can be probed using sCD4 and monoclonal antibodies directed against CD4-induced epitopes. To address this question, we compared sgp120 shedding with inhibition of single-round infection by neutralizing antibodies and entry

inhibitors (54, 68, 80). Sgp120 shedding from 7 patients (n=33 Envs from 6 patients with HAD and 1 patient with no HAD) did not correlate with sensitivity to sCD4, monoclonal CD4-binding site antibody b12, or patient sera (data not shown). Shedding from these Envs also did not correlate with inhibition by entry inhibitors, including Tak779, AD101, or T20, although there was a trend toward correlation between Envs with high levels of sgp120 shedding and T20 sensitivity (p=0.07, r=0.31) (data not shown).

Envs with high levels of shedding induce activation of bystander cells during PBMC infection. To examine whether Envs with high levels of sgp120 shedding are associated with phenotypes that may contribute to HIV pathogenesis *in vivo*, we performed a pilot study to analyze activation of lymphocytes during virus replication *in vitro*. PBMCs were infected with replication competent viruses expressing Envs with high (ADA), medium-high (UK1br), or low (UK7br) levels of sgp120 shedding as measured by Western blotting. Envs with high levels of shedding induced upregulation of cell surface CD25 on both CD4+ and CD8+ lymphocytes at day 6 post-infection (Fig. 3.7A, Fig. S3.4). On day 10 post-infection, there was a corresponding decrease in this cell population, possibly reflecting the preferential loss of the activated cells due to bystander apoptosis (Fig. 3.7B). Upregulation of IL-1β was observed at day 3 post-infection (Fig. 3.7C). Although the sample size is small, upregulation of both CD25 and IL-1β is consistent with the increased levels of sgp120 shed by the same Envs from transfected 293T cells. Importantly, the viruses replicated to similar levels, suggesting that the T cell activation was independent of an effect on levels of viral replication (Fig. 3.7D).

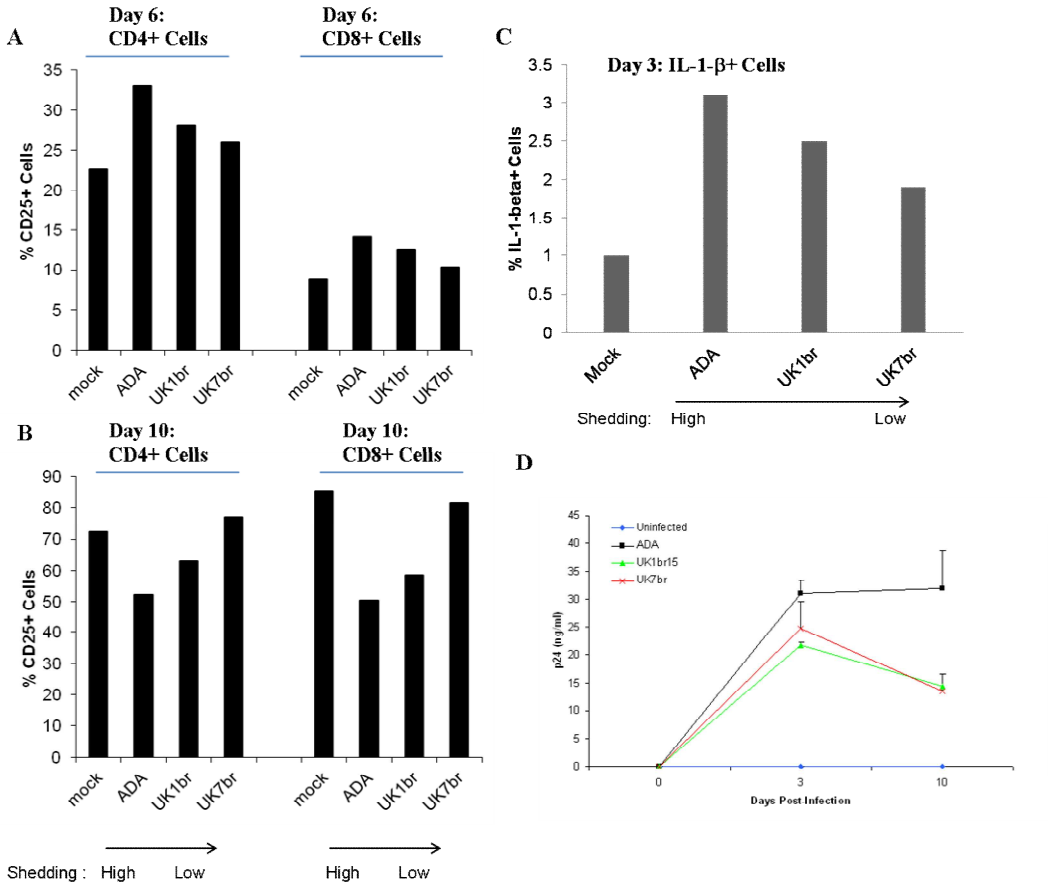

Fig. 3.7. Induction of lymphocyte activation markers is associated with Envs with high levels of sgp120 shedding. PBMC were stimulated for 24 hours with PHA-P (1 μg/ml), then the stimulation media was removed and replaced with IL-2 (10 U/ml) for 2 days. PBMCs were infected with an equivalent MOI of replication competent virus. Cells were collected on days 3 (C), 6 (A), and 10 (B) post-infection, stained for cell surface markers and cytokine production, and analyzed by flow cytometry. A/B) CD25 expression is presented as percentage of CD4+ or CD8+ T cells. C) Percent IL-1β+ cells from the activated lymphocyte population. D) Supernatants were collected every 3–4 days, and replication was monitored by p24 ELISA. Results shown are from duplicate samples. Error bars represent standard deviations.

Genetic analysis of Envs with high versus low levels of shedding. Diversifying evolution of the Env gene is important for immune evasion and adaptation to target cells. To examine the molecular and evolutionary features of Envs with high and low sgp120 shedding, Envs were divided into 2 groups based on levels of sgp120 shedding detected by Western blotting. Envs with high levels of sgp120 shedding (% sgp120 shedding >20% compared to gp120 in cell

lysate; *n*=38 Envs from 13 patients; 22 brain and 16 lymphoid Envs; median=2 Envs/patient) were compared to Envs with low levels of sgp120 shedding (% sgp120 shedding < 20% compared to cell lysate; *n*=29 Envs from 9 patients; 13 brain and 16 lymphoid Envs; median=2 Envs/patient). Amino acid diversity in Envs between the 2 groups was compared by calculating Shannon's entropy (Fig. 3.8 A/C, Table S3.4). Median entropy values averaged across gp160 were significantly higher for Envs with high versus low levels of sgp120 shedding ($p<0.0001$, Mann Whitney). Mean entropy values across gp120 and gp41 were also higher for Envs with high versus low levels of sgp120 shedding (0.554 versus 0.359 and 0.511 versus 0.214, respectively). These results were confirmed by constructing neighbor joining phylogenetic trees for both groups (Fig. S3.4). Tight within-patient clustering was observed for Envs from individual patients in the low sgp120 shedding, while higher in-patient diversity was apparent in the high sgp120 shedding group.

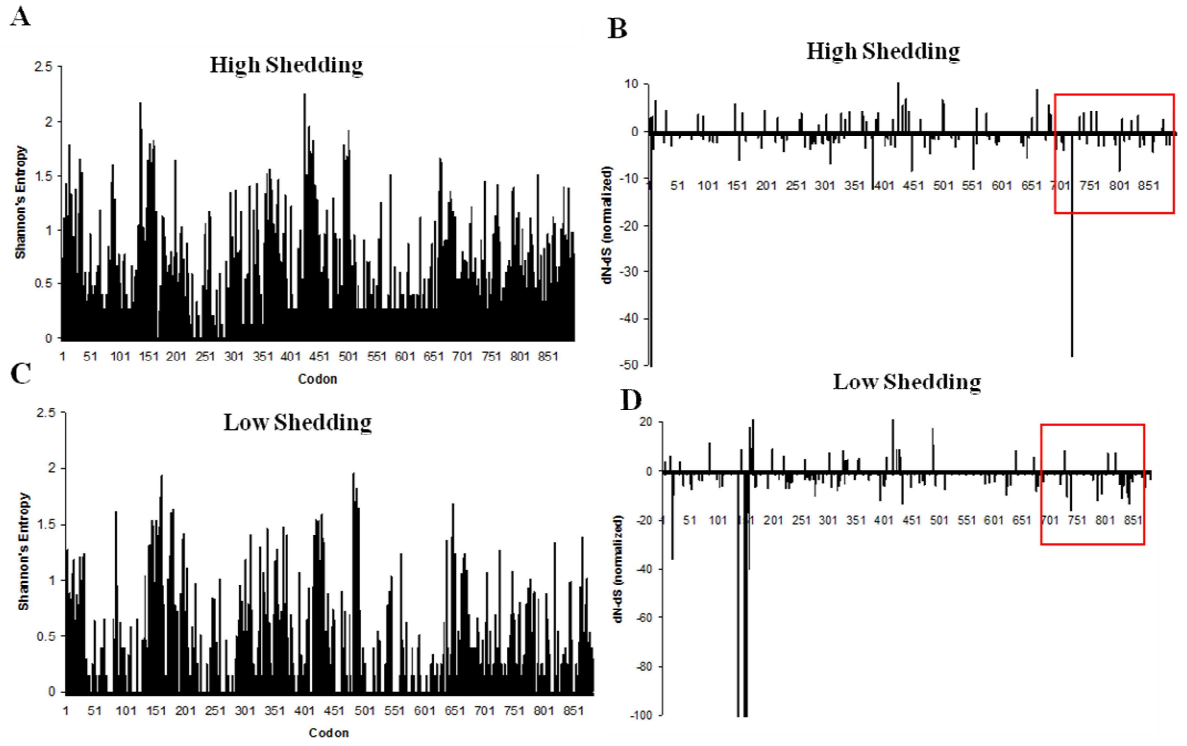

Fig. 3.8. Diversity and positive selection in sequence alignments from Envs with high and low levels of sgp120 shedding.
Primary brain and lymphoid Envs were characterized as high shedding (% sgp120 shedding >20%; *n*=38 Envs from 13 patients) or low shedding (% sgp120 shedding <20%, *n*=29 Envs from 9 patients). Nucleotide sequences for each group were aligned using Clustal X2. A/C) Shannon's entropy values were calculated from aligned sequences using Entropy One (LANL) and plotted against codon number (HXB2 numbering). (B/D) dN-dS values were estimated by SLAC, FEL, and IFEL analysis (datamonkey.org) from aligned sequences and scaled by total codon tree length. X-axis values represent codon positions (HXB2 numbering). Bars represent sites with $p<0.1$ in at least 2 analyses. Box represents area of gp41 with high number of sites predicted to be under positive selection in Envs with high levels of shedding.

To examine whether the higher *env* diversity observed in the high sgp120 shedding group is a result of increased positive selection, synonymous (dS) and nonsynonymous (dN) substitution rates were analyzed for each codon in both groups using three models of molecular evolution (63-65, 82-83). Ratios of non-synonymous and synonymous substitution rates were estimated for each codon in the Env alignments using SLAC, FEL, and IFEL analysis. Sites were considered to be under significant levels of positive selection if p-values <1.0 were estimated by

at least 2 methods. Site by site analysis revealed different patterns of positive selection between the 2 groups (Fig. 3.8 B/D and Table S3.3). An increased number of sites predicted to be under positive selection were identified in the high shedding group in regions previously demonstrated to be important for gp120-gp41 association, including the gp120 N-terminus, C2, and C4 regions and the gp41 N-terminus, HR2, MSD, and C-terminus (7-9, 17, 84-87).

To determine whether the association between Envs with high levels of sgp120 shedding and enhanced infection of cells expressing low CD4 may be due to a decrease in the number of N-linked glycosylation sites, a mechanism proposed to influence interactions between gp120 and CD4 and CCR5, the number of predicted N-glycosylation sites was compared between the 2 groups. The distribution of predicted N-glycans was similar between the 2 groups, although there was a higher number of N-glycans predicted in >90% of sequences in the low compared to high sgp120 shedding group (17 versus 12) (Table S3.3). Therefore, high sgp120 shedding was not associated with a significant decrease in N-linked glycosylation sites.

DISCUSSION

In this study, we demonstrated that sgp120 is spontaneously shed from a significant proportion of primary brain and lymphoid HIV Envs, but the phenotype is highly variable between and within patients ($p<0.0001$), representing a spectrum rather than a categorical phenotype. Levels of sgp120 shed by a subset of primary Envs overlapped with concentrations previously shown to induce biological effects *in vitro*. Moreover, viruses expressing Envs that spontaneously shed sgp120 at high levels induced higher levels of bystander T cell activation during infection of PBMC compared to those that shed sgp120 at low levels, despite similar levels of viral replication. Genetic analysis demonstrated greater median entropy ($p<0.0001$) and more codons under position selection in *env* sequences from patients with high versus low levels of sgp120 shedding (45 versus 29 positively selected codons, respectively; Fig. 3.8, Table S3.3). Thus, diversifying evolution may select for Env determinants that decrease gp120-gp41 association.

The main target cells of HIV in the CNS are macrophages and microglia, which express low levels of CD4. These cell types are preferentially infected by viruses that can utilize low levels of CD4 for entry (3, 58, 68-69, 77-81). Here, we found an association between enhanced fusion and infection with cells expressing low CD4 and brain Envs with high levels of sgp120 shedding ($p=0.06$, $r=0.4$ and $p=0.01$, $r=0.6$, respectively; Fig. 3.5). Because brain-derived Envs are generally M-tropic, we expected to find an association between levels of macrophage infection and sgp120 shedding by Envs from brain. However, we did not find this association (Fig. 3.6). The lack of correlation was unexpected, and may reflect different mechanisms of M-tropism. While brain Envs exhibited an association between reduced CD4 dependence and high levels of sgp120 shedding, not all M-tropic Envs preferentially infect cells expressing low CD4.

Other mechanisms that may contribute to M-tropism include enhanced Env affinity for CCR5 (53, 77, 88-89) (see Chapter 2) or increased interactions with high mannose oligosaccharides expressed on the macrophage cell surface (90-91). Enhanced Env-CD4 interactions can result from increased exposure of the CD4 binding site through shifting of the V1/V2 and V3 loops, thereby leading to increased spontaneous sgp120 shedding (5, 8). Future work is needed to determine if specific mechanisms contributing to M-tropism are associated with high levels of sgp120 shedding.

Purified HIV sgp120 induces biological effects *in vitro* that include cellular activation and bystander cell apoptosis, raising the possibility that sgp120 may contribute to the immune activation and immune dysregulation characteristic of HIV infection. However, a link between sgp120 and HIV pathogenesis *in vivo* has not been demonstrated. We found that viruses expressing brain Envs with high levels of sgp120 shedding had an increased capacity to induce lymphocyte activation, resulting in increased cell surface expression levels of CD25 and IL-1β (Fig. 3.6). Furthermore, CD4+ and CD8+ cells expressing high CD25 were lost over the course of PBMC infection despite similar levels of viral replication. Although this study was small (n=3 viruses), these results raise the possibility that sgp120 shed from virions and infected cells may contribute to bystander T cells activation during HIV infection.

Low concentrations (<100 ng/ml) of purified HIV sgp120 are required to induce apoptosis of uninfected neurons *in vitro* (19, 41, 43-45), a mechanism proposed to contribute to the development of HIV-associated neurological disorders (HAND) (19, 46). The low levels of antibodies in the CNS (19, 92) combined with adaptation to target cells expressing low CD4, can result in adoption of more open Env conformations with increased exposure of the CD4 and CCR5-binding sites and neutralization epitopes (1, 3, 53, 58, 66-69). Structural and functional

studies raise the possibility a consequence of these conformations may be increased spontaneous shedding of sgp120 (5, 7-8). Therefore, we expected to find that brain Envs shed sgp120 at higher levels than lymphoid Envs. However, although there was a trend towards higher median levels of sgp120 shedding from brain Envs compared to lymphoid Envs, these differences did not reach statistical significance (Fig. 3.1D). Furthermore, brain-derived Envs from patients with or without HAD had similar median levels of sgp120 shedding. The lack of correlation between sgp120 shedding and tissue of origin or disease status may be due to sample collection during late-stage AIDS.

One caveat of this study is that we measured spontaneous sgp120 shedding from a large panel of primary brain and lymphoid Envs from transfected 293T cells, which results in overexpression of Env trimer spikes on the cell surface, thereby facilitating detection of shed sgp120. These results may therefore exaggerate levels of sgp120 shedding compared to physiological conditions. We calculated our results as % sgp120 shedding, which takes into account differences in cell-associated gp120 production. As such, we expect that our results are indicative of relative levels of sgp120 shedding during physiological conditions.

In summary, this study demonstrated a wide range of sgp120 shedding from primary HIV Envs in brain and lymphoid tissues from AIDS patients with advanced disease. Sgp120 shedding from primary Envs represents a spectrum rather than a categorical phenotype. Envs with high levels of sgp120 shedding were associated with enhanced infection of cells expressing low CD4 and bystander T cell activation during PBMC infection. Thus, increased sgp120 shedding may be a viral phenotype that contributes to HIV pathogenesis.

ACKNOWLEDGEMENTS

We thank J. Cunningham, J. Sodroski, and B. Chen for helpful discussions, N. Letvin for providing TZM-bl cells, B. Lee for providing Affinofile cells, and P. Peters and P. Clapham for providing Env expression plasmids from patients NA20, NA420, and NA118. The following reagent was obtained through the NIH AIDS Research and Reference Reagent Program, Division of AIDS, NIAID: monoclonal antibody 2G12 from Dr. Herman Kattinger and b12 from Dr. Dennis Burton and Carlos Barbas. This work was supported by NIH Grants NS37277 and MH83588. M.M. was supported in part by NIH fellowship 1F31NS060611-01. Core facilities were supported by Harvard Medical School Center for AIDS Research (CFAR) and DFCI/Harvard Cancer Center grants.

.

REFERENCES

1. Thomas ER, Dunfee RL, Stanton J, Bogdan D, Taylor J, Kunstman K, et al. Macrophage entry mediated by HIV Envs from brain and lymphoid tissues is determined by the capacity to use low CD4 levels and overall efficiency of fusion. Virology. 2007;360(1):105-19.

2. Gorry PR, Bristol G, Zack JA, Ritola K, Swanstrom R, Birch CJ, et al. Macrophage tropism of human immunodeficiency virus type 1 isolates from brain and lymphoid tissues predicts neurotropism independent of coreceptor specificity. J Virol. 2001;75(21):10073-89.

3. Peters PJ, Bhattacharya J, Hibbitts S, Dittmar MT, Simmons G, Bell J, et al. Biological analysis of human immunodeficiency virus type 1 R5 envelopes amplified from brain and lymph node tissues of AIDS patients with neuropathology reveals two distinct tropism phenotypes and identifies envelopes in the brain that confer an enhanced tropism and fusigenicity for macrophages. J Virol. 2004;78(13):6915-26.

4. Kwong PD, Wyatt R, Majeed S, Robinson J, Sweet RW, Sodroski J, et al. Structures of HIV-1 gp120 envelope glycoproteins from laboratory-adapted and primary isolates. Structure. 2000;8(12):1329-39.

5. Liu J, Bartesaghi A, Borgnia MJ, Sapiro G, Subramaniam S. Molecular architecture of native HIV-1 gp120 trimers. Nature. 2008;455(7209):109-13.

6. Melikyan GB. Membrane fusion mediated by human immunodeficiency virus envelope glycoprotein. Curr Top Membr. 2011;68:81-106.

7. Finzi A, Xiang SH, Pacheco B, Wang L, Haight J, Kassa A, et al. Topological layers in the HIV-1 gp120 inner domain regulate gp41 interaction and CD4-triggered conformational transitions. Mol Cell. 2010;37(5):656-67. PMCID: 2854584.

8. Xiang SH, Finzi A, Pacheco B, Alexander K, Yuan W, Rizzuto C, et al. A V3 loop-dependent gp120 element disrupted by CD4 binding stabilizes the human immunodeficiency virus envelope glycoprotein trimer. J Virol. 2010;84(7):3147-61. PMCID: 2838131.

9. Poumbourios P, el Ahmar W, McPhee DA, Kemp BE. Determinants of human immunodeficiency virus type 1 envelope glycoprotein oligomeric structure. J Virol. 1995;69(2):1209-18.

10. Doms RW. The plasma membrane as a combat zone in the HIV battlefield. Genes & Development. 2000;14:2677-88.

11. Hammonds J, Chen X, Ding L, Fouts T, De Vico A, zur Megede J, et al. Gp120 stability on HIV-1 virions and Gag-Env pseudovirions is enhanced by an uncleaved Gag core. Virology. 2003;314(2):636-49.

12. Moore JP, McKeating JA, Jones IM, Stephens PE, Clements G, Thomson S, et al. Characterization of recombinant gp120 and gp160 from HIV-1: binding to monoclonal antibodies and soluble CD4. Aids. 1990;4(4):307-15.

13. Moore JP, McKeating JA, Norton WA, Sattentau QJ. Direct measurement of soluble CD4 binding to human immunodeficiency virus type 1 virions: gp120 dissociation and its implications for virus-cell binding and fusion reactions and their neutralization by soluble CD4. J Virol. 1991;65(3):1133-40. PMCID: 239879.

14. Moore JP, McKeating JA, Weiss RA, Sattentau QJ. Dissociation of gp120 from HIV-1 virions induced by soluble CD4. Science. 1990;250(4984):1139-42.

15. Moore JP, Sattentau QJ, Clapham PR. Enhancement of soluble CD4-mediated HIV neutralization and gp 120 binding by CD4 autoantibodies and monoclonal antibodies. AIDS Res Hum Retroviruses. 1990;6(11):1273-9.

16. Thali M, Furman C, Helseth E, Repke H, Sodroski J. Lack of correlation between soluble CD4-induced shedding of the human immunodeficiency virus type 1 exterior envelope glycoprotein and subsequent membrane fusion events. J Virol. 1992;66(9):5516-24. PMCID: 289110.

17. Affranchino JL, Gonzalez SA. Mutations at the C-terminus of the simian immunodeficiency virus envelope glycoprotein affect gp120-gp41 stability on virions. Virology. 2006;347(1):217-25.

18. Zhang JL, Choe H, Dezube BJ, Farzan M, Sharma PL, Zhou XC, et al. The bis-azo compound FP-21399 inhibits HIV-1 replication by preventing viral entry. Virology. 1998;244(2):530-41.

19. Kaul M, Garden GA, Lipton SA. Pathways to neuronal injury and apoptosis in HIV-associated dementia. Nature. 2001;410(6831):988-94.

20. Selliah N, Shackelford J, Wang JF, Traynor F, Yin J, Finkel TH. T cell signaling and apoptosis in HIV disease. Immunol Res. 2003;27(2-3):247-60.

21. Rychert J, Strick D, Bazner S, Robinson J, Rosenberg E. Detection of HIV gp120 in plasma during early HIV infection is associated with increased proinflammatory and immunoregulatory cytokines. AIDS Res Hum Retroviruses. 2010;26(10):1139-45. PMCID: 2982714.

22. Mogensen TH, Melchjorsen J, Larsen CS, Paludan SR. Innate immune recognition and activation during HIV infection. Retrovirology. 2010;7:54. PMCID: 2904714.

23. Gemma C, Smith EM, Hughes TK, Jr., Opp MR. Human immunodeficiency virus glycoprotein 160 induces cytokine mRNA expression in the rat central nervous system. Cell Mol Neurobiol. 2000;20(4):419-31.

24. Ullrich CK, Groopman JE, Ganju RK. HIV-1 gp120- and gp160-induced apoptosis in cultured endothelial cells is mediated by caspases. Blood. 2000;96(4):1438-42.

25. Garg H, Blumenthal R. HIV gp41-induced apoptosis is mediated by caspase-3-dependent mitochondrial depolarization, which is inhibited by HIV protease inhibitor nelfinavir. J Leukoc Biol. 2006;79(2):351-62.

26. Anand AR, Ganju RK. HIV-1 gp120-mediated apoptosis of T cells is regulated by the membrane tyrosine phosphatase CD45. J Biol Chem. 2006;281(18):12289-99.

27. Anand AR, Prasad A, Bradley RR, Deol YS, Nagaraja T, Ren X, et al. HIV-1 gp120-induced migration of dendritic cells is regulated by a novel kinase cascade involving Pyk2, p38 MAP kinase, and LSP1. Blood. 2009;114(17):3588-600. PMCID: 2766677.

28. Green DS, Center DM, Cruikshank WW. Human immunodeficiency virus type 1 gp120 reprogramming of CD4+ T-cell migration provides a mechanism for lymphadenopathy. J Virol. 2009;83(11):5765-72. PMCID: 2681967.

29. Chougnet C, Gessani S. Role of gp120 in dendritic cell dysfunction in HIV infection. J Leukoc Biol. 2006;80(5):994-1000.

30. Oh SK, Cruikshank WW, Raina J, Blanchard GC, Adler WH, Walker J, et al. Identification of HIV-1 envelope glycoprotein in the serum of AIDS and ARC patients. J Acquir Immune Defic Syndr. 1992;5(3):251-6.

31. Gilbert M, Kirihara J, Mills J. Enzyme-linked immunoassay for human immunodeficiency virus type 1 envelope glycoprotein 120. J Clin Microbiol. 1991;29(1):142-7. PMCID: 269718.

32. Klasse PJ, Moore JP. Is there enough gp120 in the body fluids of HIV-1-infected individuals to have biologically significant effects? Virology. 2004;323(1):1-8.

33. Santosuosso M, Righi E, Lindstrom V, Leblanc PR, Poznansky MC. HIV-1 envelope protein gp120 is present at high concentrations in secondary lymphoid organs of individuals with chronic HIV-1 infection. J Infect Dis. 2009;200(7):1050-3.

34. Stevceva L, Yoon V, Carville A, Pacheco B, Santosuosso M, Korioth-Schmitz B, et al. The efficacy of T cell-mediated immune responses is reduced by the envelope protein of the chimeric HIV-1/SIV-KB9 virus in vivo. J Immunol. 2008;181(8):5510-21.

35. Trushin SA, Bren GD, Badley AD. CD4 T Cells Treated with gp120 Acquire a CD45R0+/CD45RA+ Phenotype. Open Virol J. 2009;3:21-5. PMCID: 2703203.

36. Yang B, Akhter S, Chaudhuri A, Kanmogne GD. HIV-1 gp120 induces cytokine expression, leukocyte adhesion, and transmigration across the blood-brain barrier: modulatory effects of STAT1 signaling. Microvasc Res. 2009;77(2):212-9.

37. Cicala C, Arthos J, Censoplano N, Cruz C, Chung E, Martinelli E, et al. HIV-1 gp120 induces NFAT nuclear translocation in resting CD4+ T-cells. Virology. 2006;345(1):105-14.

38. Ameglio F, Capobianchi MR, Castilletti C, Cordiali Fei P, Fais S, Trento E, et al. Recombinant gp120 induces IL-10 in resting peripheral blood mononuclear cells; correlation with the induction of other cytokines. Clin Exp Immunol. 1994;95(3):455-8. PMCID: 1535081.

39. Kinter AL, Umscheid CA, Arthos J, Cicala C, Lin Y, Jackson R, et al. HIV envelope induces virus expression from resting CD4+ T cells isolated from HIV-infected individuals in the absence of markers of cellular activation or apoptosis. J Immunol. 2003;170(5):2449-55.

40. Biancotto A, Iglehart SJ, Vanpouille C, Condack CE, Lisco A, Ruecker E, et al. HIV-1 induced activation of CD4+ T cells creates new targets for HIV-1 infection in human lymphoid tissue ex vivo. Blood. 2008;111(2):699-704. PMCID: 2200839.

41. Medders KE, Sejbuk NE, Maung R, Desai MK, Kaul M. Activation of p38 MAPK is required in monocytic and neuronal cells for HIV glycoprotein 120-induced neurotoxicity. J Immunol. 2010;185(8):4883-95.

42. Garg H, Joshi A, Blumenthal R. Altered bystander apoptosis induction and pathogenesis of enfuvirtide-resistant HIV type 1 Env mutants. AIDS Res Hum Retroviruses. 2009;25(8):811-7. PMCID: 2791676.

43. Garden GA, Guo W, Jayadev S, Tun C, Balcaitis S, Choi J, et al. HIV associated neurodegeneration requires p53 in neurons and microglia. FASEB J. 2004;18(10):1141-3.

44. Jana A, Pahan K. Human immunodeficiency virus type 1 gp120 induces apoptosis in human primary neurons through redox-regulated activation of neutral sphingomyelinase. J Neurosci. 2004;24(43):9531-40. PMCID: 1955476.

45. Singh IN, Goody RJ, Dean C, Ahmad NM, Lutz SE, Knapp PE, et al. Apoptotic death of striatal neurons induced by human immunodeficiency virus-1 Tat and gp120: Differential involvement of caspase-3 and endonuclease G. J Neurovirol. 2004;10(3):141-51.

46. Kaul M, Zheng J, Okamoto S, Gendelman HE, Lipton SA. HIV-1 infection and AIDS: consequences for the central nervous system. Cell Death Differ. 2005;12 Suppl 1:878-92.

47. Nazli A, Chan O, Dobson-Belaire WN, Ouellet M, Tremblay MJ, Gray-Owen SD, et al. Exposure to HIV-1 directly impairs mucosal epithelial barrier integrity allowing microbial translocation. PLoS Pathog. 2010;6(4):e1000852. PMCID: 2851733.

48. Masci AM, Galgani M, Cassano S, De Simone S, Gallo A, De Rosa V, et al. HIV-1 gp120 induces anergy in naive T lymphocytes through CD4-independent protein kinase-A-mediated signaling. J Leukoc Biol. 2003;74(6):1117-24.

49. Mascola JR, Louwagie J, McCutchan FE, Fischer CL, Hegerich PA, Wagner KF, et al. Two antigenically distinct subtypes of human immunodeficiency virus type 1: viral genotype predicts neutralization serotype. J Infect Dis. 1994;169(1):48-54.

50. Albright AV, Martin J, O'Connor M, Gonzalez-Scarano F. Interactions between HIV-1 gp120, chemokines, and cultured adult microglial cells. J Neurovirol. 2001;7(3):196-207.

51. Becker C, Taube C, Bopp T, Michel K, Kubach J, Reuter S, et al. Protection from graft-versus-host disease by HIV-1 envelope protein gp120-mediated activation of human CD4+CD25+ regulatory T cells. Blood. 2009;114(6):1263-9.

52. Kohler JJ, Tuttle DL, Coberley CR, Sleasman JW, Goodenow MM. Human immunodeficiency virus type 1 (HIV-1) induces activation of multiple STATs in CD4+ cells of lymphocyte or monocyte/macrophage lineages. J Leukoc Biol. 2003;73(3):407-16.

53. Gorry PR, Taylor J, Holm GH, Mehle A, Morgan T, Cayabyab M, et al. Increased CCR5 affinity and reduced CCR5/CD4 dependence of a neurovirulent primary human immunodeficiency virus type 1 isolate. J Virol. 2002;76(12):6277-92.

54. Etemad-Moghadam B, Sun Y, Nicholson EK, Fernandes M, Liou K, Gomila R, et al. Envelope glycoprotein determinants of increased fusogenicity in a pathogenic simian-human immunodeficiency virus (SHIV-KB9) passaged in vivo. J Virol. 2000;74(9):4433-40. PMCID: 111962.

55. Johnston SH, Lobritz MA, Nguyen S, Lassen K, Delair S, Posta F, et al. A quantitative affinity-profiling system that reveals distinct CD4/CCR5 usage patterns among human immunodeficiency virus type 1 and simian immunodeficiency virus strains. J Virol. 2009;83(21):11016-26.

56. Mefford ME, Gorry PR, Kunstman K, Wolinsky SM, Gabuzda D. Bioinformatic prediction programs underestimate the frequency of CXCR4 usage by R5X4 HIV type 1 in brain and other tissues. AIDS Res Hum Retroviruses. 2008;24(9):1215-20.

57. Ohagen A, Devitt A, Kunstman KJ, Gorry PR, Rose PP, Korber B, et al. Genetic and functional analysis of full-length human immunodeficiency virus type 1 env genes derived from brain and blood of patients with AIDS. J Virol. 2003;77(22):12336-45.

58. Dunfee RL, Thomas ER, Gorry PR, Wang J, Taylor J, Kunstman K, et al. The HIV Env variant N283 enhances macrophage tropism and is associated with brain infection and dementia. Proc Natl Acad Sci U S A. 2006;103(41):15160-5. PMCID: 1586182.

59. Si Z, Madani N, Cox JM, Chruma JJ, Klein JC, Schon A, et al. Small-molecule inhibitors of HIV-1 entry block receptor-induced conformational changes in the viral envelope glycoproteins. Proc Natl Acad Sci U S A. 2004;101(14):5036-41.

60. Agrawal N, Leaman DP, Rowcliffe E, Kinkead H, Nohria R, Akagi J, et al. Functional stability of unliganded envelope glycoprotein spikes among isolates of human immunodeficiency virus type 1 (HIV-1). PLoS One. 2011;6(6):e21339. PMCID: 3124497.

61. Moore PL, Gray ES, Choge IA, Ranchobe N, Mlisana K, Abdool Karim SS, et al. The c3-v4 region is a major target of autologous neutralizing antibodies in human immunodeficiency virus type 1 subtype C infection. J Virol. 2008;82(4):1860-9.

62. Bowley DR, Labrijn AF, Zwick MB, Burton DR. Antigen selection from an HIV-1 immune antibody library displayed on yeast yields many novel antibodies compared to selection from the same library displayed on phage. Protein Eng Des Sel. 2007;20(2):81-90.

63. Pond SL, Frost SD, Grossman Z, Gravenor MB, Richman DD, Brown AJ. Adaptation to different human populations by HIV-1 revealed by codon-based analyses. PLoS Comput Biol. 2006;2(6):e62.

64. Pond SLK, A.F.Y. Poon, S. Zarate, D.M. Smith, S.J. Little, S.K. Pillai, R.J. Ellis, J.K. Wong, A.J. Leigh Brown, D.D. Richman, and S.D.W. Frost. Estimating selection pressures on HIV-1 using phylogenetic likelihood models. Stastistics in Medicine. 2008;27(23):4779-89.

65. Poon AF, Frost SD, Pond SL. Detecting signatures of selection from DNA sequences using Datamonkey. Methods Mol Biol. 2009;537:163-83.

66. Dunfee RL, Thomas ER, Wang J, Kunstman K, Wolinsky SM, Gabuzda D. Loss of the N-linked glycosylation site at position 386 in the HIV envelope V4 region enhances macrophage tropism and is associated with dementia. Virology. 2007;367(1):222-34. PMCID: 2201988.

67. Peters PJ, Duenas-Decamp MJ, Sullivan WM, Brown R, Ankghuambom C, Luzuriaga K, et al. Variation in HIV-1 R5 macrophage-tropism correlates with sensitivity to reagents that block envelope: CD4 interactions but not with sensitivity to other entry inhibitors. Retrovirology. 2008;5:5.

68. Duenas-Decamp MJ, Peters P, Burton D, Clapham PR. Natural resistance of human immunodeficiency virus type 1 to the CD4bs antibody b12 conferred by a glycan and an arginine residue close to the CD4 binding loop. J Virol. 2008;82(12):5807-14.

69. Duenas-Decamp MJ, Peters PJ, Burton D, Clapham PR. Determinants flanking the CD4 binding loop modulate macrophage tropism of human immunodeficiency virus type 1 R5 envelopes. J Virol. 2009;83(6):2575-83.

70. Holman AG, Mefford ME, O'Connor N, Gabuzda D. HIVBrainSeqDB: a database of annotated HIV envelope sequences from brain and other anatomical sites. AIDS Res Ther. 2010;7:43. PMCID: 3018377.

71. Chien MP, Jiang S, Chang DK. The function of coreceptor as a basis for the kinetic dissection of HIV type 1 envelope protein-mediated cell fusion. FASEB J. 2008;22(4):1179-92.

72. Pancera M, Wyatt R. Selective recognition of oligomeric HIV-1 primary isolate envelope glycoproteins by potently neutralizing ligands requires efficient precursor cleavage. Virology. 2005;332(1):145-56.

73. Groenink M, Moore JP, Broersen S, Schuitemaker H. Equal levels of gp120 retention and neutralization resistance of phenotypically distinct primary human immunodeficiency virus type 1 variants upon soluble CD4 treatment. J Virol. 1995;69(1):523-7. PMCID: 188603.

74. Orloff SL, Kennedy MS, Belperron AA, Maddon PJ, McDougal JS. Two mechanisms of soluble CD4 (sCD4)-mediated inhibition of human immunodeficiency virus type 1 (HIV-1) infectivity and their relation to primary HIV-1 isolates with reduced sensitivity to sCD4. J Virol. 1993;67(3):1461-71. PMCID: 237516.

75. Moore JP, McKeating JA, Huang YX, Ashkenazi A, Ho DD. Virions of primary human immunodeficiency virus type 1 isolates resistant to soluble CD4 (sCD4) neutralization differ in sCD4 binding and glycoprotein gp120 retention from sCD4-sensitive isolates. J Virol. 1992;66(1):235-43. PMCID: 238280.

76. Martin-Garcia J, Cocklin S, Chaiken IM, Gonzalez-Scarano F. Interaction with CD4 and antibodies to CD4-induced epitopes of the envelope gp120 from a microglial cell-adapted human immunodeficiency virus type 1 isolate. J Virol. 2005;79(11):6703-13.

77. Gray L, Sterjovski J, Churchill M, Ellery P, Nasr N, Lewin SR, et al. Uncoupling coreceptor usage of human immunodeficiency virus type 1 (HIV-1) from macrophage tropism reveals biological properties of CCR5-restricted HIV-1 isolates from patients with acquired immunodeficiency syndrome. Virology. 2005;337(2):384-98.

78. Walter BL, Wehrly K, Swanstrom R, Platt E, Kabat D, Chesebro B. Role of low CD4 levels in the influence of human immunodeficiency virus type 1 envelope V1 and V2 regions on entry and spread in macrophages. J Virol. 2005;79(8):4828-37.

79. Wang J, Crawford K, Yuan M, Wang H, Gorry PR, Gabuzda D. Regulation of CC chemokine receptor 5 and CD4 expression and human immunodeficiency virus type 1 replication in human macrophages and microglia by T helper type 2 cytokines. J Infect Dis. 2002;185(7):885-97.

80. Bannert N, Schenten D, Craig S, Sodroski J. The level of CD4 expression limits infection of primary rhesus monkey macrophages by a T-tropic simian immunodeficiency virus and macrophagetropic human immunodeficiency viruses. J Virol. 2000;74(23):10984-93.

81. Martin-Garcia J, Cao W, Varela-Rohena A, Plassmeyer ML, Gonzalez-Scarano F. HIV-1 tropism for the central nervous system: Brain-derived envelope glycoproteins with lower CD4 dependence and reduced sensitivity to a fusion inhibitor. Virology. 2006;346(1):169-79.

82. Ahr B, Robert-Hebmann V, Devaux C, Biard-Piechaczyk M. Apoptosis of uninfected cells induced by HIV envelope glycoproteins. Retrovirology. 2004;1:12.

83. Barroso H, Borrego P, Bartolo I, Marcelino JM, Familia C, Quintas A, et al. Evolutionary and structural features of the C2, V3 and C3 envelope regions underlying the differences in HIV-1 and HIV-2 biology and infection. PLoS One. 2011;6(1):e14548. PMCID: 3024314.

84. Kassa A, Madani N, Schon A, Haim H, Finzi A, Xiang SH, et al. Transitions to and from the CD4-bound conformation are modulated by a single-residue change in the human immunodeficiency virus type 1 gp120 inner domain. J Virol. 2009;83(17):8364-78.

85. Koito A, Harrowe G, Levy JA, Cheng-Mayer C. Functional role of the V1/V2 region of human immunodeficiency virus type 1 envelope glycoprotein gp120 in infection of primary macrophages and soluble CD4 neutralization. J Virol. 1994;68(4):2253-9. PMCID: 236701.

86. Poumbourios P, Maerz AL, Drummer HE. Functional evolution of the HIV-1 envelope glycoprotein 120 association site of glycoprotein 41. J Biol Chem. 2003;278(43):42149-60.

87. York J, Nunberg JH. Role of hydrophobic residues in the central ectodomain of gp41 in maintaining the association between human immunodeficiency virus type 1 envelope glycoprotein subunits gp120 and gp41. J Virol. 2004;78(9):4921-6. PMCID: 387687.

88. Shieh JT, Martin J, Baltuch G, Malim MH, Gonzalez-Scarano F. Determinants of syncytium formation in microglia by human immunodeficiency virus type 1: role of the V1/V2 domains. J Virol. 2000;74(2):693-701.

89. Sterjovski J, Roche M, Churchill MJ, Ellett A, Farrugia W, Gray LR, et al. An altered and more efficient mechanism of CCR5 engagement contributes to macrophage tropism of CCR5-using HIV-1 envelopes. Virology. 2010;404(2):269-78.

90. Duncan CJ, Sattentau QJ. Viral determinants of HIV-1 macrophage tropism. Viruses. 2011;3(11):2255-79. PMCID: 3230851.

91. Lai J, Bernhard OK, Turville SG, Harman AN, Wilkinson J, Cunningham AL. Oligomerization of the macrophage mannose receptor enhances gp120-mediated binding of HIV-1. J Biol Chem. 2009;284(17):11027-38. PMCID: 2670108.

92. Goudsmit J, Lange JM, Krone WJ, Teunissen MB, Epstein LG, Danner SA, et al. Pathogenesis of HIV and its implications for serodiagnosis and monitoring of antiviral therapy. J Virol Methods. 1987;17(1-2):19-34.

CHAPTER 4: BIOINFORMATIC PREDICTION PROGRAMS UNDERESTIMATE THE FREQUENCY OF CXCR4 USAGE BY R5X4 HIV-1 IN BRAIN AND OTHER TISSUES

Megan E. Mefford[a], Paul R. Gorry[b, c], Kevin Kunstman[d], Steven M. Wolinsky[d], and Dana Gabuzda[a, e*]

[a]Department of Cancer Immunology and AIDS, Dana-Farber Cancer Institute, Boston, MA, USA
[b]Macfarlane Burnet Institute for Medical Research and Public Health, Melbourne, Victoria, Australia
[c]Department of Medicine, Monash University, Melbourne, Victoria, Australia
[d]Northwestern University Medical School, Chicago, IL, USA
[e]Department of Neurology, Harvard Medical School, Boston, MA, USA

Running title: Bioinformatic predictors of R5X4 HIV-1

*Corresponding Author.
Mailing Address:
Dana-Farber Cancer Institute, JFB 816
44 Binney St.
Boston, MA 02115
Phone: (617) 632-2154
Fax: (617) 632-3113
e-mail: dana_gabuzda@dfci.harvard.edu

ABSTRACT

Human immunodeficiency virus (HIV-1) variants in brain primarily use CCR5 for entry into macrophages and microglia, but dual-tropic (R5X4) HIV-1 has been detected in brain and cerebral spinal fluid (CSF) of some patients with HIV-associated dementia (HAD). Here, we sequenced the gp120 coding region of 9 full-length dual-tropic (R5X4) *env* genes cloned directly from autopsy brain and spleen tissue from an AIDS patient with severe HAD. We then compiled a dataset of 30 unique clade B R5X4 Env V3 sequences from this subject and 16 additional patients (*n*=4 brain and 26 lymphoid/blood) and used it to compare the ability of 6 bioinformatic algorithms to correctly predict CXCR4-usage in R5X4 Envs. Only one program ($SVM_{geno2pheno}$) correctly predicted the ability of R5X4 Envs in this dataset to use CXCR4 with 90% accuracy (n=27/30 predicted to use CXCR4). The $PSSM_{SINSI}$, Random Forest, and $SVM_{genomiac}$ programs and the commonly used charge rule correctly predicted CXCR4-usage with >50% accuracy (22/30, 16/30, 19/30, and 25/30, respectively), while the $PSSM_{X4R5}$ matrix and "11/25" rule correctly predicted CXCR4-usage in <50% of the R5X4 Envs (10/30 and 13/30, respectively). Two positions in the V3 loop (19 and 32) influenced coreceptor usage predictions of 9 R5X4 Envs from patient MACS1 and a total of 12 Envs from the dataset (40% of unique V3 sequences). These results demonstrate that most predictive algorithms underestimate the frequency of R5X4 HIV-1 in brain and other tissues. $SVM_{geno2pheno}$ is the most accurate predictor of CXCR4-usage by R5X4 HIV-1.

INTRODUCTION

Human immunodeficiency virus type I (HIV-1) infects macrophages and microglia in the central nervous system (CNS) and causes HIV-associated dementia (HAD) or mild neurocognitive impairment in 10-20% of AIDS patients. HIV-1 variants in brain are genetically distinct from those in lymphoid tissues and other organs, and specific sequences in the envelope glycoprotein (Env) coding region of gp160 have been associated with brain compartmentalization (1). HIV-1 tropism is influenced by the interaction of Env with CD4 and a coreceptor, typically CCR5 or CXCR4. CCR5 (R5) is the primary coreceptor for HIV-1 infection of macrophages and microglia. Several studies identified HIV-1 brain or CSF isolates capable of mediating entry using CXCR4 (X4 isolates) or both CCR5 and CXCR4 (R5X4 or dual-tropic isolates) (1-4). However, the frequency of X4 or R5X4 strains in the brain of AIDS patients is unknown.

The third hypervariable loop of Env gp120 (V3), a disulfide-linked loop of approximately 35 amino acids, makes direct contact with the coreceptor and is the primary determinant for R5- or X4-tropism (5). Bioinformatic algorithms that use V3 sequence to predict HIV-1 coreceptor usage have been developed as a timely and cost-effective alternative to traditional phenotypic assays (6-10). However, database sequence sets are heavily dependent on R5 sequences and may underestimate X4-usage and dual-tropism. Furthermore, the ability of bioinformatic algorithms to reliably predict X4-usage by R5X4 isolates has not been addressed. Here, we cloned and sequenced 9 full-length R5X4 HIV-1 Envs from autopsy brain and spleen tissues from an AIDS patient with severe HAD. We then added these sequences to a larger dataset of unique clade B R5X4

V3 sequences and compared the ability of freely available bioinformatic algorithms to accurately predict X4-usage.

RESULTS

MACS1, a male homosexual patient in the Chicago component of the Multicenter AIDS Cohort Study with no history of antiretroviral therapy, had severe HAD and a CD4+ T-cell count of 2 cells/μl at the time of death (3-4). Analysis of CCR5 alleles by PCR demonstrated that the patient was homozygous wild type for CCR5. At autopsy, sections through the frontal and parietal cortex showed pathology consistent with HIV encephalitis (i.e. multiple microscopic foci of necrosis and focal perivascular lesions throughout the white matter occasionally associated with multinucleated giant cells). HIV vacuolar myelopathy and leukoencephalopathy was unusually advanced within the brain stem and cerebellum. We previously isolated four R5X4 HIV-1 viruses from brain (br) and spleen (spln) tissue from this patient [MACS1-br (pbmc), MACS1-br (mdm), MACS1-spln (pbmc), and MACS1-spln (mdm)]. These viruses were isolated from cultures with CD8-depleted peripheral blood mononuclear cells (PBMC) or monocyte-derived macrophages (MDM) as indicated. These R5X4 isolates replicated efficiently in MDM and microglia and induced syncytia formation in >90% of cells by day 10 post-infection. The brain- and spleen-derived isolates entered macrophages and microglia primarily via CXCR4 and induced neuronal apoptosis in primary brain cultures, suggesting that R5X4 variants may be pathogenic in the CNS (3-4).

To investigate the frequency of R5X4 variants in tissues from patient MACS1, *env* genes were amplified from genomic DNA isolated from autopsy brain and spleen

tissues and cloned into the pCR3.1 expression plasmid as described (4, 11). A single-round infection assay screen yielded 28 clones that encoded functional Envs (*n*=10 brain and 18 spleen clones). Ten Envs from this set (*n*=5 brain and 5 spleen) were selected for sequencing and further analysis. Expression and processing of 9/10 Envs on 293T cells was verified *via* Western blotting with antibodies directed against gp120 (goat anti-gp120 from the National Institutes of Health AIDS Research and Reference Reagent Program) (data not shown) (2, 4, 11). Coreceptor usage was investigated using a cell-cell fusion assay as previously described (Table 4.1) (4, 11). We previously showed that CCR5 and CXCR4 usage determined in this cell-cell fusion assay correlates well with coreceptor usage determined in viral infection assays (2-3, 12-13). The well characterized ADA (R5), 89.6 (R5X4), and HxB2 (X4) Envs were used as controls. Nine of ten MACS1 Envs tested (*n*=5/5 brain and 4/5 spleen) were equally capable of using CCR5 and CXCR4 for fusion in CD4-expressing cells (Table 4.1). None of the Envs showed a reduced dependence on CD4 levels in the cell-cell fusion assay (data not shown). One Env (spleen-derived clone sp7a-14) was non-functional based on cell-cell fusion assays using either CCR5 or CXCR4; this Env contains an amino acid variant (R507) at the gp120/gp41 interface, disrupting the REKR motif required for furin cleavage which is critical for HIV fusion (14). Thus, Env sp7a-14 is probably non-functional due to loss of gp160 cleavage.

Table 4.1. MACS1 Envs use both CCR5 and CXCR4 to mediate fusion[a]

Envelope	CCR5	CXCR4
ADA	++++	-
89.6	+++	++++
HXB2	-	++++
MACS1br6b-8[1]	++	++
MACS1br6b-9[1]	++	++
MACS1br6b-3	+++	+++
MACS1br6b-13[2]	++++	+++
MACS1br6a-9	++++	++++
MACS1sp7b-11	+++	++++
MACS1sp8a-2	+++	++++
MACS1sp7a-14[2]	-	-
MACS1sp7a-13	+++	++++
MACS1sp7b-9	+++	++++

[a]293T cells cotransfected with pCR3.1Env and pLTR-Tat were mixed with Cf2-Luc cells cotransfected with pcDNA3-CD4 and either pcDNA3-CCR5 or pcDNA3-CXCR4. Cells were harvested following an 8-hour incubation. The levels of fusion in cells expressing CD4 and CCR5 or CXCR4 as measured by luciferase activity are indicated as follows: -, +, ++, +++, and ++++ representing levels that were at background, 1-25%, 25-50%, 50-75%, and 75-100% of control Envs, respectively. Unless otherwise indicated, results are representative of 5 independent assays. [1]Results from 1 fusion assay. [2]Results from 2 fusion assays.

Analysis of amino acid sequences revealed that 9 *envs* (4 brain and 5 spleen) encode a full-length gp120 protein. One brain-derived *env* clone (br6b-9) has a short N-terminal truncation with sequence initiating at the second methionine (position 26) due to a frameshift at position 15 in the N-terminus; this truncation did not affect Env function in the cell-cell fusion assay. Phylogenetic analysis of gp120 nucleotide sequences confirmed distinct compartmentalization of brain- and spleen-derived Env clones (Fig. 4.1). Phylogenetic analysis of V1V2 amino acid sequences showed tight clustering of

brain V1V2 sequences and separation of brain- and spleen-derived Env V1V2 sequences (Fig. 4.1). MACS1 brain-derived Env clone br6b-8 was more closely related to V1V2 sequences derived from spleen than from brain.

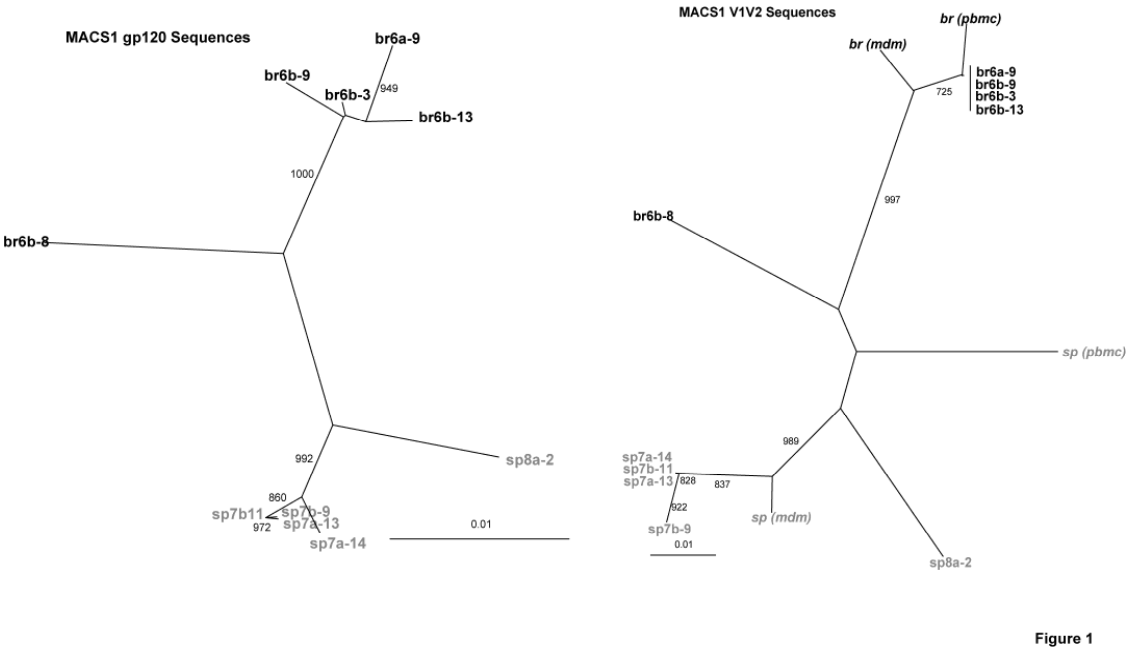

Figure 4.1. Phylogenetic analysis of HIV-1 gp120 and V1V2 sequences.
Sequences from brain and spleen tissues are color-coded black and gray, respectively. Numbers associated with each branch are bootstrap values, which represent the number of trees, out of 1000 replicates performed, in which the same branching order was found. Only values above 800 for the major branches are shown. Branch lengths are proportional to the amount of sequence divergence. Scale bars indicate 1% sequence divergence. The left panel depicts the phylogenetic relationship among gp120 nucleotide sequences amplified directly from brain and spleen tissues from patient MACS1. The right panel depicts V1V2 amino acid sequences derived from patient MACS1. MACS1 brain and spleen viral isolates obtained by PBMC coculture are shown in italics.(3-4)

The gp120 V3 loop contains important determinants of coreceptor usage and syncytium-induction in MT-2 cells (5). Consequently, patterns of V3 amino acid variation are frequently used to predict coreceptor usage of primary HIV strains (6-10, 15-16). To determine the ability of freely available bioinformatic algorithms to predict X4-usage in R5X4 Envs, we compiled a dataset containing 30 unique clade B R5X4 V3

sequences (27 unique V3 sequences from 16 patients in 9 published studies and 3 unique V3 sequences from patient MACS1; *n*=4 brain- and 26 lymphoid/blood-derived sequences) (Fig. 4.2) (2, 12-13, 17-22). Envs in this dataset were cloned and sequenced directly from tissue or from low passage isolates, and coreceptor usage of the clones was experimentally determined using viral infection assays (12-13, 17, 20-22), or a combination of viral infection assays and cell-cell fusion assays (2, 13). We then used this dataset to determine the ability of 6 bioinformatic algorithms to accurately predict X4-usage by R5X4 Envs (Fig. 4.2).

Figure 4.2. Prediction of coreceptor usage by R5X4 V3 sequences using bioinformatic prediction algorithms.
A. Unique R5X4 V3 amino acid sequences (*n*=30) from 17 patients were aligned using ClustalX. The sequences are shown aligned to the CCR5-tropic Clade B consensus sequence. Sequences are grouped by patient. Sequences derived from brain (*n*=4) are underlined. Positions 11 and 25 in the V3 loop are highlighted in the sequence alignments. Algorithms that correctly predict the ability to use CXCR4 are indicated following each sequence. 1= 11/24/25 rule; 2=Charge rule; 3= PSSM (X4R5); 4= PSSM (SINSI);5= Random Forest; 6= $SVM_{genomiac}$; 7= $SVM_{geno2pheno}$. B. Summary of total number of correct predictions for each bioinformatic algorithm and the program's specificity for the 30 R5X4 V3 sequences.

Figure 4.2, Continued

A

```
Clade B       CTRPNNNTRKSIHIGPGRAFYTTGEIIGDIRQAHC
MACS1br6b-8   ..........MSL...K......Q......K...(2,7)
MACS1br6b-9   .I........MSL...KV.....Q......K...(2,4,6,7)
MACS1br&sp    ..........MSL...KV.....Q......K...(2,4,6,7)
aBR01         .........R.VTM.........D..........
aBL01         ........KR..TR....VY....D.V........(2,3,4,6,7)
dBR02/07      .........RKGSM......LAREQ...N......(1,2,3,4,5,6,7)
15888         .........RG.Y......I...DK.V....K.Y.(1,2,3,4,5,6,7)
C2-3/16       ..........TM....VY.................(7)
C2-22         ..........TM....VY...I...........(4,7)
C2-24         ..........TM....VD.....V.........(7)
DR-1          .I........MTL...KV.....-VT.S..K...(2,4,5,6,7)
DR-8/17       .I........MTL...KV.....-VT....K...(2,4,6,7)
DR-19         .I........MTL...KV.....-VT....KE..(2,4,6,7)
89.6          .........RRLS........ARRN..........(1,2,3,4,5,6,7)
DH12          ..........G.TL....V.......V....K...(2,4,7)
T5-R5X4-1/2   ..........R.TM....VY.............K...(1,2,3,4,5,6,7)
3921F12+3     ..........R.SLS...V.............K...(1,2,3,4,5,6,7)
20813B1       .........RR.Y..Q...V...RQ......K.Y.(1,2,3,4,5,6,7)
92HT594       ..........R.S......S....Q......K...(1,2,3,4,5,6,7)
17141raf5     ....G....RR.S..........EQ...N......(1,2,3,4,5,6,7)
17136roe11    ....G.....R.S..........EQ...N......(1,2,3,4,5,6,7)
17131rog6     ....G.....R............EQ...N......(1,2,4,5,6,7)
17129roa10    ....G.....R............RQ...N......(1,2,4,5,6,7)
17136rod11    ....G.....R.S..........EQ..........(1,2,4,5,6,7)
QH1520c.2     ..........RM.IR.....RE-...........(2,5,7)
QH1549c.13    ........I..RM.IR.....RE-...........(2,4,5,7)
96USHIPS9     ..........G.N.....TV.A..K..........(1,2,4,5,7)
49030rog6     ..........G..L.....L.A..G.V........(2)
409028rod7    ............L..........G...N......(2)
QH1521c.34    ..........H..L.A.K....GE-..........(6,7)
```

B

Predictive Algorithm	Correct Predictions/ Total # R5X4 Envs	Accuracy
11/24/25 Rule	13/30	43.3%
Charge Rule	25/30	83.3%
$PSSM_{X4R5}$	10/30	33.3%
$PSSM_{SINSI}$	22/30	73.3%
Random Forest	16/30	53.3%
$SVM_{genomiac}$	19/30	63.3%
$SVM_{geno2pheno}$	27/30	90.0%

Two simple and commonly used prediction methods are the "11/25" rule and the charge rule. In the "11/25" rule, the presence of a positively-charged amino acid at either position 11 or 25 of the V3 loop predicts that the virus can use X4 to mediate entry (6-9, 15-16). This prediction method is significantly less accurate for X4 than for strictly R5-tropic viruses, with <50% and >90% accuracy, respectively (6, 9, 16). The charge rule states that an increase in the net charge of the V3 loop (>3) is strongly associated with CXCR4-usage (10). The Position-Specific Scoring Matrix (PSSM) detects nonrandom distributions of V3 amino acids at adjacent sites associated with an empirically determined group of sequences (8, 15). Two separate matrices are available for clade B Envs at: http://ubik.microslu.washington.edu/computing/pssm. $PSSM_{X4R5}$ bases predictions on sequences of known coreceptor-usage phenotype. $PSSM_{SINSI}$ bases predictions on known syncytium-inducing phenotypes on the MT-2 cell line (8). Random forest (http://yjxy.ujs.edu.cn/R5-X4 pred.rar) evaluates the relative importance of 37 features of the V3 loop including amino acid variation at each position, net charge, and polarity (10). Finally, two versions of the Support Vector Machine (SVM) algorithm can be used for coreceptor phenotype predictions (9). $SVM_{genomiac}$ (http://genomiac2.ucsd.edu:8080/wetcat/v3.html) outputs a categorical score (CCR5 or CXCR4) using a dataset aligned to a standard amino acid sequence. $SVM_{geno2pheno}$ (http://coreceptor.bioinf.mpi-sb.mpg.de/cgi-bin/coreceptor.pl) similarly outputs a

categorical score based on alignment of V3 nucleotide sequences. The accuracy of these methods in predicting coreceptor usage of R5X4 Envs has not been reported.

Coreceptor usage predictions for the R5X4 V3 sequence dataset using the "11/25" rule were comparable to those reported for X4-tropic V3 sequences, with an accuracy of 43.3% (13/30 Envs). Including position 24 in this rule ("11/24/25" rule) is reported to increase accuracy of prediction of X4-tropic sequences (6). However, including position 24 did not affect the prediction accuracy of this R5X4 dataset. The Cardozo et al model was constructed using strictly R5- or X4-tropic Envs. However, R5X4 Envs contain V3 loops that can adopt conformations capable of interacting with either CCR5 and CXCR4, and may therefore contain surface patches that do not conform to the static models of V3 structure in this proposed model (6). A second commonly used coreceptor-prediction method, the charge rule, predicted that 83.3% of the V3 data set could use CXCR4 for entry (25/30 Envs). Of the two PSSM matrices, $PSSM_{X4R5}$ matrix correctly predicted X4 usage for 10/30 V3 sequences (33.3% accuracy). $PSSM_{X4R5}$ predicted that 3/3 MACS1 unique V3 sequences would be strictly R5-tropic (0% accuracy). The $PSSM_{SINSI}$ matrix correctly predicted X4-usage in 22/30 V3 sequences, thereby increasing the accuracy of prediction for our dataset of R5X4 Envs from 33.3% to 73.3%. X4-usage was correctly predicted for 2/3 unique MACS1 V3 sequences (66.6% accuracy). The random forest program predicted X4-usage for 16/30 Envs, with an accuracy of 53.3%, and predicted that 3/3 unique MACS1 Envs were strictly R5-tropic (0% accuracy). $SVM_{genomiac}$ correctly predicted 19/30 Envs could use CXCR4 to mediate entry, with an accuracy of 63.3%. As with $PSSM_{SINSI}$, X4-usage was correctly predicted for 2/3 unique MACS1 V3 sequences (66.6% accuracy). Finally, $SVM_{geno2pheno}$ predicted that 27/30 R5X4 Envs

could use X4 for entry, with an accuracy of 90.0% (specificity, defined here as rate of false positives, set at 10%). Prediction of X4-usage for the unique MACS1 Envs was 3/3 (100%). X4-usage predictions were most accurate when specificity levels were at 5-10%. Increasing the stringency of predictions through decreasing the specificity rate to <5% resulted in a concurrent decrease in prediction accuracy, but could be overcome by inputting clinical data (CCR5-genotype and CD4+ counts).

SUMMARY AND DISCUSSION

While no single variant appears to affect the accuracy of coreceptor prediction in every genetic background, changing the Env V3 sequence entered into bioinformatic programs to assess the effects of specific amino acids on prediction accuracy in our R5X4 dataset identified several positions that may contribute to the accuracy of coreceptor prediction using bioinformatic approaches. Both the X4R5 and SINSI PSSM matrices incorrectly predict that MACS1 brain Env clone br6b-8 is R5-tropic. Env br6b-8 contains the consensus alanine at position 19 in the V3 loop, while the other eight MACS1 Env clones contain a valine at this position. Changing the amino acid sequence from our dataset of 30 unique V3 sequences from valine to alanine at position 19 also changes the PSSM prediction from X4- to R5-tropic in 9 additional Envs. These results suggest that an alanine-to-valine change at position 19 may be associated with a change from R5- to X4-tropism in sequences from the training sets of both matrices. Another interesting finding from the PSSM matrix predictions is that a glutamine to lysine variant at position 32 in the V3 loop changed the prediction for our set of MACS-1 Env clones from R5-tropic to X4-tropic. This trend is applicable to additional V3 sequences from our dataset

that contain the lysine variant at position 32. These results suggest that inclusion of V3 amino acid sequences from more X4 or R5X4 Envs to algorithm training sets will further increase the prediction accuracy of these matrices.

In summary, we identified R5X4 HIV-1 in brain from a patient with severe HAD. Comparison of the ability of bioinformatic algorithms to correctly predict X4-usage by R5X4 Envs in our dataset showed that the frequency of R5X4 HIV-1 is underestimated by most commonly used predictive algorithms. $SVM_{geno2pheno}$ is the most accurate predictor of CXCR4-usage by R5X4 HIV-1 in brain and other tissues. Bioinformatic prediction tools provide a convenient method to screen for coreceptor usage, an issue of increasing importance for clinicians considering the use of CCR5 antagonists in HIV-infected patients. It will therefore be important for future studies to increase X4 and R5X4 sequences associated with bioinformatic algorithm training set sequences in the development of prediction tools in order to better define the patterns of amino acid variation that contribute to inaccurate predictions.

SEQUENCE DATA

Sequences reported here were assigned Genbank accession numbers EU401895-EU401904.

ACKNOWLEDGEMENTS

We thank Mark Jensen for helpful discussions. This work was supported by NIH grants NS37277 and MH83588. M.M. was supported in part by NIH fellowship 1F31NS060611-01. P.R.G. is the recipient of an Australian National Health and Medical Research Council (NHMRC) R. Douglas Wright Biomedical Career Development Award and was supported, in part, by a grant from the Australian NHMRC (433915). Core facilities were supported by Harvard Medical School Center for AIDS Research (CFAR) and DFCI/Harvard Cancer Center grants.

REFERENCES

1. Dunfee R, Thomas ER, Gorry PR, Wang J, Ancuta P, Gabuzda D. Mechanisms of HIV-1 neurotropism. Curr HIV Res. 2006;4(3):267-78.

2. Ohagen A, Devitt A, Kunstman KJ, Gorry PR, Rose PP, Korber B, et al. Genetic and functional analysis of full-length human immunodeficiency virus type 1 env genes derived from brain and blood of patients with AIDS. J Virol. 2003;77(22):12336-45.

3. Gorry PR, Bristol G, Zack JA, Ritola K, Swanstrom R, Birch CJ, et al. Macrophage tropism of human immunodeficiency virus type 1 isolates from brain and lymphoid tissues predicts neurotropism independent of coreceptor specificity. J Virol. 2001;75(21):10073-89.

4. Gorry PR, Taylor J, Holm GH, Mehle A, Morgan T, Cayabyab M, et al. Increased CCR5 affinity and reduced CCR5/CD4 dependence of a neurovirulent primary human immunodeficiency virus type 1 isolate. J Virol. 2002;76(12):6277-92.

5. LaBranche CC, Hoffman TL, Romano J, Haggarty BS, Edwards TG, Matthews TJ, et al. Determinants of CD4 independence for a human immunodeficiency virus type 1 variant map outside regions required for coreceptor specificity. J Virol. 1999;73(12):10310-9.

6. Cardozo T, Kimura T, Philpott S, Weiser B, Burger H, Zolla-Pazner S. Structural basis for coreceptor selectivity by the HIV type 1 V3 loop. AIDS Res Hum Retroviruses. 2007;23(3):415-26.

7. Resch W, Hoffman N, Swanstrom R. Improved success of phenotype prediction of the human immunodeficiency virus type 1 from envelope variable loop 3 sequence using neural networks. Virology. 2001;288(1):51-62.

8. Jensen MA, Li FS, van 't Wout AB, Nickle DC, Shriner D, He HX, et al. Improved coreceptor usage prediction and genotypic monitoring of R5-to-X4 transition by motif analysis of human immunodeficiency virus type 1 env V3 loop sequences. J Virol. 2003;77(24):13376-88.

9. Low AJ, Dong W, Chan D, Sing T, Swanstrom R, Jensen M, et al. Current V3 genotyping algorithms are inadequate for predicting X4 co-receptor usage in clinical isolates. Aids. 2007;21(14):F17-24.

10. Xu S, Huang X, Xu H, Zhang C. Improved prediction of coreceptor usage and phenotype of HIV-1 based on combined features of V3 loop sequence using random forest. J Microbiol. 2007;45(5):441-6.

11. Thomas ER, Dunfee RL, Stanton J, Bogdan D, Taylor J, Kunstman K, et al. Macrophage entry mediated by HIV Envs from brain and lymphoid tissues is determined

by the capacity to use low CD4 levels and overall efficiency of fusion. Virology. 2007;360(1):105-19.

12. Gray L, Churchill MJ, Keane N, Sterjovski J, Ellett AM, Purcell DF, et al. Genetic and functional analysis of R5X4 human immunodeficiency virus type 1 envelope glycoproteins derived from two individuals homozygous for the CCR5delta32 allele. J Virol. 2006;80(7):3684-91.

13. Gorry PR, Dunfee RL, Mefford ME, Kunstman K, Morgan T, Moore JP, et al. Changes in the V3 region of gp120 contribute to unusually broad coreceptor usage of an HIV-1 isolate from a CCR5 Delta32 heterozygote. Virology. 2007;362(1):163-78.

14. Bosh VMP. Mutational analysis of the human immunodeficiency virus type I env gene product proteolytic cleavage site. J Virol. 1990;64:2337-44.

15. Shah M, Smit TK, Morgello S, Tourtellotte W, Gelman B, Brew BJ, et al. Env gp120 sequence analysis of HIV type 1 strains from diverse areas of the brain shows preponderance of CCR5 usage. AIDS Res Hum Retroviruses. 2006;22(2):177-81.

16. Hoffman NG, Seillier-Moiseiwitsch F, Ahn J, Walker JM, Swanstrom R. Variability in the human immunodeficiency virus type 1 gp120 Env protein linked to phenotype-associated changes in the V3 loop. J Virol. 2002;76(8):3852-64.

17. Yi Y, Shaheen F, Collman RG. Preferential use of CXCR4 by R5X4 human immunodeficiency virus type 1 isolates for infection of primary lymphocytes. J Virol. 2005;79(3):1480-6.

18. Gao F, Morrison SG, Robertson DL, Thornton CL, Craig S, Karlsson G, et al. Molecular cloning and analysis of functional envelope genes from human immunodeficiency virus type 1 sequence subtypes A through G. The WHO and NIAID Networks for HIV Isolation and Characterization. J Virol. 1996;70(3):1651-67.

19. Sullivan PS, Schable C, Koch W, Do AN, Spira T, Lansky A, et al. Persistently negative HIV-1 antibody enzyme immunoassay screening results for patients with HIV-1 infection and AIDS: serologic, clinical, and virologic results. Seronegative AIDS Clinical Study Group. Aids. 1999;13(1):89-96.

20. Skrabal K, Saragosti S, Labernardiere JL, Barin F, Clavel F, Mammano F. Human immunodeficiency virus type 1 variants isolated from single plasma samples display a wide spectrum of neutralization sensitivity. J Virol. 2005;79(18):11848-57.

21. van Rij RP, Blaak H, Visser JA, Brouwer M, Rientsma R, Broersen S, et al. Differential coreceptor expression allows for independent evolution of non-syncytium-inducing and syncytium-inducing HIV-1. J Clin Invest. 2000;106(12):1569.

22. Hu QX, Barry AP, Wang ZX, Connolly SM, Peiper SC, Greenberg ML. Evolution of the human immunodeficiency virus type 1 envelope during infection reveals

molecular corollaries of specificity for coreceptor utilization and AIDS pathogenesis. J Virol. 2000;74(24):11858-72.

CHAPTER 5: DISCUSSION

Summary

HIV infection of macrophages in brain and other tissues plays an important role in the development of HIV-associated neurological disorders (HAND) and other aspects of disease pathogenesis. Macrophages express low levels of CD4, and envelope glycoproteins (Envs) from macrophage-tropic (M-tropic) HIV strains adapt to overcome this restriction to virus entry by mechanisms that are not well characterized. One mechanism that influences this phenotype is increased exposure of the CD4 or CCR5 binding sites, which may also increase dissociation of soluble gp120 (sgp120) from the Env trimer based on structural models. Little is known about spontaneous sgp120 shedding from primary HIV Envs or its biological significance.

In Chapter 2, we sought to identify determinants in M-tropic brain-derived Envs that contribute to reduced CD4-dependence by enhancing gp120 interactions with CCR5. To accomplish this goal, we examined brain and lymphoid gp120 sequences from the bridging sheet region of the CCR5 binding site from AIDS patients with or without HIV-associated dementia (HAD). Two determinants in the surface exposed β3 strand of the bridging sheet were identified. D197, which results in the elimination of an N-linked glycosylation site, was associated with brain infection and dementia. Position 200 was under positive selection in HAD patients. D197 and T/V200 enhanced fusion and entry with macrophages and other cells expressing low CD4 by enhancing gp120 binding to CCR5. The influence of T/V200 on fusion and entry was additive when combined with D197, suggesting that variants in the β3 strand might act cooperatively enhance M-tropism. In Chapter 3, we analyzed spontaneous sgp120 shedding from a panel of 65 primary brain and lymphoid Envs from 12 AIDS patients. Sgp120 shedding from primary brain and lymphoid Envs was highly variable within and between patients, representing a spectrum rather than a categorical phenotype, and for 66% of Envs

reached levels overlapping those shown to induce biological effects *in vivo*. Brain Envs with high sgp120 shedding mediated enhanced fusion and infection with cells expressing low CD4. Furthermore, viruses expressing brain Envs with high sgp120 shedding demonstrated an increased capacity to induce lymphocyte activation during infection of PBMC, despite similar levels of viral replication. Genetic analysis demonstrated greater entropy and positive selection in Envs with high versus low levels of sgp120 shedding, suggesting that diversifying evolution influences gp120-gp41 association. Finally, in Chapter 4 we sequenced the gp120 coding region of nine full-length dual-tropic (R5X4) *env* genes cloned directly from autopsy brain and spleen tissue from an AIDS patient with severe HAD. We then compiled a dataset of 30 unique clade B R5X4 Env V3 sequences from this subject and 16 additional patients (*n*=4 brain and 26 lymphoid/blood Envs) and used it to compare the ability of six bioinformatic algorithms to correctly predict CXCR4 usage in R5X4 Envs. The results demonstrated that most predictive algorithms underestimated the frequency of R5X4 HIV-1 in brain and other tissues. $SVM_{geno2pheno}$ was the most accurate predictor of CXCR4 usage by R5X4 HIV-1.

Together, our work provides a better understanding of the mechanisms by which gp120 determinants in brain Envs influence M-tropism. In addition, our findings demonstrate that spontaneous sgp120 shedding from primary brain and lymphoid Envs represents a phenotypic spectrum that may influence HIV pathogenesis by contributing to immune activation and bystander cell apoptosis. The following sections will discuss these phenotypes in greater detail.

Mechanisms of HIV-1 Macrophage Tropism

Macrophages express lower levels of CD4 than CD4+ T cells in peripheral blood, and are preferentially infected by viruses that can utilize low levels of CD4 for entry (1-9). The major viral determinant of M-tropism is Env. Mechanisms that enhance Env interactions with CD4 have been elucidated in a number of studies, and include increased binding affinity for CD4 and increased exposure of the CD4-binding site (1, 6, 9-12). One mechanism by which HIV Envs may overcome the restriction imposed by reduced CD4 on macrophages is through enhanced Env interactions with CCR5. Although several studies described M-tropic Envs with reduced CCR5 dependence, the determinants in M-tropic Envs that contribute to this phenotype are poorly understood (13-15). Gorry et al (14) characterized brain-derived Env clones with increased affinity for CCR5. These Envs mediated cell-cell fusion with target cells expressing low CD4 or CCR5, and were sensitive to CCR5-targeted small molecule inhibitors, suggesting that high-affinity Env-CCR5 interactions might contribute to infection of target cells expressing low CD4. Other studies have also identified M-tropic R5 viruses that can use low levels of CD4 and CCR5 for entry (2, 15-17), raising the possibility that enhanced gp120-CCR5 interactions may be a mechanism that contributes to M-tropism in brain-derived Envs. Possible mechanisms that may contribute to these interactions include increased exposure of the CCR5 binding site, increased affinity of Env for CCR5, adoption of conformations that facilitate the rearrangements that occur following CD4 and/or coreceptor binding, and sampling of the CD4-bound conformation of gp120.

In Chapter 2, we investigated whether D197 and T/V200 in the HIV gp120 β3 strand of the bridging sheet enhanced gp120-CCR5 interactions of M-tropic Envs. Viruses expressing Envs containing D197 and T/V200 mediated enhanced entry into Affinofile cells expressing low

CD4 and CCR5 (Fig. 2.3). The UK1br T200V Env exhibited increased gp120 binding to CCR5 at levels 10-fold those of the parental Env (Fig. 2.4), suggesting that D197 and T/V200 contribute to high-affinity interactions between M-tropic brain-derived Envs and CCR5.

The increased interactions between gp120 and CCR5 were not due to increased exposure of the CCR5 binding site, as was previously reported for mutagenesis studies in which the N-linked glycosylation site (PNGS) at position 197 was eliminated (14, 18-20). Differences in neutralization sensitivity were detected between the UK1br and M2br Envs, indicating that the mechanism by which D197 and T/V200 contribute to M-tropism is context-specific. None of the parental or mutant Envs exhibited neutralization sensitivity to monoclonal antibodies 17b or 412d (Table 2.3, Fig. S2.2, data not shown). However, although the M2br Envs were resistant to neutralization by sCD4, viruses expressing M2br N197D and N197D/V200T were sensitive to neutralization by 17b following preincubation with sCD4. This suggests that D197 and T200 in this context may influence the formation or stability of the 17b epitope following binding to low levels of sCD4, or influence the kinetics of post-CD4 binding conformational rearrangements. In contrast, the UK1br Envs remained neutralization resistant to 17b following incubation with sCD4, but were neutralization sensitive to sCD4 alone. There was a 12-fold increase in resistance to sCD4 neutralization for UK1br D197N compared to the parental Env, as was previously reported (18-19, 21-22). Haim et al demonstrated that Envs have different susceptibilities to inactivation by sCD4, which may be linked to reactivity and a propensity to sample different conformations, resulting in increased sCD4-induced sgp120 shedding and virus inactivation (23-24). Thus, D197 and T/V200 seem to enhance gp120-CCR5 affinity by distinct mechanisms that may include sampling conformations that enhance gp120 binding to CCR5 and stabilizing the CCR5-binding site region following interactions with low levels of CD4.

Gp120 interactions with CCR5 are dependent on the tyrosine-rich and highly acidic CCR5 amino terminus and the second extracellular loop (ECL2). In particular, sulfation of the tyrosines at positions 10, 14, and 15 appears to be the most critical (25-27). Recent studies have suggested that brain Envs with increased affinity for the CCR5 ECL-2 region demonstrate increased efficiency of CCR5 usage (15, 28-29). This model has been predicted to contribute to M-tropism through alterations in the gp120 V3 loop, CD4-binding site, and gp41 interaction sites in the N- and C-termini (15). To examine whether D197 and T/V200 influenced interactions with CCR5, we analyzed cell-cell fusion with cells expressing CD4 and CCR5 coreceptors containing amino acid alterations in the N-terminus and ECL-2 regions (provided by D. Kabat) (25). However, there were only minor differences in the ability of the parental and mutant Envs to mediate fusion with cells expressing these attenuated CCR5s (data not shown). These results indicate that enhancement of M-tropism observed for these Envs was not due to increased dependence on the CCR5 ECL-2 region.

Model for Enhanced Infection of Target Cells Expressing Low CD4 by Envs with High Levels of sgp120 Shedding

HIV entry into cells is initiated by a high affinity interaction between gp120 and CD4. CD4 binding induces conformational changes in gp120 that involve rearrangements of the V1/V2 and V3 variable loops and formation and exposure of the CCR5 binding site (30-31). The V1/V2 and V3 loops in the unliganded Env trimer are thought to both protect the CD4 and CCR5 binding sites and neutralization epitopes and provide contact points at the apex of the trimer (32-33). The interactions between the variable loops in the context of the trimer are supported by

functional studies, which suggest that the V1/V2 loops on one protomer may mask neutralization epitopes by interacting with the V3 loop of an adjacent protomer (33-37). Adaptations to target cells expressing low CD4 may result in increased exposure of the CD4-binding site or CD4-induced epitopes, or adoption of an "open" conformation with partial formation of the CCR5 binding site and exposure of the gp41 prehairpin intermediate (8, 10-11, 33, 38-39), possibly due to repositioning of the variable loops. This is turn may destabilize the unliganded Env trimer, resulting in spontaneous sgp120 shedding.

In Chapter 3, we demonstrated that brain-derived Envs with high levels of sgp120 shedding mediated enhanced fusion and entry into cells expressing low levels of CD4 (Fig. 3.5). However, we did not find any correlations between Envs with high levels of sgp120 shedding and neutralization sensitivity to sCD4, monoclonal antibody b12, or patient sera (data not shown), which may reflect context-specific differences in adaptation to target cells expressing low CD4. In support of this idea, we found associations between neutralization sensitivity to b12 and high levels of shedding for Envs from three patients, although the sample size was too small to be considered significant (n=11 Envs, p=0.03, r=-0.68, Spearman correlation) (data not shown). Because enhanced affinity of Env for CCR5 may also contribute to reduced CD4-dependence, we analyzed correlations between Envs with high levels of sgp120 shedding and sensitivity to entry inhibitors targeting CCR5 (TAK779 and AD101, data not shown), but found no associations. Published results showed that a subset of the Envs used in our study mediate fusion and infection of cells expressing low CCR5 (7, 13), but the sample size was too small to analyze correlations between Envs with enhanced interactions with CCR5 and TAK-779 sensitivity. There was a trend towards an association between sensitivity to the entry inhibitor T20 and Envs with high levels of shedding (p=0.07, r=0.31, data not shown). T20 is an antiviral

C-peptide which targets gp41 HR1 and blocks gp41 conformational changes, including formation of the six-helix bundle (40). The gp41 HR1 and HR2 regions are exposed following gp120 binding to CD4 (31); therefore, sensitivity of Envs with high levels of sgp120 shedding to T20 suggests that some of these Envs may sample a CD4-bound conformation. Thus, Envs that mediate enhanced fusion and entry with cells expressing low levels of CD4 may increase sgp120 shedding in a context-dependent manner by influencing positioning of the variable loops or adopting an "open" conformation.

Possible Contributions of sgp120 to HIV Pathogenesis

The HIV Env sgp120 subunit induces biological effects *in vitro* at concentrations ranging from <800 pM to in excess of 40 nM. In contrast, concentrations of sgp120 detected by ELISA *in vivo* range from less than 20 to 800 pM in plasma and in excess of 4 nM in lymph nodes and spleen (41-45). These concentrations overlap the lower range of concentrations used *in vitro*, and bring into question the physiological relevance of some of the *in vitro* data. Moreover, questions have been raised concerning the validity of detection of sgp120 in plasma and tissues by ELISA (46). Sgp120 in excess of that associated with virions is detected in only a subset of patients (42-45), and the presence of plasma antibodies is proposed to interfere with accurate detection of free sgp120 (46). Therefore, the most accurate assessment of the technique may be from the studies that measured sgp120 in plasma and tissues during the acute and early stages of infection (41-43) when nonneutralizing anti-gp41 antibodies predominate (47). However, a recent study by Liu et al showed that during chronic infection in a subset of patients, levels of HIV in plasma complexed to gp120-specific IgG antibodies only approached 50% of free virus, suggesting that even during the later stages of HIV/AIDS free sgp120 in plasma may be available to activate

bystander cells (47). Indeed, sgp120 levels measured in plasma in one study remained constant before and after seroconversion, suggesting that plasma antibodies may not invariably impede detection (42). Therefore, sgp120 concentrations measured *in vivo*, especially during the early stages of infection, may be a fairly accurate measure of free sgp120.

The question remains whether sgp120 in plasma and tissues can reach the concentrations detected *in vivo*. Env trimers are expressed on the surface of virions and infected cells. Limited numbers of Env trimer spikes are found on virions, with an average of 14 spikes on HIV-1 (48). However, while the concentration of Env on the surface of infected cells *in vivo* is not known (46), higher concentrations of Env are found on the surface of infected cells compared to virions *in vitro*. These results suggest that to reach high concentrations locally, sgp120 must be shed from the surface of infected cells. Therefore, during periods of viral replication, sgp120 shed from virions and infected cells in tissue compartments with high local cell density and low extracellular space, including lymph node and spleen, has the potential to reach concentrations shown to induce biological effects *in vitro* (41, 46). This is especially true in brain, where low levels of neutralizing antibodies provide a milieu conducive to sgp120-induced activation of macrophages and potential involvement in development of HAND (46).

In Chapter 3, we present evidence that brain-derived virions with high levels of sgp120 shedding upregulated CD25 expression and induced IL-1β production from bystander CD4+ and CD8+ T cells during viral replication *in vitro* (Fig. 3.7). The observed lymphocyte activation was independent of levels of viral replication, but instead was associated with levels of sgp120 shedding detected by Western blotting *in vitro*. However, the question remains whether sgp120 induces biological effects relevant for disease pathogenesis *in vivo*. Purified sgp120 at concentrations overlapping those detected *in vivo* has been shown to induce many biological

effects *in vitro*. A large number of studies have demonstrated that sgp120 binds to CD4 on uninfected T cells and macrophages, resulting in cellular activation and production of proinflammatory cytokines, including IL-1α, IL-1β, IL-6, IL-8, TNF-α, IFN-α/β, and IFN-γ (42, 49-56). A recent study showed that sgp120 concentrations measured by ELISA in plasma from patients in the early stages of HIV infection correlated with higher levels of plasma IL-6, IL-10, and TNF-α compared to subjects without detectable sgp120 in plasma, suggesting that Envs that readily shed sgp120 *in vivo* may also induce cytokine production (42). Activation of both HIV-infected and bystander T cells and macrophages can induce apoptosis of uninfected T cells and neurons, (49, 55, 57-66), which may contribute to T-cell depletion and development of HIV-associated neurological disorders (HAND) (58, 62, 67). Interestingly, low dose exposures of sgp120 are associated with upregulation of lymphocyte activation markers including HLA-DR, CD25, and CD69 (41, 49, 53), while high dose exposures (>1 mg) induced T cell anergy and inhibited proliferation to mitogens including tetanus toxin (68-72). These results are in agreement with a study investigating proliferation of lymphocytes isolated from lymph node and plasma from SHIV-KB9-infected rhesus macaques (41). In this study, CD4+ and CD8+ T cells from plasma responded to a KB9 Env peptide pool *in vitro*, while responses from lymphocytes isolated from lymph nodes were suppressed. When plasma lymphocytes were incubated with concentrations of SHIV-KB9 Env overnight at concentrations equivalent to those detected in macaque lymph nodes, responses from CD4+ and CD8+ T cells were suppressed similarly to those isolated from lymph nodes. Therefore, long-term exposure to high doses of sgp120 may induce anergy and contribute to lack of immune-mediated clearance of HIV from reservoirs such as lymph node.

Sgp120 has been shown to be capable of disrupting epithelial barriers *in vitro*, including models of both mucosal epithelia and the blood brain barrier (BBB) (52, 73). Furthermore, results from *in vitro* assays showed that sgp120 independent from viral replication increased monocyte adhesion and migration across BBB models, providing a possible mechanism for enhanced virus penetration into the central nervous system (CNS) (52). Incubation with sgp120 has also been shown to impair the barrier function of primary epithelial cells *in vitro*, allowing translocation of virus and bacteria across a model of the mucosal epithelium (73). This translocation promotes systemic immune activation (74), suggesting that sgp120 shed from cells in the brain and gut-associated lymphoid tissues (GALT) might contribute to HIV pathogenesis.

While the amounts of sgp120 needed to induce cytopathic effects in some model systems may exceed physiologically relevant concentrations, concentrations of sgp120 required to induce neuronal apoptosis (<100 ng/ml) *in vitro* are significantly lower than amounts of sgp120 detected in tissues such as lymph node and spleen (41, 43, 57, 64-66). Because antibodies are present at low levels in the CNS (62, 75), there is a lower probability of antibody-mediated clearance of sgp120 from brain tissue. In addition to inducing neuronal apoptosis, sgp120 induces the production of toxic intermediates such as proinflammatory cytokines and arachidonic acid metabolites from activated cells, including macrophages/microglia (76-78). Sgp120 has been implicated in inducing nitric oxide synthase from astrocytes *in vitro* through binding to CXCR4 (77), which may impair their ability to protect neurons from damage. Thus, sgp120 at low concentrations may contribute to HIV neurological complications by increasing trafficking of infected lymphocytes and monocytes across the BBB and inducing production of neurotoxic factors from activated macrophages, microglia, astrocytes, and BMVECs.

Identification of Viral Determinants Associated with Brain Compartmentalization and Dementia

The genetic evolution of HIV variants in brain is distinct from that in lymphoid tissues and other organs (13, 79-83). Genetic compartmentalization of HIV within the brain suggests that selection and/or adaptive evolution may occur in the CNS in response to unique constraints of the brain microenvironment, including different target cell populations and immune selection pressures. However, the selection pressures *in vivo* that drive changes in M-tropism of R5 Envs are poorly understood (84).

Three main approaches are used to identify genetic determinants associated with brain infection. The first approach uses mutagenesis to identify determinants that contribute to the phenotype of a specific brain-derived Env (7, 9, 28, 34, 85-86). The second approach identifies determinants or signature sequences associated with brain using sequence analysis and bioinformatic tools (80, 87-89). The third approach uses a combination of molecular and bioinformatic approaches to identify variants associated with brain in a large dataset and determine whether the determinant contributes to a phenotype associated with brain infection (1, 11). The third approach is the one we chose for our studies.

In Chapter 2, we analyzed brain- and lymphoid-derived Env sequences from a large dataset of Envs from published studies and identified the loss an N-linked glycosylation site (PNGS) at position 197 as being associated with brain infection (Table 2.2). Further analysis of brain-derived sequences from patients with or without HAD determined that the loss of the PNGS was also associated with dementia. Functional studies confirmed that D197 influenced macrophage entry (Fig. 2.2). Thus, the combination of bioinformatic and molecular approaches

identified a viral determinant that, while rare, is associated with brain infection in a large dataset of primary Envs and contributes to HIV infection.

We analyzed diversifying selection in the bridging sheet region of the CCR5-binding site in Env sequences from patients with or without HAD. By this approach, we identified one codon (position 200 in the β3 strand of the gp120 bridging sheet) under positive selection in HAD patients (Fig. 2.1, Table 2.1). Position 200 was under positive selection in both brain and blood/lymphoid sequences from patients with HAD, and evolution was therefore not due to CNS-specific selection pressures. Position 200 is located in several overlapping immunodominant CTL epitopes (LANL CTL/CD8+ T Cell Database); diversifying selection at this position may therefore be a consequence of immune escape. T200 is found in matched brain and lymphoid sequences from 4 patients. In these patients, T200 was present in 100% of brain-derived sequences, and 60-100% of lymphoid sequences. This suggests that Thr could be the result of a founder effect in these patients, or the result of immune escape from CTL responses.

In summary, the combination of sequence analysis approaches described above allowed us to identify two genetic determinants that contribute to reduced CD4-dependence in brain-derived Env clones in an additive manner. The combination of approaches therefore identified variants that would have not been identified by either approach alone. Thus, studies that investigate both the genetic and molecular contributions of viral determinants of brain infection may provide a better understanding of mechanisms by which viral evolution and selection in the CNS contribute to HIV-associated neurological diseases.

Conclusions

Over the 28 years since its discovery, HIV infection has resulted in over 25 million deaths worldwide, and an estimated 35 million people are currently living with HIV infection (UNAIDS 2011). However, the use of HAART has resulted in a decline in incidence in 33 countries, and advances continue to be made. One of the main barriers to eradication of HIV infection is the seclusion of virus in reservoirs in the infected host. Cells of the macrophage lineage are reservoirs for HIV, contributing to virus persistence and disease pathogenesis (90-91). Persistently infected macrophages are less susceptible to the cytopathic effects of HIV infection than activated T cells and continue to shed virus for the duration of their normal lifespan (91). Furthermore, HIV-infected macrophages in tissues with low antiretroviral penetration, such as perivascular macrophages in brain, create sanctuaries of HIV infection that may persist for years (77). Env is the main determinant of M-tropism. Molecular and bioinformatic approaches provide a way to identify determinants in brain-derived Envs that contribute to M-tropism. A better understanding of the mechanisms by which brain-derived M-tropic Envs enhance interactions with CD4 and CCR5 will facilitate the development of therapeutics aimed at blocking these interactions.

In summary, we demonstrated that genetic determinants in the gp120 bridging sheet influence M-tropism by enhancing gp120 binding to CCR5. Furthermore, we demonstrated that a significant proportion of brain and lymphoid Envs readily shed sgp120 and present evidence that this phenotype is associated with enhanced interactions between gp120 from brain-derived Envs and CD4 and/or CCR5 and possibly with lymphocyte activation during PBMC infection. Our finding that spontaneous sgp120 shedding represents a spectrum rather than a categorical

phenotype has implications for HIV pathogenesis and optimization of therapeutics, including native Env mimetics and vaccines.

REFERENCES

1. Dunfee RL, Thomas ER, Gorry PR, Wang J, Taylor J, Kunstman K, et al. The HIV Env variant N283 enhances macrophage tropism and is associated with brain infection and dementia. Proc Natl Acad Sci U S A. 2006;103(41):15160-5. PMCID: 1586182.

2. Gray L, Sterjovski J, Churchill M, Ellery P, Nasr N, Lewin SR, et al. Uncoupling coreceptor usage of human immunodeficiency virus type 1 (HIV-1) from macrophage tropism reveals biological properties of CCR5-restricted HIV-1 isolates from patients with acquired immunodeficiency syndrome. Virology. 2005;337(2):384-98.

3. Walter BL, Wehrly K, Swanstrom R, Platt E, Kabat D, Chesebro B. Role of low CD4 levels in the influence of human immunodeficiency virus type 1 envelope V1 and V2 regions on entry and spread in macrophages. J Virol. 2005;79(8):4828-37.

4. Wang J, Crawford K, Yuan M, Wang H, Gorry PR, Gabuzda D. Regulation of CC chemokine receptor 5 and CD4 expression and human immunodeficiency virus type 1 replication in human macrophages and microglia by T helper type 2 cytokines. J Infect Dis. 2002;185(7):885-97.

5. Bannert N, Schenten D, Craig S, Sodroski J. The level of CD4 expression limits infection of primary rhesus monkey macrophages by a T-tropic simian immunodeficiency virus and macrophagetropic human immunodeficiency viruses. J Virol. 2000;74(23):10984-93.

6. Martin-Garcia J, Cao W, Varela-Rohena A, Plassmeyer ML, Gonzalez-Scarano F. HIV-1 tropism for the central nervous system: Brain-derived envelope glycoproteins with lower CD4 dependence and reduced sensitivity to a fusion inhibitor. Virology. 2006;346(1):169-79.

7. Peters PJ, Bhattacharya J, Hibbitts S, Dittmar MT, Simmons G, Bell J, et al. Biological analysis of human immunodeficiency virus type 1 R5 envelopes amplified from brain and lymph node tissues of AIDS patients with neuropathology reveals two distinct tropism phenotypes and identifies envelopes in the brain that confer an enhanced tropism and fusigenicity for macrophages. J Virol. 2004;78(13):6915-26.

8. Duenas-Decamp MJ, Peters P, Burton D, Clapham PR. Natural resistance of human immunodeficiency virus type 1 to the CD4bs antibody b12 conferred by a glycan and an arginine residue close to the CD4 binding loop. J Virol. 2008;82(12):5807-14.

9. Duenas-Decamp MJ, Peters PJ, Burton D, Clapham PR. Determinants flanking the CD4 binding loop modulate macrophage tropism of human immunodeficiency virus type 1 R5 envelopes. J Virol. 2009;83(6):2575-83.

10. Peters PJ, Duenas-Decamp MJ, Sullivan WM, Brown R, Ankghuambom C, Luzuriaga K, et al. Variation in HIV-1 R5 macrophage-tropism correlates with sensitivity to reagents that block envelope: CD4 interactions but not with sensitivity to other entry inhibitors. Retrovirology. 2008;5:5.

11. Dunfee RL, Thomas ER, Wang J, Kunstman K, Wolinsky SM, Gabuzda D. Loss of the N-linked glycosylation site at position 386 in the HIV envelope V4 region enhances macrophage tropism and is associated with dementia. Virology. 2007;367(1):222-34. PMCID: 2201988.

12. Sterjovski J, Churchill MJ, Ellett A, Gray LR, Roche MJ, Dunfee RL, et al. Asn 362 in gp120 contributes to enhanced fusogenicity by CCR5-restricted HIV-1 envelope glycoprotein variants from patients with AIDS. Retrovirology. 2007;4:89. PMCID: 2225424.

13. Thomas ER, Dunfee RL, Stanton J, Bogdan D, Taylor J, Kunstman K, et al. Macrophage entry mediated by HIV Envs from brain and lymphoid tissues is determined by the capacity to use low CD4 levels and overall efficiency of fusion. Virology. 2007;360(1):105-19. PMCID: 1890014.

14. Gorry PR, Taylor J, Holm GH, Mehle A, Morgan T, Cayabyab M, et al. Increased CCR5 affinity and reduced CCR5/CD4 dependence of a neurovirulent primary human immunodeficiency virus type 1 isolate. J Virol. 2002;76(12):6277-92.

15. Sterjovski J, Roche M, Churchill MJ, Ellett A, Farrugia W, Gray LR, et al. An altered and more efficient mechanism of CCR5 engagement contributes to macrophage tropism of CCR5-using HIV-1 envelopes. Virology. 2010;404(2):269-78.

16. Peters PJ, Duenas-Decamp MJ, Sullivan WM, Clapham PR. Variation of macrophage tropism among HIV-1 R5 envelopes in brain and other tissues. J Neuroimmune Pharmacol. 2007;2(1):32-41.

17. Li S, Juarez J, Alali M, Dwyer D, Collman R, Cunningham A, et al. Persistent CCR5 utilization and enhanced macrophage tropism by primary blood human immunodeficiency virus type 1 isolates from advanced stages of disease and comparison to tissue-derived isolates. J Virol. 1999;73(12):9741-55. PMCID: 113021.

18. Kolchinsky P, Kiprilov E, Sodroski J. Increased neutralization sensitivity of CD4-independent human immunodeficiency virus variants. J Virol. 2001;75(5):2041-50.

19. Li Y, Cleveland B, Klots I, Travis B, Richardson BA, Anderson D, et al. Removal of a single N-linked glycan in human immunodeficiency virus type 1 gp120 results in an enhanced ability to induce neutralizing antibody responses. J Virol. 2008;82(2):638-51. PMCID: 2224603.

20. Huang X, Jin W, Hu K, Luo S, Du T, Griffin GE, et al. Highly conserved HIV-1 gp120 glycans proximal to CD4-binding region affect viral infectivity and neutralizing antibody induction. Virology. 2012;423(1):97-106.

21. Rizzuto CD, Wyatt R, Hernandez-Ramos N, Sun Y, Kwong PD, Hendrickson WA, et al. A conserved HIV gp120 glycoprotein structure involved in chemokine receptor binding. Science. 1998;280(5371):1949-53.

22. Pikora C, Wittish C, Desrosiers RC. Identification of two N-linked glycosylation sites within the core of the simian immunodeficiency virus glycoprotein whose removal enhances sensitivity to soluble CD4. J Virol. 2005;79(19):12575-83.

23. Haim H, Si Z, Madani N, Wang L, Courter JR, Princiotto A, et al. Soluble CD4 and CD4-mimetic compounds inhibit HIV-1 infection by induction of a short-lived activated state. PLoS Pathog. 2009;5(4):e1000360.

24. Haim H, Strack B, Kassa A, Madani N, Wang L, Courter JR, et al. Contribution of intrinsic reactivity of the HIV-1 envelope glycoproteins to CD4-independent infection and global inhibitor sensitivity. PLoS Pathog. 2011;7(6):e1002101. PMCID: 3121797.

25. Platt EJ, Shea DM, Rose PP, Kabat D. Variants of human immunodeficiency virus type 1 that efficiently use CCR5 lacking the tyrosine-sulfated amino terminus have adaptive mutations in gp120, including loss of a functional N-glycan. J Virol. 2005;79(7):4357-68.

26. Kuhmann SE, Platt EJ, Kozak SL, Kabat D. Cooperation of multiple CCR5 coreceptors is required for infections by human immunodeficiency virus type 1. J Virol. 2000;74(15):7005-15.

27. Farzan M, Choe H, Vaca L, Martin K, Sun Y, Desjardins E, et al. A tyrosine-rich region in the N terminus of CCR5 is important for human immunodeficiency virus type 1 entry and mediates an association between gp120 and CCR5. J Virol. 1998;72(2):1160-4.

28. Gray L, Roche M, Churchill MJ, Sterjovski J, Ellett A, Poumbourios P, et al. Tissue-specific sequence alterations in the human immunodeficiency virus type 1 envelope favoring CCR5 usage contribute to persistence of dual-tropic virus in the brain. J Virol. 2009;83(11):5430-41.

29. Platt EJ, Kuhmann SE, Rose PP, Kabat D. Adaptive mutations in the V3 loop of gp120 enhance fusogenicity of human immunodeficiency virus type 1 and enable use of a CCR5 coreceptor that lacks the amino-terminal sulfated region. J Virol. 2001;75(24):12266-78.

30. Doms RW. The plasma membrane as a combat zone in the HIV battlefield. Genes & Development. 2000;14:2677-88.

31. Melikyan GB. Membrane fusion mediated by human immunodeficiency virus envelope glycoprotein. Curr Top Membr. 2011;68:81-106.

32. Liu J, Bartesaghi A, Borgnia MJ, Sapiro G, Subramaniam S. Molecular architecture of native HIV-1 gp120 trimers. Nature. 2008;455(7209):109-13.

33. Xiang SH, Finzi A, Pacheco B, Alexander K, Yuan W, Rizzuto C, et al. A V3 loop-dependent gp120 element disrupted by CD4 binding stabilizes the human immunodeficiency virus envelope glycoprotein trimer. J Virol. 2010;84(7):3147-61. PMCID: 2838131.

34. Musich T, Peters PJ, Duenas-Decamp MJ, Gonzalez-Perez MP, Robinson J, Zolla-Pazner S, et al. A conserved determinant in the V1 loop of HIV-1 modulates the V3 loop to prime low CD4 use and macrophage infection. J Virol. 2011;85(5):2397-405. PMCID: 3067776.

35. Pan Y, Ma B, Nussinov R. CD4 binding partially locks the bridging sheet in gp120 but leaves the beta2/3 strands flexible. J Mol Biol. 2005;350(3):514-27.

36. Zhu CB, Zhu L, Holz-Smith S, Matthews TJ, Chen CH. The role of the third beta strand in gp120 conformation and neutralization sensitivity of the HIV-1 primary isolate DH012. Proc Natl Acad Sci U S A. 2001;98(26):15227-32.

37. Rusert P, Krarup A, Magnus C, Brandenberg OF, Weber J, Ehlert AK, et al. Interaction of the gp120 V1V2 loop with a neighboring gp120 unit shields the HIV envelope trimer against cross-neutralizing antibodies. J Exp Med. 2011;208(7):1419-33. PMCID: 3135368.

38. Kolchinsky P, Kiprilov E, Bartley P, Rubinstein R, Sodroski J. Loss of a single N-linked glycan allows CD4-independent human immunodeficiency virus type 1 infection by altering the position of the gp120 V1/V2 variable loops. J Virol. 2001;75(7):3435-43.

39. Arrildt KT, Joseph SB, Swanstrom R. The HIV-1 env protein: a coat of many colors. Curr HIV/AIDS Rep. 2012;9(1):52-63.

40. Wild CT, Shugars DC, Greenwell TK, McDanal CB, Matthews TJ. Peptides corresponding to a predictive alpha-helical domain of human immunodeficiency virus type 1 gp41 are potent inhibitors of virus infection. Proc Natl Acad Sci U S A. 1994;91(21):9770-4. PMCID: 44898.

41. Stevceva L, Yoon V, Carville A, Pacheco B, Santosuosso M, Korioth-Schmitz B, et al. The efficacy of T cell-mediated immune responses is reduced by the envelope protein of the chimeric HIV-1/SIV-KB9 virus in vivo. J Immunol. 2008;181(8):5510-21.

42. Rychert J, Strick D, Bazner S, Robinson J, Rosenberg E. Detection of HIV gp120 in plasma during early HIV infection is associated with increased proinflammatory and immunoregulatory cytokines. AIDS Res Hum Retroviruses. 2010;26(10):1139-45. PMCID: 2982714.

43. Santosuosso M, Righi E, Lindstrom V, Leblanc PR, Poznansky MC. HIV-1 envelope protein gp120 is present at high concentrations in secondary lymphoid organs of individuals with chronic HIV-1 infection. J Infect Dis. 2009;200(7):1050-3.

44. Gilbert M, Kirihara J, Mills J. Enzyme-linked immunoassay for human immunodeficiency virus type 1 envelope glycoprotein 120. J Clin Microbiol. 1991;29(1):142-7. PMCID: 269718.

45. Oh SK, Cruikshank WW, Raina J, Blanchard GC, Adler WH, Walker J, et al. Identification of HIV-1 envelope glycoprotein in the serum of AIDS and ARC patients. J Acquir Immune Defic Syndr. 1992;5(3):251-6.

46. Klasse PJ, Moore JP. Is there enough gp120 in the body fluids of HIV-1-infected individuals to have biologically significant effects? Virology. 2004;323(1):1-8.

47. Liu P, Overman RG, Yates NL, Alam SM, Vandergrift N, Chen Y, et al. Dynamic antibody specificities and virion concentrations in circulating immune complexes in acute to chronic HIV-1 infection. J Virol. 2011;85(21):11196-207. PMCID: 3194959.

48. Zhu P, Liu J, Bess J, Jr., Chertova E, Lifson JD, Grise H, et al. Distribution and three-dimensional structure of AIDS virus envelope spikes. Nature. 2006;441(7095):847-52.

49. Trushin SA, Bren GD, Badley AD. CD4 T Cells Treated with gp120 Acquire a CD45R0+/CD45RA+ Phenotype. Open Virol J. 2009;3:21-5. PMCID: 2703203.

50. Mogensen TH, Melchjorsen J, Larsen CS, Paludan SR. Innate immune recognition and activation during HIV infection. Retrovirology. 2010;7:54. PMCID: 2904714.

51. Gemma C, Smith EM, Hughes TK, Jr., Opp MR. Human immunodeficiency virus glycoprotein 160 induces cytokine mRNA expression in the rat central nervous system. Cell Mol Neurobiol. 2000;20(4):419-31.

52. Yang B, Akhter S, Chaudhuri A, Kanmogne GD. HIV-1 gp120 induces cytokine expression, leukocyte adhesion, and transmigration across the blood-brain barrier: modulatory effects of STAT1 signaling. Microvasc Res. 2009;77(2):212-9.

53. Cicala C, Arthos J, Censoplano N, Cruz C, Chung E, Martinelli E, et al. HIV-1 gp120 induces NFAT nuclear translocation in resting CD4+ T-cells. Virology. 2006;345(1):105-14.

54. Ameglio F, Capobianchi MR, Castilletti C, Cordiali Fei P, Fais S, Trento E, et al. Recombinant gp120 induces IL-10 in resting peripheral blood mononuclear cells; correlation with the induction of other cytokines. Clin Exp Immunol. 1994;95(3):455-8. PMCID: 1535081.

55. Kinter AL, Umscheid CA, Arthos J, Cicala C, Lin Y, Jackson R, et al. HIV envelope induces virus expression from resting CD4+ T cells isolated from HIV-infected individuals in the absence of markers of cellular activation or apoptosis. J Immunol. 2003;170(5):2449-55.

56. Biancotto A, Iglehart SJ, Vanpouille C, Condack CE, Lisco A, Ruecker E, et al. HIV-1 induced activation of CD4+ T cells creates new targets for HIV-1 infection in human lymphoid tissue ex vivo. Blood. 2008;111(2):699-704. PMCID: 2200839.

57. Medders KE, Sejbuk NE, Maung R, Desai MK, Kaul M. Activation of p38 MAPK is required in monocytic and neuronal cells for HIV glycoprotein 120-induced neurotoxicity. J Immunol. 2010;185(8):4883-95.

58. Selliah N, Shackelford J, Wang JF, Traynor F, Yin J, Finkel TH. T cell signaling and apoptosis in HIV disease. Immunol Res. 2003;27(2-3):247-60.

59. Ullrich CK, Groopman JE, Ganju RK. HIV-1 gp120- and gp160-induced apoptosis in cultured endothelial cells is mediated by caspases. Blood. 2000;96(4):1438-42.

60. Garg H, Blumenthal R. HIV gp41-induced apoptosis is mediated by caspase-3-dependent mitochondrial depolarization, which is inhibited by HIV protease inhibitor nelfinavir. J Leukoc Biol. 2006;79(2):351-62.

61. Garg H, Joshi A, Blumenthal R. Altered bystander apoptosis induction and pathogenesis of enfuvirtide-resistant HIV type 1 Env mutants. AIDS Res Hum Retroviruses. 2009;25(8):811-7. PMCID: 2791676.

62. Kaul M, Garden GA, Lipton SA. Pathways to neuronal injury and apoptosis in HIV-associated dementia. Nature. 2001;410(6831):988-94.

63. Anand AR, Ganju RK. HIV-1 gp120-mediated apoptosis of T cells is regulated by the membrane tyrosine phosphatase CD45. J Biol Chem. 2006;281(18):12289-99.

64. Garden GA, Guo W, Jayadev S, Tun C, Balcaitis S, Choi J, et al. HIV associated neurodegeneration requires p53 in neurons and microglia. FASEB J. 2004;18(10):1141-3.

65. Jana A, Pahan K. Human immunodeficiency virus type 1 gp120 induces apoptosis in human primary neurons through redox-regulated activation of neutral sphingomyelinase. J Neurosci. 2004;24(43):9531-40. PMCID: 1955476.

66. Singh IN, Goody RJ, Dean C, Ahmad NM, Lutz SE, Knapp PE, et al. Apoptotic death of striatal neurons induced by human immunodeficiency virus-1 Tat and gp120: Differential involvement of caspase-3 and endonuclease G. J Neurovirol. 2004;10(3):141-51.

67. Kaul M, Zheng J, Okamoto S, Gendelman HE, Lipton SA. HIV-1 infection and AIDS: consequences for the central nervous system. Cell Death Differ. 2005;12 Suppl 1:878-92.

68. Masci AM, Galgani M, Cassano S, De Simone S, Gallo A, De Rosa V, et al. HIV-1 gp120 induces anergy in naive T lymphocytes through CD4-independent protein kinase-A-mediated signaling. J Leukoc Biol. 2003;74(6):1117-24.

69. Chirmule N, Kalyanaraman VS, Oyaizu N, Slade HB, Pahwa S. Inhibition of functional properties of tetanus antigen-specific T-cell clones by envelope glycoprotein GP120 of human immunodeficiency virus. Blood. 1990;75(1):152-9.

70. Chirmule N, McCloskey TW, Hu R, Kalyanaraman VS, Pahwa S. HIV gp120 inhibits T cell activation by interfering with expression of costimulatory molecules CD40 ligand and CD80 (B71). J Immunol. 1995;155(2):917-24.

71. Fernando K, Hu H, Ni H, Hoxie JA, Weissman D. Vaccine-delivered HIV envelope inhibits CD4(+) T-cell activation, a mechanism for poor HIV vaccine responses. Blood. 2007;109(6):2538-44. PMCID: 1852208.

72. Hu H, Fernando K, Ni H, Weissman D. HIV envelope suppresses CD4+ T cell activation independent of T regulatory cells. J Immunol. 2008;180(8):5593-600.

73. Nazli A, Chan O, Dobson-Belaire WN, Ouellet M, Tremblay MJ, Gray-Owen SD, et al. Exposure to HIV-1 directly impairs mucosal epithelial barrier integrity allowing microbial translocation. PLoS Pathog. 2010;6(4):e1000852. PMCID: 2851733.

74. Geldmacher C, Koup RA. Pathogen-specific T cell depletion and reactivation of opportunistic pathogens in HIV infection. Trends Immunol. 2012.

75. Goudsmit J, Lange JM, Krone WJ, Teunissen MB, Epstein LG, Danner SA, et al. Pathogenesis of HIV and its implications for serodiagnosis and monitoring of antiviral therapy. J Virol Methods. 1987;17(1-2):19-34.

76. Albright AV, Martin J, O'Connor M, Gonzalez-Scarano F. Interactions between HIV-1 gp120, chemokines, and cultured adult microglial cells. J Neurovirol. 2001;7(3):196-207.

77. Rotta I, Almeida SM. Genotypical diversity of HIV clades and central nervous system impairment. Arq Neuropsiquiatr. 2011;69(6):964-72.

78. Corasaniti MT, Bagetta G, Rotiroti D, Nistico G. The HIV envelope protein gp120 in the nervous system: interactions with nitric oxide, interleukin-1beta and nerve growth factor signalling, with pathological implications in vivo and in vitro. Biochem Pharmacol. 1998;56(2):153-6.

79. Dunfee R, Thomas ER, Gorry PR, Wang J, Ancuta P, Gabuzda D. Mechanisms of HIV-1 neurotropism. Curr HIV Res. 2006;4(3):267-78.

80. Gartner S, McDonald RA, Hunter EA, Bouwman F, Liu Y, Popovic M. Gp120 sequence variation in brain and in T-lymphocyte human immunodeficiency virus type 1 primary isolates. J Hum Virol. 1997;1(1):3-18.

81. Ohagen A, Devitt A, Kunstman KJ, Gorry PR, Rose PP, Korber B, et al. Genetic and functional analysis of full-length human immunodeficiency virus type 1 env genes derived from brain and blood of patients with AIDS. J Virol. 2003;77(22):12336-45.

82. Power C, McArthur JC, Johnson RT, Griffin DE, Glass JD, Dewey R, et al. Distinct HIV-1 env sequences are associated with neurotropism and neurovirulence. Curr Top Microbiol Immunol. 1995;202:89-104.

83. Wang TH, Donaldson YK, Brettle RP, Bell JE, Simmonds P. Identification of shared populations of human immunodeficiency virus type 1 infecting microglia and tissue macrophages outside the central nervous system. J Virol. 2001;75(23):11686-99.

84. Richards KH, Aasa-Chapman MM, McKnight A, Clapham PR. Modulation of HIV-1 macrophage-tropism among R5 envelopes occurs before detection of neutralizing antibodies. Retrovirology. 2010;7:48. PMCID: 2890664.

85. Shieh JT, Martin J, Baltuch G, Malim MH, Gonzalez-Scarano F. Determinants of syncytium formation in microglia by human immunodeficiency virus type 1: role of the V1/V2 domains. J Virol. 2000;74(2):693-701.

86. Peters PJ, Sullivan WM, Duenas-Decamp MJ, Bhattacharya J, Ankghuambom C, Brown R, et al. Non-macrophage-tropic human immunodeficiency virus type 1 R5 envelopes

predominate in blood, lymph nodes, and semen: implications for transmission and pathogenesis. J Virol. 2006;80(13):6324-32. PMCID: 1488974.

87. Lamers SL, Salemi M, Galligan DC, de Oliveira T, Fogel GB, Granier SC, et al. Extensive HIV-1 intra-host recombination is common in tissues with abnormal histopathology. PLoS One. 2009;4(3):e5065.

88. Shapshak P, Segal DM, Crandall KA, Fujimura RK, Zhang BT, Xin KQ, et al. Independent evolution of HIV type 1 in different brain regions. AIDS Res Hum Retroviruses. 1999;15(9):811-20.

89. Pillai SK, Pond SL, Liu Y, Good BM, Strain MC, Ellis RJ, et al. Genetic attributes of cerebrospinal fluid-derived HIV-1 env. Brain. 2006;129(Pt 7):1872-83.

90. Coiras M, Lopez-Huertas MR, Perez-Olmeda M, Alcami J. Understanding HIV-1 latency provides clues for the eradication of long-term reservoirs. Nat Rev Microbiol. 2009;7(11):798-812.

91. Gorry PR, Churchill M, Crowe SM, Cunningham AL, Gabuzda D. Pathogenesis of macrophage tropic HIV-1. Curr HIV Res. 2005;3(1):53-60.

APPENDIX A

SUPPLEMENTAL FIGURES:

CHAPTER 2

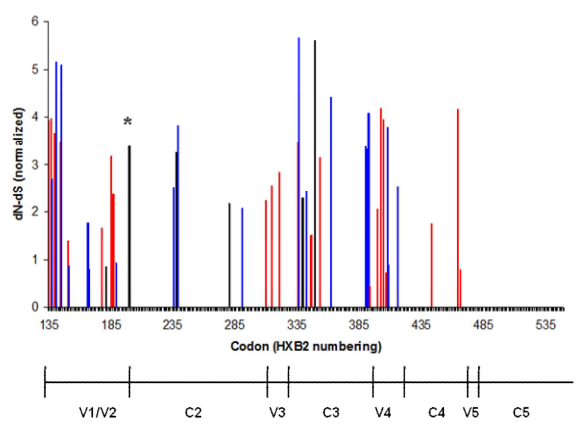

Figure S2.1. Predicted sites of positive selection in brain and lymphoid Envs from patients with HAD. Brain and lymphoid Env sequences from patients with HAD were aligned using ClustalX2 (*n*=336 brain sequences from 19 HAD patients and 171 blood/lymphoid sequences from 15 HAD patients). dN-dS values were estimated by SLAC, FEL, and IFEL and normalized by total codon tree length using HyPhy software. dN-dS values shown are averages calculated for any codon with $p<0.05$ by at least 2 of the programs. Sites from brain sequences are shown in red, sites from lymphoid sequences are shown in blue, and sites predicted from both brain and lymphoid sequences are shown in black. Codons were numbered according to codon *env* position of HIV-1 HXB2 reference strain. * indicates position 200 in the β3 strand of the bridging sheet.

Table S2.1. Codons under positive selection detected by SLAC, FEL, and IFEL in brain and lymphoid sequences from patients with and without HAD.

HAD Brain

Region	Codon[a]	SLAC[b]		FEL[b]		IFEL[b]	
	135	6.96	(0.014)	1.69	(0.005)	3.14	(0.0002)
	137	7.24	(0.003)	1.81	(0.002)	2.83	(0.0001)
	138	4.93	(0.008)	0.70	(0.027)	0.58	(0.07)
	140	8.69	(0.0003)	1.06	(0.003)	1.24	(0.002)
	145	6.92	(0.066)	1.47	(0.011)	2.04	(0.004)
	151	4.55	(0.059)	1.03	(0.045)	1.74	(0.01)
	178	3.44	(0.038)	0.67	(0.016)	0.87	(0.008)
	181	2.27	(0.067)	0.44	(0.025)	0.47	(0.026)
	186	6.80	(0.001)	1.40	(0.0007)	1.32	(0.001)
	187	5.17	(0.008)	1.01	(0.004)	0.97	(0.006)
β3	**200**	3.26	(0.067)	0.68	(0.032)	0.91	(0.015)
	238	3.47	(0.031)	0.77	(0.004)	0.64	(0.010)
	(287)	5.46	(0.014)	1.28	(0.007)	1.88	(0.001)
	281	6.26	(0.0005)	1.14	(0.0002)	1.32	(0.001)
	310	4.44	(0.012)	0.91	(0.004)	1.35	(0.0009)
	315	5.52	(0.003)	1.01	(0.002)	1.12	(0.002)
	321	5.86	(0.004)	1.12	(0.002)	1.53	(0.0007)
C3	336	6.72	(0.019)	1.55	(0.003)	2.14	(0.001)
	340		NS	1.04	(0.009)	1.28	(0.005)
	350	4.22	(0.060)	0.92	(0.007)	1.27	(0.002)
	354	5.98	(0.036)	1.22	(0.013)	2.24	(0.0006)
	394		NS	0.39	(0.038)	0.52	(0.023)
	400		NS	2.00	(0.030)	2.13	(0.030)
	403	6.18	(0.041)	1.92	(0.048)	4.45	(0.0004)
	405	7.81	(0.004)	1.77	(0.00007)	2.27	(0.00003)
	407		NS	0.58	(0.025)	0.89	(0.008)
	444	3.99	(0.044)	0.63	(0.021)	0.70	(0.019)
	465	6.14	(0.047)	1.26	(0.053)	2.19	(0.009)
	467		NS	0.62	(0.043)	0.96	(0.012)

Table S2.1, Continued

HAD Lymphoid

Region	Codon[a]	SLAC[b]		FEL[b]		IFEL[b]	
	138	4.42	(0.044)	1.37	(0.021)	1.93	(0.008)
	141	11.00	(0.023)	1.88	(0.040)	2.58	(0.021)
	143	8.23	(0.050)		NS	2.72	(0.014)
	146	8.99	(0.015)	2.30	(0.014)	3.99	(0.002)
	152		NS	0.80	(0.016)	0.95	(0.013)
	167	3.48	(0.039)	0.86	(0.017)	1.02	(0.013)
	168	3.12	(0.069)	0.74	(0.039)	0.91	(0.028)
	181	3.14	(0.032)	0.76	(0.013)	0.57	(0.042)
	(236)	3.93	(0.044)	1.03	(0.019)	1.19	(0.015)
	190	3.42	(0.057)	0.082	(0.022)	1.05	(0.014)
β3	**200**	4.96	(0.012)	1.43	(0.001)	1.42	(0.002)
	236	3.97	(0.039)	1.07	(0.026)		NS
	238	2.87	(0.039)	0.72	(0.015)	1.25	(0.003)
	240	7.26	(0.0009)	2.05	(0.0003)	2.18	(0.0006)
	281	2.84	(0.042)	0.70	(0.015)	0.85	(0.012)
	291	3.57	(0.018)	0.96	(0.005)	1.67	(0.0006)
C3	337	8.06	(0.001)	1.39	(0.008)	1.87	(0.003)
	340	7.38	(0.003)	1.33	(0.003)	1.56	(0.003)
	343	5.51	(0.011)	0.91	(0.026)	0.90	(0.035)
	350	10.28	(0.0002)	1.37	(0.018)	1.90	(0.009)
	363	7.46	(0.008)	0.91	(0.098)	1.33	(0.048)
	391		NS	2.59	(0.010)	4.18	(0.002)
	392	5.77	(0.019)	1.51	(0.013)	2.67	(0.002)
	393	9.05	(0.005)	1.73	(0.003)	1.47	(0.009)
	408	7.76	(0.003)	1.35	(0.003)	2.22	(0.0004)
	409	3.45	(0.053)	0.64	(0.039)	1.17	(0.009)
	417	5.41	(0.003)	0.95	(0.008)	1.24	(0.005)

Table S2.1, Continued

non-HAD Brain

Region	Codon[a]	SLAC[b]		FEL[b]		IFEL[b]	
	143	10.54	(0.080)	4.34	(0.018)	6.24	(0.006)
	183	5.85	(0.086)	2.18	(0.034)	2.22	(0.041)
	238		NS	1.93	(0.045)	2.36	(0.034)
	252		NS	1.96	(0.034)	2.34	(0.025)
	283	8.43	(0.032)	3.41	(0.004)	3.19	(0.008)
	290	8.11	(0.068)	3.43	(0.023)	4.50	(0.013)
	310	7.53	(0.088)	3.81	(0.015)	7.22	(0.004)
C3	347	10.90	(0.033)	4.00	(0.033)	5.50	(0.017)
	388		NS	2.62	(0.032)	3.91	(0.013)
	396		NS	5.89	(0.043)	10.58	(0.008)
	404	11.94	(0.043)	4.94	(0.008)	8.52	(0.002)
	405	9.91	(0.087)	3.90	(0.019)	4.20	(0.020)
	429	10.70	(0.045)	3.90	(0.029)	5.77	(0.011)
	466		NS	5.72	(0.050)	9.74	(0.017)

non-HAD Lymphoid

Region	Codon[a]	SLAC[b]		FEL[b]		IFEL[b]	
C3	343	2.24	(0.096)	9.31	(0.047)	15.17	(0.020)
	466		NS	13.40	(0.031)	23.24	(0.012)

[a]Codon: codons with $p<0.05$ by a minimum of 2 methods are numbered according to codon env position for HIV-1 HXB2. Codons selected by all 3 methods are underlined.
[b]SLAC, FEL, and IFEL: the first numbers are the dN-dS differences (normalized and scaled by total codon tree length), the numbers in parentheses are p-values for corresponding test of non-synonymous rate being higher than synonymous rate (dN>dS). Sites in the bridging sheet strands are indicated in bold.
NS, $p>0.1$

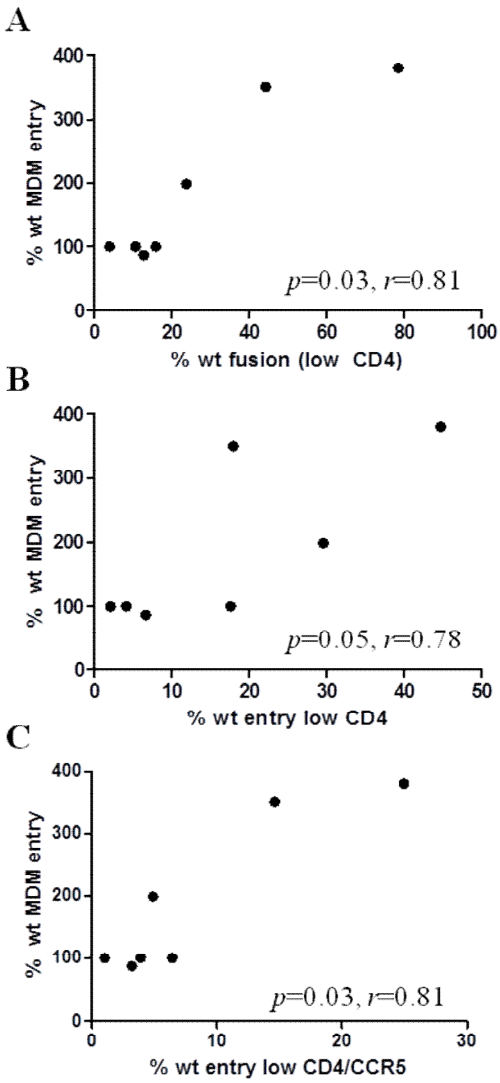

Figure S2.2. Fusion and entry into cells expressing low CD4 and CCR5 correlates with macrophage entry. Percent wild-type fusion (A) and entry (B, C) with cells expressing low CD4 (A, B) and low CD4 and CCR5 (C) were compared to percent wild-type entry into MDM. P-values were calculated using Spearman correlation (GraphPad Prism software).

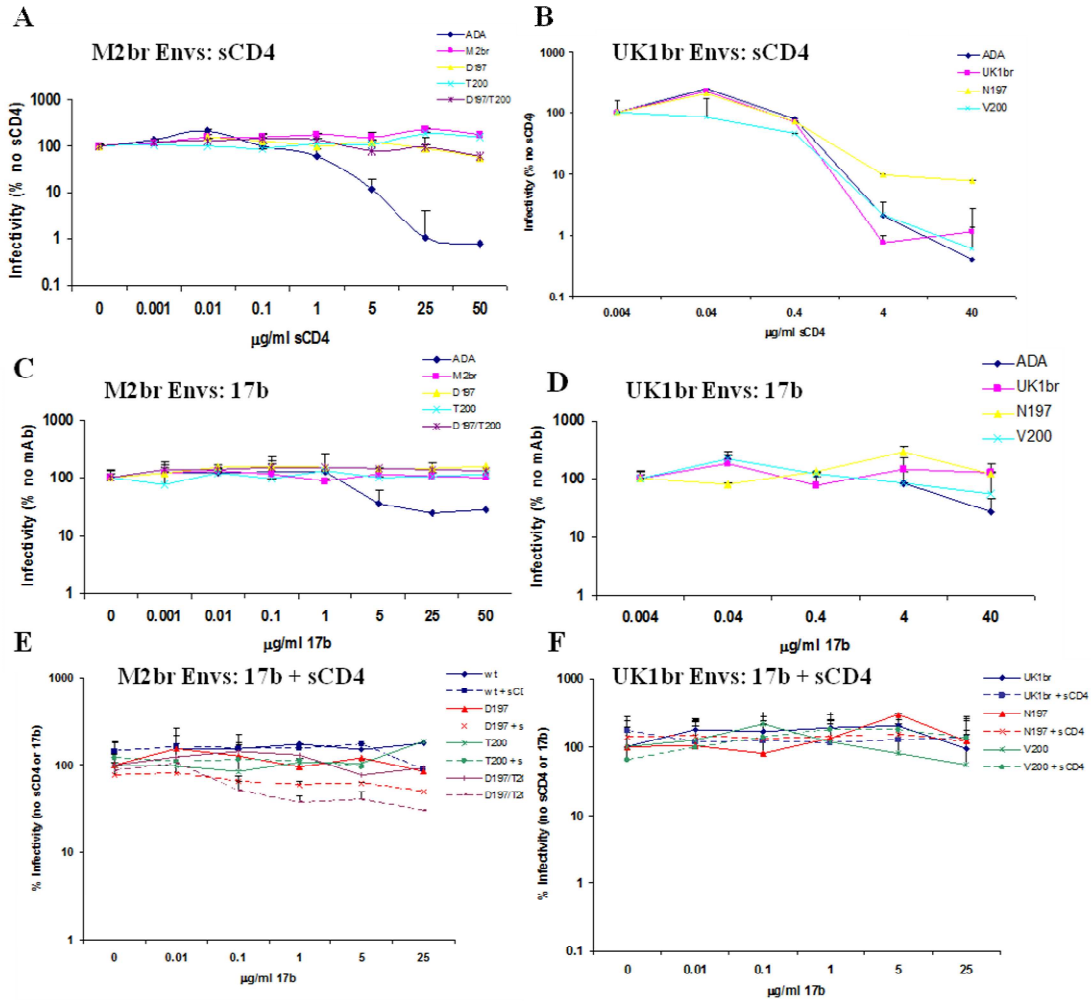

Figure S2.3. Neutralization sensitivity of the parental and mutant Envs to sCD4 and 17b is strain-dependent. HIV luciferase reporter viruses expressing the wild-type and mutant Envs and the control ADA Env were incubated with sCD4 (A-B), mAb 17b (C-D), or a mix of sCD4 and 17b (E-F) for 1 hour prior to infection of TZM-bl cells. Cells were lysed 48 hours post-infection and analyzed for luciferase activity. Results are expressed as percentages of maximum infection for each virus when incubated with no sCD4 or 17b and are representative of 2 separate experiments. Error bars represent standard deviations from duplicate wells in a single assay

SUPPLEMENTAL FIGURES:

CHAPTER 3

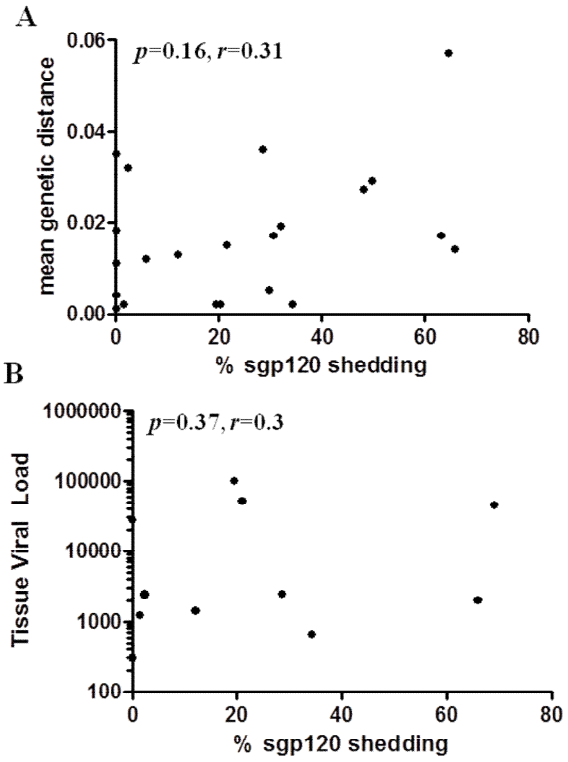

Fig. S3.1. Levels of sgp120 shedding are not associated with *env* genetic diversity or tissue viral load.

For brain and lymphoid Envs from each patient, average % sgp120 shedding was compared with mean genetic distance calculated from *env* sequence alignments using MEGA5.0 (A) or tissue viral load represented as HIV copies per million cells (B) (1-3). P values were determined using Spearman correlation (GraphPad Prism software).

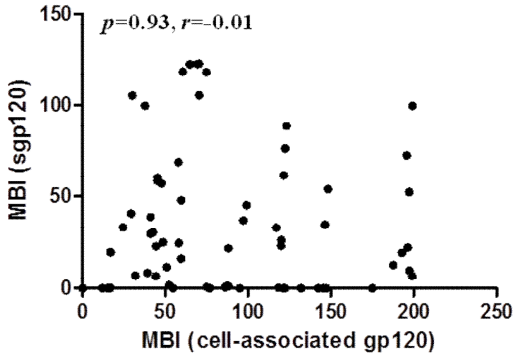

Fig. S3.2. Levels of sgp120 detected in supernatants of transfected 293T cells are not dependent on cell surface expression levels.

Mean band intensities of gp120 bands in cell lysates and supernatants analyzed by Western blot in a single experiment were determined using Photoshop and compared using GraphPad Prism software. P and R values were determined using Spearman correlation**.**

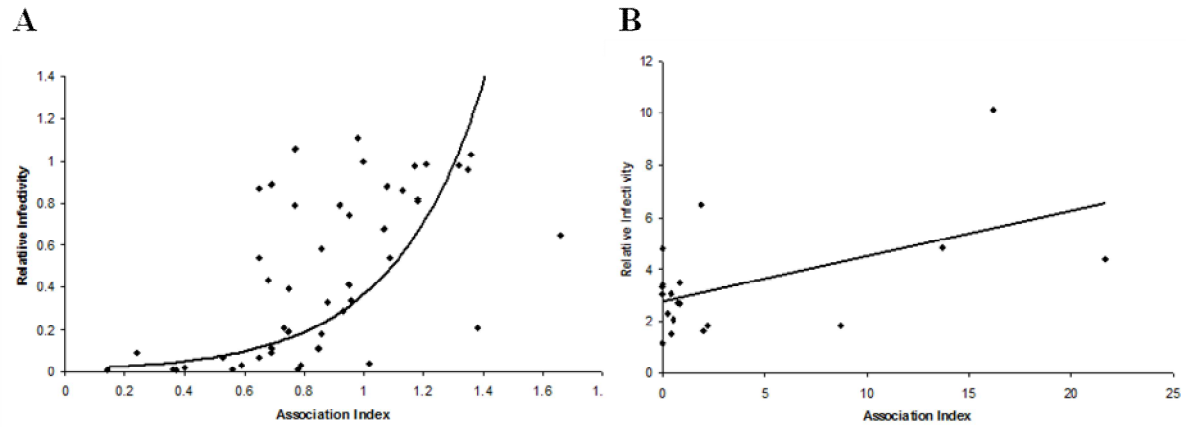

Fig. S3.3. High levels of sgp120 shedding from primary Envs does not inhibit infectivity. A) sgp120 shedding from a panel of mutants constructed in the YU2 Env was calculated as an association index [($mutant_{cell}$ x wt_{sup})/($mutant_{sup}$ x wt_{cell})] and plotted against relative infectivity of CF2-CD4/CCR5 cells as previously reported (7). Envs with high levels of sgp120 shedding exhibited reduced infectivity (bottom left portion of the curve). B) Percent sgp120 shedding from primary HIV Envs was calculated as a modified association index, with expression of the control ADA Env in cell lysates and supernatants replacing wild type Env and compared to infectivity of TZM-bl cells. Envs with high levels of shedding (left side of graph) exhibited comparable infectivity to Envs with low levels of shedding (right side of graph).

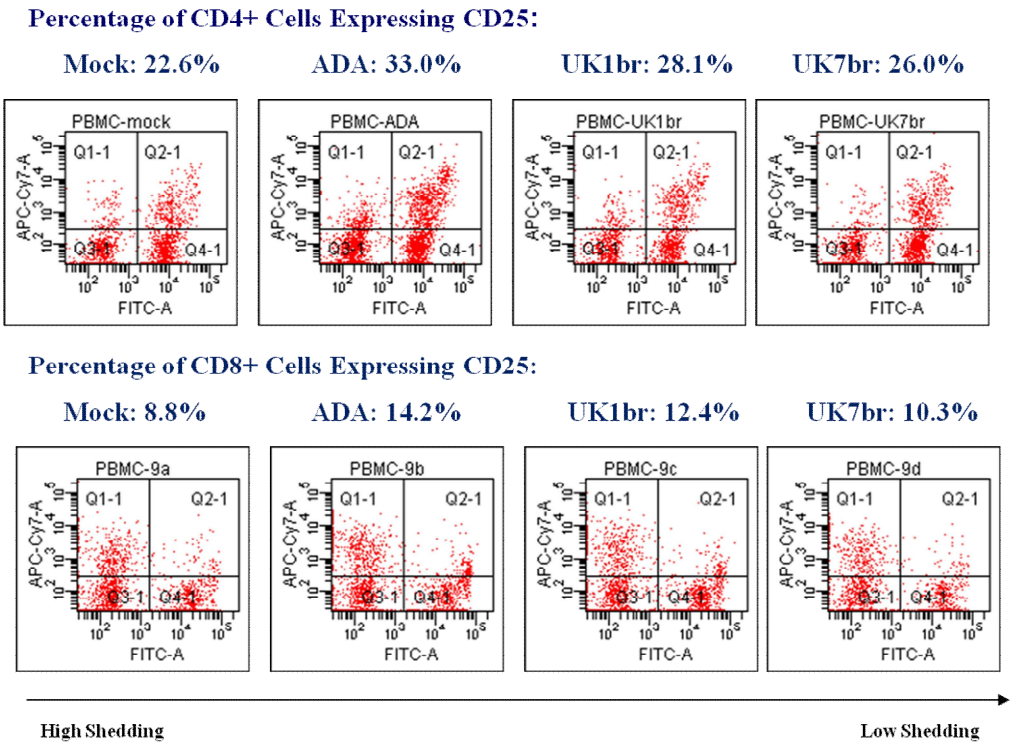

Fig. S3.4. Envs with high levels of spontaneous sgp120 shedding induce upregulation of CD25 on CD4+ and CD8+ lymphocytes.
PBMCs were infected as described in Materials and Methods. Cells were collected on day 6 post-infection, stained for expression of cell surface markers, and analyzed by flow cytometry. CD25 expression levels were analyzed for CD4+ T cells (A) and CD8+ T cells (B). Mock infected cells are shown on the left. Order of sgp120 shedding is ADA>UK1br>UK7br.

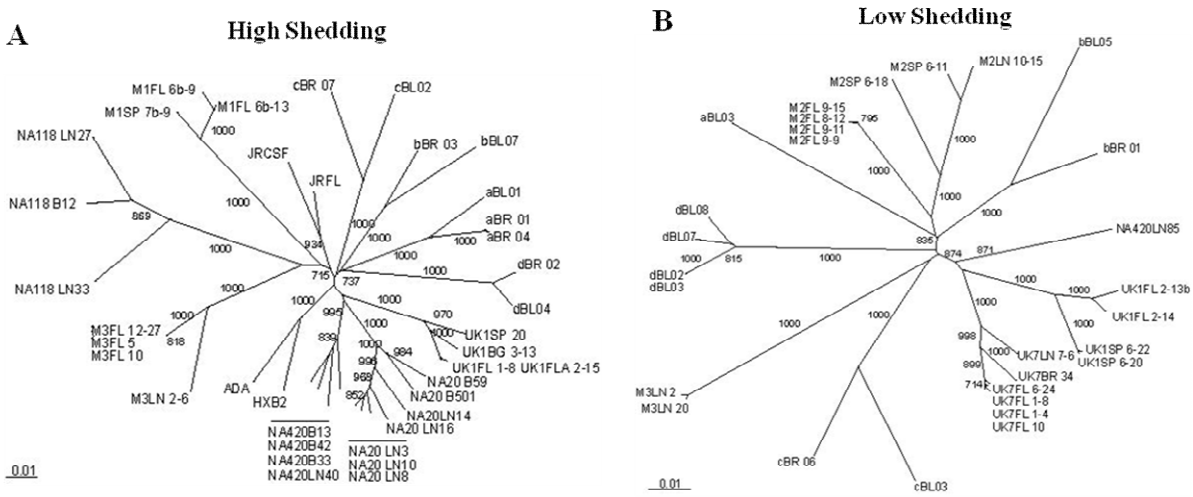

Fig. S3.5. Comparison of phylogenetic trees for Envs with high versus low shedding. Primary brain and lymphoid Envs were characterized as high shedding (% sgp120 shedding >20%; *n*=38 Envs from 13 patients) or low shedding (% sgp120 shedding <20%, *n*=29 Envs from 9 patients). Nucleotide sequence alignments of each group were created using Clustal X2 Numbers associated with each branch are bootstrap values, which represent the number of trees, out of 1000 replicates performed, in which the same branching order was found. Only values above 800 for the major branches are shown. Branch lengths are proportional to the amount of sequence divergence. Scale bars indicate 1% sequence divergence. Panels depict the phylogenetic relationship among gp120 nucleotide sequences amplified from Envs with high levels (A) and low levels (B) of % sgp120 shedding relative to gp120 in cell lysate by Western blotting. High levels of sgp120 shedding= % sgp120 shedding >20%; low levels of sgp120 shedding = % sgp120 <20%.

Table S3.1. Diversity and Compartmentalization Between Patients and Tissue Compartments

Patient	Tissue	Viral Load[a]	Genetic Distance[b]	Slatkin-Maddison P-value[c]
MACS2	Brain	1234.5	0.002	0.0007
	Lymphoid	2451.0	0.032	
MACS3	Brain	658.0	0.002	0.0007
	Lymphoid	100841.0	0.002	
UK1	Brain	51539.0	0.017	0.002
	Lymphoid	1444.0	0.013	
UK7	Brain	27826.0	0.004	0.089
	Lymphoid	301.0	0.035	
MACS1	Brain	2018.1	0.014	0.397
	Lymphoid	25267.0	ND[d]	
NA118	Brain	NA[e]	ND[d]	ND[d]
	Lymphoid	NA[e]	0.057	
NA20	Brain	NA[e]	0.029	0.086
	Lymphoid	NA[e]	0.017	
NA420	Brain	NA[e]	0.027	0.200
	Lymphoid	NA[e]	0.015	
A	Brain	NA[e]	0.002	0.167
	Blood	NA[e]	0.019	
B	Brain	NA[e]	0.005	0.333
	Blood	NA[e]	0.012	
C	Brain	NA[e]	0.011	0.167
	Blood	NA[e]	0.036	
D	Brain	NA[e]	0.001	0.238
	Blood	NA[e]	0.018	

[a] Tissue viral load is represented as HIV copies per million cells.
[b] Genetic distance is the number of nucleotide substitutions per 100 sites calculated with the maximum composite likelihood method in Mega 5.0 software. The average pairwise genetic distances for brain and blood/lymphoid sequences within each patient are shown.
[c] The Slatkin-Maddison test for gene flow between populations was used to measure genetic compartmentalization between the brain and blood/lymphoid populations. Migration events describe the number of env migration events between the brain and blood/lymphoid Env populations for each phylogenetic tree. A P-value >0.05 indicates statistically significant genetic compartmentalization between brain and b1ood/lymphoid populations.
[d] ND, not determined because <2 sequences/tissue were available.
[e] NA, not available

Table S3.2. Sgp120 detected in 293T cell lysates and supernatants by Western blotting and ELISA

Patient	Tissue	Clone	MBI[a]	% sgp120[b]	ng/ml[c]
M2	BR	8-12	0	1.1 ± 0.8	94.6 ± 13.0
		9-15	0	0 ± 0	50.9 ± 5.7
		9-11	0	3.4 ± 4.8	51.7 ± 31.6
		9-9	3.5	1.7 ± 1.2	1.6 ± 1.8
	SP	6-18	32.2	4.1 ± 0.1	0 ± 0
		10-15	34.1	0.8 ± 0.6	0 ± 0.5
		6-11	11	2.5 ± 0.1	160.3 ± 23.0
M3	BR	5	50	30.4 ± 11.8	31 ± 1.5
		12-27	42.2	39.3	5.1 ± 7.3
		10	45.6	33.1 ± 9.2	94.2 ± 2.2
	LN	20	66.7	23.7	40.3 ± 5.4
		2	77.9	36.4	177.4 ± 0.5
		2-6	37.6	20 ± 12.4	59.5 ± 28.1
UK1	BR	2-13b	24.9	13.9 ± 21.6	81.9 ± 6.1
		3-13	71.3	69.1 ± 24.5	87.5 ± 16.2
		2-14	2.9	16.4 ± 27.2	0 ± 6.6
		1-8	0	30.3 ± 27.6	27.3 ± 0.07
		2-15	0	23.4 ± 19.2	118.9 ± 26.8
	SP	20	5.7	19.6 ± 2.1	0 ± 0
		6-20	0	11.7 ± 14.6	92.8 ± 7.8
		6-22	7.5	5 ± 7.1	119.7 ± 14.0
UK7	BR	1-4	0	0 ± 0	14.2 ± 21.3
		34	0	0 ± 0	12.3 ± 13.0
		6-24	0	0 ± 0	0 ± 1.5
		1-8	54	0.1 ± 0.2	84 ± 3.7
		10	61.5	0 ± 0	73.1 ± 30.9
	LN	7-6	4.5	0 ± 0	92.2 ± 9.5
M1	BR	3b-6	5.2	38 ± 15.5	125 ± 26.1
		7b-9	0	28.6	4.7 ± 6.7
		6b-13	3.8	75.1	205.2 ± 103.8
		6b-9	7	84.6	58.0 ± 39.4
	SP	8a-2	0	0	0 ± 0
NA118	BR	12	98.7	47.5	710.5 ± 24.2
	LN	27	109.5	59.7	735.7 ± 72.3
		33	130	69.6	645.4 ± 6.2

Table S3.2, Continued

Patient	Tissue	Clone	MBI[a]	% sgp120[b]	ng/ml[c]
NA20	BR	59	49.3	46.4 ± 19.3	410.6 ± 64.7
		36	0	47.7 ± 24.8	480.9 ± 29.0
		501	0	55.5 ± 30.1	0 ± 0
	LN	3	38.7	75.4 ± 26.3	154.8 ± 61.6
		8	63.3	78.0 ± 26.0	725 ± 74.3
		10	95.1	70.6 ± 22.5	619.6 ± 39.1
		14	15.6	29 ± 2.7	330.3 ± 27.9
		16	36.6	62.9 ± 15.0	327.8 ± 67.3
NA420	BR	13	109.6	37.9	748.1 ± 61.1
		33	0	54.6	510.1 ± 37.4
		42	27.4	51.9	575.9 ± 42.8
	LN	40	18.5	32.2	377.1 ± 14.1
		85	14	11	570.9 ± 51.7
A	BR	01	41.1	21.2	235.9 ± 97.7
		04	58.8	32.8 ± 11.1	207.5 ± 47.5
	BL	01	6.8	22.8	0 ± 0
		03	8.2	11	194.9 ± 72.5
B	BR	01	32.2	12.5	91.8 ± 69.4
		03	73.2	20.6	105.7 ± 70.2
	BL	05	26.5	11.9	260.7 ± 12.0
		07	128.1	82.6	548.4 ± 42.5
C	BR	06	44	14.1	128 ± 6.1
		07	73.8	25.3	662.3 ± 47.6
	BL	02	171.5	50.2 ± 30.6	1711.2 ± 48.6
		03	27	0	22.5 ± 23.0
D	BR	02	88	38.2	462.6 ± 64.4
	BL	02	23.1	0 ± 0	62.9 ± 55.4
		03	25	0 ± 0	19.1 ± 13.5
		04	52.8	45.8	932.2 ± 71.8
		07	0	0 ± 0	53.9 ± 18.8
		08	0	15	73.9 ± 59.4
Control		ADA	96.2	52 ± 14.5	1366.1 ± 284.5
		JRFL		89.1 ± 20.8	2172.8 ± 476.2
		JRCSF		97.8	6671.0 ± 94.4
		HXB2		45.7	1315 ±
		YU2		24.4	1391.0 ± 141.3

[a] MBI, mean band intensity of sgp120 in supernatant of 293T cells detected by Western blotting
[b] % sgp120 shedding calculated at [sgp120 (supernatant)/gp120 (cell lysate)] x 100. Detected by Western blotting.
[c] ng/ml sgp120 measured by ELISA against a standard curve of purified HIV_{IIIB}.

Table S3.3. Analysis of within group variation

Analysis	Program	Condition	Region	High Shedding[d]	Low Shedding[d]
Shannon's Entropy	Entropy One[a]	Average[a]	gp120	0.554	0.359
			gp41	0.511	0.214
dN-dS	SLAC/FEL/ IFEL[b]	Positive[b]	gp120	21	24
			gp41	24	5
		Negative[b]	gp120	56	53
			gp41	35	27
N-glycosylation sites	Glycosite[c]	All frequencies[c]	gp120	55	47
			gp41	8	5
		>90%[c]	gp120	10	12
			gp41	2	4

[a] Shannon's entropy for each codon in gp160 calculated using Entropy One from Los Alamos National Laboratories online sequence analysis tools. Results are presented as Shannon's entropy values averaged across gp120 and gp41.

[b] Single likelihood ancestor counting (SLAC), fixed effects likelikhood (FEL), and internal fixed effects likelihood (IFEL) methods (HyPhy software package) were used to reconstruct ancestral sequences at each node of a phylogenetic tree (method) (data not shown). Synonymous (dS) and nonsynonymous (dN) substitutions are calculated at each branch and terminal node. Numbers of sites estimated to be under positive or negative selection in gp120 and gp41 indicate codons with P-values 0.1 using at least 2 methods.

[c] Number of predicted N-glycosylation sites across gp120 and gp41 for each group were calculated using Glycosite from Los Alamos National Laboratories online analysis tools. Total sites represents all predicted N-glycosylation sites across each group (high and low shedding). >90% represents N-glycosylation sites predicted to be present in >90% of sequences from each group.

[d] Primary brain and lymphoid Envs were characterized as high shedding (% sgp120 shedding >20%; *n*=38 Envs from 13 patients) or low shedding (% sgp120 shedding <20%, *n*=29 Envs from 9 patients).

APPENDIX B

RESEARCH Open Access

HIVBrainSeqDB: a database of annotated HIV envelope sequences from brain and other anatomical sites

Alexander G Holman[1], Megan E Mefford[1], Niall O'Connor[2], Dana Gabuzda[1,3*]

Abstract

Background: The population of HIV replicating within a host consists of independently evolving and interacting sub-populations that can be genetically distinct within anatomical compartments. HIV replicating within the brain causes neurocognitive disorders in up to 20-30% of infected individuals and is a viral sanctuary site for the development of drug resistance. The primary determinant of HIV neurotropism is macrophage tropism, which is primarily determined by the viral envelope (*env*) gene. However, studies of genetic aspects of HIV replicating in the brain are hindered because existing repositories of HIV sequences are not focused on neurotropic virus nor annotated with neurocognitive and neuropathological status. To address this need, we constructed the HIV Brain Sequence Database.

Results: The HIV Brain Sequence Database is a public database of HIV envelope sequences, directly sequenced from brain and other tissues from the same patients. Sequences are annotated with clinical data including viral load, CD4 count, antiretroviral status, neurocognitive impairment, and neuropathological diagnosis, all curated from the original publication. Tissue source is coded using an anatomical ontology, the Foundational Model of Anatomy, to capture the maximum level of detail available, while maintaining ontological relationships between tissues and their subparts. 44 tissue types are represented within the database, grouped into 4 categories: (i) brain, brainstem, and spinal cord; (ii) meninges, choroid plexus, and CSF; (iii) blood and lymphoid; and (iv) other (bone marrow, colon, lung, liver, etc). Patient coding is correlated across studies, allowing sequences from the same patient to be grouped to increase statistical power. Using Cytoscape, we visualized relationships between studies, patients and sequences, illustrating interconnections between studies and the varying depth of sequencing, patient number, and tissue representation across studies. Currently, the database contains 2517 envelope sequences from 90 patients, obtained from 22 published studies. 1272 sequences are from brain; the remaining 1245 are from blood, lymph node, spleen, bone marrow, colon, lung and other non-brain tissues. The database interface utilizes a faceted interface, allowing real-time combination of multiple search parameters to assemble a meta-dataset, which can be downloaded for further analysis.

Conclusions: This online resource, which is publicly available at http://www.HIVBrainSeqDB.org, will greatly facilitate analysis of the genetic aspects of HIV macrophage tropism, HIV compartmentalization and evolution within the brain and other tissue reservoirs, and the relationship of these findings to HIV-associated neurological disorders and other clinical consequences of HIV infection.

* Correspondence: dana_gabuzda@dfci.harvard.edu
[1]Department of Cancer Immunology and AIDS, Dana-Farber Cancer Institute, Dana-Farber Cancer Institute, 44 Binney Street, Boston, Massachusetts, 02115, USA
Full list of author information is available at the end of the article

Introduction

The population of HIV replicating within a host consists of independently evolving and interacting sub-populations, as demonstrated by the various degrees of phylogenetic compartmentalization seen across and within anatomical compartments and various rates of decay in viral load during HAART therapy [1,2]. Several factors contribute to this genetic compartmentalization: (i) viral target cell tropism–HIV infects CD4+ T cells and macrophages in the periphery, and primarily infects macrophages and microglia (and rarely, astrocytes) in the brain [3]; (ii) viral adaptation in response to immune selection pressures that differ between anatomical compartments [3,4]; (iii) physical barriers such as the blood-brain barrier [5]; and (iv) variable antiretroviral drug penetration into different tissues [6,7]. An important viral sub-population is HIV replicating within the brain [8-10]. HIV replicating in the brain causes neurocognitive and neuropathological disorders in up to 20-30% of infected individuals, particularly in later stages of disease; in the era of HAART, HIV-associated neurocognitive disorders (HAND) have emerged as a significant cause of mortality and morbidity [4,6]. Additionally, the brain is a sanctuary site for the development of drug resistance, because poor antiretroviral drug penetration into the CNS leads to sub-therapeutic drug concentrations and incomplete suppression of viral replication [6]. The primary determinant of HIV neurotropism is macrophage tropism, which is primarily determined by genetic variation in the viral envelope (*env*) gene [8]. Phylogenetically related populations of macrophage-tropic virus are found across brain and other macrophage-rich tissues, such as lung and bone marrow [11,12]. Thus, studies of the genetics of HIV replicating in the brain are pertinent to important clinical aspects of HIV, as well as the biology of the virus replicating within specific anatomical compartments.

There are several excellent existing repositories of HIV sequences in the public domain, two of the most widely used being Genbank at the NCBI [13] and the HIV Sequence Database at the Los Alamos National Laboratory (LANL) (http://hiv.lanl.gov). However, neither is focused on neurotropic virus nor contains clinical annotations of neurocognitive and neuropathological diagnosis. Though more than 20 publications have clonally sequenced HIV *env* from the brain, assembling a meta-dataset of these sequences presents significant technical challenges. To address these challenges, we constructed the HIV Brain Sequence Database (HBSD), the first comprehensive database of HIV envelope sequences clonally sequenced from brain and non-brain tissues, which is publicly available at http://HIVBrainSeqDB.org

Table 1 Publications describing the cloning of sequences included in the HBSD

Publication	Number of Sequences
Keele, Burton (2008) [19]	51
Power, Chesebro (1994) [20]	15
Peters, Clapham (2004) [21]	31
Mefford, Gabuzda (unpublished)	33
Mefford, Gabuzda (2008) [22]	10
Ohagen, Gabuzda (2003) [23]	35
Thomas, Gabuzda (2007) [24]	55
Liu, Gartner (2000) [25]	31
Martín-García, González-Scarano (2006) [26]	12
Shapshak, Goodkin (1999) [15]	65
Li, Hahn (1991) [27]	2
Gatanaga, Iwamoto (1999) [28]	17
Lamers, McGrath (2009) [29]	715
Salemi, McGrath (2005) [12]	88
Shah, Saksena (2006) [30]	30
Smit, Saksena (2001) [31]	11
Hughes, Simmonds (1997) [32]	87
McCrossan, Simmonds (2006) [18]	259
Morris, Simmonds (1999) [33]	252
Wang, Simmonds (2001) [11]	470
Monken, Srinivasan (1995) [34]	39
Korber, Wolinsky (1994) [17]	209

First author, last author and publication year of included publications, sorted by last author is shown in the left column. Total number of sequences included in the database from each publication is shown in the right column. In some cases, publications may contain additional sequences that did not meet our inclusion criteria–for example, sequences from isolates or patients with no brain sequences–and were therefore omitted.

The HIV Brain Sequence Database

The HBSD contains 2517 envelope sequences from 90 patients. Sequences were obtained from 22 published studies (Table 1) ranging in publication date from 1991 to 2009 and in number of sequences per publication from 1 to over 700. 1272 of these sequences are brain-derived; the remaining approximately 1245 are derived from blood, lymph node, spleen, bone marrow, colon, lung and other non-brain tissues. 44 independent tissue types are represented within the database. These tissue types are grouped into 4 categories: (i) brain, brainstem, and spinal cord; (ii) meninges, choroid plexus, and CSF; (iii) blood and lymphoid; and (iv) other (bone marrow, lung, liver, etc) (Table 2). Figure 1 shows the database sequence content aligned to the *env* gene of HXB2. V3 region and near full-length gp120 region sequences comprise the majority of the database, with approximately 1100 and 800 sequences, respectively. There are also approximately 200 near full-length *env* sequences, 150 V4-V5 region, and 100 V1-V2 region. As new publications emerge, facilitated by new sequencing technologies, we expect the size of the HBSD to follow the

Table 2 Classification of tissues represented in the database, with their respective Foundational Model of Anatomy (FMA) codes

Brain, brainstem, and spinal cord (n = 1272)	FMA Code	Number of sequences
Brain	FMA:50801	171
Brainstem	FMA:79876	16
Caudate nucleus	FMA:61833	7
Cortex of frontal lobe	FMA:242199	67
Cortex of occipital lobe	FMA:242205	20
Cortex of temporal lobe	FMA:242201	77
Frontal lobe	FMA:61824	91
Left frontal lobe	FMA:72970	214
Left hemisphere of cerebellum	FMA:83877	1
Left occipital lobe	FMA:72976	12
Left parietal lobe	FMA:72974	5
Left temporal lobe	FMA:72972	17
Middle frontal gyrus	FMA:61859	10
Occipital lobe	FMA:67325	25
Parietal lobe	FMA:61826	3
Putamen	FMA:61834	1
Right frontal lobe	FMA:72969	43
Right hemisphere of cerebellum	FMA:83876	1
Right occipital lobe	FMA:72975	16
Right parietal lobe	FMA:72973	18
Right temporal lobe	FMA:72971	15
Set of basal ganglia	FMA:84013	87
Spinal cord	FMA:7647	12
Temporal lobe	FMA:61825	41
White matter of frontal lobe	FMA:256178	111
White matter of neuraxis	FMA:83929	29
White matter of occipital lobe	FMA:256188	140
White matter of temporal lobe	FMA:256186	22
Meninges, choroid plexus, and CSF (n = 184)		
Choroid plexus of cerebral hemisphere	FMA:61934	44
CSF	FMA:20935	1
Set of meninges	FMA:76821	139
Blood and lymphoid (n = 776)		
Blood	FMA:9670	122
Infraclavicular lymph node	FMA:14193	4
Lymph node	FMA:5034	417
Mesenteric lymph node	FMA:12795	28
Peripheral blood mononuclear cell	FMA:86713	15
Spleen	FMA:7196	129
T-lymphocyte	FMA:62870	61
Other (n = 285)		
Bone marrow	FMA:9608	31
Colon	FMA:14543	135
Epithelial lining fluid	FMA:276456	5
Liver	FMA:7197	34
Lung	FMA:7195	78
Right lung	FMA:7309	2

exponential expansion seen by other sequence databases [13].

Collection and assembly of HIV sequences

The HBSD attempts to contain all available, published HIV sequences meeting stringent inclusion criteria. For inclusion in the HBSD, sequences must meet the following criteria: (i) be deposited in Genbank; (ii) include some portion of the HIV *env* region; (iii) be clonal, amplified directly from tissue; and (iv) be sampled from the brain, or sampled from a patient for which the HBSD already contains brain sequences. We identified sequences for inclusion both by searching the public sequence databases–Genbank and the LANL HIV sequence database–and by identifying publications that sequenced HIV from the brain. In several cases, we communicated directly with study authors to encourage deposition of sequences that had not been previously submitted to Genbank. Additionally, BLAST alignment was used to screen for possible contamination with commonly used lab strains (i.e., ADA, HXB2, JR-CSF, NL4-3, SF2, BaL, IIIB, MN, SF162, and JR-FL)

Annotation Structure

The HIV Brain Sequence Database contains three categories of annotations: publication references, patient and sampling information, and sequence properties (Table 3). The publication annotations include bibliographic information identifying the study that generated the sequences. Patient sampling annotations contain information describing the individual patients, as well as clinical information at the time of sampling. This information was obtained by manual curation of the original publications and in some cases direct communications with the study authors. In cases where multiple studies examined tissue samples from the same patient, the resulting sequences are linked to the same patient code to increase statistical power. Sample timepoint annotations describe the patient's clinical health status, neurocognitive, neuropathological status, CD4 counts, viral load, and anti-retroviral treatment history at the time of sampling. Clone and sequence annotations describe the individual sequences, the tissue from which they were cloned, and the method of PCR amplification and cloning. This includes the sequence start and end locations numbered based on alignment to the HXB2 reference genome, and tissue source coded using terms from a formal anatomical ontology. Alignment to HXB2 was performed using the HIV Sequence Locator tool located at the LANL HIV Sequence Database (http://hiv.lanl.gov). Currently, amplification and cloning methods included in the database are: bulk PCR then cloning (1736 sequences) and limiting-dilution PCR then cloning (781 sequences). As new sequencing projects are completed, we hope to expand the database to include significant numbers of sequences cloned via single genome amplification.

Annotation of Tissue Type

Annotation of tissue source presented several challenges. First, the granularity of tissue annotation varied by publication–we encountered tissue type annotations as general as "Brain" and as specific as "White matter of occipital lobe". However, within the HBSD a search for a more general tissue type, such as cerebrum should also return sequences from sub-parts of the cerebrum, such as caudate nucleus and putamen. Second, publications utilize non-standard tissue names that are human-readable but difficult to parse in a database search. To address these challenges, we utilized a formal anatomical ontology, the Foundational Model of Anatomy (FMA) to code tissue source [14]. The FMA defines terms for approximately 75,000 human anatomical structures, ranging in scale from biological macromolecules to whole organ systems. These terms are linked by ontological relationships defining subpart relationships, allowing the calculation of transitive closure within the database. In addition, we assigned sequences into one of four classes: (i) Brain; (ii) Meninges, choroid plexus, and CSF; (iii) Blood and lymphoid; and (iv) Other. Meninges, choroid plexus, and CSF were grouped separately from Brain because phylogenetic evidence suggests that the CSF represents an intermediate compartment, containing virus from both the brain and periphery [8]. "Other" includes organs such as lung, liver, stomach and prostate, bone marrow, and fluid samples such as lung epithelial lining fluid.

Annotation of Neurocognitive and Neuropathological Diagnosis

Neurocognitive and neuropathological status were classified for each patient at the sampling timepoint, usually perimortem (Table 4). Neuropathological and neurocognitive disorders can be due either to virus replicating in the brain or to non-HIV related causes such as toxoplasmosis, CMV encephalitis, or CNS lymphoma. Neuropathological status was coded as HIV encephalitis (HIVE) of varying severity, lymphocytic perivascular cuffing, or "Other", specifying the predominant non-HIV neurological pathology. Neurocognitive diagnosis was annotated using the nomenclature consensus published in Antinori et al, 2007 [4]. We further classified the HAD diagnosis into mild, moderate, and severe to capture information included in the publication as mild, moderate, or severe (most commonly) or MSK scores (rarely). Additionally, there were several unique cases that fell outside the AAN or HNRC criteria, but which we felt were important to annotate within the database.

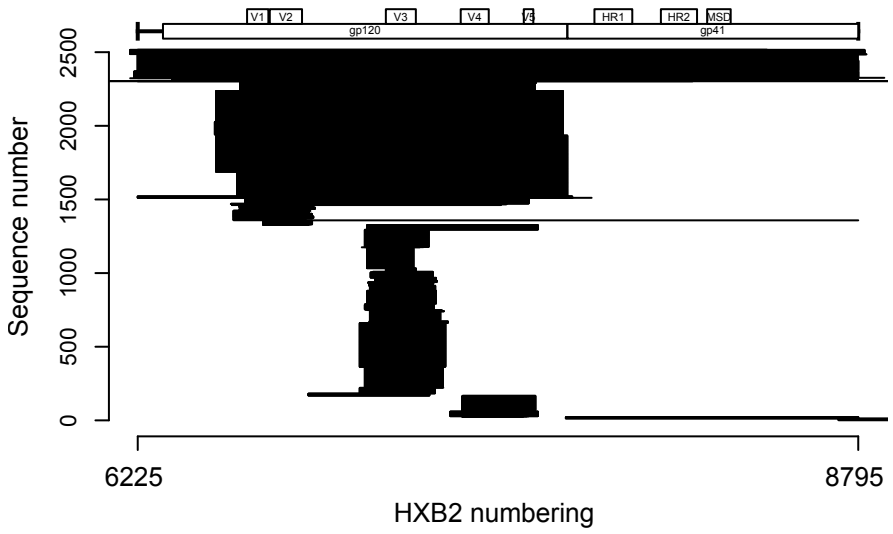

Region Coverage	Sequence Count
Full-length env	215
V1-V5	792
V1-V4	49
V1-V2	103
V2	31
V2-gp41	1
V3	1127
V3-V5	32
V4	5
V4-V5	140
gp41	10
other	12

Figure 1 Sequence coverage of the HIV *env* gene, numbered according to HXB2. Start and end coordinates are represented, but sequences are not internally aligned so gaps are not represented. The x-axis shows HXB2 nucleotide numbering with a schematic of the *env* gene plotted above. The y-axis shows arbitrary numbering of the plotted sequences.

Diagnosis for patient 196 stated: "insufficient information for patient 196 for the diagnosis of HAD, though there was evidence for neuropsychiatric disease."[15]. Given that we lacked the further information to meet the strict criteria for an ANI or MND diagnosis, we chose the more general NPI: unknown defined in Woods et al. 2004 [16]. Diagnoses for patients 1 through 6 stated, "Clinical material was obtained from six HIV-1 infected patients with significant neurological signs and symptoms requiring image-guided stereotactic brain biopsy for definitive diagnosis. ... Neurological signs and symptoms were consistent with the onset of global neurological dysfunction, with clinical evidence supporting acute rather than chronic HIV-1-associated neurological disease."[17]. As an acute diagnosis, this does not fit the criteria for HAD, so it was annotated in the database as acute HIV encephalopathy [17].

Design and Implementation

The HBSD structure is sequence-centric and uses NCBI GI and Genbank accession numbers as identifiers, simplifying correlations with other databases. The database exists in two forms. The master version is kept internally as a relational SQL database utilized for sequence management and curation. This is replicated to an external interface that uses the Apache Solr search platform to optimize for flexible search and data retrieval. The search interface (Figure 2) is based on a filtering paradigm; the user begins with the set of all sequences and narrows by applying filtering criteria to the sequence annotations. Filtering criteria are specified by two means. A faceted search interface presents all values for categorical annotations, such as tissue class or neurocognitive status. Clicking on a value adds it to the search criteria and filters for matching sequences. Additionally, a global search box allows direct entry of search terms. Multiple searches in the global search box sequentially add filtering criteria, allowing the construction of complex searches. Sequences are initially presented with a default set of annotations, however, users can select to add or remove columns from the set of all annotations available. The final filtered set of sequences and annotations can be downloaded for local analysis in tab-separated and FASTA formats.

Visualization of the contents of the database

To better understand the highly complex network of publications, patients, and sequences, we used Cytoscape to visualize the connections between patients and the publications that sequenced virus from those patients (Figure 3). This network visualization demonstrates that, while most publications examine a unique set of patients, there is an emerging network of patients from the Edinburgh MRC HIV Brain and Tissue Bank (coded as NA#) that are shared among multiple publications. Additionally, Figure 3 illustrates the dramatic differences in sequencing depth between patients, and in number of patients between studies.

Many experimental designs examining compartmentalization or tissue specific effects depend on overlap in the viral regions sequenced and matched tissue source. In order to quantify the power of the database to make these comparisons, we visualized the total number of across-tissue and within-tissue comparisons possible with

Table 3 Annotation categories

Patient	Column Definition
Patient code	patient code
Sex	gender
Risk factor	HIV risk factor
Tissue bank	tissue bank distributing samples
Patient year of death	patient year of death
Sampling timepoint	
Sampling geo-region	patient geo-region at time of sampling
Sampling country	patient country at time of sampling
Sampling city	patient city at time of sampling
Patient age	patient age at sampling
Health status	patient health status at sampling
Subtype	predominant subtype at time of sampling
Drug naïve (ART)	has patient had ART
Antiretroviral treatment (ART)	patient ART history
Viral load plasma (copies/mL)	plasma viral load
Viral load brain (copies/million cells)	brain viral load
Viral load lymphoid (copies/million cells)	lymphoid viral load
CD4 count (cells/uL)	CD4 count
Neurocognitive diagnosis	neurocognitive diagnosis
Neuropathological diagnosis	neuropathological diagnosis
Giant cells	were giant cells present in the brain
Sequence	
Genbank accession	Genbank accession number
GI	Genbank GI number
PubMed ID	Pubmed ID for original publicaiton
Sequence length	sequence length
Clone name	publication assigned clone name
Cloning strategy	methods of genome amplification and cloning
Sample tissue class	global tissue class (Brain, Blood & Lymphoid, etc...)
Sample tissue name	tissue source
Sample tissue FMA code	tissue FMA code
Nucleic acid type	was proviral DNA or viral RNA sequenced
Start and end coordinates	sequence start and end referenced to HXB2
Sequence	viral sequence

the current database content (Figure 4). Panel A visualizes, for each tissue pair, how many patients contain overlapping sequences. Each comparison is ontologically inclusive–for example entries under Frontal lobe also consider sequences from White matter of frontal lobe, Cortex of frontal lobe, etcetera. This visualization reveals structures within the dataset useful for experimental design. For example, while a large number of patients contain overlapping sequences from lymph node and another tissue, in 8, 11, and 7 patients, respectively, it is possible to compare frontal lobe to occipital, temporal, or parietal lobes. Figure 4B is a complementary visualization counting the number of pairwise patient to patient comparisons possible within each tissue type. This illustrates, for example, that while many patients have overlapping sequences from the cerebrum, frontal lobe is a particularly well-represented tissue. Conversely, though the database contains sequences from the cerebellum, there are no across patient comparisons that can be made. The numbers in both A and B of Figure 4 do not represent simple sums or permutations, because each considers sequence overlap. If hypothetical patients A, B, and C contained full-length *env*, V3 region, and V5 region sequences, respectively, then only 2 pair-wise comparisons would be possible (A to B and A to C), not the 3 given by a simple permutation.

Table 4 Neurocognitive and neuropathological annotations in the database

Neurocognitive Diagnosis	Number of Patients	Number of Sequences
None	42	739
Acute HIV encephalopathy	6	209
HAD: mild	7	46
HAD: moderate	4	8
HAD: severe	11	424
HAD: severity not specified	19	810
NPI-unknown	1	10
No diagnosis	7	271
Neuropathological Diagnosis		
None	37	369
HIVE: mild	5	276
HIVE: moderate	3	100
HIVE: severe	6	117
HIVE: severity not specified	17	938
Lymphocytic perivascular cuffing	1	31
Other: cerebral atrophy	1	39
Other: CMV encephalitis	1	5
Other: CNS lymphoma	7	242
Other: necrotizing encephalitis, not HIV-related	1	23
Other: progressive multifocal leukoencephalopathy	2	36
Other: toxoplasmosis	3	83
Other: widespread atherosclerosis	1	87
No diagnosis	12	171

An annotation of "none" indicates a diagnosis of no impairment or neuropathology, whereas "no diagnosis" indicates that clinical annotation information was not available.

Discussion

The HBSD is a public database designed to facilitate the assembly of a large meta-dataset of HIV *env* sequences that will be invaluable to investigations into the different patterns of viral evolution in the brain and other tissue reservoirs, and the relationship of these findings to each other and to clinical consequences of HIV infection, particularly development of HAND. The database contains 2517 *env* sequences cloned from 90 patients and 44 tissues sources. 1272 of these sequences are brain-derived; the remaining 1245 are derived from blood, lymph node, spleen, bone marrow, colon, lung, and other non-brain tissues. The majority of these sequences are from the V3 region (45%) or near full-length gp120 region (31%), with the remainder being near full-length *env* (9%), V4-V5 region (6%), V1-V2 region (4%) and others (5%) (Figure 1). The HBSD is unique compared to other sequence databases, such as the LANL HIV Sequence Database or Genbank, because of its specific focus on HIV in the brain, its stringent inclusion of only clonal sequences from patients with brain sequences, and its rigorous curation with detailed clinical, patient, and HAND annotations.

An HIV *env* meta-dataset annotated with detailed clinical information will allow studies that previously have not been feasible. Combining datasets to increase the number of sequences and tissue-types increases the statistical power available. This increased statistical power can be used to examine questions such as the genetic variations within *env* important for macrophage tropism, which is the primary requirement for HIV replication in the brain, and nucleotide positions within *env* under positive genetic selection during HIV replication in the CNS. Annotation of neurocognitive status, neuropathological status, and AIDS progression will facilitate correlation of viral genotype to clinical phenotypes, and may help to reveal how viral genotypes affect the development of HAND.

During the assembly and annotation of the HBSD, we encountered a number of challenges. Non-uniform tissue coding made consistent database annotation difficult. To overcome this obstacle, we utilized the FMA anatomical ontology to convert various tissue source descriptions into a set of defined terms with ontological linkages. We encountered several instances of ambiguous patient coding. Because tissue samples are shared

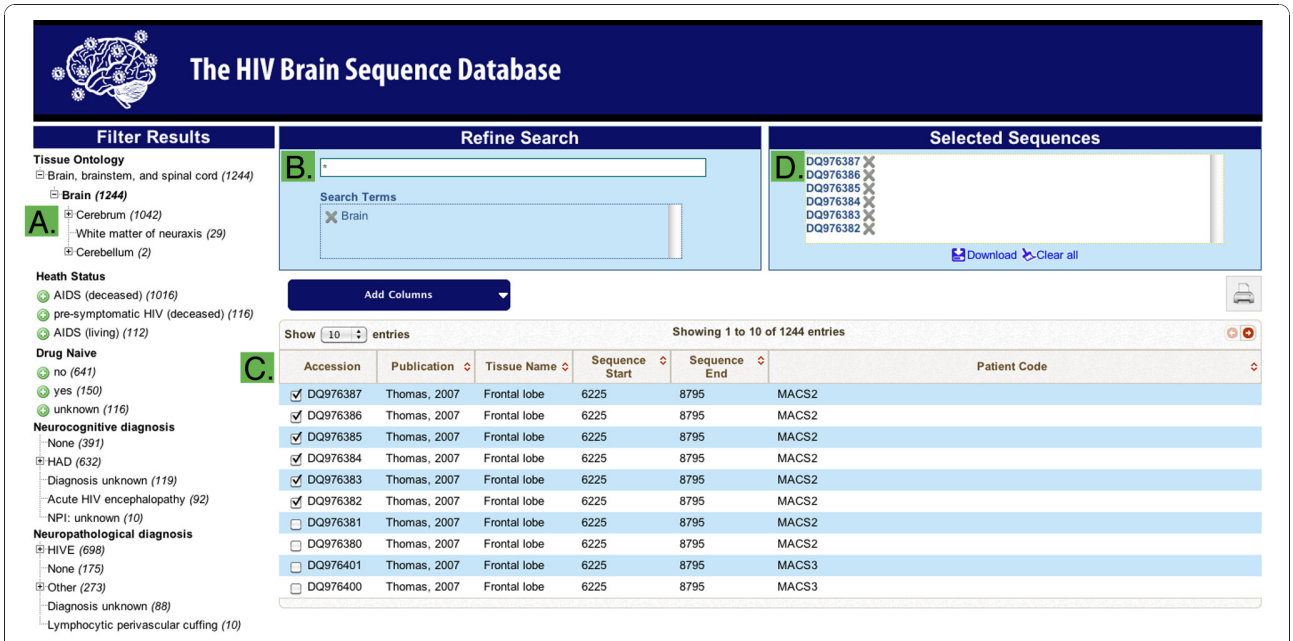

Figure 2 Search interface of the HBSD. A. Database facets for filtering results. All possible values for each category are presented, along with a count of the number of sequences for each value. Clicking on a value adds it to the search box (B), filters the results list (C), and updates the facet list and sequence counts (A). B. Universal search box and search term list. Performs a global search across categories, for example, a search for "right" returns sequences from both "Right frontal lobe" and "Right lung". Upon searching, the facet list (A) and results (C) are updated. All searches and faceting terms applied are placed in the Search Terms box and can be removed individually by clicking the "X" next to a term. C. Results list. Displays the current list of sequences matching the filters within the Search Terms box (B). Columns can be added or removed through the Add Columns button. Clicking the checkbox by a sequence adds it to the Selected Sequences box (D). D. Selected Sequences and Downloads. Clicking the download button presents options to download: (i) Current Results–all sequences matching the search terms, (ii) Current Selection–all selected sequences in box D, (iii) Entire Collection–the entire HBSD. Downloads consist of a zip file containing a FASTA formatted file of all sequences, named by Genbank accession number, and a tab-separated file of all selected annotation columns, ready for import to Excel.

within laboratories, and tissue banks distribute samples from the same patient to multiple laboratories, viruses from one patient may be sequenced in multiple publications. By examining patient annotation data and corresponding with study authors, we identified 3 patients that were coded differently by multiple studies (NA118_p5, NA420_p6 and NA21_UK1) and 2 cases of separate patients that were coded identically by different studies (NA20 and NA234). Combining sequences from multiple publications and grouping by patient can increase the diversity of tissue types and the depth of sequencing available, while carefully tracking patient coding can avoid incorrect grouping of non-identical patients. Many publications included in the HBSD contain duplicate sequences cloned from the same tissue sample. These duplicate sequences could result either from PCR resampling in studies utilizing bulk PCR before cloning, or could represent valid cloning of copies of a majority viral variant. Fifteen publications utilized bulk PCR then cloning, 5 utilized limiting dilution then cloning, and 2 used both approaches, based on patient. The database contains 490 repeated sequences in 161 groups. However, 217 of these repeated sequences were obtained by limiting dilution PCR and therefore are unlikely to represent PCR resampling. Comparison of the distribution of the percentage of duplicated sequences between bulk PCR and limiting dilution demonstrated that studies utilizing bulk PCR then cloning did not show a higher rate of sequence duplication than those utilizing limiting dilution (data not shown). Thus duplicated sequences in the database likely represent appropriate cloning of majority viral variants.

The HBSD includes several unique datasets, which, though previously available in the public domain, are now collected in a standardized annotation format for meta-analysis. 15 patients included in McCrossan, 2006 [18] are pre-symptomatic, having died from HIV-unrelated causes [alcohol/drug overdose (n = 11), cirrhosis (n = 2), suicide (n = 1), and bronchopneumonia (n = 1)]. During late-stage AIDS, declining CD4 counts lead to immune deficiency and reduced selection pressure, allowing viral population expansion that may alter the distribution of sequence variants. Based on

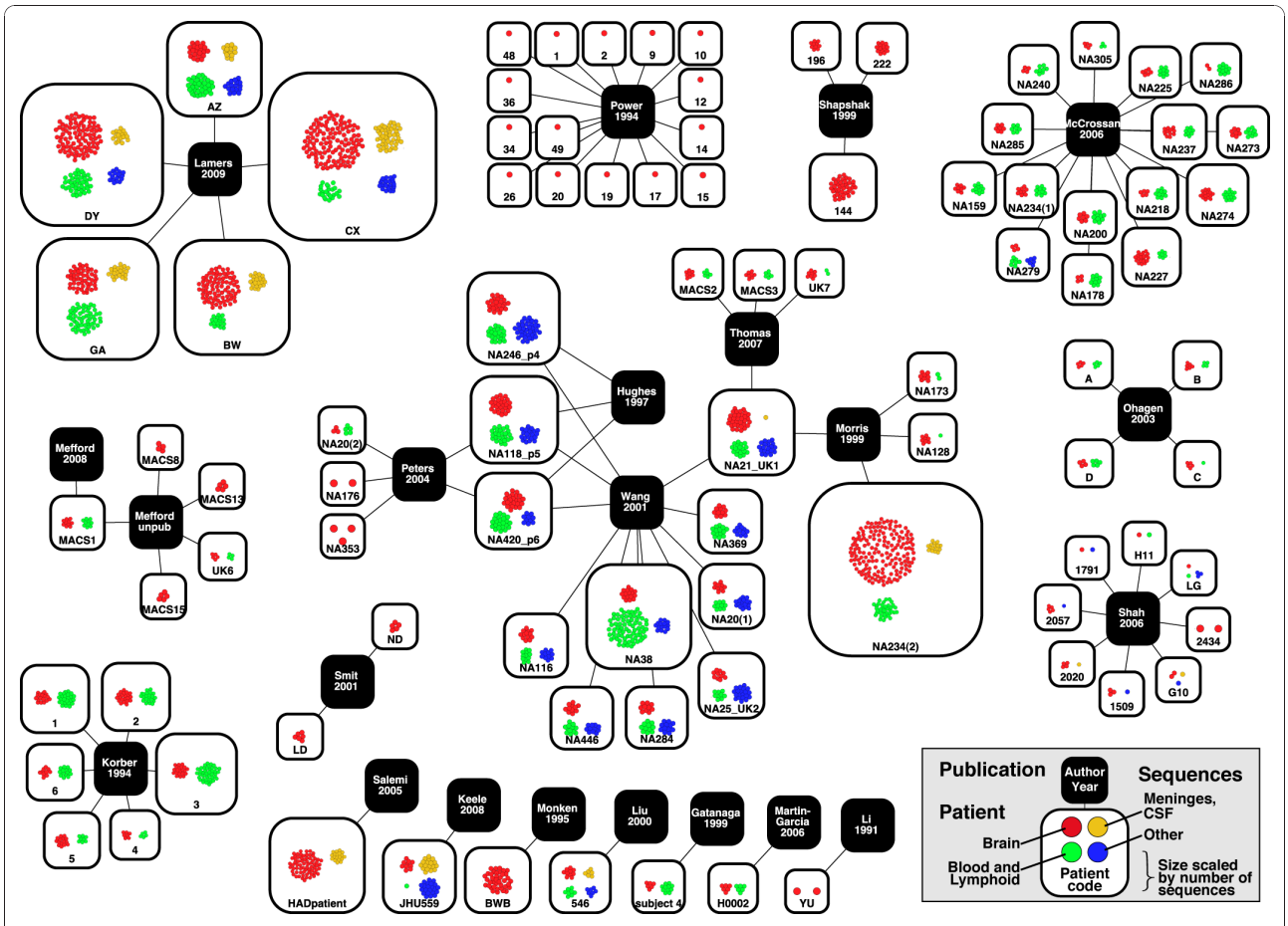

Figure 3 Network representation of interconnections between publications, the patients they sequenced, and the number and tissue classes of sequences available for each patient. The network was constructed using Cytoscape. Black nodes, containing the name of the first author, represent publications. Publication nodes are connected by edges to the patients they sequenced, represented by clear nodes with patient code printed at the bottom. In cases where multiple publications sequenced virus from the same patient, multiple publication nodes connect to a single patient node (patient NA118 in the upper right). Individual HIV sequences for each patient are represented by the colored dots within patient nodes: Brain-red, Meninges, choroid plexus, and CSF-yellow, Blood and Lymphoid-green, Other-blue. The total number of sequences for each patient scales the size of the patient node.

treatment history and year of death, the majority of patients in the HBSD died prior to the HAART era. 49 out of 90 patients have annotations for antiretroviral treatment history. Of these 49 patients, 19 are drug naïve and 30 received antiretroviral drugs. The majority of antiretroviral treated patients were on pre-HAART regimens, and 9 received only AZT. Different ART drugs have differing CNS penetration, affecting selection pressures on virus replicating in the brain [6]. Additionally, the majority of neurocognitive diagnoses occurred before the 2007 HNRC consensus document [4] that defined criteria for asymptomatic neurocognitive impairment (ANI). Future improvement of the quality and relevance of the database to the current epidemic requires generating more sequences sampled from the brains of pre-symptomatic patients at earlier stages of disease and HAART-treated patients.

Our laboratory will continue to maintain the HBSD as new sequences are deposited in the public domain. We expect the HBSD to expand in several ways. New deep sequencing projects will increase the number of sequences and expand the diversity of patients, sampling a wider spectrum of stages of disease and HAART treatment regimens. Curation of patient coding may allow us to identify longitudinal sets of sequences sampled from the periphery, which can be paired with brain sequences sampled from the same patient at autopsy. Finally, we chose to focus on *env* for the initial database release because it plays a key role in brain infection and provides a tractable scope for development of a highly curated database. As we consider further database additions, we will continue to weigh the benefits of inclusion against the resources required to maintain our high standards of database curation.

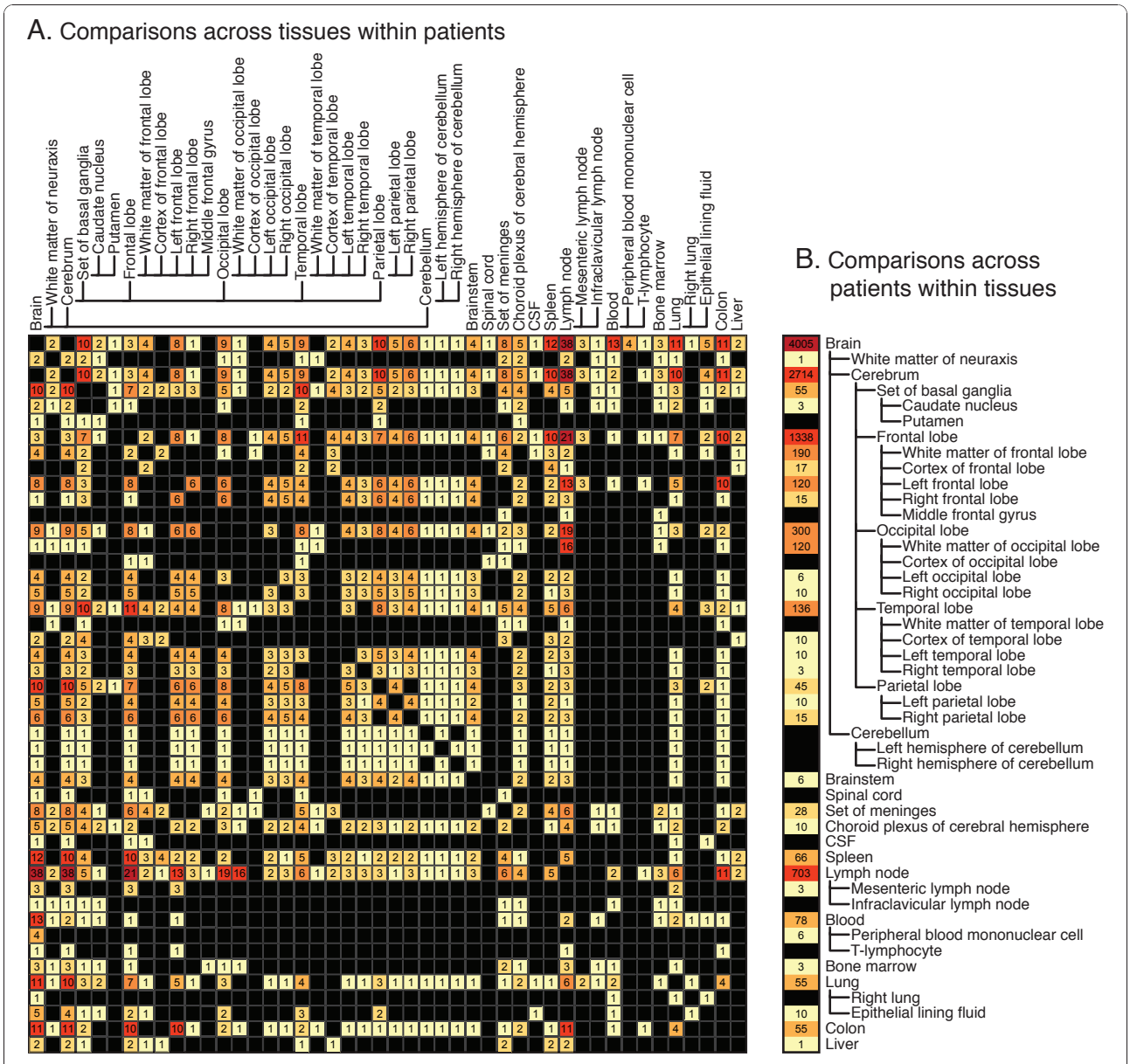

Figure 4 Heatmap representation and counts of all possible comparisons between sets of overlapping sequences within the database. Counts of possible comparisons were generated using 2 custom Perl scripts and SQL statements, then visualized as a heatmap using R. A. Number of patients for which within-patient comparisons across tissue-types can be made. For pairs of tissues from the X and Y-axis, numbers indicate the number of patients for which overlapping sequences from both tissues are available. For example, there are 11 patients with overlapping sequences from both Frontal lobe and Temporal lobe. B. Number of possible pair-wise comparisons across patients within each tissue type. For each tissue on the Y-axis, numbers indicate the count of possible pair-wise comparisons between patients. For example, there are 2 patients with overlapping sequences from White matter of neuroaxis, giving 1 possible comparison, and 4 patients with overlapping sequence from Left occipital lobe, giving 6 possible pair-wise comparisons. Tissue definitions are ontologically inclusive, i.e. Frontal lobe also includes White matter of frontal lobe, Cortex of frontal lobe, etc. Cells are colored as a heat map accentuating high values, and range from light yellow (low values) to dark red (high values). Black indicates no comparisons possible.

Tat and *nef* are two logical next steps, as these genes influence brain infection and development of neurocognitive disorders. Drug resistance mutations in *pol* and RT would also be a useful addition that will be considered in the future.

Conclusions

The HBSD is a unique resource for the research community investigating unique genetic and biological characteristics of HIV in the brain. Though nearly all the sequences and annotations included were previously

available in the public domain, the data did not exist in a well-annotated and accessible format and its assembly and curation represented a significant hurdle. The HBSD will be an invaluable resource for studying the viral genetics of HIV evolution within the brain and other tissue reservoirs, and the relationship of these findings to each other and to the development of HIV-associated neurocognitive disorders.

Acknowledgements

The authors wish to thank Mick Correll and Yaoyu Wang of The Center for Cancer Computational Biology, Dana-Farber Cancer Institute, Boston, MA for assistance with developing the database website and interface. We also thank the National NeuroAIDS Tissue Consortium (NNTC) for providing missing clinical data for some cases. The tissue source annotation is based on the FMA developed at the University of Washington by the FMATM Research Project and is provided under license from the University of Washington.

This work was supported by an ARRA supplement NIH/NIMH #3ROI MH83588-12S1 and the parent grant MH83588. MEM was supported in part by NIH fellowship 1F31NS060611-01. Core facilities were supported by the Harvard Center for AIDS Research and DFCI/Harvard Center for Cancer Research grants. The NNTC was supported by NIH funding through the NIMH and NINDS Institutes by the following grants: Manhattan HIV Brain Bank U01MH083501, R24MH59724 Texas NeuroAIDS Research Center U01MH083507, R24 NS45491 National Neurological AIDS Bank 5U01MH083500, NS 38841 California NeuroAIDS Tissue Network U01MH083506, R24MH59745, Statistics and Data Coordinating Center U01MH083545, N01MH32002. The funders and NNTC had no role in study design, data analysis, or preparation and submission of the publication.

Author details

[1]Department of Cancer Immunology and AIDS, Dana-Farber Cancer Institute, Dana-Farber Cancer Institute, 44 Binney Street, Boston, Massachusetts, 02115, USA. [2]Center for Cancer Computational Biology, Dana-Farber Cancer Institute, Dana-Farber Cancer Institute, 44 Binney Street, Boston, Massachusetts, 02115, USA. [3]Department of Neurology, Harvard Medical School, 25 Shattuck Street, Boston, Massachusetts, 02115, USA.

Authors' contributions

AH designed the sequence database, assembled and curated sequences, performed all bioinformatic analysis, and drafted the manuscript. MM assembled and curated sequences and clinical data. NO designed and implemented the database interface. DG conceived of the study, participated in its design and coordination, and helped to draft the manuscript. All authors read and approved the final manuscript.

Competing interests

The authors declare that they have no competing interests.

Received: 9 November 2010 Accepted: 14 December 2010
Published: 14 December 2010

References

1. Simon V, Ho DD: **HIV-1 dynamics in vivo: implications for therapy.** *Nature Reviews Microbiology* 2003, **1**:181-190.
2. Frost SD, Dumaurier MJ, Wain-Hobson S, Brown AJ: **Genetic drift and within-host metapopulation dynamics of HIV-1 infection.** *Proc Natl Acad Sci USA* 2001, **98**:6975-6980.
3. Stevenson M: **HIV-1 pathogenesis.** *Nature medicine* 2003, **9**:853-860.
4. Antinori A, Arendt G, Becker JT, Brew BJ, Byrd DA, Cherner M, Clifford DB, Cinque P, Epstein LG, Goodkin K, *et al*: **Updated research nosology for HIV-associated neurocognitive disorders.** *Neurology* 2007, **69**:1789-1799.
5. Ivey NS, MacLean AG, Lackner AA: **Acquired immunodeficiency syndrome and the blood-brain barrier.** *J Neurovirol* 2009, **15**:111-122.
6. McGee B, Smith N, Aweeka F: **HIV pharmacology: barriers to the eradication of HIV from the CNS.** *HIV Clin Trials* 2006, **7**:142-153.
7. Saksena NK, Potter SJ: **Reservoirs of HIV-1 in vivo: implications for antiretroviral therapy.** *AIDS Rev* 2003, **5**:3-18.
8. Dunfee R, Thomas ER, Gorry PR, Wang J, Ancuta P, Gabuzda D: **Mechanisms of HIV-1 neurotropism.** *Curr HIV Res* 2006, **4**:267-278.
9. González-Scarano F, Martín-García J: **The neuropathogenesis of AIDS.** *Nat Rev Immunol* 2005, **5**:69-81.
10. van Marle G, Power C: **Human immunodeficiency virus type 1 genetic diversity in the nervous system: evolutionary epiphenomenon or disease determinant?** *J Neurovirol* 2005, **11**:107-128.
11. Wang TH, Donaldson YK, Brettle RP, Bell JE, Simmonds P: **Identification of shared populations of human immunodeficiency virus type 1 infecting microglia and tissue macrophages outside the central nervous system.** *J Virol* 2001, **75**:11686-11699.
12. Salemi M, Lamers SL, Yu S, de Oliveira T, Fitch WM, McGrath MS: **Phylodynamic analysis of human immunodeficiency virus type 1 in distinct brain compartments provides a model for the neuropathogenesis of AIDS.** *J Virol* 2005, **79**:11343-11352.
13. Benson DA, Karsch-Mizrachi I, Lipman DJ, Ostell J, Sayers EW: **GenBank.** *Nucleic Acids Res* 2010, **38**:D46-51.
14. Rosse C, Mejino JLV: **A reference ontology for biomedical informatics: the Foundational Model of Anatomy.** *J Biomed Inform* 2003, **36**:478-500.
15. Shapshak P, Segal DM, Crandall KA, Fujimura RK, Zhang BT, Xin KQ, Okuda K, Petito CK, Eisdorfer C, Goodkin K: **Independent evolution of HIV type 1 in different brain regions.** *AIDS Res Hum Retroviruses* 1999, **15**:811-820.
16. Woods SP, Rippeth JD, Frol AB, Levy JK, Ryan E, Soukup VM, Hinkin CH, Lazzaretto D, Cherner M, Marcotte TD, *et al*: **Interrater reliability of clinical ratings and neurocognitive diagnoses in HIV.** *J Clin Exp Neuropsychol* 2004, **26**:759-778.
17. Korber BT, Kunstman KJ, Patterson BK, Furtado M, McEvilly MM, Levy R, Wolinsky SM: **Genetic differences between blood- and brain-derived viral sequences from human immunodeficiency virus type 1-infected patients: evidence of conserved elements in the V3 region of the envelope protein of brain-derived sequences.** *J Virol* 1994, **68**:7467-7481.
18. McCrossan M, Marsden M, Carnie FW, Minnis S, Hansoti B, Anthony IC, Brettle RP, Bell JE, Simmonds P: **An immune control model for viral replication in the CNS during presymptomatic HIV infection.** *Brain* 2006, **129**:503-516.
19. Keele BF, Tazi L, Gartner S, Liu Y, Burgon TB, Estes JD, Thacker TC, Crandall KA, McArthur JC, Burton GF: **Characterization of the follicular dendritic cell reservoir of human immunodeficiency virus type 1.** *J Virol* 2008, **82**:5548-5561.
20. Power C, McArthur JC, Johnson RT, Griffin DE, Glass JD, Perryman S, Chesebro B: **Demented and nondemented patients with AIDS differ in brain-derived human immunodeficiency virus type 1 envelope sequences.** *J Virol* 1994, **68**:4643-4649.
21. Peters PJ, Bhattacharya J, Hibbitts S, Dittmar MT, Simmons G, Bell J, Simmonds P, Clapham PR: **Biological analysis of human immunodeficiency virus type 1 R5 envelopes amplified from brain and lymph node tissues of AIDS patients with neuropathology reveals two distinct tropism phenotypes and identifies envelopes in the brain that confer an enhanced tropism and fusigenicity for macrophages.** *J Virol* 2004, **78**:6915-6926.
22. Mefford ME, Gorry PR, Kunstman K, Wolinsky SM, Gabuzda D: **Bioinformatic prediction programs underestimate the frequency of CXCR4 usage by R5X4 HIV type 1 in brain and other tissues.** *AIDS Res Hum Retroviruses* 2008, **24**:1215-1220.
23. Ohagen A, Devitt A, Kunstman KJ, Gorry PR, Rose PP, Korber B, Taylor J, Levy R, Murphy RL, Wolinsky SM, Gabuzda D: **Genetic and functional analysis of full-length human immunodeficiency virus type 1 env genes derived from brain and blood of patients with AIDS.** *J Virol* 2003, **77**:12336-12345.
24. Thomas ER, Dunfee RL, Stanton J, Bogdan D, Taylor J, Kunstman K, Bell JE, Wolinsky SM, Gabuzda D: **Macrophage entry mediated by HIV Envs from brain and lymphoid tissues is determined by the capacity to use low CD4 levels and overall efficiency of fusion.** *Virology* 2007, **360**:105-119.
25. Liu Y, Tang XP, McArthur JC, Scott J, Gartner S: **Analysis of human immunodeficiency virus type 1 gp160 sequences from a patient with HIV dementia: evidence for monocyte trafficking into brain.** *J Neurovirol* 2000, **6(Suppl 1)**:S70-81.

26. Martín-García J, Cao W, Varela-Rohena A, Plassmeyer ML, González-Scarano F: **HIV-1 tropism for the central nervous system: Brain-derived envelope glycoproteins with lower CD4 dependence and reduced sensitivity to a fusion inhibitor.** *Virology* 2006, **346**:169-179.
27. Li Y, Kappes JC, Conway JA, Price RW, Shaw GM, Hahn BH: **Molecular characterization of human immunodeficiency virus type 1 cloned directly from uncultured human brain tissue: identification of replication-competent and -defective viral genomes.** *J Virol* 1991, **65**:3973-3985.
28. Gatanaga H, Oka S, Ida S, Wakabayashi T, Shioda T, Iwamoto A: **Active HIV-1 redistribution and replication in the brain with HIV encephalitis.** *Arch Virol* 1999, **144**:29-43.
29. Lamers SL, Salemi M, Galligan DC, de Oliveira T, Fogel GB, Granier SC, Zhao L, Brown JN, Morris A, Masliah E, McGrath MS: **Extensive HIV-1 intra-host recombination is common in tissues with abnormal histopathology.** *PLoS ONE* 2009, **4**:e5065.
30. Shah M, Smit TK, Morgello S, Tourtellotte W, Gelman B, Brew BJ, Saksena NK: **Env gp120 sequence analysis of HIV type 1 strains from diverse areas of the brain shows preponderance of CCR5 usage.** *AIDS Res Hum Retroviruses* 2006, **22**:177-181.
31. Smit TK, Wang B, Ng T, Osborne R, Brew B, Saksena NK: **Varied tropism of HIV-1 isolates derived from different regions of adult brain cortex discriminate between patients with and without AIDS dementia complex (ADC): evidence for neurotropic HIV variants.** *Virology* 2001, **279**:509-526.
32. Hughes ES, Bell JE, Simmonds P: **Investigation of population diversity of human immunodeficiency virus type 1 in vivo by nucleotide sequencing and length polymorphism analysis of the V1/V2 hypervariable region of env.** *J Gen Virol* 1997, **78(Pt 11)**:2871-2882.
33. Morris A, Marsden M, Halcrow K, Hughes ES, Brettle RP, Bell JE, Simmonds P: **Mosaic structure of the human immunodeficiency virus type 1 genome infecting lymphoid cells and the brain: evidence for frequent in vivo recombination events in the evolution of regional populations.** *J Virol* 1999, **73**:8720-8731.
34. Monken CE, Wu B, Srinivasan A: **High resolution analysis of HIV-1 quasispecies in the brain.** *AIDS* 1995, **9**:345-349.

doi:10.1186/1742-6405-7-43
Cite this article as: Holman *et al.*: HIVBrainSeqDB: a database of annotated HIV envelope sequences from brain and other anatomical sites. *AIDS Research and Therapy* 2010 **7**:43.

APPENDIX C

Reprinted from Virology, Vol. 362, Gorry, P.R., R.L. Dunfee, M.E. Mefford, K. Kunstman, T. Morgan, J.P. Moore, J.R. Mascola, K. Agopian, G.H. Holm, A. Mehle, J. Taylor, M. Farzan, H. Wang, P. Ellery, S.J. Willey, P.R. Clapham, S.M. Wolinsky, S.M. Crowe, and D. Gabuzda, Changes in the V3 region of gp120 contribute to unusually broad coreceptor usage of an HIV-1 isolate from a CCR5 Δ32 heterozygote, pp. 163-178,

Available online at www.sciencedirect.com
ScienceDirect
Virology 362 (2007) 163 – 178
VIROLOGY
www.elsevier.com/locate/yviro

Changes in the V3 region of gp120 contribute to unusually broad coreceptor usage of an HIV-1 isolate from a CCR5 Δ32 heterozygote

Paul R. Gorry [a,b,1], Rebecca L. Dunfee [a,b], Megan E. Mefford [a,b], Kevin Kunstman [d], Tom Morgan [e], John P. Moore [e], John R. Mascola [f], Kristin Agopian [a,b], Geoffrey H. Holm [a,b], Andrew Mehle [a,b], Joann Taylor [d], Michael Farzan [a,b], Hui Wang [a], Philip Ellery [g,h], Samantha J. Willey [i], Paul R. Clapham [i], Steven M. Wolinsky [d], Suzanne M. Crowe [g,h], Dana Gabuzda [a,c,*]

[a] *Department of Cancer Immunology and AIDS, Dana-Farber Cancer Institute, Harvard Medical School, Boston, MA 02115, USA*
[b] *Department of Pathology, Harvard Medical School, Boston, MA 02115, USA*
[c] *Department of Neurology, Harvard Medical School, Boston, MA 02115, USA*
[d] *Department of Medicine, Northwestern University Medical School, Chicago, IL 60611, USA*
[e] *Weill Medical College of Cornell University, New York, NY 10021-4896, USA*
[f] *Vaccine Research Center, National Institutes of Allergy and Infectious Diseases, National Institutes of Health, Bethesda, MD 20892, USA*
[g] *Macfarlane Burnet Institute for Medical Research and Public Health, Melbourne, Victoria, Australia*
[h] *Department of Medicine, Monash University, Melbourne, Victoria, Australia*
[i] *Program in Molecular Medicine, Department of Molecular Genetics and Microbiology, University of Massachusetts Medical School, Worcester, MA 01655, USA*

Received 6 October 2006; returned to author for revision 30 October 2006; accepted 16 November 2006
Available online 18 January 2007

Abstract

Heterozygosity for the CCR5 Δ32 allele is associated with delayed progression to AIDS in human immunodeficiency virus type 1 (HIV-1) infection. Here we describe an unusual HIV-1 isolate from the blood of an asymptomatic individual who was heterozygous for the CCR5 Δ32 allele and had reduced levels of CCR5 expression. The primary virus used CCR5, CXCR4, and an unusually broad range of alternative coreceptors to enter transfected cells. However, only CXCR4 and CCR5 were used to enter primary T cells and monocyte-derived macrophages, respectively. Full-length Env clones had an unusually long V1/V2 region and rare amino acid variants in the V3 and C4 regions. Mutagenesis studies and structural models suggested that Y308, D321, and to a lesser extent K442 and E444, contribute to the broad coreceptor usage of these Envs, whereas I317 is likely to be a compensatory change. Furthermore, database analysis suggests that covariation can occur at positions 308/317 and 308/321 *in vivo*. Y308 and D321 reduced dependence on the extracellular loop 2 (ECL2) region of CCR5, while these residues along with Y330, K442, and E444 enhanced dependence on the CCR5 N-terminus compared to clade B consensus residues at these positions. These results suggest that expanded coreceptor usage of HIV-1 can occur in some individuals without rapid progression to AIDS as a consequence of changes in the V3 region that reduce dependence on the ECL2 region of CCR5 by enhancing interactions with conserved structural elements in G-protein-coupled receptors.

Keywords: HIV-1; CCR5 Δ32; Env; V3; CCR5

Introduction

Human immunodeficiency virus type 1 (HIV-1) enters cells via interaction of the viral envelope glycoproteins (Env) with CD4 and a coreceptor. Macrophage (M)-tropic HIV-1 viruses primarily use CCR5 (R5) as a coreceptor, whereas T cell line-

* Corresponding author. Dana-Farber Cancer Institute, 44 Binney Street-JF816, Boston, MA 02115, USA. Fax: +1 617 632 3113.
E-mail address: dana_gabuzda@dfci.harvard.edu (D. Gabuzda).
[1] Present address: Macfarlane Burnet Institute for Medical Research and Public Health, Melbourne, Victoria, Australia.

0042-6822/$ - see front matter © 2006 Elsevier Inc. All rights reserved.
doi:10.1016/j.virol.2006.11.025

tropic HIV-1 viruses use CXCR4 (X4) (Berger et al., 1999; Doms and Trono, 2000; Moore et al., 2004). Dual-tropic viruses (R5X4) use both coreceptors. A subset of viruses can also use alternative coreceptors including CCR3, CCR2b, CCR8, Apj, Strl33 (BONZO/CXCR6), Gpr1, Gpr15 (BOB), CX3CR1, ChemR23, or RDC1 for entry (Berger et al., 1999; Doms and Trono, 2000; Moore et al., 2004). However, usage of coreceptors other than CCR5 and CXCR4 by primary viruses *in vitro* is rare (Zhang et al., 1998), and infection of primary cells occurs, with few exceptions, exclusively via CCR5 or CXCR4 (Cilliers et al., 2005; Moore et al., 2004). R5 strains predominate during primary infection and the asymptomatic phase, whereas expansion of viral coreceptor usage and emergence of X4 or R5X4 strains is frequently associated with rapid disease progression.

Delayed or slow HIV-1 disease progression can be defined by the lack of development of an AIDS defining illness for at least 10 years after infection with a slowly declining CD4+ T cell count. Viral genetic factors associated with slow progression or nonprogression include mutations in the HIV-1 *gag*, *rev*, *vif*, *vpr*, *vpu*, *env* and *nef* genes (Churchill et al., 2004, 2006; Deacon et al., 1995; Kirchhoff et al., 1995; Michael et al., 1997; Shioda et al., 1997; Wang et al., 2000). Host genetic factors linked to a delay in the onset of AIDS and prolonged survival include the CCR5 Δ32 mutation, CCR2b-V64I polymorphism, and certain HLA haplotypes (Dean et al., 1996; Eugen-Olsen et al., 1997; Huang et al., 1996; Smith et al., 1997) (reviewed in O'Brien and Moore, 2000; Roger, 1998). The CCR5 Δ32 mutation, which results in a 32-nucleotide deletion, is common in Caucasians, with heterozygosity in 15 to 20% and homozygosity in 1%. Individuals homozygous for the CCR5 Δ32 allele are highly resistant to HIV-1 transmission (O'Brien and Moore, 2000), whereas heterozygotes are susceptible but typically have delayed CD4+ T cell decline and prolonged survival compared to CCR5 wt/wt individuals (Dean et al., 1996; Eugen-Olsen et al., 1997; Huang et al., 1996; Michael et al., 1997). Among CCR5 Δ32/wt heterozygotes, there is large variation in levels of CCR5 expression (Cohen et al., 1997; de Roda Husman et al., 1999). Slow progression of HIV-1 disease has been correlated with reduced levels of CCR5 expression on CD4+ T lymphocytes and monocytes compared to levels in CCR5 wt/wt individuals (Cohen et al., 1997; de Roda Husman et al., 1999). Nonetheless, there is considerable overlap between CCR5 expression levels in CCR5 Δ32/wt heterozygotes and individuals with the CCR5 wt/wt genotype (de Roda Husman et al., 1999).

In this study, we isolated and characterized HIV-1 from the blood of an asymptomatic individual who was heterozygous for the CCR5 Δ32 allele and had reduced levels of CCR5 cell surface expression. In addition to using CCR5 and CXCR4, the virus has highly expanded utilization of alternative coreceptors that is broader than that of any previously described HIV-1 virus. Mutagenesis studies and structural models suggested Y308 and D321 in the V3 region of gp120, and to a lesser extent K442 and E444 in the C4 region, contribute to the broad coreceptor usage of Envs cloned from the viral isolate. Furthermore, studies using mutant CCR5 coreceptors indicated that Y308, D321, Y330, K442, and E444 alter dependence on the N-terminal and extracellular loop 2 (ECL2) regions of CCR5. The results suggest that expanded coreceptor usage of HIV-1 can occur in some individuals without rapid progression to AIDS as a consequence of changes in the V3 region that enhance interactions with conserved structural elements in G-protein-coupled receptors (GPCRs).

Results

Clinical history and isolation of HIV-1

The subject is a homosexual male who was infected with HIV-1 via sexual contact and first tested seropositive for HIV-1 in May 1989. As of 2006, the subject remained asymptomatic with no AIDS defining illness. His antiretroviral therapy (ART), plasma HIV-1 RNA levels, and CD4 counts are summarized in Supplementary Table 3. The subject was seropositive for cytomegalovirus, hepatitis A, hepatitis C, and *Toxoplasma gondii*. Genetic analysis of CCR5 alleles by PCR demonstrated heterozygosity for the CCR5 Δ32 deletion (data not shown). Two-color FACS staining of peripheral blood mononuclear cells (PBMC) collected in October 2003 demonstrated that the mean percentage of CCR5+ cells in the CD4+ T lymphocyte fraction was 0.9% ($n=2$, SD=0.08) as compared with 19.3% in healthy HIV-1-negative control subjects ($n=7$, SD=10.15). HIV-1 was isolated from PBMC collected in August 2000 by coculture with CD8-depleted donor PBMC as described (Gorry et al., 2001). Attempts to isolate HIV-1 from cryopreserved PBMC collected in October 1998 and March 1999 were unsuccessful.

Coreceptor usage

The ability of the primary virus isolate to utilize CCR5, CXCR4, or alternative coreceptors for virus entry was first determined in canine Cf2-Luc cells (Gorry et al., 2001) (Fig. 1A). The X4 NL4-3, R5 ADA, and R5X4 89.6 HIV-1 viruses were used as positive controls (Gorry et al., 2001, 2002b). The primary virus used both CCR5 and CXCR4 for virus entry. Efficient usage of CCR2b, CCR3, CCR8, Gpr1, Gpr15, Strl33 and Apj was also demonstrated. Compared to 89.6, usage of CCR2b, Gpr1, and Apj by the primary virus was approximately 5-, 20- and 2-fold greater, respectively. Compared to ADA, usage of CCR8, Gpr15 and Strl33 by the primary virus was approximately 5-, 6- and 2-fold greater. The virus could also enter canine Cf2-Luc cells transfected with CD4 alone, albeit at low levels. Coreceptor usage in human U87 astrocytoma cells was similar to that in Cf2-Luc cells with the exception that virus entry was not detected in U87 cells transfected with CD4 alone (data not shown), suggesting that entry in Cf2-Luc cells expressing CD4 alone was mediated by an endogenous canine coreceptor. The promiscuous pattern of coreceptor usage resembles that of some SIV and HIV-2 virus strains (Edinger et al., 1998; Morner et al., 1999; Reeves et al., 1997, 1999; Rucker et al., 1997), which can infect certain cell types lacking CD4. However, virus entry mediated by CCR3, CCR5, CXCR4, or the endogenous coreceptor expressed on Cf2-Luc

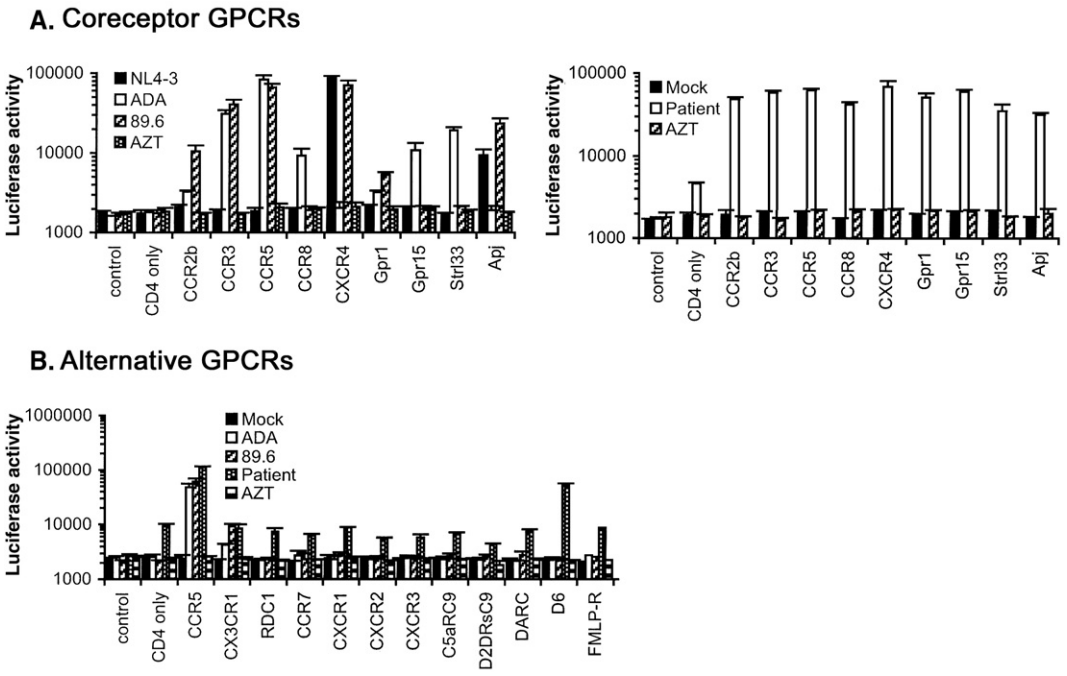

Fig. 1. Coreceptor usage. (A) Cf2-Luc cells were transfected with pcDNA3-CD4 alone or cotransfected with pcDNA3-CD4 and pcDNA3 expressing CCR2b, CCR3, CCR5, CCR8, CXCR4, Gpr1, Gpr15, Strl33 or Apj and infected with equivalent amounts of each control HIV-1 virus (left panel) or patient-derived virus (right panel). Control cells were transfected with pcDNA3 plasmid only. Mock-infected cells were treated with culture medium. Cell lysates were prepared at 48 h post-infection and assayed for luciferase activity. (B) Cf2-Luc cells transfected with pcDNA3-CD4 alone or cotransfected with pcDNA3-CD4 and plasmids expressing CCR5, CX3CR1, RDC1, CCR7, CXCR1, CXCR2, CXCR3, C5aRC9, D2DRsC9, DARC, D6 or FMLP-R were infected with equivalent amounts of each HIV-1 virus. HIV-1 entry was measured as above. Data are represented as means from duplicate infections. Error bars represent standard deviations. Similar results were obtained in two independent experiments.

cells was strictly CD4-dependent (data not shown). We next tested whether the primary virus could utilize other GPCRs as coreceptors. Virus entry was detected in Cf2-Luc cells coexpressing CD4 and the promiscuous CC-chemokine receptor D6 (Nibbs et al., 1997), but not in cells coexpressing CD4 and CX3CR1, Rdc1, CCR7, CXCR1, CXCR2, CXCR3, complement 5a anaphylatoxin receptor (C5aRC9), dopamine receptor 2-short form (D2DrsC9), duffy antigen/receptor for chemokines (DARC), or formyl-methionine–leucine–phenylalanine receptor (FMLP-R) (Fig. 1B). Cell surface expression of these GPCRs was readily detected (M. Farzan and H. Choe, unpublished observations). Preincubation with zidovudine (AZT) abolished infection (data not shown). The broad and efficient usage of alternative coreceptors by the patient virus was unique by comparison to over 50 other primary HIV-1 viruses analyzed in similar assays (Gorry et al., 2001, 2002b; Gray et al., 2005; Lawson et al., 2004; Solomon et al., 2005 and data not shown). Thus, the patient virus demonstrates unusually broad and efficient usage of alternative coreceptors compared to other HIV-1 strains.

Replication kinetics

We examined the capacity of the primary virus to replicate in PBMC, CEMx174 cells, and monocyte-derived macrophages (MDM) (Fig. 2A). The ADA and NL4-3 viruses were used as positive controls for replication in PBMC; NL4-3 was used as a positive control for replication in CEMx174 cells; ADA, the R5 YU2 strain, and the X4 NDK strain (Ancuta et al., 2001; Gorry et al., 2001) were used as positive controls for replication in MDM. In PBMC, the primary virus replicated to low levels compared to NL4-3 and ADA, reaching peak levels of replication at day 10 post-infection compared to days 4 and 7 for NL4-3 and ADA, respectively. In CEMx174 cells, the primary virus reached peak levels of virus replication at day 24 post-infection compared to day 7 for NL4-3. In MDM, the primary virus replicated at low levels compared to ADA, YU2 and NDK. These results, together with experiments showing that the same primary virus stock had similar infectivity on Cf2-Luc cells coexpressing CD4 and CCR5 or CXCR4 compared to the control viruses (Fig. 1), suggest that the primary virus has reduced replication capacity in PBMC, CEMx174, and MDM compared to several laboratory and primary HIV-1 strains.

Sensitivity to CCR5 and CXCR4 inhibitors

The efficient usage of alternative coreceptors in transfected cells raised the possibility that infection of primary CD4+ cells by the primary virus might be mediated by alternative coreceptors. Therefore, sensitivity to small molecule inhibitors of CCR5 or CXCR4 (TAK-779 and AMD3100, respectively) was tested in PBMC and MDM. We first determined sensitivity to AMD3100 and TAK-779 in PBMC at a range of concentrations previously shown to be effective at inhibiting infection by other primary HIV-1 viruses (Gorry et al., 2002a). AMD3100 or AMD3100 and TAK-779 in combination abolished infection of

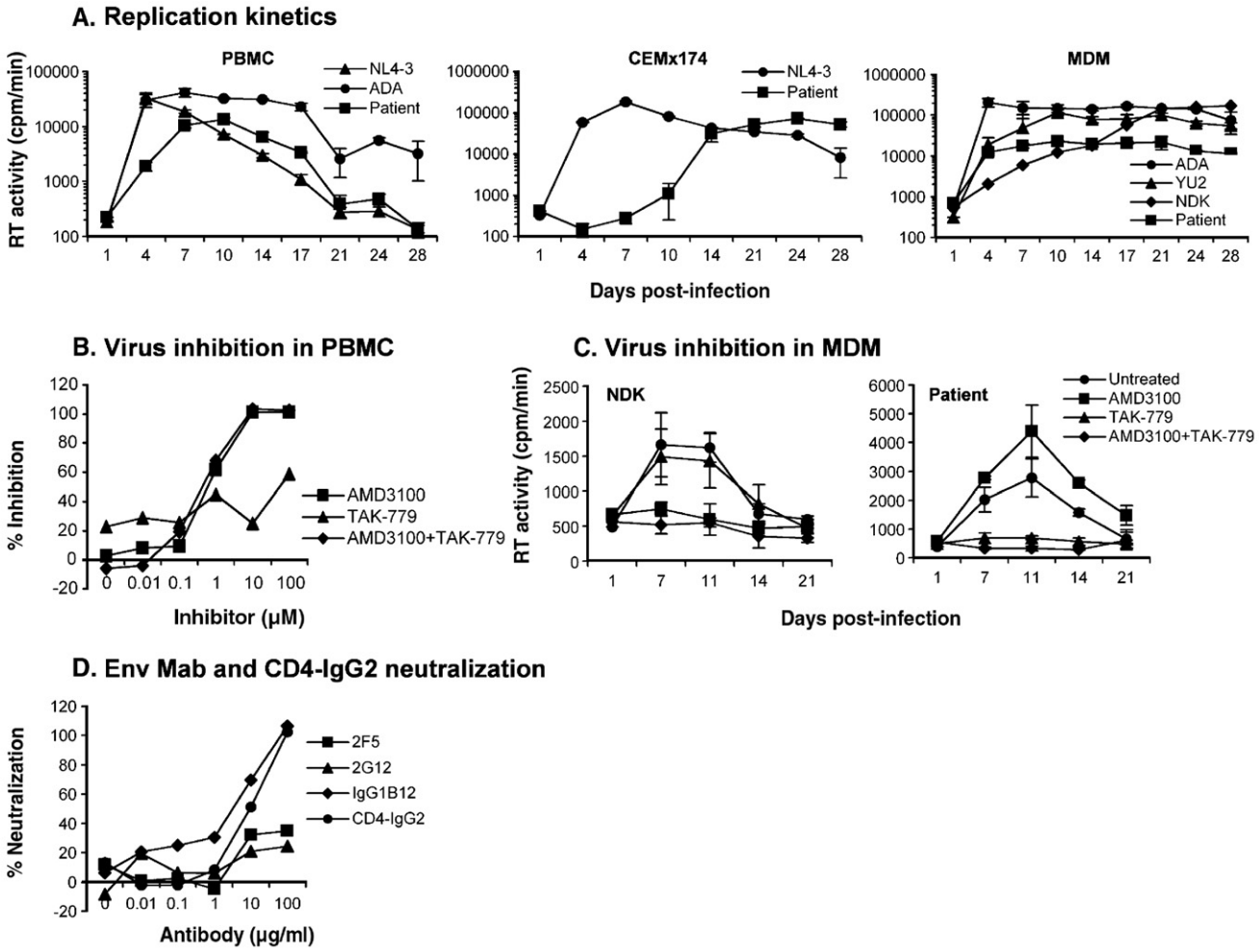

Fig. 2. Replication kinetics and sensitivity to coreceptor inhibitors and antibody neutralization. (A) PBMC, CEMx174 cells and MDM were infected with equivalent amounts of each HIV-1 virus, as described in Materials and methods, and cultured for 28 days. Virus production in culture supernatants was measured by RT assays. (B) PBMC were treated with concentrations of CCR5 (TAK-779) or CXCR4 inhibitors (AMD3100), or both inhibitors increasing 10-fold from 0.01 to 100 μM, and infected with the patient virus in the presence of each concentration of inhibitor. Virus production in culture supernatants at day 14 post-infection was measured by quantitation of soluble HIV-1 p24 Ag. Production of p24 Ag was calculated as a percentage of the amount produced in the absence of inhibitors, and then expressed as the percentage of inhibition relative to cultures containing no inhibitor. (C) MDM were treated with TAK-779 (100 nM), AMD3100 (1.2 μM) or both for 1 h prior to infection. Untreated cells contained no inhibitor. Cells were infected with equivalent amounts of HIV-1 NDK or the patient isolate and cultured for 21 days in the presence of each inhibitor. HIV-1 production in culture supernatants was measured by RT assays. (D) Virus stocks were treated with concentrations of MAbs or CD4-IgG2 increasing 10-fold from 0.01 to 100 μM for 30 min, and used to infect PBMC. Virus production in culture supernatants and calculation of percent neutralization was determined as per panel (B). Values shown are means from duplicate infections. Error bars represent standard deviations (A, C). Results are representative of two independent experiments using cells obtained from different donors.

PBMC at day 14 post-infection, whereas treatment with TAK-779 alone had only a modest inhibitory effect (Fig. 2B). Similar results were obtained at days 7 and 10 post-infection (data not shown). The 50% inhibitory concentration (IC_{50}) and IC_{90} of AMD3100 at day 14 post-infection was 0.65 μM and 5.5 μM, respectively, whereas the IC_{50} and IC_{90} of TAK-779 at day 14 was 58 μM and >100 μM, respectively. PBMC from a donor homozygous for the CCR5 Δ32 allele supported replication of the primary virus, which was completely abolished by AMD3100 (data not shown). These results demonstrate that the virus primarily uses CXCR4 for infection of PBMC. We then determined sensitivity to AMD3100 and TAK-779 in MDM at concentrations previously shown to completely inhibit infection of MDM or microglia (Gorry et al., 2001; Simmons et al., 1998) (Fig. 2C). AMD3100 abolished infection of MDM by NDK, but had no inhibitory effect on the primary virus. TAK-779 abolished infection of MDM by the primary virus, but had no inhibitory effect on NDK. AMD3100 and TAK-779 in combination abolished infection of MDM by either virus. These results demonstrate exclusive use of CCR5 for infection of MDM. Thus, despite broad coreceptor utilization in transfected cells, infection of PBMC and MDM was mediated only by CXCR4 and CCR5, respectively.

We previously showed that primary human adult astrocytes transduced with CD4 via an adenovirus vector and primary brain microvascular endothelial cells (BMVECs) that express low levels of CD4 can support infection by a subset of HIV-1, HIV-2 and SIV isolates in a CCR5- and CXCR4-independent manner (Willey et al., 2003). To further investigate whether the primary virus can use alternative coreceptors for virus entry in

primary human cells, we infected these cells with the primary virus, as previously described (Willey et al., 2003). No evidence of infection of CD4-expressing astrocytes or BMVECs by the primary virus was observed, whereas both cell types supported productive virus replication by the R5X4 HIV-1 viruses GUN-1v and HAN-2, the HIV-2 strain TER, and the SIV strain 17Efr (data not shown). These studies provide further evidence that infection of primary cells by the virus is unlikely to be mediated by alternative coreceptors.

Sensitivity to antibody neutralization

We next measured the sensitivity of the primary virus to neutralization by Env monoclonal antibodies (MAbs) and CD4-IgG2, as previously described (Trkola et al., 1995) (Fig. 2D). The neutralizing reagents were human MAbs 2F5 (Muster et al., 1994; Trkola et al., 1995), 2G12 (Trkola et al., 1995, 1996), IgG1b12 (Burton et al., 1991, 1994), and the tetrameric CD4-IgG2 molecule (Allaway et al., 1995). The virus was moderately sensitive to neutralization by IgG1b12 and CD4-IgG2, but showed a high level of resistance to neutralization by 2F5 and 2G12, similar to that of 2 other primary viruses studied in parallel (Fig. 2D and data not shown). Thus, the primary virus is relatively resistant to neutralization by Env MAbs and CD4-IgG2, similar to the majority of primary HIV-1 viruses.

Neutralization of heterologous viruses by the subject's plasma

We determined the ability of the subject's plasma (obtained in September 2001; see Supplementary Table 3) to inhibit infection of PBMC by 6 clade B and 2 clade A HIV-1 viruses as compared with HIVIG and MAbs IgG1b12, 2F5, and 2G12, as previously described (Mascola et al., 2002). The IC_{50}s and IC_{90}s are summarized in Table 1. The subject's plasma and HIVIG neutralized infection by 6 diverse clade B and 1 of 2 clade A HIV-1 viruses at plasma dilutions increasing 5-fold from 1:5 to 1:625, or HIVIG concentrations increasing 10-fold from 10 μg/ml to 10 mg/ml (Mascola et al., 2002). In contrast, the MAbs IgG1b12, 2F5 and 2G12, at concentrations increasing from 0.05 μg/ml to 50 μg/ml, neutralized infection by a subset of the viruses tested. Compared to plasma and sera from other HIV-1-infected individuals, the potency and breadth of the cross-neutralizing activity of the patient's plasma were in the top 10% of HIV-1-positive plasma/sera (J. Mascola, unpublished data). Together, these studies suggest that the subject's plasma has high levels of cross-neutralizing antibodies.

Characterization of full-length gp160 Env clones

The gp160 coding region of HIV-1 Env was cloned into the pCR3.1-Uni expression vector. Full-length, functional Env clones were identified by Western blot analysis of gp120/gp160 in transfected 293T cells and by fusion assays. Four Env clones that express distinct gp160 and gp120 proteins detected by Western blot analysis of transfected 293T cells (Fig. 4A) were sequenced (Fig. 3). Env gp160 amino acid sequences were uninterrupted in Env clones 6, 16 and 30, but contained a premature truncation of 4 amino acids in the gp41 cytoplasmic region in clone 12. The net charge of the V3 variable loops was +5 in all 4 Env clones. The Env clones contained an asparagine-rich insertion of 10 amino acids at positions 131 to 140 in the V1 variable region, which is unique among 207 clade B Envs screened in the Los Alamos database. Two similar asparagine-rich insertions of 11 and 6 amino acids were identified at positions 192 to 202 and 208 to 213, respectively, in the V2 variable region. These insertions result in a net gain of one potential N-linked glycosylation site in V1, and 3 potential N-linked glycosylation sites in V2. The total number of potential N-linked glycosylation sites in gp120 was 20 to 21 compared to 25 in the clade B consensus sequence.

To determine whether the Env clones are representative of the predominant HIV-1 variants in the viral quasispecies, fusion and single round entry assays were performed (Figs. 4B, C). 293T cells expressing each Env (Fig. 4A) were fused with Cf2-Luc cells cotransfected with CD4 and a coreceptor as described (Gorry et al., 2002a) (Fig. 4B). 293T cells expressing a non-functional Env or expressing the ADA, HXB2 or 89.6 Env were used as negative and positive controls, respectively. The

Table 1
Virus neutralization studies

Plasma or Ab		Clade B HIV-1						Clade A HIV-1	
		SF162	BaL	89.6	dBR07	aBL01	6101	UG031	RW020
Patient[a]	IC_{50}	255	220	261	553	90	105	187	32
	IC_{90}	42	31	64	256	18	27	10	7
b12[b]	IC_{50}	0.4	1.1	0.3	0.6	12	>50	>50	>50
	IC_{90}	2.7	12	5.5	22	>50	>50	>50	>50
2F5	IC_{50}	2.9	1.1	0.1	1.1	3.1	50	9	0.3
	IC_{90}	>50	>50	2	>50	>50	>50	>50	4
2G12	IC_{50}	17	0.1	>50	>50	>50	29	>50	0.6
	IC_{90}	>50	10	>50	>50	>50	>50	>50	5
HIVIG	IC_{50}	40	320	13	140	685	850	5420	2004
	IC_{90}	680	6590	430	2610	>10000	8700	>10000	6050

[a] IC_{50} and IC_{90} values of patient plasma neutralization are expressed as the reciprocal of plasma dilution required to inhibit 50 or 90%, respectively, of viral infection of CD8-depleted PBMC. The patient plasma was obtained in September, 2001 (see Supplementary Table 3).

[b] IC_{50} and IC_{90} values of Env MAbs and HIVIG are expressed as the concentration (μg/ml) required to inhibit 50 or 90%, respectively, of viral infection of CD8-depleted PBMC.

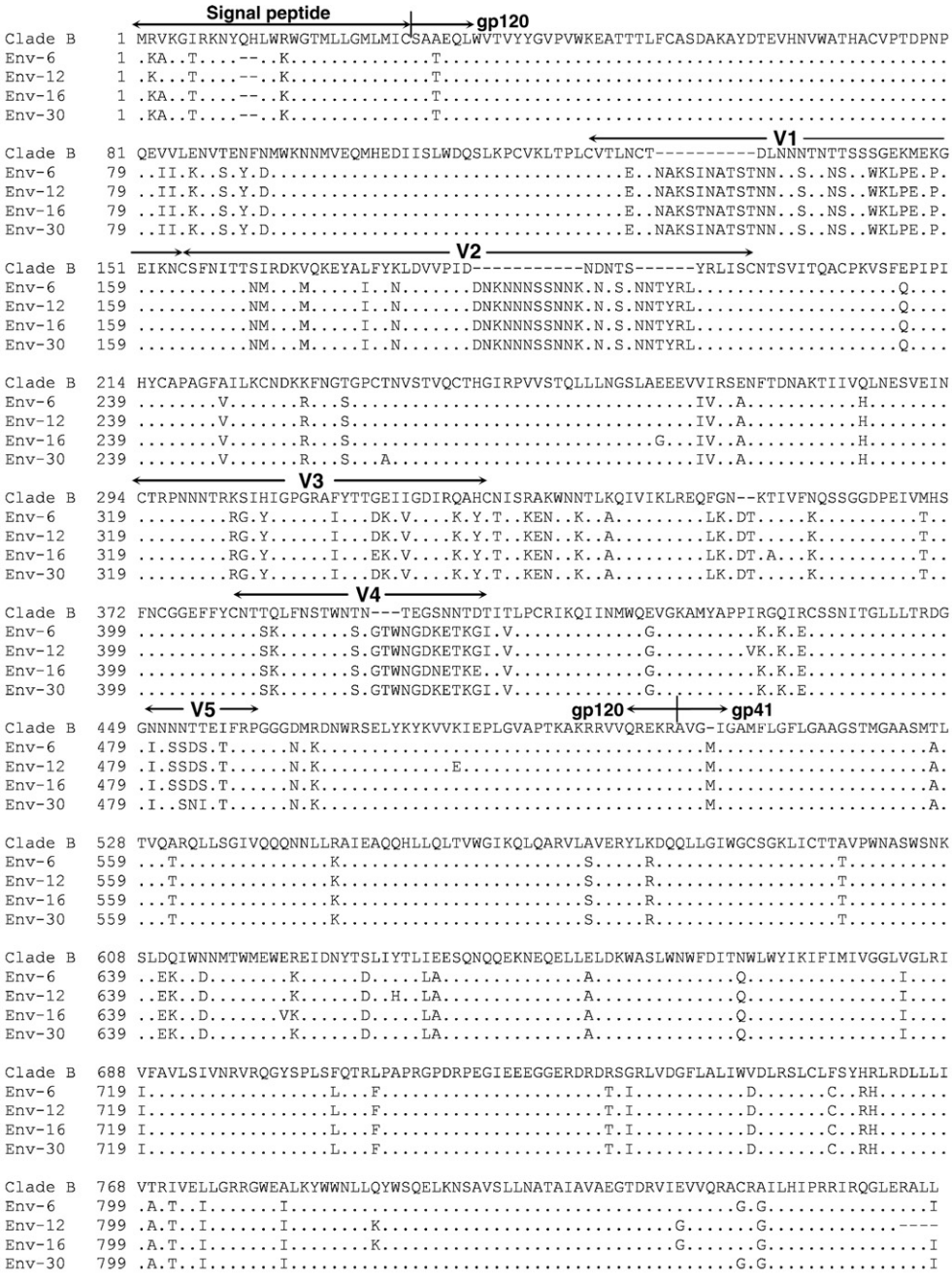

Fig. 3. Env amino acid sequences. Amino acid sequences were obtained from gp160 *env* genes cloned from genomic DNA of PBMC infected with the primary virus as described in Materials and methods. Amino acid alignments of Envs from the patient virus are compared to the clade B consensus sequence. Dots indicate residues identical to the clade B consensus and dashes indicate gaps.

primary Env clones functioned in fusion assays with Cf2-Luc cells coexpressing CD4 and CCR2b, CCR3, CCR5, CCR8, CXCR4, Gpr1, Gpr15, Strl33, Apj or D6. A low level of fusion was also observed with Cf2-Luc cells expressing CD4 only. We performed single round entry assays in Cf2th cells expressing CD4 only or coexpressing CD4 and each of the coreceptors (Fig. 4C). HIV-1 pseudotyped with Env clones 6 and 30 entered cells expressing CD4 alone, or coexpressing CD4 and CCR2b, CCR3, CCR5, CCR8, CXCR4, Gpr1, Gpr15, Strl33, Apj or D6. In contrast, HIV-1 pseudotyped with Env clones 12 and 16 entered cells coexpressing CD4 and CCR2b, CCR3, CCR5, CXCR4, Gpr15, Strl33 or Apj, but not cells expressing CD4 alone or coexpressing CD4 and CCR8, Gpr1 or D6. The levels of virus entry mediated by Env clones 12 and 16 were lower than those mediated by Env clones 6 and 30. Together, these results demonstrate broad coreceptor usage by 4 Env clones in fusion and single round entry assays, similar to the pattern of coreceptor usage of the primary virus isolate (Fig. 1).

Analysis of Env determinants contributing to broad coreceptor usage

To investigate mechanisms underlying the broad coreceptor usage of these primary Envs, we analyzed sequences of the V3

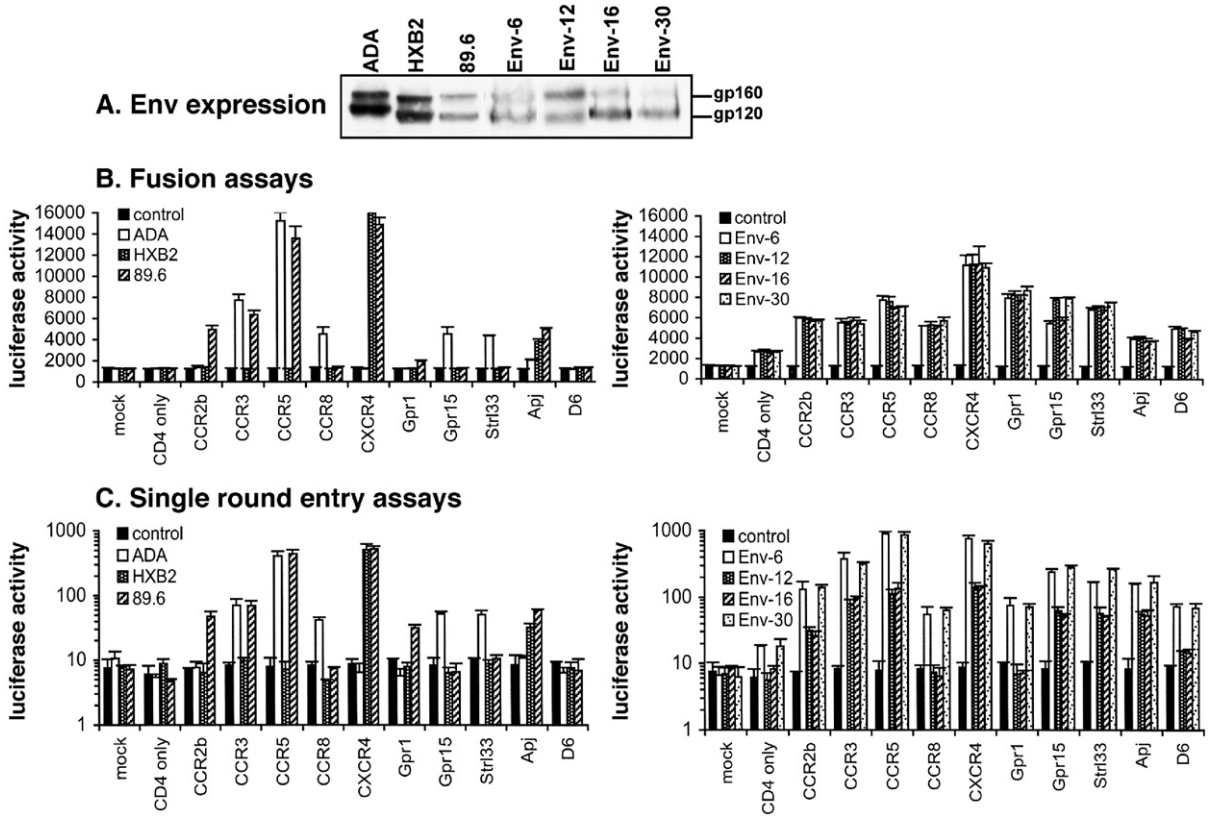

Fig. 4. Expression and function of full-length Env clones in cell–cell fusion and infection assays. (A) 293T cells were cotransfected with 15 μg pCR3.1 Env-expressing plasmid (Envs 6, 12, 16 and 30) or pSVIII Env-expressing plasmid (ADA, HXB2 and 89.6 Envs) and 2 μg pLTR-Tat. At 72 h post-transfection, cell lysates were analyzed by Western blotting using rabbit anti-gp120. The positions of gp160 and gp120 are indicated on the right. (B) 293T effector cells transfected with Env and Tat as above were mixed with Cf2-Luc cells transfected with pcDNA3-CD4 only or cotransfected with pcDNA3-CD4 and pcDNA3 expressing CCR2b, CCR3, CCR5, CCR8, CXCR4, Gpr1, Gpr15, Strl33, Apj or D6 and incubated at 37 °C for 12 h. Control 293T cells were transfected with ΔKS Env. Mock-transfected Cf2-Luc cells were transfected with pcDNA3 only. Cell lysates were then prepared and assayed for luciferase activity. (C) HIV-1 luciferase reporter viruses pseudotyped with each Env were generated and used to infect Cf2th cells transfected with pcDNA3-CD4 only or cotransfected with pcDNA3-CD4 and pcDNA3 expressing CCR2b, CCR3, CCR5, CCR8, CXCR4, Gpr1, Gpr15, Strl33, Apj or D6. Control virus was produced by pseudotyping with a non-functional Env (ΔKS Env). Cell lysates were prepared at 60 h post-infection and assayed for luciferase activity. Data are represented as means from duplicate wells in one experiment. Error bars represent standard deviations. Results are representative of two independent experiments, each performed in duplicate.

region, which modulates coreceptor usage (reviewed in Hartley et al., 2005), and the conserved coreceptor binding site on the Env core (Rizzuto et al., 1998) to identify amino acid variants that might influence Env–GPCR interactions. In the V3 region, patient Envs had Y308, a rare amino acid variant (1.5% of Clade B Envs, $n=23{,}470$) at a position implicated in modulating resistance to neutralizing antibodies (Zhang et al., 2002) and a small molecule CCR5 inhibitor (Kuhmann et al., 2004); I317, an amino acid that contributed to the ability of JR-CSF to use an N-terminal deletion mutant of CCR5 (Platt et al., 2001); D321 (or E321) and Y330, amino acid changes that affect the overall charge of V3 and thus may alter interactions with the tyrosine-sulfated N-terminal region of GPCRs; and T332, a change that results in the loss of a potential N-linked glycosylation site relative to the Clade B consensus (Fig. 5A). In the conserved coreceptor binding site on the Env core, patient Envs had K442 and E444 in the β22 strand near the base of V3, amino acid variants that could potentially affect electrostatic interactions at the Env–GPCR interface.

To investigate the contribution of these amino acid variants to broad coreceptor usage, we used site-directed mutagenesis to change each of these amino acids to the Clade B consensus residue in patient Env-30. The parental and mutant Envs were expressed at similar levels as determined by Western blotting (Fig. 5B, inset). The ability of Envs to use CCR5, CXCR4, and alternate coreceptors Gpr1, Gpr15, Strl33, and D6 was analyzed in cell-to-cell fusion and single round virus entry assays (Fig. 5B and data not shown). The Y308H mutation resulted in an increased ability to use CCR5, and to a lesser extent CXCR4, but reduced the capacity of Env-30 to use Gpr1, Gpr15, Strl33, and D6 ($p=0.001$, 0.02, 0.02, and 0.04, respectively; Student's t test). Additionally, a D321G mutation in Env-30 resulted in an increased utilization of CCR5, CXCR4, and D6 ($p=0.002$, 0.049, and 0.006, respectively), but decreased utilization of Gpr1 and Gpr15 ($p=0.006$ and 0.048, respectively). In contrast, a I317F mutation drastically reduced the capacity of Env-30 to use all coreceptors tested ($p<0.01$). A K442Q mutation resulted in a significant decrease in utilization of Gpr1 and Strl33 ($p=0.001$ and 0.01, respectively) and a minor decrease in utilization of D6 that did not reach statistical significance, while a E444R change reduced utilization of CXCR4 and Gpr15 ($p<0.01$). A Y330H mutation reduced the ability of Env-30 to

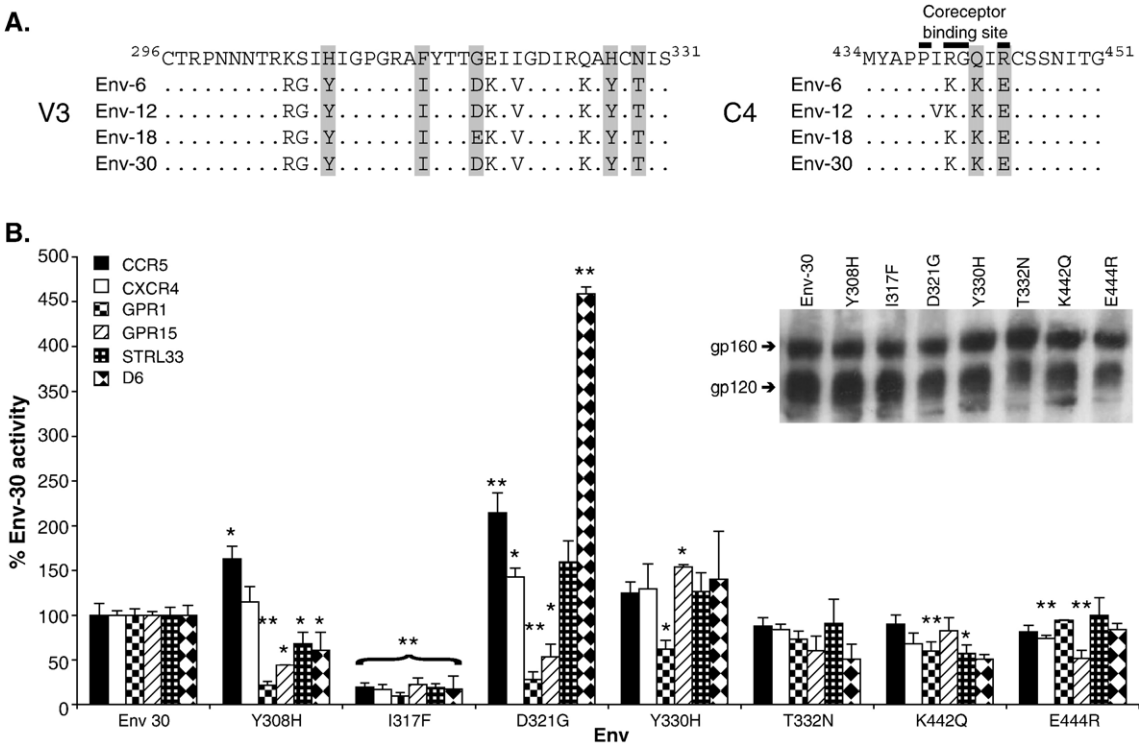

Fig. 5. Analysis of Env determinants contributing to broad coreceptor usage (A) V3 and C4 amino acid sequences of the Clade B consensus and patient Env clones were aligned with Clustal X. Dots represent amino acids identical to the Clade B consensus sequence. Residues important for CCR5 binding (Rizzuto et al., 1998) in the C4 region are indicated. Amino acid variants analyzed in mutagenesis studies are highlighted in gray. (B) HIV-1 luciferase reporter viruses pseudotyped with each Env were generated and used to infect Cf2th cells cotransfected with pcDNA3-CD4 and pcDNA3 expressing CCR5, CXCR4, Gpr1, Gpr15, Strl33, or D6. Control virus was produced by pseudotyping with ΔKS Env. Cell lysates were prepared at 60 h post-infection and assayed for luciferase activity. Data were normalized to parental Env-30 activity and are represented as means from two to three independent experiments, each performed in duplicate. Error bars represent standard error of the mean. *, $p<0.05$; **, $p<0.01$, Student's t test. Inset, 293T cells were cotransfected with 15 μg Env-expressing plasmids and 2 μg pLTR-Tat. At 72 h post-transfection, cell lysates were analyzed by Western blotting using goat anti-gp120. The positions of gp160 and gp120 are indicated on the left.

use Gpr1 ($p=0.04$), but enhanced utilization of Gpr15 ($p=0.01$) and had no significant effect on utilization of Strl33 and D6. A T332N mutation had no significant effect on entry efficiencies and patterns of coreceptor usage compared to the parental Env-30 (Fig. 5B). These results suggest that Y308, D321, and to a lesser extent K442 and E444, contribute to enhanced gp120 interactions with alternate coreceptors, and raise the possibility that I317 may be a compensatory change in patient Env-30.

Molecular modeling of V3 determinants

To elucidate a mechanism for enhanced gp120–coreceptor interactions in Env-30, we used Swiss PDB viewer to model the amino acids at positions 308, 317, and 321 on the JRFL gp120-CD4-X5 CD4i Ab crystal structure (2B4C) (Huang et al., 2005). The Clade B consensus amino acids at positions 308 and 317 in the V3 tip region are His and Phe, respectively (Fig. 6A). If the His at 308 is changed to Tyr, there is an increased potential for steric clashing when the aromatic ring of Phe is present at position 317 (Fig. 6B), whereas the smaller side chain of Ile at this position can accommodate the Tyr at 308 (Fig. 6C). This finding suggests that the loss of Env function in the I317F mutant may be due to the lack of a compensatory change at position 308. Consistent with this prediction, when Y308 is present in Clade B Envs ($n=360$), there is a decreased frequency of amino acids with bulky aromatic side chains such as Phe and Trp, but an increased frequency of amino acids with small hydrophobic chains such as Ile and Val at position 317 compared to Clade B Envs ($n=23{,}470$) (Table 2), suggesting that covariation may occur at positions 308/317 *in vivo*. In Envs with Y308 ($n=360$ Env sequences from 77 patients), I317 appeared in 23.9% ($n=86$ Env sequences from 11 patients) compared to 4.1% ($n=959$) of Clade B Envs in the database ($n=23{,}470$) (Table 2). At position 321, Gly may increase the flexibility of the V3 stem, allowing increased gp120 binding to GPCRs. An Asp at this position may decrease the flexibility of the stem, but may also enhance the ability of Env-30 to interact with some GPCRs that contain positive charges in the N-terminus, such as Gpr1 and Gpr15. In Envs with Y308, there is an increased frequency of charged amino acids at position 321 compared to Clade B Envs, raising the possibility that covariation may also occur at 308/321 (Table 2).

Analysis of Env interactions with attenuated CCR5 coreceptors

GPCRs are 7-transmembrane receptors with an extracellular, post-translationally modified acidic N-terminal region and three

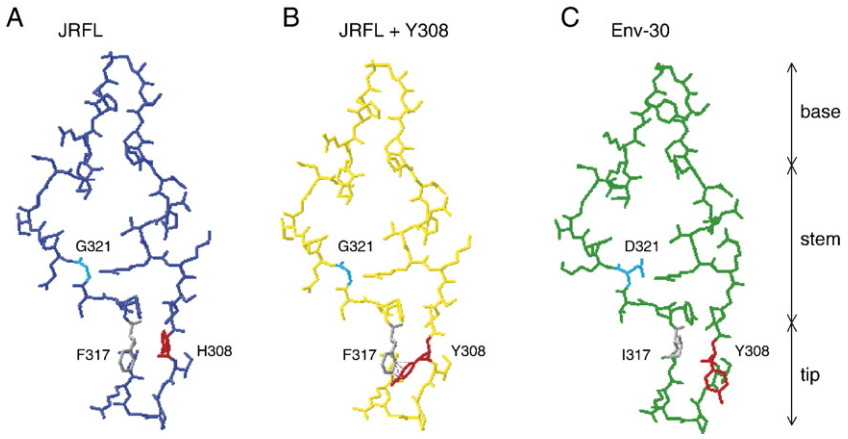

Fig. 6. Structural modeling of Env V3 determinants contributing to broad coreceptor usage. Swiss PDB viewer was used to model amino acid changes at positions 308, 317, and 321 on the V3 region of the JRFL gp120-CD4-X5 CD4i Ab crystal structure (2B4C) (Huang et al., 2005). JRFL V3 has a single amino acid change relative to the clade B consensus (N301Q). Red, position 308. Gray, position 317. Cyan, position 321. (A) V3 region of JRFL with H308, F317, and G321. (B) A Y308 change in JRFL results in steric clashing with F317 (dotted lines). (C) Changes Q301N, K305R, S306G, Y308H, F317I, G321D, E322K, I324V, Q328K, H330Y, and N332T were introduced in JRFL to produce a model of the V3 region of Env-30. Positions Y308, I317, and D321 are indicated.

extracellular loops (ECLs). The N-terminal region and ECL2 contain the major determinants for gp120 binding and coreceptor activity (Dragic et al., 1998; Farzan et al., 1998, 1999; Kuhmann et al., 1997; Lee et al., 1999; Olson et al., 1999; Rabut et al., 1998; Rucker et al., 1996). The N-terminus of CCR5 has Tyr sulfation modifications at several sites that are important for mediating HIV entry (Farzan et al., 1999). To determine whether amino acid variants in Env-30 influence interactions with the N-terminus or ECL2 regions of GPCRs, Cf2 cells expressing CD4 and either wild-type CCR5 (CCR5 (wt)), CCR5 (Y14N) which has a point mutation in the N-terminal region that changes a Tyr sulfation site important for mediating HIV-1 entry to an N-linked glycosylation site (Farzan et al., 1999; Kuhmann et al., 2000), CCR5 (Δ18) which contains a deletion of the first 18 amino acids of the N-terminal region, or CCR5 (G163R) which contains a point mutation in the transmembrane region associated with a conformational change in ECL2 that is detrimental to HIV-1 entry (Platt et al., 2001; Siciliano et al., 1999), were infected with viruses expressing wild-type or mutant Envs. Primary, macrophage tropic R5 viral isolates use CCR5 (Y14N) and CCR5 (G163R) at low efficiencies (1.5% and 10–20% compared to CCR5 (wt), respectively) (Kuhmann et al., 2000; Platt et al., 2001) and are unable to use CCR5 (Δ18) (Platt et al., 2005). In contrast to primary R5 Envs, Env-30 used CCR5 (wt) and CCR5 (G163R) with similar efficiencies (Fig. 7). Y308H and D321G had reduced utilization of CCR5 (G163R) relative to CCR5 (wt) compared to Env-30 (Fig. 7), suggesting that amino acid variants at these positions in patient Env-30 reduce dependence on the ECL2 region of CCR5. The Y308H, Y330H, K442Q, and E444R mutants used CCR5 (Y14N) for entry more efficiently compared to Env-30 (Fig. 7). None of the Envs could use CCR5 (Δ18) efficiently, consistent with the critical role of the N-terminal region of GPCRs in binding and entry (Dragic et al., 1998; Farzan et al., 1998, 1999; Kuhmann et al., 1997; Rabut et al., 1998; Rucker et al., 1996). However, the Y308H, D321G, T332N, and E444R mutations resulted in an increase in the ability of Env-30 to use CCR5 (Δ18), albeit at very low efficiencies. Cell surface expression levels of CD4 and CCR5 on transfected Cf2th cells were similar based on staining with CD4-FITC (RPA-T4) and CCR5-PE (2D7) and FACS analysis (data not shown). Together, these results suggest that Y308 and D321 reduce dependence on the ECL2 region of CCR5, while these residues along with Y330, K442, and E444 increase dependence on the

Table 2
Frequency and co-variation of unusual amino acid variants *in vivo*

Position	Amino Acid	Clade B Envs (n=23470)[a]		Envs with Y308 (n=360)		
		Frequency (%)[b]	n	Frequency (%)	n	Significance[c]
317	F	78.6	18446	23.6	85	**
	W	6.4	1500	0.6	2	**
	L	5.1	1194	5.0	18	
	I	4.1	959	23.9	86[d]	**
	V	2.7	644	45.3	163	**
	Y	1.8	411	0.0	0	**
	Other	1.3	316[e]	1.7	6[f]	
321	G	79.8	18740	36.7	132	**
	E	4.1	970	19.7	71	**
	D	2.8	667	7.5	27	**
	K	2.0	460	26.9	97	**
	R	1.7	389	8.1	29	**
	Other	9.6	2244[g]	1.1	4[h]	

[a] V3 sequence alignment was obtained from the Los Alamos database in October 2005. Sequence data for Envs with Y308 are from 77 patients.
[b] Frequency was calculated as [(n/total number of sequences)×100].
[c] Differences between groups were significant as calculated by Fisher's Exact Test. **, $p<0.005$.
[d] Envs with Y308/I317 are from 11 patients.
[e] Other indicates amino acids M, S, K, R, C, Q, H, P, T, G, A, D, and E (in descending order of frequency), or could not be determined.
[f] Other indicates amino acids M, S, K, E, and P (in descending order of frequency).
[g] Other indicates amino acids T, A, Q, N, S, I, and V (in descending order of frequency), a gap in the alignment, or could not be determined.
[h] Other indicates amino acid Q or could not be determined.

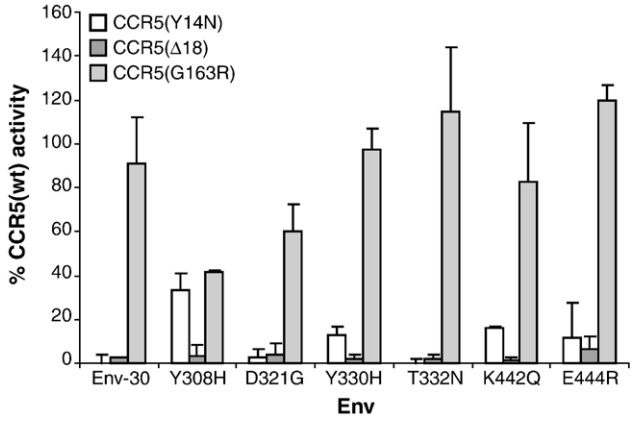

Fig. 7. Env interactions with attenuated CCR5 coreceptors. HIV-1 luciferase reporter viruses pseudotyped with each Env were generated and used to infect Cf2th cells cotransfected with pcDNA3-CD4 and pcDNA3 expressing CCR5 (Y14N), CCR5 (Δ18), or CCR5 (G163R). Control virus was produced by pseudotyping with ΔKS Env. Cell lysates were prepared at 60 h post-infection and assayed for luciferase activity. Results for each mutant CCR5 were normalized to levels of luciferase activity in cells expressing CCR5 (wt) for each Env and are represented as means from two independent experiments, each performed in duplicate. Error bars represent standard deviations.

CCR5 N-terminus compared to clade B consensus residues at these positions.

Discussion

In this study, we isolated and characterized an unusual HIV-1 strain from the blood of an asymptomatic individual who was heterozygous for the CCR5 Δ32 allele and had reduced levels of CCR5 expression. The primary virus is dual-tropic and exhibits unusually broad and efficient utilization of alternative coreceptors. The repertoire of alternative coreceptors used is greater than that of any previously described HIV-1 virus, and more closely resembles that of some SIV and HIV-2 viruses than that of HIV-1 viruses (Morner et al., 1999; Rucker et al., 1997; Siciliano et al., 1999). However, in contrast to some SIV and HIV-2 strains that can infect cells in the absence of CD4 (Reeves et al., 1997, 1999), CCR5- and CXCR4-mediated entry by the primary virus is strictly CD4-dependent. Previous studies suggest that expanded use of alternative coreceptors is associated with rapid HIV-1 disease progression (Bjorndal et al., 1997; Connor et al., 1997). However, the virus we described here was isolated from an individual who was asymptomatic for 18 years and had slow disease progression, suggesting that expanded tropism of HIV-1 can occur in some individuals who do not have rapid disease progression.

Despite efficient usage of many alternative coreceptors in transfected cells, the virus exclusively used CXCR4 or CCR5 to enter primary T cells and monocyte-derived macrophages, respectively. A similar pattern of coreceptor preference for infection of these primary cells was described for the R5X4 89.6 isolate. CD4-expressing astrocytes and BMVECS were not infected by the primary virus, whereas both cell types supported infection by other unusual HIV-1 and HIV-2 strains. Thus, infection of primary cells was mediated only by CXCR4 and CCR5.

In addition to using CCR2b, CCR3, CCR5, CCR8, CXCR4, Gpr1, Gpr15, Strl33 and Apj, the patient virus also utilized the promiscuous CC-chemokine receptor D6 (Nibbs et al., 1997). Only two previous studies demonstrated HIV-1 entry mediated via D6 (Choe et al., 1998; Neil et al., 2005). D6 is expressed on lymphatic endothelial cells, but not on peripheral blood cells or vascular endothelial cells (Nibbs et al., 2001). In addition to entry mediated by D6, entry mediated by an endogenous canine coreceptor was demonstrated, albeit at very low levels. This property was not observed for over 50 other primary HIV-1 isolates tested in similar assays (data not shown). The identity of the endogenous canine coreceptor is unknown. However, entry via this coreceptor was not inhibited by AMD3100, suggesting it most likely is not CXCR4 (data not shown).

CCR5 cell surface expression levels were very low on the study subject's PBMC compared to other CCR5 Δ32 heterozygotes (Cohen et al., 1997; de Roda Husman et al., 1999). Previous studies demonstrated an increased frequency of R5X4 viruses in CCR5 Δ32 heterozygotes compared to CCR5 wt/wt individuals (Lathey et al., 2001; Zhang et al., 1998). We speculate that structural features that enhance interaction of the primary virus Env described herein with conserved structural elements in GPCRs may have resulted from adaptive evolution in the setting of very low levels of CCR5 cell surface expression. However, validation of this hypothesis would require longitudinal analysis of Env sequences in the patient's plasma and their functional characterization. The primary virus did not show enhanced sensitivity to antibody neutralization, but the subject's plasma had potent neutralizing activity against a wide variety of HIV-1 strains. This finding raises the possibility that the Env from the subject's virus may express epitopes that are immunogenic and neutralization functional, and may be responsible for at least some of the cross-reactive neutralizing activity of his plasma. A better understanding of these epitopes and their relationship to expanded coreceptor usage may provide insights relevant for improving HIV-1 immunogenicity and the elicitation of anti-HIV-1 neutralizing antibodies.

The broad usage of alternate coreceptors suggests that the Env of this primary virus has unique structural features that enhance interaction with conserved structural elements in GPCRs. In the V3 region, patient Envs had the unusual amino acid variants Y308 (present in 1.5% of Clade B Envs, $n=23{,}470$), I317 (4.1%), and D321 (2.8%). Y308H and D321G mutations increased the capacity of Env-30 to use CCR5 and to a lesser extent CXCR4, but decreased the utilization of alternate coreceptors, and an I317F mutation drastically decreased the capacity of the Env to use any coreceptor. Structural modeling suggests that a Y308 change in the JRFL crystal structure results in steric clashing with F317 (the clade B consensus residue), whereas the smaller side chain of Ile at this position is accommodated. Thus, I317 is likely to be a compensatory change for Y308. D321 may enhance electrostatic interactions with the positively charged N-terminus of CCR5 and other GPCRs. These observations, together with evidence for covariation of amino acids at positions 308/317 and 308/321 *in vivo* based on database analysis, suggest that Y308, I317, and D321 may act cooperatively to enhance Env–GPCR interactions. Env-30 used

CCR5(G163R), a mutant CCR5 which does not affect entry of SIV_{mac251} but reduces entry of primary macrophage tropic isolates such as ADA and SF162 (Kuhmann et al., 1997), for entry at levels comparable to those mediated by CCR5 (wt). This finding is consistent with the promiscuous coreceptor usage of the patient isolate and Env-30, which resembles that of SIV or HIV-2 (Edinger et al., 1998; Morner et al., 1999; Reeves et al., 1997, 1999; Rucker et al., 1997). In addition to enhancing utilization of alternative coreceptors, Y308 and D321 reduced the dependence of Env-30 on the ECL2 region of CCR5, while introducing the clade B consensus residues H308, H330, K442, and E444 resulted in reduced dependence on the CCR5 N-terminus. These findings are consistent with a proposed model in which the tip of V3 interacts with ECL2 of GPCRs, while the more conserved stem and base of V3 interact with the N-terminal region (Huang et al., 2005; Xiang et al., 2005). K442 and E444 in the C4 region may work in concert with the changes in V3 by facilitating interactions with the highly acidic N-terminal region of CCR5 and other GPCRs. Changes in other regions of Env, such as those in the V1/V2 region that cooperatively modulate coreceptor usage with V3 (Nabatov et al., 2004; Pastore et al., 2006; Sullivan et al., 1993), may further enhance Env–coreceptor interactions. Based on our results, we propose that changes in the V3 region of Env-30 cooperatively enhance interactions with conserved structural elements in GPCRs, while changes in the base of V3 and the C4 region may enhance electrostatic interactions with the N-terminus of GPCRs.

Analysis of patient Env sequences revealed a unique insertion of 10 amino acids in the V1 region, and two asparagine-rich insertions of 11 and 6 amino acids in the V2 region. Similar extensions in the V2 region have been associated with slow HIV-1 progression or nonprogression (Shioda et al., 1997; Wang et al., 2000). The V1 insertion in this subject is unusual compared to other clade B Envs, and the V1/V2 region is longer than that of other Envs in the database. Changes in Env that reposition the V1/V2 loops can increase exposure of the coreceptor binding site (Kolchinsky et al., 2001). These findings raise the possibility that the unusually long V1/V2 region may reposition the V1/V2 loops, resulting in a conformation that enhances interaction of gp120 with conserved elements in GPCRs. Conserved elements in GPCRs important for HIV-1 entry include the tyrosine-rich sulfated regions in the N-terminus, which are important for CCR5-mediated HIV-1 entry (Farzan et al., 1999). GPCRs that mediate entry by the primary virus have many tyrosine residues within the N-terminus that are probably sulfated in close proximity, similar to the pattern of sulfated tyrosine residues in CCR5. Thus, the tyrosine-rich region in the N-terminus is likely to be one of the conserved elements in GPCRs involved in HIV-1 binding and virus entry.

The subject's slow disease progression despite harboring a dual-tropic HIV-1 strain with highly expanded coreceptor usage may reflect additional viral and/or host factors that can influence HIV-1 progression. The primary virus had attenuated replication kinetics in PBMC, CEMx174, and MDM compared to several laboratory strains (Fig. 3A) and other primary viruses (Gorry et al., 2001). However, we did not determine whether the virus studied here was one of the majority sequences present in the patient. Mutations in the *nef* gene can cause viral attenuation and reduced pathogenicity of HIV-1 strains (Deacon et al., 1995; Kirchhoff et al., 1995). However, we found no deletions or other obvious defects in *nef* genes cloned from the primary virus, which were fully functional for CD4 and MHC-I down-regulation (K. Agopian and D. Gabuzda, unpublished data). Further studies are required to determine whether the primary virus contains any mutations in other viral genes that might be associated with slow disease progression, and whether it is a major variant in the patient viral quasispecies in vivo.

In summary, we describe an unusual dual-tropic HIV-1 strain with highly expanded coreceptor usage isolated from an asymptomatic individual who was heterozygous for the CCR5 Δ32 allele and had low CCR5 cell surface expression. In this subject, highly expanded coreceptor usage of HIV-1 occurred without progression to AIDS, suggesting that R5X4 HIV-1 strains with broadened coreceptor usage can be harbored by some individuals without rapid disease progression. Our results suggest that changes in the V3 and C4 regions, possibly a consequence of adaptive evolution in the setting of very low levels of CCR5 expression and viral escape from neutralizing antibodies, act cooperatively to broaden coreceptor usage by enhancing interactions with conserved structural elements in GPCRs. These results lead to a better understanding of HIV Env–GPCR interactions and provide insights that may facilitate development of vaccines and therapeutics that target virus entry.

Materials and methods

Cells

Peripheral blood mononuclear cells were purified from blood of healthy HIV-1-negative donors by Ficoll-Hypaque density gradient centrifugation, stimulated with 2 μg/ml phytohemagglutinin (PHA) for 3 days and cultured in RPMI 1640 medium supplemented with 10% (v/v) fetal bovine serum (FBS) and 20 U/ml interleukin-2 (IL-2; Boehringer Mannheim, Germany). CD8+ T cells were depleted by magnetic separation with anti-CD8-conjugated magnetic beads (Miltenyi Biotech, Auburn, CA). Monocyte-derived macrophages were purified from PBMC by plastic adherence and cultured for 5 days in RPMI 1640 medium supplemented with 10% (v/v) human AB+ serum and 12.5 ng/ml M-CSF. Cf2-Luc cells (Etemad-Moghadam et al., 2000), derived from the Cf2th canine thymocyte cell line (Choe et al., 1996), stably express the luciferase gene under the control of the HIV-1 LTR. Cf2-Luc cells were cultured in DMEM medium supplemented with 10% (v/v) FBS, and 0.7 mg/ml G418. Cf2th cells were cultured in the same medium without G418. CEMx174 cells were cultured in RPMI 1640 medium supplemented with 10% (v/v) FBS.

Isolation of HIV-1

HIV-1 was isolated from patient PBMC by coculture with CD8-depleted donor PBMC as described previously (Gorry et al., 2001). Briefly, 2×10^6 patient cells were added to

5×10^6 CD8-depleted PBMC from a normal uninfected donor, incubated at 37 °C for 1 h, and then cultured in 10 ml growth media containing 20 U/ml IL-2. Fifty percent media changes were performed twice weekly. Five million fresh PHA-activated, CD8-depleted PBMC from a different donor were added at every second media change. Supernatants were tested for reverse transcriptase (RT) activity using [^{3}H]dTTP incorporation. Supernatants testing positive for RT were filtered through 0.45 μm filters and stored at −80 °C.

Coreceptor usage

To determine coreceptor usage by the patient HIV-1 isolate, Cf2-Luc cells were cotransfected with 10 μg of plasmid pcDNA3-CD4 and 20 μg of plasmid pcDNA3 containing CCR2b, CCR3, CCR5, CCR8, CXCR4, CX3CR1, Gpr1, Gpr15, Strl33, Apj, CX3CR1, Rdc1, CCR7, CXCR1, CXCR2, CXCR3, C5aRC9, D2DrsC9, DARC, D6 or FMLP-R using the calcium phosphate method, and infected 48 h later by incubation with 10,000 ^{3}H cpm RT units of HIV-1 in the presence of 2 μg/ml polybrene as described previously (Gorry et al., 2001). Mock-infected cells were treated with culture medium. Cf2-Luc cells mock-transfected or transfected with pcDNA3-CD4 alone were used as negative controls. After overnight infection, virus was removed and the cells were cultured for an additional 48 h prior to lysis in 200 μl cell lysis buffer. Cell lysates were cleared by centrifugation, and assayed for luciferase activity according to the manufacturers' protocol (Promega).

HIV-1 replication kinetics

Five million PHA-activated PBMC were infected by incubation with 50,000 ^{3}H cpm RT units of virus supernatant in a volume of 2 ml for 3 h at 37 °C. Virus was then removed and PBMC were washed 3 times with PBS and cultured in media containing 20 U/ml IL-2 for 28 days. Monocyte-derived macrophages were isolated from PBMC by plastic adherence and allowed to mature for 5 days prior to seeding in 6-well tissue culture plates at approximately 90% confluence. Virus equivalent to 50,000 ^{3}H cpm RT units in a volume of 2 ml was allowed to adsorb to the cell monolayers for 3 h at 37 °C. Virus was then removed and cells were rinsed 3 times with PBS prior to addition of 2 ml culture medium. Five million CEMx174 cells were infected by incubation with 50,000 ^{3}H cpm RT units of virus supernatant in a volume of 2 ml for 3 h at 37 °C. Virus was then removed and cells were washed 3 times with PBS and cultured for 28 days. Fifty percent media changes were performed twice weekly and supernatants were tested for HIV-1 by RT assays.

Virus inhibition studies

The effects of the coreceptor inhibitors TAK-779 (Baba et al., 1999) and AMD-3100 (Donzella et al., 1998; Schols et al., 1997) on virus replication in PBMC were assayed as described elsewhere (Gorry et al., 2002a; Trkola et al., 1998). Briefly, PBMC were incubated for 30 min with a range of concentrations of each inhibitor (0.01 to 100 μM) prior to infection with the patient virus isolate. Virus replication was measured by production of HIV-1 p24 antigen in culture supernatants for 14 days (Trkola et al., 1995). The production of p24 antigen in the presence of an inhibitor was expressed as a percentage of the amount produced in control cultures containing no inhibitor. For virus inhibition studies in MDM, cells were preincubated with 100 nM TAK-779 or 1.2 μM AMD3100 for 1 h prior to infection with HIV-1 isolates containing the same concentration of inhibitor, as described previously (Gorry et al., 2001). Infected cells were cultured for 21 days in the presence of each inhibitor. Fifty percent media changes were performed weekly and supernatants were tested for HIV-1 by RT assays.

Neutralization assays

Human monoclonal antibodies (MAb) against HIV-1 gp120 (IgG1b12 and 2G12) and gp41 (2F5), the tetrameric CD4-immunoglobulin (CD4-IgG2) molecule, and purified polyclonal anti-HIV immunoglobulin (HIVIG) have been described previously (Allaway et al., 1995; Burton et al., 1991, 1994; Mascola et al., 2002; Muster et al., 1994; Trkola et al., 1995, 1996). Neutralization of replication of the patient virus isolate in PBMC was assessed as described previously (Trkola et al., 1995). Briefly, virus was incubated for 30 min with a range of concentrations of each Mab or CD4-Ig2 (0.01 to 100 μg/ml) prior to infection. Virus replication and calculation of percent neutralization were measured as described above. Neutralization of heterologous viruses by the subject's plasma was assessed as described by Mascola et al. (2002).

PCR amplification, HIV-1 Env cloning and sequence analysis

Genomic DNA was extracted from PBMC infected with the patient virus isolate using the DNeasy DNA extraction kit (Qiagen). Full-length *Env* genes were amplified from genomic DNA with RTth XL polymerase and nested primers using hot start AmpliWax PCR Gem 50 (Applied Biosystems), as described previously (Gorry et al., 2002a). Env PCR-product DNA was gel purified and cloned into pCR3.1-Uni (Invitrogen). Functional full-length Env clones were identified by Western blot analysis of gp120/gp160 in transfected 293T cells and by fusion assays. Env clones were sequenced using a model 3100 Genetic Analyzer (Applied Biosystems). Y308H, I317F, D321G, Y330H, T332N, K442Q, and E444R mutant Env plasmids were created by PCR-based mutagenesis and changes were verified by DNA sequencing.

Western blot analysis

For analysis of Env expression, 293T cells were transfected with 15 μg of different pCR3.1 Env clones, or 15 μg pSVIII plasmid expressing ADA, HXB2 or 89.6 Env plus 2 μg pLTR-Tat plasmid. At 72 h after transfection, cells were rinsed twice in PBS and resuspended in 400 μl of ice-cold lysis buffer for 20 min, followed by centrifugation at 15,300×*g* for 10 min to remove cellular debris. Cell lysates were separated in 8.5%

SDS-PAGE gels, and analyzed by Western blotting using rabbit anti-gp120 polyclonal antisera (American Biotechnologies Inc.) or goat anti-gp120 polyclonal antisera (NIH AIDS Research and Reference Reagent program). Env proteins were visualized using horseradish peroxidase-conjugated anti-rabbit or anti-goat immunoglobulin G antibodies and enhanced chemiluminescence (Perkin Elmer).

Fusion assays

293T cells (1×10^5) cotransfected with 15 μg Env-expressing plasmid and 2 μg pLTR-Tat were mixed with Cf2-Luc cells (1×10^6) that had been cotransfected with 10 μg pcDNA3-CD4 and 20 μg pcDNA3 expressing an alternative coreceptor as indicated, then incubated at 37 °C in 0.75 ml culture medium. Mock-transfected Cf2-Luc cells were transfected with pLTR-Tat only. Control 293T cells were cotransfected with pLTR-Tat and a non-functional Env (pSVIII-ΔKS Env). Twelve hours later, cells were harvested and assayed for luciferase activity as described above.

Single round entry assays

An Env complementation assay was used to quantitate HIV-1 entry as described (Choe et al., 1996). Briefly, recombinant HIV-1 luciferase reporter viruses were generated by cotransfection of 293T cells by the calcium phosphate method with 16 μg of pNL4-3env$^-$ Luc, which contains an HIV-1 provirus with a deletion in the *env* gene and a replacement of the *nef* gene with a luciferase gene, and 6 μg of pCR3.1Env or pSVIIIEnv plasmid. Cf2th cells intended for use as target cells were cotransfected with 10 μg pcDNA3-CD4 and 20 μg pcDNA3 expressing an alternative coreceptor as indicated. Plasmids expressing CCR5 (Y14N), CCR5 (Δ18), and CCR5 (G163R) were kindly provided by D. Kabat. Approximately 48 h after transfection, these cells were infected by incubation with 20,000 ^{3}H cpm RT units of recombinant luciferase reporter viruses. Reporter viruses pseudotyped with a non-functional Env (pSVIII-ΔKSenv) were used as negative controls. Sixty hours later, cells were harvested and assayed for luciferase activity.

Nucleotide sequence accession numbers

Nucleotide sequences were submitted to GenBank (accession numbers AY624304 through AY624307).

Acknowledgments

We are indebted to the subject who provided blood samples and details of his clinical history for this study. We thank J. Sodroski, P. Kwong, D. McPhee, N. Saksena, and J. Wang for their helpful discussions, A. Dunne for the preparation of clinical samples, and L. Gray for assistance with figures. We are also grateful to J. Sodroski for providing Cf2th and Cf2-Luc cells, J. Sodroski, R. Doms, S. Peiper and D. Kabat for the coreceptor plasmids, H. Choe for D2DRsC9 and DARC plasmids, D. Montefiore for HIV-1 6101, and the NIH AIDS Research and Reference Reagent program, Division of AIDS, NIAID, NIH, for primary HIV-1 isolates (contributed by H. Gendelman, J. Levy, S. Gartner, and the UNAIDS Network for HIV Isolation and Characterization, DAIDS, NIAID), TAK-779, AMD3100 (DAIDS, NIAID), antibodies used in neutralization assays (contributed by D. Burton, P. Parren, and H. Katinger), and goat anti-sera used in Western blotting.

This work was supported by NIH NS37277 to D.G. and AI41420 to J.P.M. Core facilities were supported by Center for AIDS Research grants and the DFCI/Harvard Center for Cancer Research grant. S.M.C. was supported by the Australian National Center in HIV Virology Research and by an Australian National Health and Medical Research Council (NHMRC) Principal Research Fellowship. P.R.G. was supported in part by NHMRC 251520 and NIH R21 AI054207. P.C. was supported by NIH MH64408 and amfAR 02802-30-RG. A.M. was supported in part by a NSF fellowship. P.R.G. is a recipient of an NHMRC R. Douglas Wright Biomedical Career Development Award. D.G., J.P.M., and P.C. are Elizabeth Glaser Scientists who were supported by the Pediatric AIDS Foundation.

Appendix A. Supplementary data

Supplementary data associated with this article can be found, in the online version, at doi:10.1016/j.virol.2006.11.025.

References

Allaway, G.P., Davis-Bruno, K.L., Beaudry, G.A., Garcia, E.B., Wong, E.L., Ryder, A.M., Hasel, K.W., Gauduin, M.C., Koup, R.A., McDougal, J.S., et al., 1995. Expression and characterization of CD4-IgG2, a novel heterotetramer that neutralizes primary HIV type 1 isolates. AIDS Res. Hum. Retroviruses 11 (5), 533–539.

Ancuta, P., Bakri, Y., Chomont, N., Hocini, H., Gabuzda, D., Haeffner-Cavaillon, N., 2001. Opposite effects of IL-10 on the ability of dendritic cells and macrophages to replicate primary CXCR4-dependent HIV-1 strains. J. Immunol. 166 (6), 4244–4253.

Baba, M., Nishimura, O., Kanzaki, N., Okamoto, M., Sawada, H., Iizawa, Y., Shiraishi, M., Aramaki, Y., Okonogi, K., Ogawa, Y., Meguro, K., Fujino, M., 1999. A small-molecule, nonpeptide CCR5 antagonist with highly potent and selective anti-HIV-1 activity. Proc. Natl. Acad. Sci. U.S.A. 96 (10), 5698–5703.

Berger, E.A., Murphy, P.M., Farber, J.M., 1999. Chemokine receptors as HIV-1 coreceptors: roles in viral entry, tropism, and disease. Annu. Rev. Immunol. 17, 657–700.

Bjorndal, A., Deng, H., Jansson, M., Fiore, J.R., Colognesi, C., Karlsson, A., Albert, J., Scarlatti, G., Littman, D.R., Fenyo, E.M., 1997. Coreceptor usage of primary human immunodeficiency virus type 1 isolates varies according to biological phenotype. J. Virol. 71 (10), 7478–7487.

Burton, D.R., Barbas III, C.F., Persson, M.A., Koenig, S., Chanock, R.M., Lerner, R.A., 1991. A large array of human monoclonal antibodies to type 1 human immunodeficiency virus from combinatorial libraries of asymptomatic seropositive individuals. Proc. Natl. Acad. Sci. U.S.A. 88 (22), 10134–10137.

Burton, D.R., Pyati, J., Koduri, R., Sharp, S.J., Thornton, G.B., Parren, P.W., Sawyer, L.S., Hendry, R.M., Dunlop, N., Nara, P.L., et al., 1994. Efficient neutralization of primary isolates of HIV-1 by a recombinant human monoclonal antibody. Science 266 (5187), 1024–1027.

Choe, H., Farzan, M., Sun, Y., Sullivan, N., Rollins, B., Ponath, P.D., Wu, L., Mackay, C.R., LaRosa, G., Newman, W., Gerard, N., Gerard, C., Sodroski, J., 1996. The beta-chemokine receptors CCR3 and CCR5 facilitate infection by primary HIV-1 isolates. Cell 85 (7), 1135–1148.

Choe, H., Farzan, M., Konkel, M., Martin, K., Sun, Y., Marcon, L., Cayabyab, M., Berman, M., Dorf, M.E., Gerard, N., Gerard, C., Sodroski, J., 1998. The orphan seven-transmembrane receptor Apj supports the entry of primary T-cell-line-tropic and dualtropic human immunodeficiency virus type 1. J. Virol. 72 (7), 6113–6118.

Churchill, M., Sterjovski, J., Gray, L., Cowley, D., Chatfield, C., Learmont, J., Sullivan, J.S., Crowe, S.M., Mills, J., Brew, B.J., Wesselingh, S.L., McPhee, D.A., Gorry, P.R., 2004. Longitudinal analysis of nef/long terminal repeat-deleted HIV-1 in blood and cerebrospinal fluid of a long-term survivor who developed HIV-associated dementia. J. Infect. Dis. 190 (12), 2181–2186.

Churchill, M.J., Rhodes, D.I., Learmont, J.C., Sullivan, J.S., Wesselingh, S.L., Cooke, I.R., Deacon, N.J., Gorry, P.R., 2006. Longitudinal analysis of human immunodeficiency virus type 1 nef/long terminal repeat sequences in a cohort of long-term survivors infected from a single source. J. Virol. 80 (2), 1047–1052.

Cilliers, T., Willey, S., Sullivan, W.M., Patience, T., Pugach, P., Coetzer, M., Papathanasopoulos, M., Moore, J.P., Trkola, A., Clapham, P., Morris, L., 2005. Use of alternate coreceptors on primary cells by two HIV-1 isolates. Virology 339, 136–144.

Cohen, O.J., Vaccarezza, M., Lam, G.K., Baird, B.F., Wildt, K., Murphy, P.M., Zimmerman, P.A., Nutman, T.B., Fox, C.H., Hoover, S., Adelsberger, J., Baseler, M., Arthos, J., Davey Jr., R.T., Dewar, R.L., Metcalf, J., Schwartzentruber, D.J., Orenstein, J.M., Buchbinder, S., Saah, A.J., Detels, R., Phair, J., Rinaldo, C., Margolick, J.B., Pantaleo, G., Fauci, A.S., 1997. Heterozygosity for a defective gene for CC chemokine receptor 5 is not the sole determinant for the immunologic and virologic phenotype of HIV-infected long-term nonprogressors. J. Clin. Invest. 100 (6), 1581–1589.

Connor, R.I., Sheridan, K.E., Ceradini, D., Choe, S., Landau, N.R., 1997. Change in coreceptor use coreceptor use correlates with disease progression in HIV-1-infected individuals. J. Exp. Med. 185 (4), 621–628.

Deacon, N.J., Tsykin, A., Solomon, A., Smith, K., Ludford-Menting, M., Hooker, D.J., McPhee, D.A., Greenway, A.L., Ellett, A., Chatfield, C., et al., 1995. Genomic structure of an attenuated quasi species of HIV-1 from a blood transfusion donor and recipients. Science 270 (5238), 988–991.

Dean, M., Carrington, M., Winkler, C., Huttley, G.A., Smith, M.W., Allikmets, R., Goedert, J.J., Buchbinder, S.P., Vittinghoff, E., Gomperts, E., Donfield, S., Vlahov, D., Kaslow, R., Saah, A., Rinaldo, C., Detels, R., O'Brien, S.J., 1996. Genetic restriction of HIV-1 infection and progression to AIDS by a deletion allele of the *CKR5* structural gene. Hemophilia Growth and Development Study, Multicenter AIDS Cohort Study, Multicenter Hemophilia Cohort Study, San Francisco City Cohort, ALIVE Study. Science 273 (5283), 1856–1862.

de Roda Husman, A.M., van Rij, R.P., Blaak, H., Broersen, S., Schuitemaker, H., 1999. Adaptation to promiscuous usage of chemokine receptors is not a prerequisite for human immunodeficiency virus type 1 disease progression. J. Infect. Dis. 180 (4), 1106–1115.

Doms, R.W., Trono, D., 2000. The plasma membrane as a combat zone in the HIV battlefield. Genes Dev. 14 (21), 2677–2688.

Donzella, G.A., Schols, D., Lin, S.W., Este, J.A., Nagashima, K.A., Maddon, P.J., Allaway, G.P., Sakmar, T.P., Henson, G., De Clercq, E., Moore, J.P., 1998. AMD3100, a small molecule inhibitor of HIV-1 entry via the CXCR4 co-receptor. Nat. Med. 4 (1), 72–77.

Dragic, T., Trkola, A., Lin, S.W., Nagashima, K.A., Kajumo, F., Zhao, L., Olson, W.C., Wu, L., Mackay, C.R., Allaway, G.P., Sakmar, T.P., Moore, J.P., Maddon, P.J., 1998. Amino-terminal substitutions in the CCR5 coreceptor impair gp120 binding and human immunodeficiency virus type 1 entry. J. Virol. 72 (1), 279–285.

Edinger, A.L., Hoffman, T.L., Sharron, M., Lee, B., Yi, Y., Choe, W., Kolson, D.L., Mitrovic, B., Zhou, Y., Faulds, D., Collman, R.G., Hesselgesser, J., Horuk, R., Doms, R.W., 1998. An orphan seven-transmembrane domain receptor expressed widely in the brain functions as a coreceptor for human immunodeficiency virus type 1 and simian immunodeficiency virus. J. Virol. 72 (10), 7934–7940.

Etemad-Moghadam, B., Sun, Y., Nicholson, E.K., Fernandes, M., Liou, K., Gomila, R., Lee, J., Sodroski, J., 2000. Envelope glycoprotein determinants of increased fusogenicity in a pathogenic simian-human immunodeficiency virus (SHIV-KB9) passaged in vivo. J. Virol. 74 (9), 4433–4440.

Eugen-Olsen, J., Iversen, A.K., Garred, P., Koppelhus, U., Pedersen, C., Benfield, T.L., Sorensen, A.M., Katzenstein, T., Dickmeiss, E., Gerstoft, J., Skinhoj, P., Svejgaard, A., Nielsen, J.O., Hofmann, B., 1997. Heterozygosity for a deletion in the *CKR-5* gene leads to prolonged AIDS-free survival and slower CD4 T-cell decline in a cohort of HIV-seropositive individuals. Aids 11 (3), 305–310.

Farzan, M., Choe, H., Vaca, L., Martin, K., Sun, Y., Desjardins, E., Ruffing, N., Wu, L., Wyatt, R., Gerard, N., Gerard, C., Sodroski, J., 1998. A tyrosine-rich region in the N terminus of CCR5 is important for human immunodeficiency virus type 1 entry and mediates an association between gp120 and CCR5. J. Virol. 72 (2), 1160–1164.

Farzan, M., Mirzabekov, T., Kolchinsky, P., Wyatt, R., Cayabyab, M., Gerard, N.P., Gerard, C., Sodroski, J., Choe, H., 1999. Tyrosine sulfation of the amino terminus of CCR5 facilitates HIV-1 entry. Cell 96 (5), 667–676.

Gorry, P.R., Bristol, G., Zack, J.A., Ritola, K., Swanstrom, R., Birch, C.J., Bell, J.E., Bannert, N., Crawford, K., Wang, H., Schols, D., De Clercq, E., Kunstman, K., Wolinsky, S.M., Gabuzda, D., 2001. Macrophage tropism of human immunodeficiency virus type 1 isolates from brain and lymphoid tissues predicts neurotropism independent of coreceptor specificity. J. Virol. 75 (21), 10073–10089.

Gorry, P.R., Taylor, J., Holm, G.H., Mehle, A., Morgan, T., Cayabyab, M., Farzan, M., Wang, H., Bell, J.E., Kunstman, K., Moore, J.P., Wolinsky, S.M., Gabuzda, D., 2002a. Increased CCR5 affinity and reduced CCR5/CD4 dependence of a neurovirulent primary human immunodeficiency virus type 1 isolate. J. Virol. 76 (12), 6277–6292.

Gorry, P.R., Zhang, C., Wu, S., Kunstman, K., Trachtenberg, E., Phair, J., Wolinsky, S., Gabuzda, D., 2002b. Persistence of dual-tropic HIV-1 in an individual homozygous for the CCR5 Delta 32 allele. Lancet 359 (9320), 1832–1834.

Gray, L., Sterjovski, J., Churchill, M., Ellery, P., Nasr, N., Lewin, S.R., Crowe, S.M., Wesselingh, S., Cunningham, A.L., Gorry, P.R., 2005. Uncoupling coreceptor usage of human immunodeficiency virus type 1 (HIV-1) from macrophage tropism reveals biological properties of CCR5-restricted HIV-1 isolates from patients with acquired immunodeficiency syndrome. Virology 337, 384–398.

Hartley, O., Klasse, P.J., Sattentau, Q.J., Moore, J.P., 2005. V3: HIV's switch-hitter. AIDS Res. Hum. Retroviruses 21 (2), 171–189.

Huang, Y., Paxton, W.A., Wolinsky, S.M., Neumann, A.U., Zhang, L., He, T., Kang, S., Ceradini, D., Jin, Z., Yazdanbakhsh, K., Kunstman, K., Erickson, D., Dragon, E., Landau, N.R., Phair, J., Ho, D.D., Koup, R.A., 1996. The role of a mutant CCR5 allele in HIV-1 transmission and disease progression. Nat. Med. 2 (11), 1240–1243.

Huang, C.C., Tang, M., Zhang, M.Y., Majeed, S., Montabana, E., Stanfield, R.L., Dimitrov, D.S., Korber, B., Sodroski, J., Wilson, I.A., Wyatt, R., Kwong, P.D., 2005. Structure of a V3-containing HIV-1 gp120 core. Science 310 (5750), 1025–1028.

Kirchhoff, F., Greenough, T.C., Brettler, D.B., Sullivan, J.L., Desrosiers, R.C., 1995. Brief report: absence of intact nef sequences in a long-term survivor with nonprogressive HIV-1 infection. N. Engl. J. Med. 332 (4), 228–232.

Kolchinsky, P., Kiprilov, E., Bartley, P., Rubinstein, R., Sodroski, J., 2001. Loss of a single N-linked glycan allows CD4-independent human immunodeficiency virus type 1 infection by altering the position of the gp120 V1/V2 variable loops. J. Virol. 75 (7), 3435–3443.

Kuhmann, S.E., Platt, E.J., Kozak, S.L., Kabat, D., 1997. Polymorphisms in the *CCR5* genes of African green monkeys and mice implicate specific amino acids in infections by simian and human immunodeficiency viruses. J. Virol. 71 (11), 8642–8656.

Kuhmann, S.E., Platt, E.J., Kozak, S.L., Kabat, D., 2000. Cooperation of multiple CCR5 coreceptors is required for infections by human immunodeficiency virus type 1. J. Virol. 74 (15), 7005–7015.

Kuhmann, S.E., Pugach, P., Kunstman, K.J., Taylor, J., Stanfield, R.L., Snyder, A., Strizki, J.M., Riley, J., Baroudy, B.M., Wilson, I.A., Korber, B.T., Wolinsky, S.M., Moore, J.P., 2004. Genetic and phenotypic analyses of human immunodeficiency virus type 1 escape from a small-molecule CCR5 inhibitor. J. Virol. 78 (6), 2790–27807.

Lathey, J.L., Tierney, C., Chang, S.Y., D'Aquila, R.T., Bettendorf, D.M., Alexander, H.C., Santini, C.D., Hughes, A.M., Barroga, C.F., Spector, S.A., Landes, J.E., Hammer, S.M., Katzenstein, D.A., 2001. Associations of

CCR5, CCR2, and stromal cell-derived factor 1 genotypes with human immunodeficiency virus disease progression in patients receiving nucleoside therapy. J. Infect. Dis. 184 (11), 1402–1411.

Lawson, V.A., Silburn, K.A., Gorry, P.R., Paukovic, G., Purcell, D.F., Greenway, A.L., McPhee, D.A., 2004. Apoptosis induced in synchronized human immunodeficiency virus type 1-infected primary peripheral blood mononuclear cells is detected after the peak of CD4+ T-lymphocyte loss and is dependent on the tropism of the gp120 envelope glycoprotein. Virology 327 (1), 70–82.

Lee, B., Sharron, M., Blanpain, C., Doranz, B.J., Vakili, J., Setoh, P., Berg, E., Liu, G., Guy, H.R., Durell, S.R., Parmentier, M., Chang, C.N., Price, K., Tsang, M., Doms, R.W., 1999. Epitope mapping of CCR5 reveals multiple conformational states and distinct but overlapping structures involved in chemokine and coreceptor function. J. Biol. Chem. 274 (14), 9617–9626.

Mascola, J.R., Louder, M.K., Winter, C., Prabhakara, R., De Rosa, S.C., Douek, D.C., Hill, B.J., Gabuzda, D., Roederer, M., 2002. Human immunodeficiency virus type 1 neutralization measured by flow cytometric quantitation of single-round infection of primary human T cells. J. Virol. 76 (10), 4810–4821.

Michael, N.L., Chang, G., Louie, L.G., Mascola, J.R., Dondero, D., Birx, D.L., Sheppard, H.W., 1997. The role of viral phenotype and *CCR-5* gene defects in HIV-1 transmission and disease progression. Nat. Med. 3 (3), 338–340.

Morner, A., Bjorndal, A., Albert, J., Kewalramani, V.N., Littman, D.R., Inoue, R., Thorstensson, R., Fenyo, E.M., Bjorling, E., 1999. Primary human immunodeficiency virus type 2 (HIV-2) isolates, like HIV-1 isolates, frequently use CCR5 but show promiscuity in coreceptor usage. J. Virol. 73 (3), 2343–2349.

Moore, J.P., Kitchen, S.G., Pugach, P., Zack, J.A., 2004. The CCR5 and CXCR4 coreceptors-central to understanding the transmission and pathogenesis of human immunodeficiency virus type 1 infection. AIDS Res. Hum. Retroviruses 20 (1), 111–126.

Muster, T., Guinea, R., Trkola, A., Purtscher, M., Klima, A., Steindl, F., Palese, P., Katinger, H., 1994. Cross-neutralizing activity against divergent human immunodeficiency virus type 1 isolates induced by the gp41 sequence ELDKWAS. J. Virol. 68 (6), 4031–4034.

Nabatov, A.A., Pollakis, G., Linnemann, T., Kliphius, A., Chalaby, M.I., Paxton, W.A., 2004. Intrapatient alterations in the human immunodeficiency virus type 1 gp120 V1V2 and V3 regions differentially modulate coreceptor usage, virus inhibition by CC/CXC chemokines, soluble CD4, and the b12 and 2G12 monoclonal antibodies. J. Virol. 78 (1), 524–530.

Neil, S.J., Aasa-Chapman, M.M., Clapham, P.R., Nibbs, R.J., McKnight, A., Weiss, R.A., 2005. The promiscuous CC chemokine receptor D6 is a functional coreceptor for primary isolates of human immunodeficiency virus type 1 (HIV-1) and HIV-2 on astrocytes. J. Virol. 79 (15), 9618–9624.

Nibbs, R.J., Wylie, S.M., Yang, J., Landau, N.R., Graham, G.J., 1997. Cloning and characterization of a novel promiscuous human beta-chemokine receptor D6. J. Biol. Chem. 272 (51), 32078–32083.

Nibbs, R.J., Kriehuber, E., Ponath, P.D., Parent, D., Qin, S., Campbell, J.D., Henderson, A., Kerjaschki, D., Maurer, D., Graham, G.J., Rot, A., 2001. The beta-chemokine receptor D6 is expressed by lymphatic endothelium and a subset of vascular tumors. Am. J. Pathol. 158 (3), 867–877.

O'Brien, S.J., Moore, J.P., 2000. The effect of genetic variation in chemokines and their receptors on HIV transmission and progression to AIDS. Immunol. Rev. 177, 99–111.

Olson, W.C., Rabut, G.E., Nagashima, K.A., Tran, D.N., Anselma, D.J., Monard, S.P., Segal, J.P., Thompson, D.A., Kajumo, F., Guo, Y., Moore, J.P., Maddon, P.J., Dragic, T., 1999. Differential inhibition of human immunodeficiency virus type 1 fusion, gp120 binding, and CC-chemokine activity by monoclonal antibodies to CCR5. J. Virol. 73 (5), 4145–4155.

Pastore, C., Nedellec, R., Ramos, A., Pontow, S., Ratner, L., Mosier, D.E., 2006. Human immunodeficiency virus type 1 coreceptor switching: V1/V2 gain-of-fitness mutations compensate for V3 loss-of-fitness mutations. J. Virol. 80 (2), 750–758.

Platt, E.J., Kuhmann, S.E., Rose, P.P., Kabat, D., 2001. Adaptive mutations in the V3 loop of gp120 enhance fusogenicity of human immunodeficiency virus type 1 and enable use of a CCR5 coreceptor that lacks the amino-terminal sulfated region. J. Virol. 75 (24), 12266–12278.

Platt, E.J., Shea, D.M., Rose, P.P., Kabat, D., 2005. Variants of human immunodeficiency virus type 1 that efficiently use CCR5 lacking the tyrosine-sulfated amino terminus have adaptive mutations in gp120, including loss of a functional N-glycan. J. Virol. 79 (7), 4357–4368.

Rabut, G.E., Konner, J.A., Kajumo, F., Moore, J.P., Dragic, T., 1998. Alanine substitutions of polar and nonpolar residues in the amino-terminal domain of CCR5 differently impair entry of macrophage- and dual tropic isolates of human immunodeficiency virus type 1. J. Virol. 72 (4), 3464–3468.

Reeves, J.D., McKnight, A., Potempa, S., Simmons, G., Gray, P.W., Power, C.A., Wells, T., Weiss, R.A., Talbot, S.J., 1997. CD4-independent infection by HIV-2 (ROD/B): use of the 7-transmembrane receptors CXCR-4, CCR-3, and V28 for entry. Virology 231 (1), 130–134.

Reeves, J.D., Hibbitts, S., Simmons, G., McKnight, A., Azevedo-Pereira, J.M., Moniz-Pereira, J., Clapham, P.R., 1999. Primary human immunodeficiency virus type 2 (HIV-2) isolates infect CD4-negative cells via CCR5 and CXCR4: comparison with HIV-1 and simian immunodeficiency virus and relevance to cell tropism in vivo. J. Virol. 73 (9), 7795–7804.

Rizzuto, C.D., Wyatt, R., Hernandez-Ramos, N., Sun, Y., Kwong, P.D., Hendrickson, W.A., Sodroski, J., 1998. A conserved HIV gp120 glycoprotein structure involved in chemokine receptor binding. Science 280 (5371), 1949–1953.

Roger, M., 1998. Influence of host genes on HIV-1 disease progression. FASEB J. 12 (9), 625–632.

Rucker, J., Samson, M., Doranz, B.J., Libert, F., Berson, J.F., Yi, Y., Smyth, R.J., Collman, R.G., Broder, C.C., Vassart, G., Doms, R.W., Parmentier, M., 1996. Regions in beta-chemokine receptors CCR5 and CCR2b that determine HIV-1 cofactor specificity. Cell 87 (3), 437–446.

Rucker, J., Edinger, A.L., Sharron, M., Samson, M., Lee, B., Berson, J.F., Yi, Y., Margulies, B., Collman, R.G., Doranz, B.J., Parmentier, M., Doms, R.W., 1997. Utilization of chemokine receptors, orphan receptors, and herpesvirus-encoded receptors by diverse human and simian immunodeficiency viruses. J. Virol. 71 (12), 8999–9007.

Schols, D., Struyf, S., Van Damme, J., Este, J.A., Henson, G., De Clercq, E., 1997. Inhibition of T-tropic HIV strains by selective antagonization of the chemokine receptor CXCR4. J. Exp. Med. 186 (8), 1383–1388.

Shioda, T., Oka, S., Xin, X., Liu, H., Harukuni, R., Kurotani, A., Fukushima, M., Hasan, M.K., Shiino, T., Takebe, Y., Iwamoto, A., Nagai, Y., 1997. In vivo sequence variability of human immunodeficiency virus type 1 envelope gp120: association of V2 extension with slow disease progression. J. Virol. 71 (7), 4871–4881.

Siciliano, S.J., Kuhmann, S.E., Weng, Y., Madani, N., Springer, M.S., Lineberger, J.E., Danzeisen, R., Miller, M.D., Kavanaugh, M.P., DeMartino, J.A., Kabat, D., 1999. A critical site in the core of the CCR5 chemokine receptor required for binding and infectivity of human immunodeficiency virus type 1. J. Biol. Chem. 274 (4), 1905–1913.

Simmons, G., Reeves, J.D., McKnight, A., Dejucq, N., Hibbitts, S., Power, C.A., Aarons, E., Schols, D., De Clercq, E., Proudfoot, A.E., Clapham, P.R., 1998. CXCR4 as a functional coreceptor for human immunodeficiency virus type 1 infection of primary macrophages. J. Virol. 72 (10), 8453–8457.

Smith, M.W., Dean, M., Carrington, M., Winkler, C., Huttley, G.A., Lomb, D.A., Goedert, J.J., O'Brien, T.R., Jacobson, L.P., Kaslow, R., Buchbinder, S., Vittinghoff, E., Vlahov, D., Hoots, K., Hilgartner, M.W., O'Brien, S.J., 1997. Contrasting genetic influence of CCR2 and CCR5 variants on HIV-1 infection and disease progression. Hemophilia Growth and Development Study (HGDS), Multicenter AIDS Cohort Study (MACS), Multicenter Hemophilia Cohort Study (MHCS), San Francisco City Cohort (SFCC), ALIVE Study. Science 277 (5328), 959–965.

Solomon, A., Lane, N., Wightman, F., Gorry, P.R., Lewin, S.R., 2005. Enhanced replicative capacity and pathogenicity of HIV-1 isolated from individuals infected with drug-resistant virus and declining CD4+ T-cell counts. J. Acquired Immune Defic. Syndr. 40 (2), 140–148.

Sullivan, N., Thali, M., Furman, C., Ho, D.D., Sodroski, J., 1993. Effect of amino acid changes in the V1/V2 region of the human immunodeficiency virus type 1 gp120 glycoprotein on subunit association, syncytium formation, and recognition by a neutralizing antibody. J. Virol. 67 (6), 3674–3679.

Trkola, A., Pomales, A.B., Yuan, H., Korber, B., Maddon, P.J., Allaway, G.P., Katinger, H., Barbas III, C.F., Burton, D.R., Ho, D.D., et al., 1995. Cross-

clade neutralization of primary isolates of human immunodeficiency virus type 1 by human monoclonal antibodies and tetrameric CD4-IgG. J. Virol. 69 (11), 6609–6617.

Trkola, A., Purtscher, M., Muster, T., Ballaun, C., Buchacher, A., Sullivan, N., Srinivasan, K., Sodroski, J., Moore, J.P., Katinger, H., 1996. Human monoclonal antibody 2G12 defines a distinctive neutralization epitope on the gp120 glycoprotein of human immunodeficiency virus type 1. J. Virol. 70 (2), 1100–1108.

Trkola, A., Paxton, W.A., Monard, S.P., Hoxie, J.A., Siani, M.A., Thompson, D.A., Wu, L., Mackay, C.R., Horuk, R., Moore, J.P., 1998. Genetic subtype-independent inhibition of human immunodeficiency virus type 1 replication by CC and CXC chemokines. J. Virol. 72 (1), 396–404.

Wang, B., Spira, T.J., Owen, S., Lal, R.B., Saksena, N.K., 2000. HIV-1 strains from a cohort of American subjects reveal the presence of a V2 region extension unique to slow progressors and non-progressors. Aids 14 (3), 213–223.

Willey, S.J., Reeves, J.D., Hudson, R., Miyake, K., Dejucq, N., Schols, D., De Clercq, E., Bell, J., McKnight, A., Clapham, P.R., 2003. Identification of a subset of human immunodeficiency virus type 1 (HIV-1), HIV-2, and simian immunodeficiency virus strains able to exploit an alternative coreceptor on untransformed human brain and lymphoid cells. J. Virol. 77 (11), 6138–6152.

Xiang, S.H., Farzan, M., Si, Z., Madani, N., Wang, L., Rosenberg, E., Robinson, J., Sodroski, J., 2005. Functional mimicry of a human immunodeficiency virus type 1 coreceptor by a neutralizing monoclonal antibody. J. Virol. 79 (10), 6068–6077.

Zhang, L., He, T., Huang, Y., Chen, Z., Guo, Y., Wu, S., Kunstman, K.J., Brown, R.C., Phair, J.P., Neumann, A.U., Ho, D.D., Wolinsky, S.M., 1998. Chemokine coreceptor usage by diverse primary isolates of human immunodeficiency virus type 1. J. Virol. 72 (11), 9307–9312.

Zhang, P.F., Bouma, P., Park, E.J., Margolick, J.B., Robinson, J.E., Zolla-Pazner, S., Flora, M.N., Quinnan Jr., G.V., 2002. A variable region 3 (V3) mutation determines a global neutralization phenotype and CD4-independent infectivity of a human immunodeficiency virus type 1 envelope associated with a broadly cross-reactive, primary virus-neutralizing antibody response. J. Virol. 76 (2), 644–655.

APPENDIX D

This is a copy of an article printed in PLoS Pathogens, Vol. 5, p. e1000360

Soluble CD4 and CD4-Mimetic Compounds Inhibit HIV-1 Infection by Induction of a Short-Lived Activated State

Hillel Haim[1], Zhihai Si[1], Navid Madani[1], Liping Wang[1], Joel R. Courter[2], Amy Princiotto[1], Aemro Kassa[1], Marciella DeGrace[1], Kathleen McGee-Estrada[1], Megan Mefford[1], Dana Gabuzda[1], Amos B. Smith III[2], Joseph Sodroski[1,3]*

1 Department of Cancer Immunology and AIDS, Dana-Farber Cancer Institute, Division of AIDS, Harvard Medical School, Boston, Massachusetts, United States of America, **2** Department of Chemistry, University of Pennsylvania, Philadelphia, Pennsylvania, United States of America, **3** Department of Immunology and Infectious Diseases, Harvard School of Public Health, Boston, Massachusetts, United States of America

Abstract

Binding to the CD4 receptor induces conformational changes in the human immunodeficiency virus (HIV-1) gp120 exterior envelope glycoprotein. These changes allow gp120 to bind the coreceptor, either CCR5 or CXCR4, and prime the gp41 transmembrane envelope glycoprotein to mediate virus–cell membrane fusion and virus entry. Soluble forms of CD4 (sCD4) and small-molecule CD4 mimics (here exemplified by JRC-II-191) also induce these conformational changes in the HIV-1 envelope glycoproteins, but typically inhibit HIV-1 entry into CD4-expressing cells. To investigate the mechanism of inhibition, we monitored at high temporal resolution inhibitor-induced changes in the conformation and functional competence of the HIV-1 envelope glycoproteins that immediately follow engagement of the soluble CD4 mimics. Both sCD4 and JRC-II-191 efficiently activated the envelope glycoproteins to mediate infection of cells lacking CD4, in a manner dependent on coreceptor affinity and density. This activated state, however, was transient and was followed by spontaneous and apparently irreversible changes of conformation and by loss of functional competence. The longevity of the activated intermediate depended on temperature and the particular HIV-1 strain, but was indistinguishable for sCD4 and JRC-II-191; by contrast, the activated intermediate induced by cell-surface CD4 was relatively long-lived. The inactivating effects of these activation-based inhibitors predominantly affected cell-free virus, whereas virus that was prebound to the target cell surface was mainly activated, infecting the cells even at high concentrations of the CD4 analogue. These results demonstrate the ability of soluble CD4 mimics to inactivate HIV-1 by prematurely triggering active but transient intermediate states of the envelope glycoproteins. This novel strategy for inhibition may be generally applicable to high–potential-energy viral entry machines that are normally activated by receptor binding.

Citation: Haim H, Si Z, Madani N, Wang L, Courter JR, et al. (2009) Soluble CD4 and CD4-Mimetic Compounds Inhibit HIV-1 Infection by Induction of a Short-Lived Activated State. PLoS Pathog 5(4): e1000360. doi:10.1371/journal.ppat.1000360

Editor: Thomas J. Hope, Northwestern University, United States of America

Received December 4, 2008; **Accepted** March 2, 2009; **Published** April 3, 2009

Funding: This work was supported by grants from the National Institutes of Health (AI24755, GM56550, and AI67854)(http://www.nih.gov), by the International AIDS Vaccine Initiative (http://www.iavi.org), and by the late William F. McCarty-Cooper. The funders had no role in study design, data collection and analysis, decision to publish, or preparation of the manuscript.

Competing Interests: The authors have declared that no competing interests exist.

* E-mail: joseph_sodroski@dfci.harvard.edu

Introduction

The entry of human immunodeficiency virus type 1 (HIV-1) into target cells is mediated by the trimeric envelope glycoprotein complex, which consists of three gp120 exterior envelope glycoproteins and three gp41 transmembrane envelope glycoproteins [1]. Binding of gp120 to the receptor, CD4, on the target cell surface induces major conformational changes in the envelope glycoproteins [2]. These changes allow gp120 to bind the viral coreceptor, either CXCR4 or CCR5 [3–7]. CD4 binding also induces the formation of a gp41 pre-hairpin intermediate, in which three hydrophobic grooves on the surface of a coiled coil formed by the heptad repeat 1 (HR1) region of gp41 are exposed [8–10]. These hydrophobic grooves are subsequently occupied by helices from the gp41 heptad repeat 2 (HR2) region, during the formation of an energetically stable six-helix bundle that is thought to drive the fusion of the viral and target cell membranes [9,11,12].

In contrast to the activating effect of cell-surface CD4 on HIV-1 entry, the soluble form of CD4 (sCD4) demonstrates opposing effects on HIV-1 infectivity at different concentrations. At high concentrations, sCD4 neutralizes most HIV-1 strains [13]; at lower sCD4 concentrations, the infectivity of some HIV-1 strains can be modestly enhanced [14]. This enhancing effect of sCD4 is more prominent in some strains of the related primate immunodeficiency viruses, HIV-2 and simian immunodeficiency virus (SIV), where sCD4 can efficiently replace cell-surface CD4 to drive infection of $CD4^{-}CCR5^{+}$ cells [15,16].

Based on the potential of sCD4 to inhibit HIV-1 infection *in vitro*, this protein was tested for clinical efficacy in HIV-1-infected individuals; however, no effect on plasma viral loads was observed [13]. Further examination revealed that doses of sCD4 that were significantly higher than those achieved in the clinical trial were required to neutralize primary clinical isolates of HIV-1, in contrast to the relatively sensitive, laboratory-adapted strains [17].

Interest in improving the therapeutic potential of sCD4 has prompted investigation of the mechanistic basis for sCD4-induced neutralization. Competitive inhibition of envelope glycoprotein binding to the cell-surface CD4 receptor was suggested as a major

Author Summary

Human immunodeficiency virus type 1 (HIV-1) is the cause of the global AIDS epidemic. HIV-1 gains entry into its target cells by fusing with the cell membrane, a process that begins with the interaction of the viral envelope glycoproteins with cell-surface receptors. HIV-1 uses two receptors on the target cell: CD4 and CCR5/CXCR4. Binding of the virus to the primary receptor, CD4, primes the viral envelope glycoproteins to mediate the fusion of the viral membrane and the membrane of the target cell. Soluble forms of the CD4 receptor and small molecules that mimic the effects of CD4 can inhibit virus infection; however, how this inhibition occurs is still unknown. In this report, we show that soluble mimics of CD4 inhibit HIV-1 infection by prematurely triggering the viral envelope glycoproteins. The unstable activated state of the virus lasts only a few minutes, after which the virus loses the ability to infect cells. This novel strategy for inhibition may be generally applicable to other viruses besides HIV-1, some of which are also activated by binding to their receptors.

mechanism of sCD4 neutralization [17,18]. Resistance to sCD4 may thus arise by a decreased affinity of the envelope glycoprotein complex for sCD4 [13]. However, sCD4 sensitivity cannot always be predicted by measurements of affinity [17,19–21]. Binding of sCD4 to the envelope glycoprotein trimer can induce detachment (shedding) of the gp120 subunit from the envelope glycoprotein trimer [17,18,22–24]. However, the sCD4 concentrations that are required to elicit shedding are significantly higher than those required to neutralize the virus [25,26]. In addition, for some HIV-1 strains, the temperature dependence of sCD4-induced gp120 shedding and virus neutralization differs [26]. The mode of sCD4-mediated inhibition thus remains incompletely understood.

Targeting the functionally important and therefore conserved CD4-binding site on HIV-1 gp120 represents an attractive potential approach to therapy or prophylaxis. CD4-mimicking peptides and oligomeric forms of sCD4 that target this site on primary HIV-1 isolates have been developed [27–30]. Recently, a new class of small-molecule CD4 mimics was identified [31,32]. These compounds, which include the prototypic compound NBD-556 and its derivatives, mimic the effects of CD4 by inducing the exposure of the coreceptor-binding site on gp120 [31,33]. Although NBD-556 inhibits HIV-1 infection of $CD4^+CCR5^+$ cells, it can replace CD4 and thus enhance HIV-1 infection of $CD4^-CCR5^+$ cells [31]. In view of their capacity to enhance infectivity, any potential application of CD4-mimetic compounds and sCD4 derivatives, herein referred to as soluble CD4 mimics (SCMs), would benefit from a mechanistic understanding of these activating and inhibitory effects.

The study of receptor-induced conformational changes of the HIV-1 envelope glycoprotein complex is still limited by the lack of tools that enable monitoring of this dynamic multi-step process. Detection of conformational intermediates is largely based on the use of conformation-specific fusion/entry inhibitors, which are added at different times after initiation of the fusion process [34–38]. Although such assays have provided insights into the mechanisms of gp41-directed inhibitors, they fail to detect transitions to conformations that are inactive and do not differentiate between lack of inhibitor binding and lack of inhibition. Furthermore, because formation of the ternary complex between the envelope glycoproteins, CD4 and coreceptor constitutes a major rate-limiting step in the membrane fusion process, these approaches are limited in their capacity to define the progression of subsequent events [39]. Finally, due to the low temporal resolution of most systems, mainly steady-state conformations are detected, while intermediate states of the complex may be missed.

To overcome these limitations, we developed new systems that allow us to monitor the dynamic changes in conformation and function of the HIV-1 envelope glycoproteins, immediately after engagement of the activating molecules. Using these tools, we found that SCMs inactivate envelope glycoprotein function by an activation-triggered inhibition process, through induction of a metastable activated state.

Materials and Methods

Reagents and Antibodies

Four-domain sCD4 (molecular weight 50 kDa) was expressed in 293F cells after stable transfection. The protein was secreted into the cell culture medium and then purified by using the C-terminal His_6 tag, as previously described [40]. The structure of compound JRC-II-191 (herein referred to as **191**) is reported in reference [33]. The CCR5 antagonist 'Compound A' [4-nitrobenzyl 1-(3-(N-methylphenylsulfonamido)-3-phenylbutyl)piperidin-4-yl(vinyl)-carbamate] [41,42] was kindly provided by Dr. Martin Springer at Merck Research Laboratories, Rahway, NJ.

The anti-gp120 monoclonal antibody 48d, which recognizes an epitope that overlaps the coreceptor-binding site, was kindly provided by Dr. James Robinson (Tulane University Medical Center) [43]. The monoclonal antibodies IgG1 b12 and 39F recognize the CD4-binding site and the V3 loop of gp120, respectively [44,45]. The C34-Ig fusion protein consists of the Fc region of human IgG1 linked to the HR2 region of the HXBc2 envelope glycoprotein (amino acid residues 628–661, numbered according to current convention [46]). C34-Ig was produced and purified as previously described [47]. The CD4-Ig fusion protein consists of the first two N-terminal domains of the CD4 molecule and the Fc region of human IgG1. Purification was carried out as described for the C34-Ig molecule [47].

Envelope Glycoprotein Constructs

The primary viruses UK7br and UK7br34 were isolated from autopsy brain tissue from an AIDS patient with HIV-1 associated dementia [48]. These envelope glycoproteins were expressed from the pcDNA 3.1 backbone vector. All other envelope glycoproteins described were expressed from the pSVIIIenv vector [49]. The YU2, AD8, JR-FL, 89.6 and KB9 *env* sequences from Asp 718 (Kpn I) to BamH I were substituted for the corresponding HXBc2 *env* sequences in the original pSVIIIenv vector. The ΔKS construct, which contains an HIV-1 HXBc2 *env* gene with a large deletion, was used as a negative control. The YU2(Δct) protein has a truncated cytoplasmic tail of 17 amino acids, with a stop codon introduced after Ala 710 (numbered according to current convention [46]).

The YU2-GS8 construct is a cleavage-defective form of the YU2 HIV-1 envelope glycoproteins that contains an 8-amino acid glycine-serine linker at the gp120/gp41 junction. Starting with the cytoplasmic tail-deleted YU2 envelope glycoproteins, both Arg 508 and Arg 511 near the furin cleavage site were altered to Ser to render the protein cleavage-defective. The 8-amino acid linker, Gly-Gly-Gly-Ser-Gly-Gly-Gly-Ser, was then inserted between Ser 511 (the C-terminal residue of gp120) and Ala 512 (the N-terminal residue of gp41) using the overlapping PCR method.

Cell-Based Enzyme-Linked Immunosorbent Assay (ELISA)

A sensitive cell-based ELISA with high temporal resolution was developed to measure the binding of antibodies to HIV-1 envelope

glycoprotein trimers expressed on cells. COS-1 cells were seeded in 96-well plates (2.4×10^4 cells per well) and transfected the next day with 0.1 μg of a plasmid expressing the envelope glycoproteins and 0.01 μg of a Tat-expressing plasmid per well using the Effectene transfection reagent (Qiagen). Two days later, cells were washed twice with blocking buffer (35 mg/ml BSA, 10 mg/ml non-fat dry milk, 1.8 mM $CaCl_2$, 1 mM $MgCl_2$, 25 mM Tris, pH 7.5 and 140 mM NaCl). For pulse activation experiments, the COS-1 cells were incubated with sCD4 (40 μg/ml, 0.8 μM) or **191** (360 μM) suspended in blocking buffer for three minutes, washed three times with blocking buffer and incubated for different time periods until the C34-Ig or 48d antibodies were added (at 40 μg/ml or 1 μg/ml, respectively, for 30 minutes). To study the temperature dependence of HR1 groove exposure, the sCD4-pulsed cells were incubated at the requisite temperature for different lengths of time; the cells were subsequently returned to room temperature for incubation with C34-Ig. Cells were then washed four times with blocking buffer and four times with washing buffer (140 mM NaCl, 1.8 mM $CaCl_2$, 1 mM $MgCl_2$ and 20 mM Tris, pH 7.5). A horseradish peroxidase-conjugated antibody specific for the Fc region of human IgG was then incubated with the samples for 45 minutes at room temperature. Cells were washed 5 times with blocking buffer and 5 times with washing buffer. HRP enzyme activity was determined after the addition of 33 μl per well of a 1:1 mix of Western Lightning oxidizing and luminol reagents (Perkin Elmer Life Sciences) supplemented with 150 mM NaCl. Light emission was measured with a Mithras LB 940 luminometer (Berthold Technologies). For experiments that measure the rate of decay of C34-Ig or 48d antibody binding, the indicated values for the amount of antibody bound were obtained by subtracting binding measured in the absence of sCD4 from the binding measured at each time point after the sCD4 pulse.

HR1 Groove Exposure Induced by Cell-Surface CD4

293T cells cultured in 6-well plates were transfected with the pcDNA3.1-CD4 or ΔKS constructs (1 μg per 1.8×10^6 cells) using the Effectene reagent (Qiagen). COS-1 cells cultured in 96-well plates were transfected with plasmids expressing the HIV-1 envelope glycoproteins as described above. Two days later, the 293T cells were harvested using 5 mM EDTA in PBS and added at 4°C to the monolayer of COS-1 cells (3×10^5 293T cells per well). Cells were subsequently centrifuged at 1,000×g for two minutes to increase contact and incubated at 4°C for 75 minutes. Samples were then washed once with blocking buffer and rapidly equilibrated to 25°C. C34-Ig was then added at different times. Detection of C34-Ig binding was performed as described above.

Fluorescence-Activated Cell Sorting (FACS) Analysis of Ligand Binding to Cell-Surface HIV-1 Envelope Glycoproteins

Flow cytometry was used to detect the binding of C34-Ig to 293T cells that express the cytoplasmic tail-deleted (Δct) HIV-1 envelope glycoproteins [47]. Cells were cultured in 6-well plates (1.5×10^6 cells per well) and transfected with 0.6 μg of a plasmid expressing the HIV-1 envelope glycoproteins and 0.06 μg of a Tat-expressing plasmid using the Effectene transfection reagent (Qiagen). Two days later, cells were detached using PBS supplemented with 5 mM EDTA and resuspendend in FACS buffer (PBS supplemented with 10 mg/ml BSA and 0.5 mg/ml sodium azide). Cells were then incubated with C34-Ig suspended in FACS medium, with or without sCD4, at the indicated temperature for 45 minutes. Following three washes with FACS buffer, cells were incubated at room temperature for 45 minutes in FACS buffer containing a phycoerythrin-conjugated goat anti-human IgG antibody (Sigma) and an anti-CD4 fluorescein-conjugated antibody (OKT4, eBioscience) to measure C34-Ig and sCD4 binding, respectively. Cells were subsequently washed three times with FACS buffer and analyzed with a FACScan analyzer (Becton Dickinson) using Cellquest software for data acquisition and analysis.

Generation and Preparation of Recombinant Luciferase-Expressing Viruses

Single-round, recombinant HIV-1 viruses that express the luciferase reporter gene were generated by transfection of 293T cells using the calcium phosphate transfection method (Promega). Cells were seeded in 100-mm tissue culture dishes (approximately 4×10^6 cells per dish) and transfected the next day with 10 μg of the HIV-1 packaging construct pCMVΔP1ΔenvpA [50], 10 μg of the firefly luciferase-expressing construct pHIvec2.luc and 2.5 μg of the plasmid expressing the HIV-1 Rev and envelope glycoproteins. Sixteen hours following transfection, the medium was changed to culture medium (Dulbecco-modified Eagle medium supplemented with 10% fetal calf serum, DMEM/FCS 10%); 12 hours later, the medium was changed to DMEM/FCS 1%. Virus-containing supernatants were collected 12 hours later, cleared of cell debris by low speed centrifugation and filtered through 0.2 μm filters. Preparations were subsequently loaded onto Float-A-Lyzer dialysis cassettes (molecular weight cutoff 100 kDa, Spectrum Labs) and dialyzed against HS buffer (140 mM NaCl, 10 mM HEPES, pH 7.3) for 24 hours at 4°C. Viral preparations were subsequently aliquoted and stored at −80°C until use.

Magnetically Controlled Infection by sCD4-Activated HIV-1

To minimize the time interval between activation of the virus and attachment to the cells, we magnetically controlled the attachment step. As a magnetically controllable carrier, we used magnetite nanoparticles (50 nm in diameter) that are coated by a starch polymer with phosphate end groups (FluidMag PD, Chemicell). Viruses were preincubated with magnetite nanoparticles (1.2 mg/ml) for 7 minutes at room temperature, followed by incubation with sCD4 (40 μg/ml) for different time periods. Preparations were then added to a confluent monolayer of cells cultured in a 96-well plate, to which was applied a magnetic field using a Nd-Fe-B permanent magnet (OZ Biosciences). Canine thymocyte Cf2Th cells that express CCR5 or both CD4 and CCR5 were used as target cells (approximately 7×10^4 cells per well). After a one-minute incubation at room temperature, cells were washed twice with DMEM/FCS 10% and cultured for an additional 14 hours. Cells were then detached with trypsin-EDTA and seeded again at a 1:6 dilution. Forty-eight hours after infection, cells were lysed with passive lysis buffer (Promega) and lysates were assayed for luciferase activity. To each well was added 100 μl of luciferin buffer (15 mM $MgSO_4$, 15 mM KPO_4 [pH 7.8], 1 mM ATP, and 1 mM dithiothreitol) and 50 μl of 1 mM D-luciferin potassium salt (BD Pharmingen). Luminescence was recorded using a Berthold LB 960 microplate luminometer.

Decay Rate of Virus Infectivity after Pulse Activation with sCD4

The decay rate of virus infectivity after activation by sCD4 was measured using magnetically-immobilized viruses. This method allows rapid pulsing and washing of the virus before addition of

target cells; thus, virus infectivity shortly after activation can be measured. Virus preparations were preincubated with magnetite nanoparticles (1.2 mg/ml, suspended in HS buffer) for 7 minutes and then added to 96-well plates placed over a permanent Ne-Fe-B magnet (OZ Biosciences). After a 4-minute incubation at room temperature, wells were washed twice with culture medium. Immobilized viruses were then pulsed with 40 μg/ml (0.8 μM) sCD4 for 3 minutes, washed twice with culture medium and then incubated at room temperature for different time periods. Cf2Th-CCR5 cells suspended in culture medium ($\sim 1 \times 10^5$ cells) were then added to the wells and centrifuged at 1,000×g for 2 minutes to expedite contact between cells and viruses. Luciferase activity was measured two days later.

Decay Rate of Virus Infectivity after Pulse Activation with Compound 191

The affinity of NBD-556 analogues, including **191**, for the HIV-1 gp120 envelope glycoprotein is significantly lower than that of sCD4 [31,33]. Measured by isothermal titration calorimetry, the K_d of **191** binding to the YU2 gp120 envelope glycoprotein is 760 nM, compared with a K_d of approximately 2 nM for the sCD4-gp120 interaction. At achievable concentrations, **191** induced significantly lower levels of HIV-1 activation than sCD4 (see Results section); levels of infectivity were consequently too low to be monitored for decay. We therefore introduced a number of modifications to the method described above for measuring infectivity decay. Briefly, viruses were incubated with 180 μM **191** at 37°C for 10 minutes. Activation was then halted by a 20-fold dilution of the virus-compound mix in HS buffer equilibrated to 26°C. After dilution, no additional activation of HIV-1 infection was induced by **191** during the time frame of the experiment (data not shown). Samples were then incubated for different time periods, associated with magnetite nanoparticles and magnetically adsorbed to confluent cultures of Cf2Th-CCR5 cells, as described above.

Infectivity of Cell-Bound Virus Activated by sCD4

Cf2Th cells cultured in 6-well plates (6×10^5 cells per well) were transfected with different amounts of the pcDNA3.1-CCR5 plasmid, which expresses human CCR5, using the Effectene transfection reagent. Two days later, cells were detached using 5 mM EDTA in PBS and re-seeded in 96-well plates (7×10^5 cells per well). Viruses were then magnetically adsorbed to the transfected cells in the presence of 20 μg/ml (400 nM) sCD4 in the culture medium and infectivity was measured two days later.

Results

Rescue of the Infectivity of sCD4-Treated HIV-1 by Rapid Attachment to Cells

Soluble CD4 mimics (SCMs) can exert varied effects on HIV-1 infection of $CD4^+$ and $CD4^-$ target cells. Although soluble CD4 (sCD4) typically inhibits HIV-1 infection of $CD4^+CCR5^+$ cells, enhancement of HIV-1 infection of $CCR5^+$ cells lacking CD4 is sometimes seen after sCD4 treatment [14]. Sensitivity to these effects varies among different HIV-1 strains [49]. We examined the sensitivity to sCD4 of recombinant HIV-1 viruses (designated HIV-1(AD8) and HIV-1(YU2), respectively) pseudotyped with the envelope glycoproteins of the primary HIV-1 isolates AD8 and YU2, which have similar binding affinities for sCD4 [51,52]. In $CD4^+CCR5^+$ target cells, sCD4 inhibited the infectivity of HIV-1(AD8) and HIV-1(YU2) with IC_{50} values of 80 nM (4 μg/ml) and 12 nM (0.6 μg/ml), respectively (Figure 1A). In $CD4^-CCR5^+$ cells, sCD4 activated infection of HIV-1(AD8) much more efficiently than that of HIV-1(YU2).

A similar pattern of HIV-1 activation and inactivation was observed for the NBD-556 analogue, JRC-II-191, herein referred to as **191**. The affinity of **191** for the HIV-1_{YU2} gp120 envelope glycoprotein (K_d = 760 nM) is significantly lower than that of sCD4 (K_d = ~2 nM). Nevertheless, at proportionately higher concentrations, **191** resembled sCD4, inhibiting HIV-1 infection of $CD4^+CCR5^+$ cells and enhancing infection of $CD4^-CCR5^+$ cells (Figure 1B). For both sCD4 and **191**, the enhancement of infection of cells lacking CD4 became progressively less efficient at higher concentrations; in some cases, decreases in viral infectivity were associated with escalating doses. These characteristics of HIV-1 envelope glycoproteins differ from those observed with several SIV envelope glycoproteins, which demonstrate increasingly efficient infection of $CD4^-CCR5^+$ cells with increasing sCD4 concentrations (data not shown, and ref. [15]). These observations suggested the existence of a concentration-dependent, virus-inhibitory process superimposed on the HIV-1 activation process.

Because virus attachment to cells in culture progresses in a slow, diffusion-dependent manner [53,54], significant time intervals can elapse between virus binding by SCMs and the association between virus and cell. Thus, the diminished capacity of the SCMs

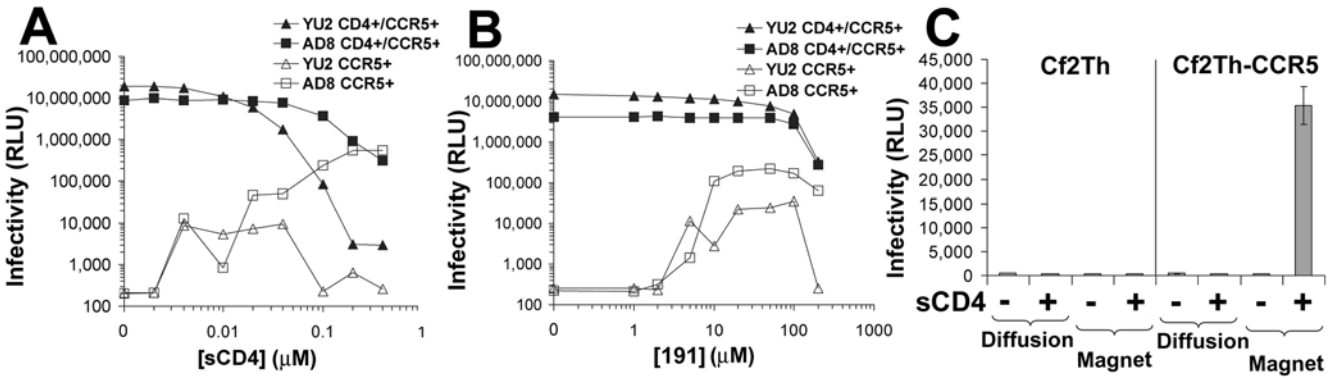

Figure 1. Inhibition and activation of infection by sCD4 and the CD4-mimetic compound 191. Recombinant HIV-1(YU2) or HIV-1(AD8) strains were incubated with $CD4^-CCR5^+$ or $CD4^+CCR5^+$ Cf2Th cells for 48 hours in the presence of sCD4 (A) or **191** (B). Infectivity was determined by measurement of luciferase activity. (C) HIV-1(YU2) was incubated for three minutes in the presence or absence of sCD4 (40 μg/ml, 0.8 μM) and then adsorbed by diffusion or magnetically to cultures of the indicated cell type. Measured luciferase activity is presented as mean relative light units (RLU)±standard error of the mean (s.e.m.) of three replicate samples.
doi:10.1371/journal.ppat.1000360.g001

to enhance HIV-1 infection of $CD4^{-}CCR5^{+}$ cells at higher concentrations might reflect the involvement of time-dependent as well as concentration-dependent processes that abrogate infectivity after activation occurs. To test this possibility, we examined the effect of neutralizing concentrations of sCD4 on HIV-1(YU2) infection when the time interval between sCD4-virus binding and virus-cell attachment was reduced. For this purpose, we applied a system that magnetically controls virus motion to eliminate viral dependence on passive diffusion for cell attachment; this system allows near-complete transfer of the virus inoculum to the cell-bound state within one minute [53,55]. When HIV-1(YU2) was briefly incubated with a high concentration of sCD4 and then added to $CD4^{-}CCR5^{+}$ cells, infection occurred only when the virus was magnetically adsorbed to the cells (Figure 1C). These results suggested the possibility of a time-dependent process that decreases HIV-1 infectivity after activation by sCD4, and prompted us to measure the stability of the sCD4-activated intermediate form of the HIV-1 envelope glycoproteins.

Conformational Stability of the CD4-Activated Intermediate

Engagement of CD4 induces a major structural rearrangement of the HIV-1 envelope glycoproteins [2]. Two functionally important regions of the HIV-1 envelope glycoproteins are formed and exposed as a result of CD4 binding: i) the coreceptor-binding site on the gp120 envelope glycoprotein [3–7,56]; and ii) the trimeric coiled coil composed of the N-terminal heptad repeat (HR1) regions of the three gp41 subunits [8–10,47]. To investigate the conformational stability of the sCD4-activated envelope glycoprotein intermediate, we monitored changes over time in the exposure of the coreceptor-binding site on gp120 and the HR1 coiled coil on gp41 after pulse activation by sCD4.

To measure the progression of conformational changes that immediately follow HIV-1 envelope glycoprotein activation, we developed a novel enzyme-linked immunosorbent assay (ELISA)-based system that utilizes live cells as a platform for expression of membrane-bound trimeric envelope glycoprotein complexes The system allowed sensitive detection of ligand binding to full-length envelope glycoproteins at high temporal resolution. COS-1 cells that express the HIV-1_{YU2} envelope glycoproteins were pulse-activated with sCD4 at 37°C for 3 minutes and incubated at 37°C for different time periods. The following probes were then added: i) monoclonal antibody 48d, which binds to a gp120 epitope that overlaps the coreceptor-binding site [43]; or ii) the C34-Ig protein, which is composed of the C34 peptide corresponding to the gp41 HR2 region linked to the Fc constant region of human IgG1 [47]. C34-Ig binds to the hydrophobic groove formed at the interface of the HR1 coiled-coil helices [10,47]. The sCD4 pulse significantly enhanced the binding of the C34-Ig protein and the 48d antibody to the HIV-1 envelope glycoproteins (Figure 2A and 2B). The time interval between the sCD4 pulse and addition of the 48d antibody did not affect the level of 48d binding observed (Figure 2B). Thus, after the sCD4-induced conformational change, the epitope of the 48d antibody remains stably exposed over the time period examined.

In contrast to the above results, the exposure of the C34-Ig binding site after the sCD4 pulse was transient at 37°C (Figure 2C). Stability of the HR1-exposed state was highly dependent on the temperature of incubation (Figure 3A). Although sCD4 efficiently bound to the envelope glycoprotein complex and induced the formation/exposure of the HR1 groove at 4, 25 and 37°C, this state was stable only at lower temperatures (Figure 3B). The loss of exposure of the HR1 groove was not reversible by repeated pulsing of the envelope glycoprotein complexes with saturating concentrations of sCD4 (data not shown). At the different temperatures examined, in the absence of sCD4, C34-Ig binding was similar to that measured for the negative control cells transfected with the ΔKS plasmid. No correlation was observed between the temperature of incubation and the binding of C34-Ig in the absence of sCD4.

Given the constant level of 48d antibody binding to the sCD4-pulsed envelope glycoprotein-expressing cells, the observed time-dependent decrease in C34-Ig binding cannot be attributed to changes in cell-surface levels of the envelope glycoproteins, as might occur due to gp120 shedding [17]. Moreover, we observed that sCD4 binding to the cells remained constant over the time period examined. We performed a kinetic experiment to measure the decay of HR1 exposure using FACS analysis. The binding of sCD4 and C34-Ig to the envelope glycoprotein-expressing cells was measured simultaneously at different time points after the sCD4 pulse, using phycoerythrin- and fluorescein-conjugated secondary antibodies. We observed a gradually decreasing capacity of C34-Ig to bind despite constant levels of bound sCD4 (Figure S1).

In summary, after engagement of sCD4, the HIV-1 envelope glycoprotein complex undergoes conformational changes that result in formation/exposure of the gp120 coreceptor-binding site and the gp41 HR1 groove. However, despite continued engagement of sCD4 and stable exposure of the 48d epitope on gp120, the induced envelope glycoprotein intermediate undergoes a spontaneous temperature-dependent and apparently irreversible change of conformation.

Decay of Exposure of the HR1 Groove on Envelope Glycoproteins from Different HIV-1 Strains

The decay profile of sCD4-induced HR1 groove exposure was determined for a panel of envelope glycoproteins from primary and laboratory-adapted HIV-1 strains. Measurements were conducted at room temperature (24–26°C) to slow the rate of decay, allowing greater accuracy. Interestingly, a wide range of stabilities of the HR1 groove-exposed state was observed in the different HIV-1 envelope glycoproteins (Figure 4A). For example, the YU2 and AD8 envelope glycoproteins exhibited half-lives of 5 and 100 minutes, respectively. The different decay rates of HR1 groove exposure could not be explained by differences in the affinity of the trimeric envelope glycoprotein complexes for sCD4 (Figure S2A), or in kinetic differences in CD4-Ig binding to these complexes (Figure S2B). We also found that the deletion of the gp41 cytoplasmic tail had no effect on the stability of the CD4-activated intermediate (Figure S2C), even though the cell-surface level of envelope glycoprotein expression was increased, as expected [57].

Envelope glycoproteins from HIV-$1_{89.6}$ and HIV-1_{KB9} exhibited highly stable sCD4-induced intermediates that did not appreciably decay at room temperature for up to 1 hour after the sCD4 pulse. For these envelope glycoproteins, the half-lives of the HR1-exposed state measured at 37°C were 16 and 17 minutes, respectively (Figure S2D).

Correlation between Stability of the HR1 Groove and Functional Stability of the HIV-1 Envelope Glycoproteins after sCD4 Exposure

Does the sCD4-induced conformational instability in the HIV-1 envelope glycoproteins have consequences for virus infectivity? To examine this question, we devised a strategy to measure changes over time in the capacity of sCD4-activated virus to infect $CD4^{-}CCR5^{+}$ cells. First, recombinant, luciferase-expressing viruses were associated with magnetite nanoparticles and immo-

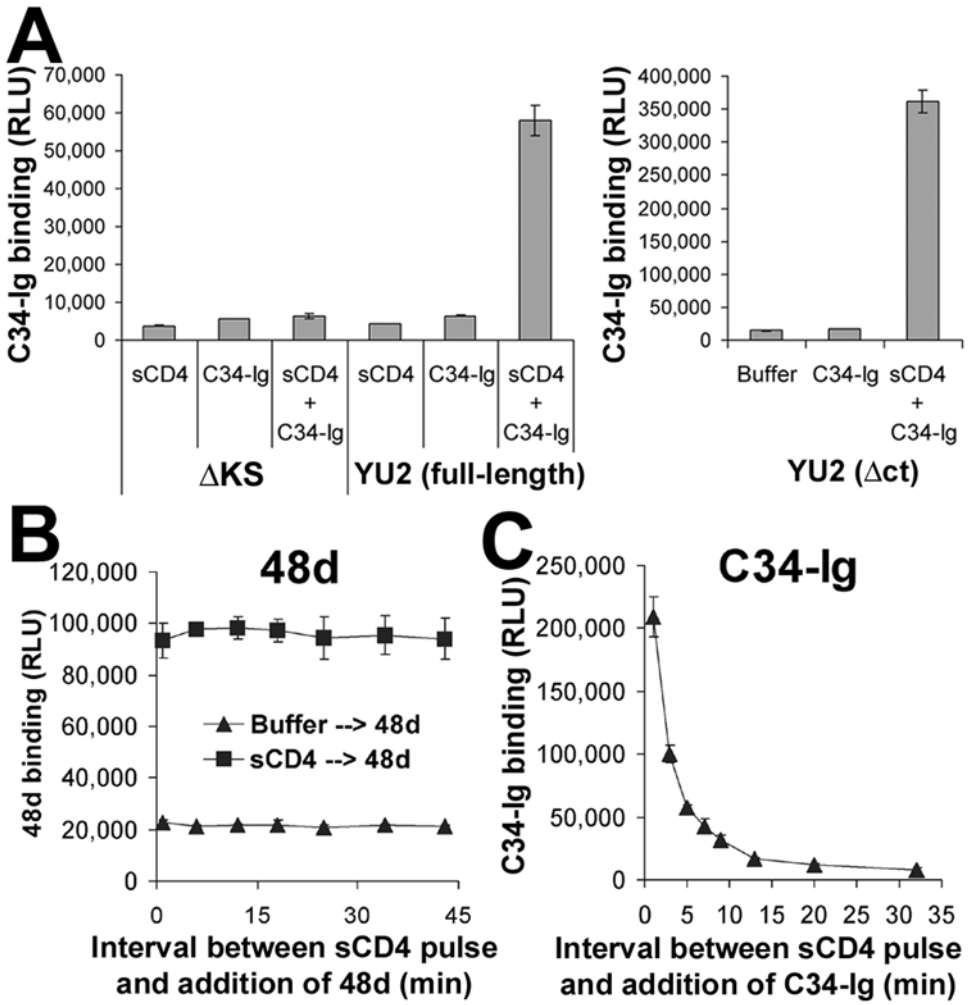

Figure 2. Soluble CD4-induced changes in the gp120 coreceptor–binding region and gp41 HR1 region. (A) A cell-based ELISA was used to measure the binding of C34-Ig, which detects the HR1 gp41 region [38,47], to the trimeric HIV-1 envelope glycoproteins. COS-1 cells were transfected with the negative control ΔKS plasmid or plasmids expressing the full-length YU2 envelope glycoproteins (left) or the cytoplasmic tail-deleted (Δct) YU2 envelope glycoproteins (right). Two days later, cells were incubated with C34-Ig (20 μg/ml), in the presence or absence of sCD4 (20 μg/ml). C34-Ig binding was measured using a secondary horseradish peroxidase-conjugated antibody. (B,C) Change over time in the exposure of CD4-induced epitopes. Cells that express the YU2(Δct) envelope glycoproteins were pulsed for three minutes with sCD4 (40 μg/ml). Cells were then washed three times and incubated for different time periods at 37°C. The monoclonal antibody 48d (B) or C34-Ig (C) was then added. The bound 48d or C34-Ig molecules were detected using a horseradish peroxidase-conjugated anti-human IgG Fc antibody, as described in Materials and Methods. Values represent the mean RLU (±s.e.m.) of two replicate samples.
doi:10.1371/journal.ppat.1000360.g002

bilized on tissue-culture plates by constant application of a magnetic field. Next, the immobilized viruses were pulsed with sCD4 for 3 minutes and incubated at 25°C for different time periods. Then, $CD4^{-}CCR5^{+}$ cells were added and immediately pelleted onto the immobilized viruses. Infectivity was assessed by measuring luciferase activity in the cells 48 hours later. The levels of initial infectivity for viruses pseudotyped with the different HIV-1 envelope glycoproteins were significantly increased by incubation with sCD4 (data not shown). However, infectivity subsequently declined at different rates for viruses with different envelope glycoproteins (Figure 4B). Similar to the stability of HR1 groove exposure, the rate of decay of infectivity was highly dependent upon temperature (Figure S3). At room temperature, the half-life of infectivity exhibited by the sCD4-treated viruses pseudotyped with different HIV-1 envelope glycoproteins correlated well with the half-life of the HR1 groove-exposed state following incubation with sCD4 ($R^2 = 0.9374$, Figure 4C).

Assuming that the linear regression model generated using the data obtained at 25°C applies to the situation at 37°C, we first estimated the half-lives of HIV-1 infectivity by fitting the half-lives of HR1 groove exposure measured at 37°C to the model. For the most stable envelope glycoproteins (derived from $HIV\text{-}1_{89.6}$ and $HIV\text{-}1_{KB9}$), we estimated a maximal half-life of infectivity of 5–7 minutes at 37°C. In accordance with the predicted values, the measured half-lives of infectivity at 37°C for viruses containing the KB9 and 89.6 envelope glycoproteins were 7 and 8 minutes, respectively, after the sCD4 pulse (Figure S2E).

We compared the infectious half-lives of viruses with different HIV-1 envelope glycoproteins following incubation with sCD4 (using $CD4^{-}CCR5^{+}$ cells, as described above) and without sCD4 treatment (using $CD4^{+}CCR5^{+}$ cells). Incubation of the viruses at 37°C for increasing time periods in the absence of sCD4, followed by infection of $CD4^{+}CCR5^{+}$ cells, revealed a gradual reduction of infectivity, with half-lives ranging from 6.9 to 12.1 hours (Figure

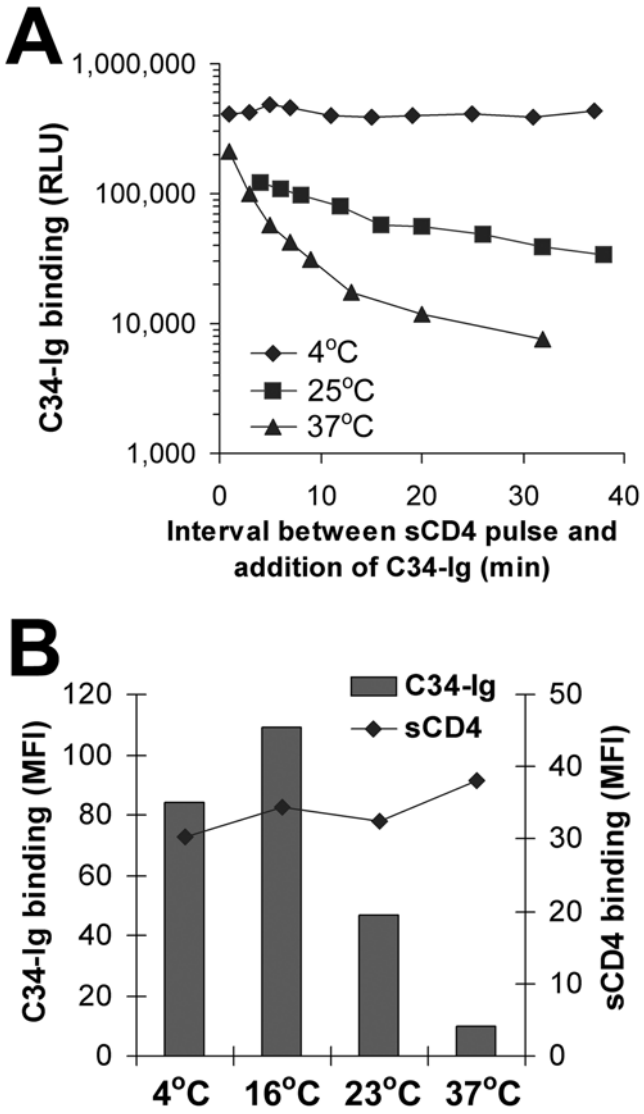

Figure 3. Temperature dependence of the decay of HR1 groove exposure. (A) Decay of HR1 groove exposure at different temperatures after pulse activation with sCD4 (40 μg/ml; 0.8 μM) was measured by a cell-based ELISA, as described in Materials and Methods. The indicated values for C34-Ig binding were obtained by subtracting the values of C34-Ig binding in the absence of sCD4 from the binding measured at each time point after the sCD4 pulse. Mean background levels of C34-Ig binding (in the absence of sCD4) were 10316, 21413, and 19028 RLU for the experiments performed at 4°C, 25°C, and 37°C, respectively. (B) Binding of C34-Ig and sCD4 to the HIV-1 envelope glycoproteins was measured at different temperatures. Cells that express the YU2(Δct) envelope glycoproteins were incubated simultaneously with both C34-Ig (20 μg/ml) and sCD4 (20 μg/ml; 0.4 μM) at the indicated temperature. Binding of sCD4 and C34-Ig was detected by FACS analysis using a fluorescein-conjugated anti-CD4 antibody and a phycoerythrin-conjugated goat anti-human IgG antibody, respectively (see Materials and Methods). The mean fluorescence intensity (MFI) of the cells in both channels is shown.

doi:10.1371/journal.ppat.1000360.g003

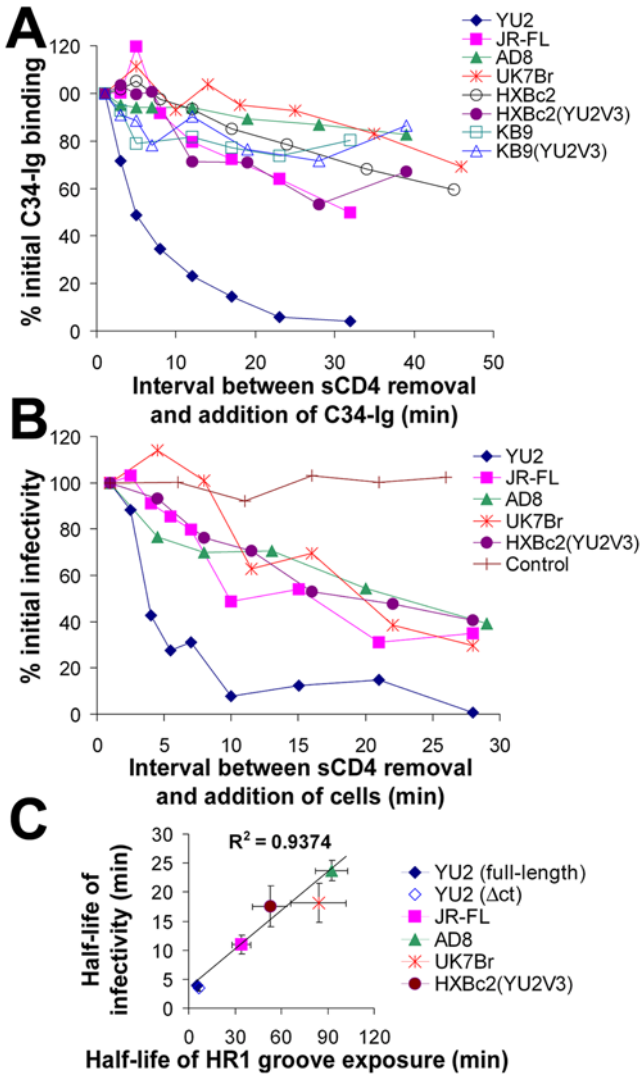

Figure 4. Relationship between infectivity decay and loss of HR1 groove exposure. (A) Decay of HR1 groove exposure of different HIV-1 envelope glycoproteins was studied at 25°C after pulse activation with sCD4. COS-1 cells expressing the indicated HIV-1 envelope glycoproteins were pulsed with sCD4 (40 μg/ml; 0.8 μM) for 3 minutes, followed by assessment of HR1 groove exposure using the cell-based ELISA method, as described in the Figure 2 legend. (B) Recombinant HIV-1 virions carrying the indicated envelope glycoproteins were pulsed with sCD4 (40 μg/ml; 0.8 μM) for 3 minutes and incubated at 25°C. After the indicated times, $CD4^{-}CCR5^{+}$ Cf2Th cells were added to the viruses. For the sample marked as control, HIV-1(YU2) was pulsed with buffer and then $CD4^{+}CCR5^{+}$ cells were added. Two days later, virus infectivity was assessed by measuring luciferase activity in the target cells. (C) The relationship between the decay rate of HR1 groove exposure and the decay rate of infectivity, both measured at 25–27°C after pulse activation with sCD4, is shown for the panel of HIV-1 envelope glycoproteins. Half-lives were determined by fitting a model function to the data using nonlinear regression. Values represent half-lives (±s.e.m. for both variables) derived from two to four separate experiments for each envelope glycoprotein variant.

doi:10.1371/journal.ppat.1000360.g004

S4). However, no correlation between the functional stability of the native and sCD4-bound states of each of the envelope glycoproteins was observed.

We conclude that after engagement of sCD4, HIV-1 undergoes a transient phase of activation, during which attachment to cells that express CCR5 will allow entry to occur. However, this activated state is short-lived and is followed by apparently irreversible structural rearrangements and loss of infectivity. Thus, at any given time point after exposure to sCD4, HIV-1 infectivity represents the combined result of an activation process and progression through the activated intermediate state to inactivation (Figure S5).

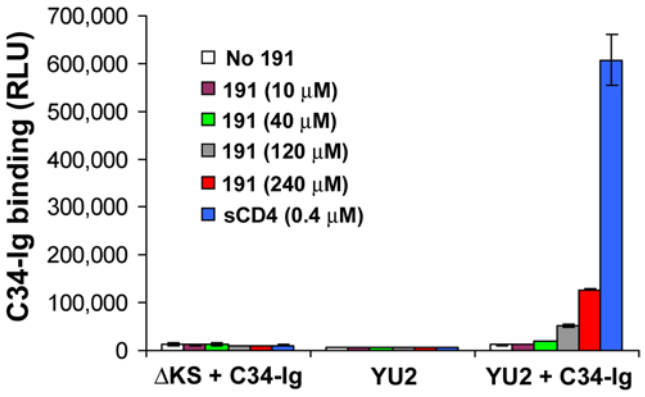

Figure 5. Effect of compound 191 on exposure of the gp41 HR1 groove. COS-1 cells transfected with a plasmid expressing the YU2(Δct) envelope glycoproteins or with the control ΔKS plasmid, which does not express an envelope glycoprotein on the cell surface, were incubated with the indicated molecules in the presence or absence of C34-Ig (20 μg/ml). The data represent the means (±s.e.m.) of two replicate samples.
doi:10.1371/journal.ppat.1000360.g005

Metastable Activation Induced by a Small-Molecule CD4 Mimic

CD4-mimetic compounds exemplified by NBD-556 and **191** induce conformational changes in the HIV-1 envelope glycoproteins similar to those induced by sCD4 [31,33]. These changes include formation/exposure of both the coreceptor-binding site on gp120 and the HR1 groove on gp41 (Figure 5). The similarity between the effects of **191** and sCD4 on HIV-1 infection of $CD4^+$ and $CD4^-$ cells (Figure 1) suggested that **191** may also induce transiently activated intermediate states in the HIV-1 envelope glycoproteins. To examine this possibility, we compared the decay profiles associated with sCD4 and **191**. We examined the YU2 and AD8 envelope glycoproteins, which exhibit dramatic differences in the decay rate of the sCD4-induced intermediate. For each of these envelope glycoproteins, sCD4 and **191** induced identical decay profiles, both for HR1 groove exposure and for infectivity (Figure 6). These results suggest that sCD4 and **191** induce a similar, transient intermediate state in the HIV-1 envelope glycoproteins. Moreover, the differences in decay rates between the AD8 and YU2 envelope glycoproteins were evident for both sCD4 and **191**, suggesting that the stability of the induced state is determined by intrinsic properties of the envelope glycoproteins rather than by the activating agent.

A More Stable Envelope Glycoprotein Intermediate Induced by Cell-Surface CD4

To examine the longevity of the activated intermediate induced during the normal HIV-1 entry process, we examined the stability of HR1 groove exposure after the binding of the envelope glycoproteins to cell-surface CD4. For this purpose, 293T cells that express CD4 (but not CCR5) were used to activate the HIV-1 envelope glycoproteins expressed on COS-1 cells. Pilot experiments demonstrated that the observed increases in C34-Ig binding to the envelope glycoproteins-expressing cells depended on the presence of CD4 on the activating cell, and were not observed for a mutant envelope glycoprotein (YU2-GS8), which binds CD4 efficiently but does not expose the HR1 groove in response (see Figure S6 and Materials and Methods). Relative to the effects of treatment with sCD4 or **191**, the HR1 groove exposure consequent to activation by cell-surface CD4 was surprisingly long-lived (Figure 7A). The AD8 and YU2 envelope glycoproteins, which exhibited significant differences in the half-lives of HR1 groove exposure after activation by sCD4, both formed stable intermediates following activation by cell-surface CD4.

During HIV-1 entry, CCR5 binding to the CD4-induced envelope glycoprotein intermediate promotes progression along the path to virus entry [58]. Differences in the longevity of the CD4-induced state would be predicted to manifest themselves as an altered dependency on the density of target cell CCR5. To test this, the CCR5 available on CD4-expressing cells for interaction with the HIV-1 envelope glycoproteins was varied in two ways: 1) the addition of increasing amounts of Compound A, a CCR5 inhibitory compound [41,42,59], to cells expressing both CD4 and CCR5; and 2) transfection of different amounts of a CCR5-expressing plasmid into cells expressing CD4. The latter method is based on the direct relationship between the amount of CCR5 DNA transfected and the cell-surface density of the expressed

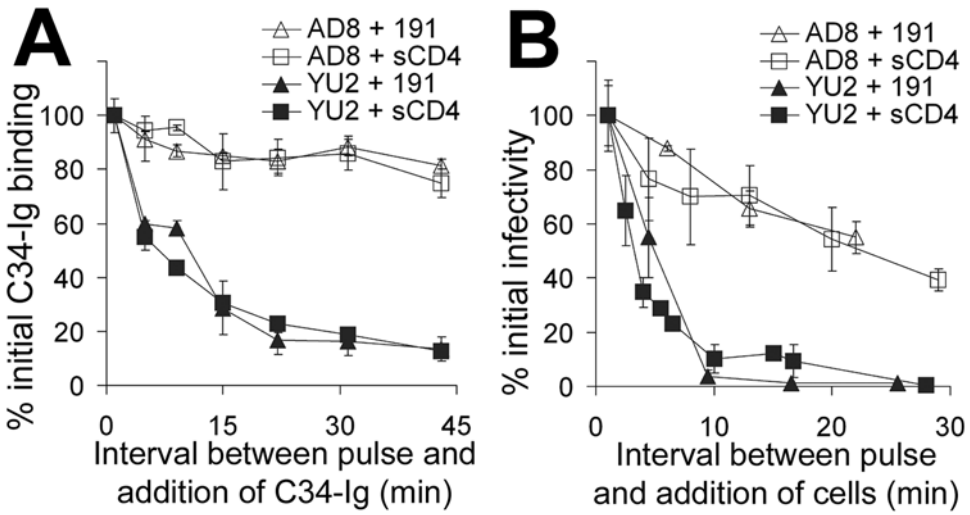

Figure 6. Longevity of the HIV-1 envelope glycoprotein intermediate at room temperature after activation by sCD4 or 191. (A) The decay of HR1 groove exposure for cell-surface–expressed YU2 and AD8 envelope glycoproteins is compared after pulse activation with **191** (360 μM) or sCD4 (40 μg/ml, 0.8 μM). (B) The decay of the ability to infect $CD4^-CCR5^+$ Cf2Th cells after pulse activation with **191** or sCD4 is compared.
doi:10.1371/journal.ppat.1000360.g006

CCR5 molecule (Figure S7). The cells were then exposed to HIV-1(AD8) or HIV-1(YU2) and the efficiency of infection measured. HIV-1(AD8) and HIV-1(YU2) behaved indistinguishably in response to variations in the CCR5 available on target cells expressing CD4 (Figure 7B and 7C). In contrast, when sCD4 was used to activate infection of Cf2Th cells expressing different levels of CCR5, entry by HIV-1(AD8) was significantly better than that of HIV-1(YU2) (Figure 7D). These results are consistent with the existence of a relatively long-lived envelope glycoprotein intermediate being induced by CD4 expressed on the target membrane.

Discussion

Clinical testing of the inhibitory efficiency of sCD4 revealed no reduction of viral loads in HIV-1-infected individuals [13]. Failure of treatment was attributed to the resistance to sCD4-mediated inhibition of primary HIV-1 isolates, relative to laboratory-adapted isolates [13]. However, lower sCD4-binding affinity could not be consistently correlated with resistance of HIV-1 isolates to inhibition [17,19]. Furthermore, in vitro observations of sCD4-mediated enhancement of infection [14] remained largely unexplained. More recently, small-molecular-weight compounds have been developed that target the highly conserved CD4-binding site of the gp120 envelope glycoprotein [31,32]. NBD-556 and its derivatives bind to the gp120 envelope glycoprotein and induce structural changes similar to those promoted by sCD4. Although currently NBD-556 and analogues are only interesting tools to study the entry process, with improvement, they could prove useful therapeutically or prophylactically. However, in view of their potential to enhance HIV-1 infection, an understanding of the mechanisms underlying the effects of SCMs is essential for the safe application of these inhibitors.

In this study, we apply a new approach to define the dynamics of conformational changes that occur in the trimeric membrane-bound form of the HIV-1 envelope glycoproteins. The binding of conformation-specific probes was directly measured at high temporal resolution, allowing us to monitor transiently exposed structures and thus to define the longevity of specific activated intermediates. The lack of dependence on indirect methods, such as the use of conformation-specific inhibitors, and the capacity to detect conformational intermediates permitted identification of an SCM-induced transition to the inactive state. In contrast to previous observations based on the interactions of envelope glycoprotein- and receptor-expressing cells [26,60], we detected no lag in the formation/exposure of either the gp120 coreceptor-binding site or the gp41 HR1 groove, two key signatures of the SCM-activated state. Even at low temperatures, both sites were immediately exposed after binding of the SCMs to gp120. This is consistent with a model in which conformational changes in the envelope glycoproteins associated with SCM binding are tightly coupled, or perhaps coincide, with the structural transitions that shape and expose the coreceptor-binding site and the HR1 coiled coil.

Except for its lower affinity for the envelope glycoproteins, the NBD-556 analogue **191** [31,33] exerted effects that were remarkably similar to those exerted by sCD4. Thus, the properties of the SCM-induced intermediate defined in this study are intrinsic to the envelope glycoproteins of the particular HIV-1 strain rather than being dependent on the individual SCMs.

During HIV-1 infection of $CD4^+$ cells, SCMs compete for cell-associated CD4. Competition for the cell-surface CD4 receptor was previously suggested as a major mechanism of HIV-1 inhibition by sCD4 [17,18]. In this work, we show that SCMs can efficiently substitute for cell-surface CD4. In this context, some inhibition of infection may result from the difference in the efficiency with which membrane-anchored CD4 and SCMs promote HIV-1 entry. Importantly, we demonstrate that SCMs inhibit HIV-1 infection by a novel mechanism that is initiated by activation of the viral envelope glycoproteins. Similar to the envelope glycoprotein intermediate that results from binding cell-surface CD4, the SCM-induced activated state is characterized by the exposure of the coreceptor-binding site on gp120 and the HR1 groove on gp41. Moreover, the SCM-activated envelope glycoproteins are able to mediate virus entry into $CCR5^+$ cells lacking CD4. However, in contrast to the stable activation induced by cell-surface CD4, the SCM-activated intermediate decays rapidly, in a manner dependent upon temperature and envelope glycoprotein

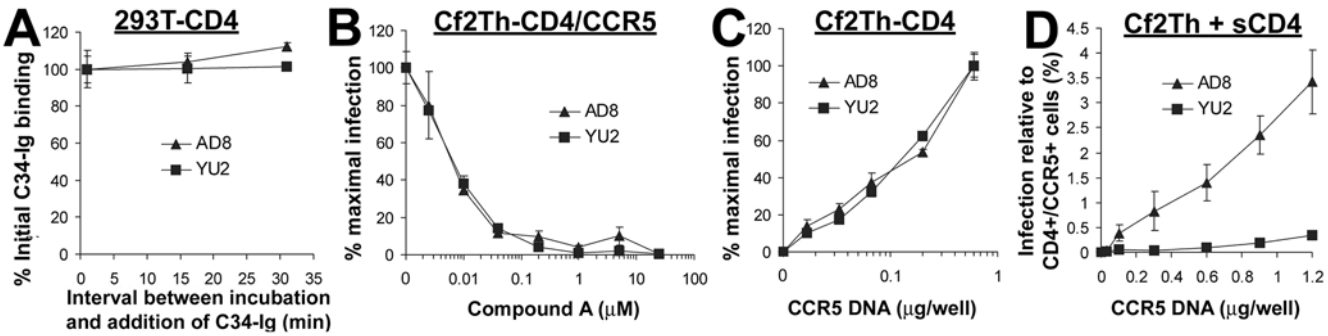

Figure 7. HIV-1 activation by native CD4 and sCD4. (A) The stability of HR1 groove exposure was measured after activation of the YU2 or AD8 envelope glycoproteins by cell-surface CD4. Background was defined as C34-Ig binding to cells transfected with the YU2-GS8 construct, which engages sCD4 with an affinity similar to that of the wild-type YU2 envelope glycoproteins but does not expose the HR1 groove (see Figure S6). The background was subtracted from all measurements, which are presented as percent (±s.e.m.) of C34-Ig binding measured at the initial time point. (B) The effect of the CCR5 antagonist "Compound A" [41,42] on infectivity of recombinant HIV-1 pseudotyped with the indicated envelope glycoproteins was investigated. Cf2Th-CD4/CCR5 cells were infected with HIV-1(AD8) or HIV-1(YU2) in the presence of increasing concentrations of Compound A. Data are presented as the percentage (±s.e.m.) of infection measured in the absence of the compound. (C) The effect of CCR5 expression on the infection of CD4-expressing cells by HIV-1(AD8) or HIV-1(YU2) was examined. Cf2Th-CD4 cells were transfected with different amounts of a plasmid that expresses human CCR5. Two days later, transfected cells were incubated with HIV-1(AD8) or HIV-1(YU2). Infectivity is expressed as the percentage (±s.e.m.) of infectivity measured for cells transfected with the highest amount of the CCR5-expressing plasmid. (D) The graph shows infection by cell-bound virus of $CD4^-$ Cf2Th cells transfected with different amounts of the CCR5-expressing plasmid in the presence of 20 μg/ml sCD4. Infectivity is expressed as the percentage (±s.e.m.) of infection measured in cells transfected with plasmids expressing CD4 and CCR5 (0.6 and 0.9 μg, respectively, of each plasmid per well).
doi:10.1371/journal.ppat.1000360.g007

strain. In the process, both exposure of the HR1 groove and membrane-fusing potential are irreversibly lost.

The SCM-induced exposure of the hydrophobic HR1 groove may be energetically unfavorable in the context of free virus, favoring a transition to a more stable but nonfunctional state. Whether this nonfunctional state involves a prematurely triggered six-helix bundle in gp41 or another, possibly off-pathway, conformation requires further investigation. Arguing against the former possibility is the expectation that six-helix bundle formation in gp41 would be incompatible with maintaining the non-covalent association with gp120. In fact, even for the most unstable envelope glycoprotein intermediate studied, no evidence of gp120 shedding after SCM treatment was observed. Despite rapid loss of function, the SCM-inactivated envelope glycoproteins retained gp120, which remained associated with the SCM and stably attached to the expressing cell surface. This finding is consistent with previous studies of dose response, temperature dependence, timing and HIV-1 strain specificity that show a lack of correlation between the HIV-1-inhibitory activity of sCD4 and the degree of gp120 shedding induced [14,17,19,21,25].

By contrast, the kinetics of the decay of SCM-induced HR1 groove exposure and the decay of HIV-1 infectivity correlate, and the ranges of SCM concentrations required for induction of the labile envelope glycoprotein intermediate and for virus neutralization overlap. These observations support the important contribution that induction of the metastable activated intermediate makes to SCM-mediated inhibition of virus infectivity. Achieving inhibition by initiating the targeted process is unusual, but two properties of the HIV-1 envelope glycoproteins render them susceptible to this strategy of inhibition: 1) initial folding and assembly into a high-potential-energy form that is prone to transform into energetically more favorable states; and 2) triggering of these conformational transitions by receptor binding, allowing a receptor mimic to take advantage of the built-in propensity of the viral envelope glycoproteins to engage the receptor and undergo global conformational changes.

The efficiency of an activation-based mechanism of inhibition is determined by the change over time in the distribution of the HIV-1 envelope glycoproteins among three states: 1) unliganded/non-activated; 2) bound/activated; and 3) post-activation decayed. This distribution is influenced by the following factors: 1) rate of SCM engagement; 2) the time interval between SCM-induced activation and progression to a step of infection that is unaffected by the decay process; and 3) the intrinsic stability of the SCM-induced activated intermediate. Forces that determine the distribution between these three states dictate the balance between enhancement and inhibition of infection, as detailed below.

Infection by cell-free virus is rate-limited by the slow diffusion-dependent attachment of the virus to the cell surface [53,54]. Activation of the diffusing virus by a soluble molecule is thus characterized by an extended lag period between activation and the next step of the infection sequence. Half-maximal productive adsorption of diffusing HIV-1 virions to a cell monolayer (i.e., attachment that culminates in an infection event) occurs after approximately 5 hours at 37°C [55]. By contrast, the half-life of infectivity of the most stable activated intermediate examined in this study at 37°C was less than 8 minutes. As the longevity of the SCM-activated intermediate is significantly shorter than the duration of the attachment step, SCM-mediated inhibition of cell-free virus is primarily determined by the rate of activation (i.e. by both the on-rate and effective concentration of the compound).

Activating effects on HIV-1 infection predominate at low concentrations of SCMs. The dependence of virus activation and inactivation on SCM concentration was particularly evident in the biphasic dose-effect curves associated with HIV-1(YU2) infection of $CD4^-$ $CCR5^+$ target cells (Figure 1A and 1B and Figure S5). The stoichiometry of SCM binding to the HIV-1 envelope glycoprotein trimers may influence the propensity of the activated intermediate(s) to proceed along entry or post-activation decay pathways. For example, the binding of two SCMs to the envelope glycoprotein trimer may be more efficient in promoting inactivation/decay than the binding of a single SCM. Such a model would explain the exceptionally long-lived sCD4 activation of SIV [15,61], the envelope glycoproteins of which have been reported to bind only one CD4 molecule per trimer [62,63].

Retrovirus transmission is significantly more efficient when virus is transferred through direct physical interaction between cells (cell-cell transmission) than by diffusion of virions in cell-free transmission [64]. During cell-cell transmission, where HIV-1 virions emerging from the infected cell rapidly achieve proximity to the target cell [65,66], SCMs are more likely to enhance infection than in the case of cell-free infection. Indeed, HIV-1 that was pre-bound to the surface of $CD4^-CCR5^+$ cells, perhaps mimicking the conditions of cell-cell transmission, infected the cells efficiently after incubation with SCM concentrations that were highly neutralizing for cell-free virus. In cell-cell transmission, the time interval between SCM-induced activation and the next step committed to the infection pathway exerts a dominant influence on the efficiency of HIV-1 inhibition by SCMs. Several observations suggest that the engagement of the coreceptor plays a major role in moving the SCM-activated HIV-1 envelope glycoproteins along the entry pathway. First, the sCD4-mediated enhancement of HIV-1 infection of $CD4^-$ cells is highly dependent on the level of CCR5 expression (Figure 7D). Second, a study of activation of infection of $CD4^-CCR5^+$ cells by NBD-556 indicated a contribution of CCR5-binding affinity to susceptibility to enhancement [33]. Finally, although SCMs allowed CCR5-using viruses to infect $CD4^-CCR5^+$ cells, SCMs did not stimulate the infection of $CD4^-CXCR4^+$ cells by CXCR4-using viruses. The lack of enhancement of CXCR4-using viruses was not due to greater lability of the activated state. The half-life of the sCD4-induced, HR1-groove-exposed state on the CXCR4-tropic HXBc2 envelope glycoproteins was 55 minutes at 26°C, and was significantly longer on the dual-tropic KB9 envelope glycoproteins. Despite this, neither of these envelope glycoproteins supported infection of $CD4^-CXCR4^+$ cells after incubation with sCD4 or **191** [ref. 33 and data not shown]. However, **191** did allow viruses with the KB9 envelope glycoproteins to infect $CD4^-CCR5^+$ cells. The apparent inability of SCM-activated viruses to utilize CXCR4 for entry may be a consequence of the significantly lower affinity of CXCR4 for the HIV-1 envelope glycoproteins, relative to that of CCR5 [67]. Together, these observations support the importance of efficient coreceptor binding to the susceptibility of HIV-1 to SCM-induced activation of infection of $CD4^-$ cells. Further work will be required to assess whether this type of enhancement can occur on primary $CD4^-CCR5^+$ cells following SCM treatment.

The mechanism of inhibition elucidated here suggests that SCMs will be most effective in settings, such as sexual transmission, in which HIV-1 is fully dependent on diffusion for successful infection. Efforts to develop small-molecule SCMs with improved rates of engaging the HIV-1 envelope glycoproteins are therefore warranted.

Binding of the HIV-1 envelope glycoproteins to native, membrane-anchored CD4 resulted in the stable exposure of the HR1 groove on gp41, in contrast to the labile structure induced by SCMs. Although additional studies will be needed to address the basis of this difference, our data rule out the contribution of CCR5

or CXCR4 on the target cell. The stable nature of the activated HIV-1 envelope glycoprotein intermediate induced by cell surface CD4 facilitates engagement of additional CD4 molecules and the coreceptor, and creates a "window of opportunity" for inhibition of downstream events in virus entry.

Supporting Information

Figure S1 Decay of HR1 groove exposure measured by FACS. Cells that express the YU2(Δct) envelope glycoproteins were incubated at room temperature with sCD4 (40 μg/ml; 0.8 μM) for 20 min, washed, and further incubated at room temperature for the indicated time periods. Then the C34-Ig protein (40 μg/ml) was added. Binding of sCD4 and C34-Ig was detected by fluorescein- and phycoerythrin-conjugated antibodies, respectively, as described in the Figure 3 legend. Note that the decrease in the mean fluorescence intensity of C34-Ig binding (right panel) was more modest than the decrease in the percentage of the double-positive cell population.
Found at: doi:10.1371/journal.ppat.1000360.s001 (0.44 MB TIF)

Figure S2 The kinetics, affinity, and consequences of soluble CD4 binding to the HIV-1 envelope glycoproteins. (A) Binding of sCD4 to the YU2 and AD8 envelope glycoprotein complexes on the surface of expressing cells was examined. COS-1 cells expressing the YU2 and AD8 full-length envelope glycoproteins were incubated with the indicated concentrations of sCD4 for 1 h at room temperature. Cells were then washed four times and incubated with the anti-CD4 monoclonal antibody OKT4 (10 μg/ml) for 30 min. Cells were subsequently washed, and binding was detected using a horseradish peroxidase-conjugated goat-anti-mouse polyclonal antibody. Results are presented as mean RLU (±s.e.m.) of two replicate samples. (B) The kinetics of CD4-Ig binding to full-length YU2 and JR-FL envelope glycoproteins expressed on the surface of COS-1 cells was measured by the cell-based ELISA method. CD4-Ig was added at 0.5 μg/ml. Results are presented as the percentage of binding measured at the final time point examined. (C) Decay of gp41 HR1 groove exposure for the indicated envelope glycoproteins at 25°C after pulse-activation with sCD4. (D) Decay of gp41 HR1 exposure at 25°C and 37°C after pulse activation by sCD4 (40 μg/ml; 0.8 μM). (E) Decay of HIV-1(KB9) and HIV-1(89.6) infectivity at 37°C after pulse activation by sCD4 (40 μg/ml; 0.8 μM).
Found at: doi:10.1371/journal.ppat.1000360.s002 (0.68 MB TIF)

Figure S3 Decay of HIV-1 infectivity at different temperatures after pulse activation with sCD4. (A) HIV-1(JR-FL) virions were magnetically immobilized on tissue-culture plates and pulsed with sCD4 (40 μg/ml; 0.8 μM) for three minutes at 26°C. Samples were then washed and incubated at the indicated temperatures for 20 min. Cf2Th-CCR5 cells were subsequently added and pelleted onto the viruses. Two days later, infectivity was measured by luciferase assays. (B) As a control, viruses were pulsed with buffer, incubated at the different temperatures, and then Cf2Th-CD4/CCR5 cells were added. Infectivity was measured two days later and is presented as mean RLU (±s.e.m.) of three replicate samples.
Found at: doi:10.1371/journal.ppat.1000360.s003 (0.31 MB TIF)

Figure S4 Decay of infectivity of viruses bearing different HIV-1 envelope glycoproteins. Recombinant, luciferase-expressing viruses that contain the indicated envelope glycoproteins were incubated in culture medium at 37°C for different time periods and then added to Cf2Th-CD4/CCR5 cells. 48 h later, luciferase activity in the target cells was measured to estimate the level of infection. Data are presented as the percentage of infectivity observed in samples not incubated at 37°C. The inset shows a comparison between the infectivity half-lives of the non-activated viruses (measured at 37°C with CD4+CCR5+ cells) and the sCD4-activated viruses (measured at 26°C with CD4−CCR5+ cells).
Found at: doi:10.1371/journal.ppat.1000360.s004 (0.43 MB TIF)

Figure S5 Change in cell-free HIV-1 infectivity after engagement of sCD4. HIV-1(YU2) or HIV-1(JR-FL) virions were associated with magnetite nanoparticles and then incubated with the indicated concentrations of sCD4 for different time periods at 26°C. Complexes were then added to confluent cultures of Cf2Th-CCR5 cells to which a magnetic field was applied. After incubation for 1 min, cells were washed and further cultured for two days. As a control, complexes of viruses and magnetite nanoparticles were incubated with buffer and then adsorbed to Cf2Th-CD4/CCR5 cells. Results are presented as mean RLU (±s.e.m.) of three replicate samples.
Found at: doi:10.1371/journal.ppat.1000360.s005 (0.66 MB TIF)

Figure S6 Activation of the HIV-1 envelope glycoproteins by cell-surface CD4. (A) The abilities of the YU2 and YU2-GS8 envelope glycoproteins to bind different ligands were compared, using the cell-based ELISA. COS-1 cells transfected with plasmids expressing the indicated envelope glycoproteins were incubated with the monoclonal antibodies 39F or IgG1b12 (both at 0.5 μg/ml), or C34-Ig (20 μg/ml), with or without sCD4 (20 μg/ml; 0.4 μM). Data are presented as mean RLU (±s.e.m.) of two replicate samples. (B,C) 293T cells transfected with a plasmid expressing wild-type human CD4 or with the control ΔKS plasmid were added to COS-1 cells transfected with plasmids expressing ΔKS, wild-type YU2, or the YU2-GS8 envelope glycoproteins. Cells were pelleted to increase approximation and incubated at 4°C for 75 minutes to allow CD4 engagement. Samples were then incubated with C34-Ig (20 μg/ml) to measure HR1 groove exposure (B) or the anti-CD4 antibody sc-70660 (Santa Cruz Biotechnology) to measure association of the 293T-CD4 cells with the COS-1 cell monolayer. Antibody binding was detected using HRP-conjugated antibodies. Data are presented as mean RLU (±s.e.m.) of two replicate samples. (D) The experiments described in (B) were repeated, expressing CD4 and the HIV-1 YU2 envelope glycoproteins (or the ΔKS control) in either COS-1 or 293T cells.
Found at: doi:10.1371/journal.ppat.1000360.s006 (0.56 MB TIF)

Figure S7 Relationship between the amount of transfected CCR5-expressing plasmid DNA and the density of CCR5 on the surface of the transfected cells. (A) COS-1 cells cultured in 96-well plates (2.4×10^4 cells per well) were transfected using Effectene reagent (Qiagen) with the indicated amounts of the pcDNA3.1-CCR5 plasmid, which expresses the CCR5 gene under the control of the hCMV-IE promoter. Each well was transfected with the same total amount of DNA (0.1 μg) by supplementing the pcDNA3.1-CCR5 plasmid with the ΔKS plasmid. Two days later, CCR5 expression was measured using the cell-based ELISA method with the anti-CCR5 monoclonal antibody 2D7 (1 μg/ml), detected with a horseradish peroxidase-conjugated goat-anti-mouse IgG2a antibody. Data are presented as mean RLU (±s.e.m.) of two replicate samples. (B) Cf2Th cells cultured in 10-cm plates were transfected using Lipofectamine 2000 reagent (Invitrogen) with the indicated amounts of the pcDNA3.1-CCR5 plasmid. Three days later, cells were analyzed for CCR5 expression with a phycoerythrin-conjugated 2D7 antibody using an EPICS XL flow cytometer (Beckman-Coulter). Data were analyzed using WinMDI 2.9 software.
Found at: doi:10.1371/journal.ppat.1000360.s007 (0.18 MB TIF)

Acknowledgments

We thank James Robinson for the 48d monoclonal antibody. We thank Ms. Yvette McLaughlin and Ms. Elizabeth Carpelan for manuscript preparation.

Author Contributions

Conceived and designed the experiments: HH NM AK JGS. Performed the experiments: HH. Analyzed the data: HH ZS JGS. Contributed reagents/materials/analysis tools: HH ZS NM LW JRC AP MD KME MM DG ABS. Wrote the paper: HH JGS.

References

1. Wyatt R, Sodroski J (1998) The HIV-1 envelope glycoproteins: fusogens, antigens, and immunogens. Science 280: 1884–1888.
2. Myszka DG, Sweet RW, Hensley P, Brigham-Burke M, Kwong PD, et al. (2000) Energetics of the HIV gp120-CD4 binding reaction. Proc Natl Acad Sci U S A 97: 9026–9031.
3. Choe H, Farzan M, Sun Y, Sullivan N, Rollins B, et al. (1996) The beta-chemokine receptors CCR3 and CCR5 facilitate infection by primary HIV-1 isolates. Cell 85: 1135–1148.
4. Deng H, Liu R, Ellmeier W, Choe S, Unutmaz D, et al. (1996) Identification of a major co-receptor for primary isolates of HIV-1. Nature 381: 661–666.
5. Dragic T, Litwin V, Allaway GP, Martin SR, Huang Y, et al. (1996) HIV-1 entry into CD4+ cells is mediated by the chemokine receptor CC-CKR-5. Nature 381: 667–673.
6. Feng Y, Broder CC, Kennedy PE, Berger EA (1996) HIV-1 entry cofactor: functional cDNA cloning of a seven-transmembrane, G protein-coupled receptor. Science 272: 872–877.
7. Alkhatib G, Combadiere C, Broder CC, Feng Y, Kennedy PE, et al. (1996) CC CKR5: a RANTES, MIP-1alpha, MIP-1beta receptor as a fusion cofactor for macrophage-tropic HIV-1. Science 272: 1955–1958.
8. Chan DC, Chutkowski CT, Kim PS (1998) Evidence that a prominent cavity in the coiled coil of HIV type 1 gp41 is an attractive drug target. Proc Natl Acad Sci U S A 95: 15613–15617.
9. Tan K, Liu J, Wang J, Shen S, Lu M (1997) Atomic structure of a thermostable subdomain of HIV-1 gp41. Proc Natl Acad Sci U S A 94: 12303–12308.
10. Wild CT, Shugars DC, Greenwell TK, McDanal CB, Matthews TJ (1994) Peptides corresponding to a predictive alpha-helical domain of human immunodeficiency virus type 1 gp41 are potent inhibitors of virus infection. Proc Natl Acad Sci U S A 91: 9770–9774.
11. Chan DC, Fass D, Berger JM, Kim PS (1997) Core structure of gp41 from the HIV envelope glycoprotein. Cell 89: 263–273.
12. Weissenhorn W, Dessen A, Harrison SC, Skehel JJ, Wiley DC (1997) Atomic structure of the ectodomain from HIV-1 gp41. Nature 387: 426–430.
13. Daar ES, Li XL, Moudgil T, Ho DD (1990) High concentrations of recombinant soluble CD4 are required to neutralize primary human immunodeficiency virus type 1 isolates. Proc Natl Acad Sci U S A 87: 6574–6578.
14. Sullivan N, Sun Y, Binley J, Lee J, Barbas CF III, et al. (1998) Determinants of human immunodeficiency virus type 1 envelope glycoprotein activation by soluble CD4 and monoclonal antibodies. J Virol 72: 6332–6338.
15. Schenten D, Marcon L, Karlsson GB, Parolin C, Kodama T, et al. (1999) Effects of soluble CD4 on simian immunodeficiency virus infection of CD4-positive and CD4-negative cells. J Virol 73: 5373–5380.
16. Clapham PR, McKnight A, Weiss RA (1992) Human immunodeficiency virus type 2 infection and fusion of CD4-negative human cell lines: induction and enhancement by soluble CD4. J Virol 66: 3531–3537.
17. Orloff SL, Kennedy MS, Belperron AA, Maddon PJ, McDougal JS (1993) Two mechanisms of soluble CD4 (sCD4)-mediated inhibition of human immunodeficiency virus type 1 (HIV-1) infectivity and their relation to primary HIV-1 isolates with reduced sensitivity to sCD4. J Virol 67: 1461–1471.
18. Moore JP, McKeating JA, Norton WA, Sattentau QJ (1991) Direct measurement of soluble CD4 binding to human immunodeficiency virus type 1 virions: gp120 dissociation and its implications for virus-cell binding and fusion reactions and their neutralization by soluble CD4. J Virol 65: 1133–1140.
19. Groenink M, Moore JP, Broersen S, Schuitemaker H (1995) Equal levels of gp120 retention and neutralization resistance of phenotypically distinct primary human immunodeficiency virus type 1 variants upon soluble CD4 treatment. J Virol 69: 523–527.
20. Moore JP, McKeating JA, Huang YX, Ashkenazi A, Ho DD (1992) Virions of primary human immunodeficiency virus type 1 isolates resistant to soluble CD4 (sCD4) neutralization differ in sCD4 binding and glycoprotein gp120 retention from sCD4-sensitive isolates. J Virol 66: 235–243.
21. Thali M, Furman C, Helseth E, Repke H, Sodroski J (1992) Lack of correlation between soluble CD4-induced shedding of the human immunodeficiency virus type 1 exterior envelope glycoprotein and subsequent membrane fusion events. J Virol 66: 5516–5524.
22. Bugelski PJ, Ellens H, Hart TK, Kirsh RL (1991) Soluble CD4 and dextran sulfate mediate release of gp120 from HIV-1: implications for clinical trials. J Acquir Immune Defic Syndr 4: 923–924.
23. Hart TK, Kirsh R, Ellens H, Sweet RW, Lambert DM, et al. (1991) Binding of soluble CD4 proteins to human immunodeficiency virus type 1 and infected cells induces release of envelope glycoprotein gp120. Proc Natl Acad Sci U S A 88: 2189–2193.
24. Moore JP, McKeating JA, Weiss RA, Sattentau QJ (1990) Dissociation of gp120 from HIV-1 virions induced by soluble CD4. Science 250: 1139–1142.
25. Chertova E, Bess JW Jr, Crise BJ, Sowder IR, Schaden TM, et al. (2002) Envelope glycoprotein incorporation, not shedding of surface envelope glycoprotein (gp120/SU), is the primary determinant of SU content of purified human immunodeficiency virus type 1 and simian immunodeficiency virus. J Virol 76: 5315–5325.
26. McDougal JS, Kennedy MS, Orloff SL, Nicholson JK, Spira TJ (1996) Mechanisms of human immunodeficiency virus Type 1 (HIV-1) neutralization: irreversible inactivation of infectivity by anti-HIV-1 antibody. J Virol 70: 5236–5245.
27. Arthos J, Cicala C, Steenbeke TD, Chun TW, Dela Cruz C, et al. (2002) Biochemical and biological characterization of a dodecameric CD4-Ig fusion protein: implications for therapeutic and vaccine strategies. J Biol Chem 277: 11456–11464.
28. Allaway GP, Davis-Bruno KL, Beaudry GA, Garcia EB, Wong EL, et al. (1995) Expression and characterization of CD4-IgG2, a novel heterotetramer that neutralizes primary HIV type 1 isolates. AIDS Res Hum Retroviruses 11: 533–539.
29. Trkola A, Pomales AB, Yuan H, Korber B, Maddon PJ, et al. (1995) Cross-clade neutralization of primary isolates of human immunodeficiency virus type 1 by human monoclonal antibodies and tetrameric CD4-IgG. J Virol 69: 6609–6617.
30. Martin L, Stricher F, Misse D, Sironi F, Pugniere M, et al. (2003) Rational design of a CD4 mimic that inhibits HIV-1 entry and exposes cryptic neutralization epitopes. Nat Biotechnol 21: 71–76.
31. Schön A, Madani N, Klein JC, Hubicki A, Ng D, et al. (2006) Thermodynamics of binding of a low–molecular-weight CD4 mimetic to HIV-1 gp120. Biochemistry 45: 10973–10980.
32. Zhao Q, Ma L, Jiang S, Lu H, Liu S, et al. (2005) Identification of N-phenyl-N′-(2,2,6,6-tetramethyl-piperidin-4-yl)-oxalamides as a new class of HIV-1 entry inhibitors that prevent gp120 binding to CD4. Virology 339: 213–225.
33. Madani N, Schön A, Princiotto AM, LaLonde JM, Courter JR, et al. (2008) Small-molecule CD4 mimics interact with a highly conserved pocket on HIV-1 gp120. Structure 16: 1689–1701.
34. Gallo SA, Puri A, Blumenthal R (2001) HIV-1 gp41 six-helix bundle formation occurs rapidly after the engagement of gp120 by CXCR4 in the HIV-1 Env-mediated fusion process. Biochemistry 40: 12231–12236.
35. Munoz-Barroso I, Durell S, Sakaguchi K, Appella E, Blumenthal R (1998) Dilation of the human immunodeficiency virus-1 envelope glycoprotein fusion pore revealed by the inhibitory action of a synthetic peptide from gp41. J Cell Biol 140.
36. Steger HK, Root MJ (2006) Kinetic dependence to HIV-1 entry inhibition. J Biol Chem 281: 25813–25821.
37. Melikyan GB, Markosyan RM, Hemmati H, Delmedico MK, Lambert DM, et al. (2000) Evidence that the transition of HIV-1 gp41 into a six-helix bundle, not the bundle configuration, induces membrane fusion. J Cell Biol 151: 413–423.
38. Furuta RA, Wild CT, Weng Y, Weiss CD (1998) Capture of an early fusion-active conformation of HIV-1 gp41. Nat Struct Biol 5: 276–279.
39. Mkrtchyan SR, Markosyan RM, Eadon MT, Moore JP, Melikyan GB, et al. (2005) Ternary complex formation of human immunodeficiency virus type 1 Env, CD4, and chemokine receptor captured as an intermediate of membrane fusion. J Virol 79: 11161–11169.
40. Yang X, Tomov V, Kurteva S, Wang L, Ren X, et al. (2004) Characterization of the outer domain of the gp120 glycoprotein from human immunodeficiency virus type 1. J Virol 78: 12975–12986.
41. Finke PE, Oates B, Mills SG, MacCoss M, Malkowitz L, et al. (2001) Antagonists of the human CCR5 receptor as anti-HIV-1 agents. Part 4. Synthesis and structure-activity relationships for 1-[*N*-(methyl)-*N*-(phenylsulfonyl)amino]-2-(phenyl)-4(4-(*N*-(alkyl)-*N*-(benzyloxycarbonyl)amino)piperidin-1-yl)-butanes. Bioorg Med Chem Lett 11: 2475–2479.
42. Hale JJ, Budhu RJ, Holson EB, Finke PE, Oates B, et al. (2001) 1,3,4-Trisubstituted pyrrolidine CCR5 receptor antagonists. Part 2: lead optimization affording selective, orally bioavailable compounds with potent anti-HIV activity. Bioorg Med Chem Lett 11: 2741–2745.
43. Thali M, Moore JP, Furman C, Charles M, Ho DD, et al. (1993) Characterization of conserved human immunodeficiency virus type 1 gp120 neutralization epitopes exposed upon gp120-CD4 binding. J Virol 67: 3978–3988.
44. Zhou T, Xu L, Dey B, Hessell AJ, Van Ryk D, et al. (2007) Structural definition of a conserved neutralization epitope on HIV-1 gp120. Nature 445: 732–737.
45. Kwong PD, Doyle ML, Casper DJ, Cicala C, Leavitt SA, et al. (2002) HIV-1 evades antibody-mediated neutralization through conformational masking of receptor-binding sites. Nature 420: 678–682.
46. Korber B, Foley B, Kuiken C, Pillai S, Sodroski J (1998) Human Retroviruses and AIDS. Los Alamos: Los Alamos Natl. Lab.

47. Si Z, Madani N, Cox JM, Chruma JJ, Klein JC, et al. (2004) Small-molecule inhibitors of HIV-1 entry block receptor-induced conformational changes in the viral envelope glycoproteins. Proc Natl Acad Sci U S A 101: 5036–5041.
48. Dunfee RL, Thomas ER, Gorry PR, Wang J, Taylor J, et al. (2006) The HIV Env variant N283 enhances macrophage tropism and is associated with brain infection and dementia. Proc Natl Acad Sci U S A 103: 15160–15165.
49. Sullivan N, Sun Y, Li J, Hofmann W, Sodroski J (1995) Replicative function and neutralization sensitivity of envelope glycoproteins from primary and T-cell line-passaged human immunodeficiency virus type 1 isolates. J Virol 69: 4413–4422.
50. Parolin C, Taddeo B, Palu G, Sodroski J (1996) Use of cis- and trans-acting viral regulatory sequences to improve expression of human immunodeficiency virus vectors in human lymphocytes. Virology 222: 415–422.
51. Zhang W, Godillot AP, Wyatt R, Sodroski J, Chaiken I (2001) Antibody 17b binding at the coreceptor site weakens the kinetics of the interaction of envelope glycoprotein gp120 with CD4. Biochemistry 40: 1662–1670.
52. Zhang CW, Chishti Y, Hussey RE, Reinherz EL (2001) Expression, purification, and characterization of recombinant HIV gp140. The gp41 ectodomain of HIV or simian immunodeficiency virus is sufficient to maintain the retroviral envelope glycoprotein as a trimer. J Biol Chem 276: 39577–39585.
53. Haim H, Steiner I, Panet A (2005) Synchronized infection of cell cultures by magnetically controlled virus. J Virol 79: 622–625.
54. Andreadis S, Lavery T, Davis HE, Le Doux JM, Yarmush ML, et al. (2000) Toward a more accurate quantitation of the activity of recombinant retroviruses: alternatives to titer and multiplicity of infection. J Virol 74: 3431–3439.
55. Haim H, Steiner I, Panet A (2007) Time frames for neutralization during the human immunodeficiency virus type 1 entry phase, as monitored in synchronously infected cell cultures. J Virol 81: 3525–3534.
56. Wu L, Gerard NP, Wyatt R, Choe H, Parolin C, et al. (1996) CD4-induced interaction of primary HIV-1 gp120 glycoproteins with the chemokine receptor CCR-5. Nature 384: 179–183.
57. Wyss S, Berlioz-Torrent C, Boge M, Blot G, Honing S, et al. (2001) The highly conserved C-terminal dileucine motif in the cytosolic domain of the human immunodeficiency virus type 1 envelope glycoprotein is critical for its association with the AP-1 clathrin adaptor [correction of adapter]. J Virol 75: 2982–2992.
58. Berger EA, Murphy PM, Farber JM (1999) Chemokine receptors as HIV-1 coreceptors: roles in viral entry, tropism, and disease. Annu Rev Immunol 17: 657–700.
59. Madani N, Hubicki AM, Perdigoto AL, Springer M, Sodroski J (2007) Inhibition of human immunodeficiency virus envelope glycoprotein- mediated single cell lysis by low-molecular-weight antagonists of viral entry. J Virol 81: 532–538.
60. Jones PL, Korte T, Blumenthal R (1998) Conformational changes in cell surface HIV-1 envelope glycoproteins are triggered by cooperation between cell surface CD4 and co-receptors. J Biol Chem 273: 404–409.
61. Allan JS, Strauss J, Buck DW (1990) Enhancement of SIV infection with soluble receptor molecules. Science 247: 1084–1088.
62. Crooks ET, Jiang P, Franti M, Wong S, Zwick MB, et al. (2008) Relationship of HIV-1 and SIV envelope glycoprotein trimer occupation and neutralization. Virology 377: 364–378.
63. Kim M, Chen B, Hussey RE, Chishti Y, Montefiori D, et al. (2001) The stoichiometry of trimeric SIV glycoprotein interaction with CD4 differs from that of anti-envelope antibody Fab fragments. J Biol Chem 276: 42667–42676.
64. Dimitrov DS, Willey RL, Sato H, Chang LJ, Blumenthal R, et al. (1993) Quantitation of human immunodeficiency virus type 1 infection kinetics. J Virol 67: 2182–2190.
65. Sherer NM, Lehmann MJ, Jimenez-Soto LF, Horensavitz C, Pypaert M, et al. (2007) Retroviruses can establish filopodial bridges for efficient cell-to-cell transmission. Nat Cell Biol 9: 310–315.
66. Carr JM, Hocking H, Li P, Burrell CJ (1999) Rapid and efficient cell-to-cell transmission of human immunodeficiency virus infection from monocyte-derived macrophages to peripheral blood lymphocytes. Virology 265: 319–329.
67. Babcock GJ, Mirzabekov T, Wojtowicz W, Sodroski J (2001) Ligand binding characteristics of CXCR4 incorporated into paramagnetic proteoliposomes. J Biol Chem 276: 38433–38440.

APPENDIX E

ATTRIBUTIONS

Chapter 2: M.E.M. and D.G. designed research; M.E.M. performed research; K.K. and S.M.W. provided sequence data.

Chapter 3: M.E.M. and D.G. designed research; M.E.M. performed research; E.T., P.J.P., and P.R.C. provided reagents and technical advice; E.T. and P.J.P. published experimental data used in comparisons in Figures 3.5 and 3.6; A.F published experimental data used in Figure S3.1; K.K. and S.M.W. provided sequence data.

Chapter 4: M.E.M. and D.G. designed research; M.E.M. performed research; P.R.G. provided reagents and technical advice; K.K. and S.M.W. provided sequence data.

Appendix A: My contribution to this work was to compile the initial set of sequences and annotations for the database.

Appendix B: My contribution to this work was to create and initially characterize the mutant Envs used in Figure 7.

Appendix C: My contribution to this work was the UK7 brain-derived Envs plasmids, other reagents, and technical assistance and advice.

PUBLICATIONS

Chapter 4: Mefford, M.E., Gorry, P.R., Kunstman, K., Wolinsky, S.M., and D. Gabuzda. 2008. Bioinformatic Prediction Programs Underestimate the Frequency CXCR4 Usage by R5X4 HIV-1 in Brain and Other Tissues. AIDS Res Hum Retroviruses 24: 1215-1220.

Appendix A: Holman, A.G., M.E. Mefford, N. O'Connor, and D. Gabuzda. 2010. HIVBrainSeqDB: a database of annotated HIV envelope sequences from brain and other anatomical sites. AIDS Res. Ther. 7: 43.

Appendix B: Gorry P. R., Dunfee, R., Mefford, M., Kunstman, K., Morgan, T., Moore, J. P., Mascola, J. R., Agopian, K., Holm, G., Mehle, A., Taylor, J., Farzan, M., Wang, H. Ellery, P, Willey, S., Clapham, S. M., Wolinsky, S. M., Crowe, S. M., and D. Gabuzda,. 2007. Adaptive changes in the V3 region of gp120 contribute to the unusually broad coreceptor usage of human immunodeficiency virus type 1 isolated from a CCR5 D32 heterozygote. Virology 362: 163-178.

Appendix C: Haim, H., Si, Z., Madani, N., Wang, L., Courter, J.R., Princiotto, A., Kassa, A., DeGrace, M., McGee-Estrada, K., Mefford, M., Gabuzda, D., Smith 3rd, A.B., and J. Sodroski. 2009. Soluble CD4 and CD4-Mimetic Compounds Inhibit HIV-1 Infection by Induction of a Short-Lived Activated State. PLOS Pathog. 5: e1000360. PMID19343205